申报	系列：教学科研
	专业：植物学
	职称：教授

业绩成果材料

（申报人的业绩成果材料包括论文、科研项目、获奖以及其他成果等）

单　位（二级单位） 生命科学院

姓　名 **龚维**

材料核对人：　　单位盖章：

核对时间：

华南农业大学制

目　录

一、教学研究业绩

1.教学研究项目：2022 年广东省本科高校高等教育教学改革项目——后疫情时代全英《植物学》国际化教学探索..... 5

2.教改论文：新时代全英课程《植物学》国际化教学改革思路探索..... 10

3.教改论文：以兴趣培养为核心的植物学教学改革..... 17

4.教改论文：生物科学双语教学模式与发展..... 26

二、科研项目

1.主持：2022 年国家自然科学基金面上项目——物种多样性空间分布格局形成机制探讨：以洲际间断分布绣球花族历史生物地理学研究为例.....34

2.主持：2015 年国家自然科学基金面上项目——北半球历史生物地理学问题探讨：基于 RAD taqs 方法的紫荆属亲缘地理学研究..... 38

3.主持：2014 年国家自然科学基金青年基金——广布种檵木及其近缘类群的亲缘地理学研究.....40

4.主持：2017 年广东省科技计划项目——南岭山区紫荆属种质资源调查和群体遗传多样性研究.....43

5.主持：2016 年广东省科技计划项目——南雄市银杏种质资源调查及雌雄株性别分子鉴定研究.....56

三、论文、著作等

1.检索证明.....69

2.以第一作者发表本专业论文情况

2.1. Evolution of the sex-determining region in *Ginkgo biloba*..76

2.2.DNA barcodes identify Chinese medicinal plants and detect geographical patterns of *Sinosenecio* (Asteraceae) 88

2.3.珍稀濒危植物伯乐树的潜在适生区预测.....96
3.以通讯作者发表本专业论文情况
3.1. The complete plastid genome provides insight into maternal plastid inheritance mode of the living fossil plant *Ginkgo biloba* 108
3.2. Population dynamics linked to glacial cycles in *Cercis chuniana* F. P. Metcalf (Fabaceae) endemic to the montane regions of subtropical China 113
3.3. The complete chloroplast genome of *Philadelphus pekinensis* Rupr. (Hydrangeaceae) 130
3.4. The complete chloroplast genome of *Deutzia pilosa* Rehd. (Hydrangeaceae) 133
3.5. Complete chloroplast genome of *Cercis chuniana* (Fabaceae) with structural and genetic comparison to six species in Caesalpinioideae.....136
3.6. Identification and characterization of microsatellites in *Aconitum reclinatum* (Ranunculaceae), a rare species endemic to North America.....153
3.7. The complete chloroplast genome of *Aristolochia hainanensis* Merr. (Aristolochiaceae) 157
3.8. Characterization of the whole chloroplast genome of a rare and endangered species *Aconitum reclinatum* (Ranunculaceae) in the United States.....161
3.9.A comparison of chloroplast genome sequences in *Aconitum* (Ranunculaceae): a traditional herbal medicinal genus 165
3.10. The complete chloroplast genome of *Sedum tricarpum* Makino. (Crassulaceae) 183

3.11. The complete chloroplast genome of *Hylotelephium erythrostictum* (Miq.) H.Ohba (Crassulaceae) 186

四、科研成果

五、其他业绩

广 东 省 教 育 厅

粤教高函〔2023〕4号

广东省教育厅关于公布2022年广东省本科高校教学质量与教学改革工程建设项目立项名单的通知

各本科高校:

按照《广东省教育厅关于开展2022年度广东省本科高校教学质量与教学改革工程项目申报推荐工作的通知》等文件安排，经学校遴选推荐、省教育厅审核、评审、公示及异议复审等环节，现将2022年省本科高校质量工程建设项目立项名单予以公布，并就有关事项通知如下:

一、立项情况

确定立项建设省级实验教学示范中心27个、校企联合实验室23个、科产教融合实践教学基地58个、大学生社会实践教学基地44个、教师教学发展中心2个、课程教研室112个、现代产业学院23个、未来技术学院1个、专项人才培养计划58个、高等教育教学改革项目781个、高等教育教学改革项目(委托类)

5个。具体立项名单见附件。

二、项目管理

（一）本次公布项目均为省质量工程建设项目，建设项目经学校组织建设、校内结题并通过省教育厅统一组织项目验收后，正式认定为省级项目。

（二）项目正式实施前，请确保已对项目建设目标、建设举措、预期成果、建设进度安排等进行科学论证，论证专家应不少于5人，且至少有三分之一来自外校。论证后的目标、任务等将作为项目结题验收时的重要依据。

（三）项目日常管理由学校主管部门负责，学校应统筹做好项目中期检查、校内结题验收等工作。校内结题时，邀请校外评审专家人数不得少于专家总人数的三分之二。满足以下条件的项目，经学校正式申请，可以参与省教育厅统一组织的项目验收：

1.项目已完成立项时设定的主要建设任务和目标；

2.项目已取得标志性建设成果，且该成果已在教学实践中得到检验和有效应用；

3.已按照要求完成项目校内结题；

4.符合当年度省统一验收规定的其他条件。

各校质量工程建设项目管理情况，将作为学校下一年度项目立项限额的参考依据。

（四）项目实施过程中，其名称、建设内容（任务）、建设目标、建设周期、主要负责人、预期成果等发生重大变更的，需

由时任项目负责人在发生变更后及时提出，经学校项目主管部门审核后由学校正式来函说明原因；擅自变更上述内容的，验收评定时列为不通过。

三、其他事项

（一）2022年度各校向省教育厅推荐并获得立项的项目，学校须将项目校内评审、推荐及论证相关材料妥善保存，留底备查。

（二）各校要统筹本校“冲补强”提升计划资金及自有资金对立项项目予以资助，项目获得学校资助情况将作为项目结题验收时重要考察因素之一。如项目建设中取得具有推广价值的优秀成果，请及时形成书面材料报省教育厅高教处。

联系人：李成军、傅兴淙，联系电话：020-37626882、37627703。

附件：2022年广东省本科高校教学质量与教学改革工程建设项目立项项目名单

广东省教育厅

2023年1月11日

公开方式：依申请公开

校对人：傅兴淙

395	高等教育教学改革项目	华南理工大学	基于量子力学课程的学生创新能力培养研究与实践	尹淼
396	高等教育教学改革项目	华南理工大学	基于六步法的计算机硬件类全英文课程教学改革与实践	俞鹤伟
397	高等教育教学改革项目	华南理工大学	高分子专业产教融合长效机制的探索与实践	张安强
398	高等教育教学改革项目	华南理工大学	新文科建设背景下基于建构主义仿真案例教学方法的领导科学课程教学改革研究	张树旺
399	高等教育教学改革项目	华南理工大学	面向先进制造拔尖创新人才培养的机器人仿真技术课程改革	占宏
400	高等教育教学改革项目	华南理工大学	螺旋式教学模式下的师生学习共同体构建研究	周文慧
401	高等教育教学改革项目	暨南大学	基于工程认证背景下仪器分析实验课程教学改革实践探索	陈永生
402	高等教育教学改革项目	暨南大学	物理化学理论课的具象化教学改革与实践	高庆生
403	高等教育教学改革项目	暨南大学	信息化背景下生物学创新人才培养模式的构建与实践	黄柏炎
404	高等教育教学改革项目	暨南大学	文化“走出去”战略背景下“商务翻译”课程思政建设路径探索与实践	黄艳琼
405	高等教育教学改革项目	暨南大学	以中华优秀传统文化传播为导向的《中国政府与政治》“浸润式”教学模式探索与推广	胡涤非
406	高等教育教学改革项目	暨南大学	“双一流”建设背景下科教融合驱动拔尖人才培养的改革与实践	高昊
407	高等教育教学改革项目	暨南大学	基于 5E 理论的医学生跨公卫课程群联动综合教学改革与实践	郜艳晖
408	高等教育教学改革项目	暨南大学	运用“五微一体”增强“改革开放史纲”课程亲和力与针对性的改革与实践	江传月
409	高等教育教学改革项目	暨南大学	港澳台侨及留学生大学英语多元融合型智慧课程的构建与实践	王璐
410	高等教育教学改革项目	暨南大学	“三个课堂”联动系统中新闻实务类课程思政体系建设	王媛
411	高等教育教学改革项目	暨南大学	面向港澳台侨学生的自然与文化敬畏素养培养：基于旅游类课程的改革与实践	徐松浚
412	高等教育教学改革项目	暨南大学	表达性艺术疗法在大学生心理健康教育课程教学中的创新与实践	刘浩鑫
413	高等教育教学改革项目	暨南大学	医文结合•叙事仁育——融入叙事医学的口腔修复学课程思政探索与实践	刘湘宁
414	高等教育教学改革项目	暨南大学	“双一流”建设背景下中药药理学与中药化学融合创新实验教学模式的改革与实践	李怡芳
415	高等教育教学改革项目	暨南大学	“新工科”背景下复合型工程结构创新人才培养模式与实践平台建设	聂振华
416	高等教育教学改革项目	暨南大学	身心两育：基于全面促进健康的高校体育教育教学改革与实践	容浩
417	高等教育教学改革项目	暨南大学	以学生为中心的审计课程教育模式改革与案例教学创新研究	石水平
418	高等教育教学改革项目	暨南大学	基于叙事护理以角色扮演为核心的 WebQuest 教学模式对本科护生综合能力的影响	田晓迎
419	高等教育教学改革项目	暨南大学	基于问题导向的“统计学习基础”课程改革与实践	王国长
420	高等教育教学改革项目	暨南大学	中华语言文化传承传播人才“共生教育”培养模式研究与实践	杨万兵
421	高等教育教学改革项目	暨南大学	基于 4C 软技能培养的 PBL 教学模式探索与实践——以“国际企业管理”课程为例	杨学军
422	高等教育教学改革项目	暨南大学	“交叉学科”人才培养体系构建与实践——以暨南大学国际学院为平台	于沛
423	高等教育教学改革项目	暨南大学	中国现代文学史课程思政教育的红色化、本土化探索与实践	张丽军
424	高等教育教学改革项目	暨南大学	工程教育专业认证背景下混合式学习教学模式研究与实践	张新征
425	高等教育教学改革项目	暨南大学	竞赛驱动的程序设计类课程融合教学改革研究与实践	张震
426	高等教育教学改革项目	暨南大学	中医药文化融入课程思政“一心二融四翼”教学模式构建与实践	朱诗平
427	高等教育教学改革项目	暨南大学	多模态混合式教学赋能驱动中医药课程优秀传统文化传播的模式构建与实践	朱晓峰
428	高等教育教学改革项目	华南农业大学	以“学以致用”为导向的《茶叶审评与检验》课程教学改革	谭新东
429	高等教育教学改革项目	华南农业大学	基于科教、产教双融合理念的《小动物临床病理学实验》教学改革与实践	李英

430	高等教育教学改革项目	华南农业大学	融合“树医生”理念的《园林植物栽植与养护》课程思政与实践教学改革研究	刘天颐
431	高等教育教学改革项目	华南农业大学	教学高质量发展视域下本科学生评教指标体系的优化	贾莉
432	高等教育教学改革项目	华南农业大学	融合课程思政的农林院校数学类公共基础课课程评价体系的建立和实践	丁仕虹
433	高等教育教学改革项目	华南农业大学	问题驱动下农业院校的数学分析课程线上线下教学改革的研究与实践	王石安
434	高等教育教学改革项目	华南农业大学	中外合作办学“学术英语”模块课程融合课程思政的探索	冯立新
435	高等教育教学改革项目	华南农业大学	助力乡村振兴的高阶性新型农商复合人才培养实践教学模式研究	齐文娥
436	高等教育教学改革项目	华南农业大学	“大思政课”视野下《中国近现代史纲要》教学改革与实践	崔芸
437	高等教育教学改革项目	华南农业大学	大数据背景下统计学专业产教融合人才培养机制的探索与实践	肖莉
438	高等教育教学改革项目	华南农业大学	基于知识地图的高校实验室安全教育微课体系构建研究	刘小波
439	高等教育教学改革项目	华南农业大学	乡村美育实施背景下农林院校音乐专业人才培养改革研究	朱虹
440	高等教育教学改革项目	华南农业大学	数学核心素养与“三农”情怀融合的《大学数学 I》课程思政探索与实践	曹静
441	高等教育教学改革项目	华南农业大学	“双一流”背景下农林高校公共基础课的教学改革与实践——以大学数学课程群为例	李朗
442	高等教育教学改革项目	华南农业大学	基于“馆校协同+合作学习”的历史实践教学模式改革与探索	龚金红
443	高等教育教学改革项目	华南农业大学	思政教育融合双创教育在专业实验课程中的研究与探索	罗霞
444	高等教育教学改革项目	华南农业大学	基于课程思政建设的高校体育课程研究	周华锋
445	高等教育教学改革项目	华南农业大学	“双一流”建设农业院校本科人才培养目标与定位研究——以大数据管理与应用专业为例	熊俊涛
446	高等教育教学改革项目	华南农业大学	后疫情时代全英《植物学》国际化教学探索	龚维
447	高等教育教学改革项目	华南农业大学	基于“知农爱农”的农业高校课程思政模式建设研究	张运红
448	高等教育教学改革项目	华南农业大学	落实“育德”教育与实践，打造《饲料生物技术》思政“金课”	孙加节
449	高等教育教学改革项目	华南农业大学	基于“五维优化，三层互助”的专业课程改革、思政建设与实践——以《家具与室内材料学》为例	孙理超
450	高等教育教学改革项目	华南农业大学	新工科背景下风景园林历史与理论课程教学改革研究	夏宇
451	高等教育教学改革项目	华南农业大学	基于“SPOC+PBL”的《形势与政策》混合式教学模式改革与实践	项赠
452	高等教育教学改革项目	华南农业大学	强综合、重实践、补短板——面向专业认证的科产教融合式建筑设计课教学改革	陈乃华
453	高等教育教学改革项目	华南农业大学	新工科课程思政一体化教学改革与实践——以《测量学》课程为例	姚朝龙
454	高等教育教学改革项目	华南农业大学	基于 PDCA 与 CDIO 的实践教学模式研究与实践——以《汽车构造实验》为例	周锡恩
455	高等教育教学改革项目	华南农业大学	习近平生态文明思想融入思政课教学机制研究	李俊宏
456	高等教育教学改革项目	华南农业大学	《用户体验设计》课程深度学习模式与效应研究	周秀
457	高等教育教学改革项目	南方医科大学	基于中医思维高阶培养的中医基础理论“IAC”教学法研究	安海燕

ISSN 1671-5691
CN 50-9221/G

中文科技期刊数据库（引文版）

教育科学

JIAOYUKEXUE

ISSN 1671-5691
10>
9 771671 569240

10
2024

中文科技期刊数据库（引文版）教育科学

二〇二四年十月

中文科技期刊数据库（引文版）

教育科学

2024 年 10 月　课程 · 教材 · 教法

主管单位：　科技部西南信息中心

主办单位：　重庆维普资讯有限公司

出版单位：　重庆维普资讯有限公司

总　　编：　车东林

电　　话：　023-63416211

网　　址：　https://oa.cqvip.com/

地　　址：　重庆市渝北区洪湖西路 18 号上丁企业公园

邮　　编：　401121

国际标准连续出版物号：
ISSN 1671-5691

国内统一连续出版物号：
CN 50-9221/G

法律顾问：　闫　军

本刊声明

本刊版权归重庆维普资讯有限公司所有。作者稿件一经录用，均视为作者同意刊载以及同意在本刊合作的数据库及互联网站传播。如作者不同意文章被收录，请在来稿时向本刊声明。

目　次

CONTENTS

课程研究

基于课程思政理念的物理因子治疗技术教学改革措施 ..... 黄婉莹　王　岩　朱　杰　李晓洁 1
高职院校《轨道施工与维护》课程思政实施中的突出问题及解决策略 ..... 杜　娇 5
《机械制造技术》实验课程思政建设策略探索 ..... 顾井飞　陈兴强　许　跃 9
课程思政融入《砌体结构》课程教学的思路与案例分析..... 焦贞贞 13
面向行政管理专业本科生的科技论文写作课程教学模式优化策略研究 ..... 刘树鑫　李润佳 17
新疆高职教育中数控技术课程的思政举措探讨——以哈密职业技术学院为例 ..... 朱　东　孙亚雯 20
中职护理教育《急救护理学》课程教学改革策略探索..... 葛媛媛 24
全国职业技能竞赛背景下《嵌入式技术》课程教学改革研究.... 李大盼 28
《航空服务心理学》课程思政教学策略研究..... 刘双玉 32
基于霍尔三维实施模型的应用型本科院校课程改革及创新路径研究 ..... 李　欣　刘玉丁 36
面向通信专业需求的大专层次数学课程建设思路与方法 ..... 杨　旸　罗屹洁　方　贵　陈学强 40
医学院校传染病学教学中融入课程思政的意义及策略分析 ..... 余　婷　刘凤君　曾　跃　王贵霞 44
思政课程中情境创设教学的理论基础与实践路径..... 李文静 48
职业院校礼仪教学与思政课程协同育人的路径研究..... 李晓慧 52
跨学科教学在历史课程设计中的应用思路与效果研究..... 吴秋容 56
“以赛促教、以赛促学”建筑设计类课程教学改革方法分析.... 喻梓琳 60
新时代全英课程《植物学》国际化教学改革思路探索 ..... 龚　维　张荣京　谢建光　郝　刚 64

科教论坛

线上教学结合 Seminar 教学方法在临床麻醉带教中作用探讨 ..... 孙　力　李　健　李洋洋 68
浅析虚拟现实在机械教学领域的应用方法..... 靳海涛 72
高职院校智慧农业视域下《plc 与电气控制》课程教学现状及优化策略 ..... 马　超　赵超阳　韩茂波　谭庆吉　赵玉冰 76
基于创造力三方思维模型（TTMC）的小学语文思辨性阅读教学模型的构建思路及教学策略 ..... 罗宇玥　张　阳 80
基于互动式教学模式的高职计算机应用技术教学策略及改革研究 ..... 许子毅 86
双一流学科建设背景下大学生专业自信的培养策略——以林产化工《香料化学与工艺》选修课为例 ..... 马春慧　李　伟　罗　沙　刘守新 90
教学医院专业课程隐形育人功能发挥的路径研究..... 强　娟　蒋　好 96
护理学专业实践教学现状分析和改革策略探究..... 徐　建 100
小学体育教学中游戏法运用策略探析..... 彭　沛 104

小学数学教学中跨学科整合的策略分析 ..... 刘晓晓 108
小学语文读写结合教学策略研究 ..... 钟明民 112
基于学习任务群的小学语文阅读教学策略 ..... 李宏霄 116
依托信息技术助力小学语文教学创新发展的策略研究 ..... 唐　丹 120
小学语文阅读教学的特点和路径探究 ..... 董智媛 124
以专业能力培养为导向的发射专业实验内容体系构建 ..... 仲启媛　谭立龙　陈恩情　薛　超 128
新时代背景下汉语言文学与黄河文化的融合探究 ..... 杨　洁 133

教学教法研究

大数据与会计专业校企联合下“双向三段六环”混合式教学模式的研究与实践..... 孙德惠 137
信息化背景下思维导图在高职英语写作教学中的应用价值与方法研究 ..... 夏叠丽 141
新时代背景下中学思政课的创新教学策略研究与实践 ..... 根　领 145
基于文化自信的高职院校思政教育课教学创新途径探索 ..... 郑沂郢 149
基于微信平台的混合式教学法在临床护理技能教学中的应用效果 ..... 薄文婷　古丽祖热·麦米提明 153
综合教学法在中医内科学教学中的实践探讨 ..... 高　玉　朱小莉　翟雪芹 157
核心素养视野下的中职数学教学策略 ..... 李　君 161
信息技术环境下的教学评一致性教学路径 ..... 吴芳蓉 165
师范生三笔字教育教学研究 ..... 祁　燕 169
实践性法律教学在法学教育改革中的实现路径分析 ..... 任　宇 174
互动教学在职高数学教学中的应用策略研究 ..... 何新飞 178
基于强化科研思维培养的免疫学实验教学改革探索 ..... 李英秀　刘洪展　王相伟 182
信息化条件下英语学科教学的现状与优化对策 ..... 姚　玄 186
情境模拟法应用于手术室护理教学中的价值探讨 ..... 蒋　薇　郭　娅 189
BOPPPS 联合情景模拟教学模式在临床麻醉教学中的应用..... 亚力·亚森　李玉倩　王　江　程　虎 193
虚拟仿真技术在核医学技能教学中的应用探讨 ..... 徐杨杨　谢　海 197
基于核心素养的古诗词群文阅读教学策略探究 ..... 张丽华 201

新时代全英课程《植物学》国际化教学改革思路探索

龚 维[1(通讯作者)] 张荣京[1] 谢建光[1] 郝 刚[2]

1.华南农业大学生命科学学院，广东 广州 510642

2.华南农业大学广州都柏林国际生命科学与技术学院，广东 广州 510642

摘要：随着全球化教育的发展，国际化教学模式成为高等教育的重要趋势。华南农业大学作为“双一流”大学，在国际化教学方面取得显著成就。随着新时代国际形式的不断发展和变化，国际化教学的创新也面临着前所未有的挑战。本文以华南农业大学与爱尔兰都柏林大学合作的全英《植物学》课程为例，探讨了新时代国际化教学模式的改革与实践。基于现有的教学情况，论文提出了一系列改革措施，包括教学理念的转变、语言环境的营造、教学资源的丰富化、教学方式的创新和考核机制的改善。

关键词：国际化教学；全英课程；植物学；教学改革

中图分类号：G640

0 引言

国际化教学在高等教育中占据重要地位。然而，长久以来，国际化教学也存在一些问题，例如，教学资源落后、师资配备不足、语言环境不充分和信息更新不及时等问题。在新时代下，国际格局发生了巨大的转变，国际合作模式也面临着前所未有的挑战，在新形势下该如何改革并完善顺应时代变化的国际化教学，已成为高等学校探讨的热点课题之一。作为中国的“双一流”大学之一，为了更好的响应国家国际化合作办学的政策、更有效的利用国外的教学资源，华南农业大学与爱尔兰都柏林大学开展合作办学，发展了不出国门对学生进行国际化联合培养的模式，其教育质量和国际影响力得以显著提升。

在国际化合作教学模式的改革和发展过程中，学科类别以及专业方向越来越多样化，涉及生命科学、金融学、计算机科学、工商管理等学科。合作的国家和大学也逐步增多，包括英国、美国、爱尔兰、澳大利亚等各国的优质名校，部分高校位列 QS 世界大学排名前 100。国际化合作方式也更加灵活多样，除学分互认、双学位联合培养，还有自主招生、短期访学、交换项目等。国际化合作办学的开展，在很大程度上促进了学校的国际化发展，为建设双一流大学提供了更多的教学、科研方面的契机。

《植物学》是高等院校生物类和农学类等一切以植物为生产和研究对象的重要学科基础课和专业必修课程，是农学、生命科学类专业人才培养体系的基础，具有十分重要的学科地位。同时，《植物学》课程也是生命科学类国际化教学的必修课之一。其中，全英《植物学》课程国际化教学体系的建立，对于培养具有国际视野的专门人才、吸引更多生命科学、农学类专业的招生对象具有重要意义。为了在教学语言环境、学习氛围和学术前沿方面更好的与相关专业学科适应和对接，亟需充分建立国际化的《植物学》教学体系。基于此，十分有必要进一步改革全英《植物学》课程的国际化教学模式，建立更加完善的教学体系。

基于此，本项目将针对现有的全英《植物学》课程国际化教学模式，结合当下中国的国情，从学校和专业的实际情况出发，探索并构建一套以培养具有国际化视野、国际竞争力的创新人才为导向的国际化教学模式。兼顾线上和线下教学，从教学氛围、语言环境、信息化教学资源、师资力量等方面将进行具体的探索和完善，对其它类似专业课程的国际化教学提供借鉴，具有一定的参考价值。

1 全英课程《植物学》国际化改革目标和意义

通过全英《植物学》国际化教学模式的探索，基于国际化合作办学模式，将实现如下几点目标。

1.1 培养具有国际化视野的优秀国际人才

收稿日期：2024年05月16日

作者简介：龚维（1979—），女，汉族，重庆人，博士，华南农业大学生命科学学院，副教授，从事植物生物地理学、分子进化和群体遗传学等方面的研究。

传授植物学知识的同时，培养学生具备良好的科学、文化素养，系统掌握植物学基础知识、基本理论和基本技能。此外，新国际形势下，充分利用国际教学资源，拓展相关学科领域的国际化视野，跟上时代步伐，培养活跃的思维和创新的精神。最终，获取在植物学相关领域继续深造的知识储备和专业素质，成为能够在相关领域从事教育、科学研究、技术研发和生产管理等工作的高素质的国际化人才。

1.2 提高教师国际化教学水平

通过讲授全英课程，要求授课教师具有扎实的专业理论知识，熟悉并掌握植物学研究相关理论知识、实验技能以及数据分析方法，并具备丰富的教学经验。同时，重视科研发展动态，紧跟最新学术热点。通过英语为主的授课，大量介绍相关研究领域的文献资料和研究成果，进一步巩固自身的知识构架，提升教学能力。

1.3 丰富教学资源

大量引入国内外教学资源，包括优秀教材、文献资料、研究报道、多媒体教学资源等，在此过程中，丰富课堂资源，活跃学术思想，让学生的学习不再单调乏味。

1.4 完善培养方案和教学体系

兼顾传统经典的基础理论知识，结合最新的教学内容和研究成果，查漏补缺，完善和补充已有的教学体系。配合灵活多变的考核方式，全面检查学生对相关专业知识的掌握程度，客观评价其学习效果，从而全面培养学生的综合能力和科学素养。

2 全英课程《植物学》国际化教学改革思路

2.1 转变教学理念

传统的《植物学》教学，主要从理论学习、结构图解和形态观察为主，教材主要基于国内各大高校主编的《植物学》教材。传统的《植物学》教学历时悠久，知识内容精炼。然而，随着《植物学》相关研究领域不断涌现出新的科学成果，一些概念和知识点也逐步产生了更新。授课过程中，不仅需要基于传统的细胞学、遗传学以及植物分类学知识，确保以经典植物学教学理论知识为基础，同时，需紧跟学科发展前沿，传授最新的相关研究成果，保证知识传递的时效性。例如，讨论细胞学说的建立，其主要内容和核心思想是否完全适用于现代生物科学领域。关于植物分类学部分，基于林奈分类系统，结合最新的 APG 系统，认识被子植物分科，正确讲解被子植物分类学等相关问题。

2.2 多元化授课方式

在遵循传统教学模式的基础上，接纳多元化的教学模式。以教师讲授为主，鼓励学生提出的新见解，允许学生对经典理论和知识点提出质疑，并尝试探索新理论、发展新的研究方法。最根本的是要实现从以“教”为中心向以“学”为中心转变，即从“教师将知识传授给学生”向“让学生自己去发现和创造知识”转变[1-2]。例如，围绕“对人类历史影响最大的植物是什么”展开讨论，同学们查阅文献资料，针对植物的起源以及植物资源在人类社会发展进程中的应用进行深入的探讨和激烈的辩论，有理有据，将植物学理论知识与人类社会的进步相联系。

2.3 营造语言氛围

双语教学，尤其是全英教学，是国际化教学的重要特征之一，全英《植物学》国际化教学也不例外。双语教学不是简单地采取两种语言教学，全英教学也不是简单的全程英语授课。无论是双语教学还是全英教学，其目的不是单纯的学习语言，而是为了传递不同语言所承载的文化知识和科学理念，培养学生运用两种语言去学习、理解和思考专业领域的学科知识。基于此，在全英《植物学》教学中，要学会运用中英文两种语言知识和学术思维去理解植物学相关概念和科学问题。通过两种语言的交汇，接纳该专业领域在不同语言国家对各种学术问题的讨论，了解该学科领域的发展历程。与此同时，逐步提高对学术论文的阅读理解能力以及英语语言的应用能力，这将为日后开展国际学术交流与合作打下良好基础。

在课题教学的过程中，教师首先需因地制宜地制作全英课件，提前准备英文专业词汇，尽可能全英文口头授课，必要时辅以中文进行阐述。此外，开展英语课堂互动和讨论，营造英语语言环境，鼓励学生运用英文进行专题汇报、课堂讨论和解答课外作业，让学生充分利用英文专业术语和句型进行学术知识交流，从而达到锻炼、提高学生英语表达能力的目的。课题

讨论要求学生 3～5 人组成研究小组，分工协作完成选题，建立由任务驱动的团队自主写作、共同学习的教学模式[3-5]。最后，在课堂考核、实验报告、期中考试和期末考试中，要求学生英文作答，尽可能与其它相关的全英课程接轨。

2.4 丰富教学资源

网络信息的大量涌现，对于最新发展方向、科研动态和热点问题的获取也越来越高效和广泛，人们接收知识信息的方式已经不再局限于书本和老师。因此，基于国际化的教学更加应当充分利用各种信息渠道来充实教学内容、创新教学方式并更新教学成果。基于此，全英《植物学》国际化教学需要进一步丰富教学资源，包括相关领域的科学成果、研究论文，通过视频、文献、图片等，引入国内外优秀教材，向学生传达最新的研究进展，将传统知识点与现有科学研究相结合，理论联系实践，更好的理解植物学概念，而不是空泛的讲授植物学知识。例如，针对苔藓植物的结构和生活史，通过简短的英文视频和形象生动的动画，直观显示苔藓植物的孢子体和配子体结构，观察苔藓植物有性生殖过程，理解世代交替。同时，在线共享教学课件、文献资料，在百度网盘、微信群等平台，存放教学资料，即使在紧急情况下无法实现或参与线下课程，学生也能随时查找阅读教材、课件和文献，充分利用网络，多媒体技术，让同学们不出国门也能获取最新的国际化教学资料。

2.5 改善考核机制

《植物学》课程一直以来以闭卷考试为主，《植物学实验》和《植物学实习》，均以实践和理论相结合的方式进行考核和考查。为了更加全面而且客观的评价学生的学习效果，考核形式应适当多样化。首先，考核语言为英语，辅以中文，要求学生以英文作答。同时，考核方式除了传统的卷面作答，也要结合课堂论文、专题讨论等，让学生主动去查阅文献资料，探讨植物学相关的科学问题。另外，完善考核机制，将线上线下相结合，灵活应对各种情况下的课程考核。考核是教学环节的重要一环，是督促学生认真学习和巩固所学知识的有效手段，也是调动学生学习积极性和主动性的有效措施。避免仅以期末考试分数作为学生成绩的唯一标准，而造成学生考前突击，不利于学习及创新能力的培养[6]。在全英《植物学》课程考试中我们采用综合评价体系，分为卷面成绩（占 50～60%）和平时成绩（40～50%）。平时成绩则包含了探究小论文、实践作业、课堂讨论和实验报告等。

3 结语

以上教学改革举措将以国际学院的学生为主，通过全英《植物学》国际化教学模式的改革和探讨，将传统《植物学》教学纳入国际化元素。在符合我国国情的前提下，既遵循传统教学方式，又发展创新的教学理念和教学手段，保证植物学基础知识的传授，同时跟上该学科国际化发展的步伐，拓展学术视野。以丰富多彩的教学资源，结合形式多样的教学方式，调动学生学习兴趣，活跃教学氛围，拓展国际视野，让原本枯燥的理论学习变得生动有趣。授课教师也可以在此过程中，积累更丰富和先进的针对国际化教学的方法和经验，最终，全英《植物学》课程将进一步适应国际化教学模式，并有助于学校在新国际形势下快速发展，也为其他高等教育机构提供了国际化教学的有益参考。在未来，该课程将继续探索和完善国际化教学模式，以更好地适应全球教育环境的变化，培养出能够在国际舞台上发挥重要作用的优秀人才，为全球高等教育的发展贡献力量。

参考文献

[1]Barr B.Robert,John Tagg.From teaching to learning-a new paradigm for undergraduate education[J].Change:The Magazine of Higher Learning,1995,27(6):12-26.

[2]刘献君.论“以学生为中心”[J].高等教育研究,2012(8):1-6.

[3]付春华,栗茂腾,蒋涛,余龙江.“以学生为中心”的植物学课程教学体系构建与实践[J].生物学杂志,2017,34(6):113-115.

[4]王雪峰,曲春香,刘超,等.基于问题探究、合作学习与团体考核的《生物化学》教学方法的研究[J].生物学杂

志,2015,32(6):122-123.
[5]尹军霞,沈国娟.由任务驱动的团队自主合作学习教学模式在微生物学课程中的探索和实践[J].微生物学通报,2016,43(2):410-416.
[6]邢万金,莫日根,苏慧敏.生物学教学中研究型教学方法与内容的探索[J].遗传,2014,36(7):732-738.
基金项目：2022 年广东省本科高校高等教育教学改革项目“后疫情时代全英《植物学》国际化教学探索”（446）。

中国知网
万方数据
维普网
龙源期刊网
博看网
收录本刊全文

ISSN 1674-9324
CN 13-1399/G4

教育教学论坛

JIAOYU JIAOXUE LUNTAN

2013年10月 第42期

EDUCATION TEACHING FORUM

ISSN 1674-9324
9 771674 932102 42>

目录 contents

特别关注

1 大学生自尊相关研究概述 …… 陈思瑶
2 小学生拖延行为心理原因及干预策略初探 …… 罗 俊,周玲玲,胡 月
4 大学新生入学教育 …… 卢冬莉
5 关于加强高职女大学生性安全教育的探讨 …… 赵艳君,王明娟
6 中学生抄袭作业现象浅议 …… 刘元新
7 高职学院市场营销专业毕业生就业与营销人才需求分析
——以郑州铁路职业技术学院为例 …… 江 欣
9 大学生志愿服务参与农村留守儿童的路径分析
——以德国多代屋项目模式为载体 …… 李荣志

科学管理

11 宽严相济 巧用其“短”
——高中班主任工作案例分析 …… 魏 巍
12 浅议民办高校教务管理工作 …… 李招弟,李 杨,赵玲玲
14 通过项目管理全面推进示范校建设 …… 孙 勇
15 高校转型过程中实验室建设与管理探析 …… 秦丽梅,邬依林,张渝荣
16 中学教务管理系统设计与实现 …… 高 飞
18 以德服人 民主管理 …… 谢侣枝,母相军
19 独立学院国有资产管理刍议 …… 唐春玉

教改创新

20 《过程设备机械基础》课程教学改革 …… 吴 静,张 青
21 以兴趣培养为核心的植物学教学改革
…… 龚 维,张荣京,谢建光,郝 刚
23 积极心理理念的心理素质教育课堂教学改革初探 …… 刘文俐
24 高职《食用菌生产技术》课程教学改革研究 …… 刘连成
25 浅谈邮政报刊发行系统改革与创新 …… 雷晓燕
27 医学教学改革中现代教育技术的应用 …… 张东威
28 理工科院校研究生英语教改中的制约因素 …… 林 易,马新英,孙爱珍
30 经管类专业《管理信息系统》课程教学改革的思考与创新
…… 赵阿平,彭海红
32 工业工程专业 CDIO 实践教学模式改革研究 …… 刘伟民,郑爱云
34 高校武术课内外一体化教学改革实践研究 …… 孙明兴,赵雁楠
35 高职院校商法课程教学改革研究 …… 张 媛
37 关于本科经济学专业课程体系和教学内容改革的若干思考 …… 张雪绸
39 职业院校计算机教学的改革分析与探讨 …… 孙永国
40 新课程改革的思考 …… 彭 骋,陶 丽

教师建设

42 做一个幸福的教师 …… 宋 莉

教育教学论坛

JIAOYU JIAOXUE LUNTAN

2013年10月 第42期 总第123期

期刊名称 教育教学论坛
主 管 河北出版传媒集团有限责任公司
主 办 河北教育出版社有限责任公司
花山文艺出版社有限责任公司
出 版 教育教学论坛杂志社
印 刷 石家庄市飞达印刷有限公司
发 行 河北省报刊发行局
出版日期 2013年10月16日
主 编 韩新保
发行范围 国内外公开
定 价 35.00元
国内统一连续出版物号 CN 13-1399/G4
国际标准连续出版物号 ISSN 1674-9324
广告许可证号 1301024D00093
地 址 石家庄市联盟路705号
邮 编 050061
订 购 处 全国各地邮局
邮发代号 18-219
电子信箱 jyjxlt@jyjxltzzs.com
联系电话 0311-87760976

主 任 韩新保
委 员 韩新保 王瑞婵 秘云霞 刘春玮 秦甜甜 王雪平 郭桂香 张保玉 康 薇
副主编 王瑞婵
市场监管 展建军
责任编辑 刘春玮 王雪平 秦甜甜 王越西 韩向军 庞国刚
美术编辑 张贵新

43　浅谈中等职业教育队伍的建设与培养 …… 石　权
44　论独立学院辅导员在大学生就业工作中的角色与定位 …… 刘益明
46　浅谈教学秘书工作中写作能力的培养 …… 贾　乙
47　高等职业教育“双师型”教师队伍的培养 …… 李洪军

学生教育

48　城区中小学惩戒教育的缺失分析 …… 王文娟
50　真心关爱　真诚合作
　　——关注外来学生成长　共建家校和谐关系 …… 孙向红
51　做学生的心灵鸡汤
　　——班主任随感 …… 楼益平
52　特别的爱给特别的你 …… 张兆艳
53　感恩父母　点滴入怀
　　——记一堂班团活动课 …… 郑华勇
55　浅议班主任在学生焦虑情绪中的心理干预 …… 陈美琴
56　以人为本　构建爱情教育的内容体系 …… 杨炎梅
58　养成教育在小学教育阶段的作用 …… 张虎杰，崔建石
59　“学生殴打老师”现象的思考 …… 孙　科
60　例谈初中班主任德育工作有效策略 …… 刘来喜
61　用心去做班主任 …… 孙淑霞，宋学军
62　赏识、宽容都是爱 …… 栗成红
63　做好个别教育　提高班级整体素质 …… 徐晓燕，杨文庆

思想品德

64　浅谈以行为习惯为核心的职校德育教育 …… 林兰花
65　网络环境下高中政治探究性学习的反思 …… 秦　毅
66　关于加强当代大学生社会主义核心价值观教育的思考 …… 周　菘
67　创新高校思想政治教育机制研究
　　——以云南大学旅游文化学院园区思想政治教育为视点 …… 朱玉福
69　高校思想政治理论课中教师和学生的地位
　　——以实践教学为中心的分析 …… 王雅娟

高教研究

70　驻济高校大学生休闲体育活动现状的调查分析 …… 牛　婷，王瑞静，李志伟
71　我国高校公共政策学课堂教学方法现状与问题 …… 张　杰
73　机械类学生三维设计能力培养方法研究 …… 刘永霞，彭如恕
74　普通高等学校钢琴教学的优化策略探析 …… 陆晨曦

教师观点

75　关注高职教育　成为理想教师 …… 周红雨
77　新课程背景下初中学生历史学习现状分析与建议 …… 谭新天
78　浅谈新课改背景下的语文教学 …… 郑　丹
79　例谈物理教学过程中的安全教育 …… 王中文
80　对农村高中兼顾美术考生专业与文化课教学管理策略的思考 …… 黄海丰
81　浅谈如何讲解多媒体美术欣赏课 …… 贺志刚
82　关于大学物理教学的几点思考 …… 陈　尧
83　物理建模与中学生思维能力培养 …… 陈国华
84　新课标下的数学教学浅析 …… 凌晓霞
86　英语写作能力培养探究 …… 张晓霞
87　中等职业学校英语课教学中面临的困惑及对策探讨 …… 王生亮
88　小学英语课堂参与问题及策略研究 …… 梁艺娟
89　浅谈数学目标教学及其评价 …… 乔智平

90　浅谈尊重学生学习主体地位的几点感悟 …… 黄学勤
91　浅谈农村初中英语教学现状及策略 …… 纪素香

专题研讨

92　发挥农广校优势　搞好农民教育培训工作 …… 张春梅
93　浅谈参考文献在毕业论文中所反映出的问题
　　——以湖南第一师范教育科学系 2012 届本专科毕业生为例 …… 汤　勇
95　油画的预防性保护研究 …… 吴晓欧,张　辉
97　关于中变催化剂使用寿命缩短的原因分析 …… 魏承涛
99　“公益积分”在志愿服务活动中的应用 …… 刘颖春
100　家庭礼仪教育缺失探析
　　——基于儒家视角 …… 黄晨洁,杨　玲
102　大学生党员教育方法的创新与实践
　　——以云南师范大学化学化工学院学生第二党支部为例 …… 刘　莹
103　广告语中的模糊现象及其语用功能探析 …… 刘　琦
104　中韩高职教育的实践教学模式比较研究 …… 白　玲
106　体能训练对预防高校篮球运动损伤的作用 …… 刘文军
107　中医院校学生《预防医学》内容设置满意度调查
　　…… 胡继宏,郑贵森,吴建军,万学忠,陈　丽
108　论新世纪大学校园的人文精神内涵 …… 杜启蓉,杜启玉
109　当前大学生权利意识状况的分析报告
　　——基于 18 所高校的调查 …… 艾阿琛
112　辽宁省优秀运动员心理健康状况调查与分析 …… 丁冬云
113　论公示语翻译的规范化问题 …… 陆相如
115　大学文化与城市文化互动关系探讨
　　——以欧洲与美国为例 …… 任　茵
116　大学生的创新、创业能力培养的调查与研究
　　——以新疆部分高校为例 …… 仇　岗

教法研究

117　浅谈技校汽修专业一体化教学的开展 …… 马卫卫
119　谈陶行知教育思想在小学语文中的渗透 …… 吴周泽
120　关于小学数学概念教学的思考 …… 杨文明
121　浅谈军队院校“马克思主义基本原理概论”课堂教学艺术
　　…… 侯莲梅,郭发仔
123　Protel 教学经验之谈 …… 吴跃虎
124　浅谈影视资源在高中地理教学中的运用 …… 王海燕
125　小学低年级写字教学探究 …… 林胜国
126　PBL 教学法在《运动解剖学》实验课教学中的实践研究 …… 王瑞静
128　CCD 成像原理教学“四步曲”
　　…… 刘　杰,周　冰,华文深,任宏岩,何永强,鲁　军,应家驹,陈玉丹
129　医学遗传学教学过程中的一点感悟 …… 粟炳南
131　中学生地理思维能力培养的影响因素及其培养策略 …… 左胜杰,左洪义
132　香豆素 -3- 甲酸乙酯的微型制备方法研究 …… 邹碧群,张　业
133　“五步式探究”数学教学思路探微 …… 郭利峰
134　点集拓扑课堂教学的几点体会 …… 姜德烁
136　少儿美术教育与创新发展 …… 郭　佳
137　初中体育课分层教学模式的实践研究 …… 宫成刚
138　重视估算教学　发展估算能力 …… 陈旺根
139　应用语言的翻译研究凝思 …… 张　蓉
140　浅谈简笔画在生物学教学中的运用 …… 曹鹏会
141　中学数学的教学探讨及乘法公式的灵活应用 …… 骆付安

142　浅谈小学数学概念教学 …… 黄柏森
143　体育课堂教学中发挥学生主动性的“六字方针” …… 何艳蕊
144　从课堂语言、情境、作业培养低年级学生的学习兴趣 …… 林葆华
145　少数民族地区小学语文低段识字教学方法初探 …… 李茹菲
146　几种数学思想在数学问题中的应用 …… 林文飞
148　激、传、动、促——谈歌曲教学中情感艺术的培养 …… 郑伟君
149　论高中历史教学中思维能力的培养 …… 王迎春
150　浅谈初中地理教学中学生读图能力的培养 …… 刘　玮

学法指导

151　浅析新高考历史主观题答题技巧 …… 杨　凯
152　利用合作学习提升高中地理复习效果 …… 徐兆刚
153　物理课程中矢量与微积分 …… 荣　健
154　谈谈分类讨论思想 …… 王　欣
156　谈谈中学生如何记忆英语单词 …… 兰清世
157　学生解题后的反思之我见 …… 亓甲明
158　论数学解题自我监控能力的培养 …… 李艳利
160　《数值天气预报》中非线性计算不稳定的举例 …… 施　宁

课题项目

161　生物工程专业《基因工程》课程实践教学初探
…… 徐　波，周　通，熊维娜，钟平安，黄　林
163　大林姬鼠与黑线姬鼠消化系统的比较研究
…… 王丛民，朴忠万，刘文洋，闫佳续，金志民
164　新疆维吾尔族受众职业背景与媒介依赖研究 …… 徐荟涵，李卓谦
166　英语师范生实习中存在的问题及对策研究 …… 宋晓龑，张娜萍，陈洁秋
167　《临床技能学》国家精品课程建设的研究与实践
…… 李　熠，沈元琼，桂庆军，文格波，游　咏，尹　凯
169　基于创新能力培养的归纳总结法
——以化学箭头为例 …… 李江胜，付冬梅，李志伟，卢翠红，王辰宇
171　影响高校贫困生就业能力的因素分析与可行性措施
…… 李鸿发，陈周鼎，纪　娜，张梦飞

研究生教育

173　研究生医学分子生物学教学改革与思考
…… 杨加伟，陈　静，陆红玲，冯赞杰，刘喜平，欧刚卫
174　医学硕士研究生选题的原则与方法
…… 秦丽娟，王艳蕾，王小君，张一兵，杨秀红
175　研究生博客学习中的人际交互促进策略初探 …… 王艳随
176　硕士研究生学位论文盲审效果研究及探索性建议 …… 安　洁

职业教育

178　高职院校提高学生“顶岗实习”质量的策略 …… 邱文华，邱珍珍
179　职业技术学校英语教学中如何培养学生有效的学习策略 …… 马　刚
180　因材施教　提高课堂教学有效性 …… 包素玲
181　职业学院学生英语听力成绩与听力策略关系的调查研究 …… 张　平
183　钳工实习教学中分段式教学模式的应用 …… 戴文进
184　高等职业院校工商企业管理专业人才培养模式探索与改革
——以呼和浩特职业学院工商企业管理专业为例 …… 张　峰

教学设计

186　“采蘑菇”式教学在高三英语一轮复习中的应用 …… 郝秀兰

187　奏响语文课堂教学的第一乐章
——谈新课改下语文课堂的导语设计 …… 赵小燕
188　关注学生需要　满足学生需要
——“认钟表”案例与反思 …… 吴福英
189　20 以内的加法说课稿 …… 宋静霞
190　《飞云湖》教学设计 …… 周永胜
191　创设真实语境　培养学生综合运用语言的能力
——7A Unit 6 Integrated Skills 教学案例 …… 吴华芝

民主教学

193　巧用历史插图　点燃思维火花 …… 王良根
194　谈谈激活语文课堂教学的几条有效途径 …… 王文萍
195　表演展示激活高中生物课堂教学 …… 张宝平
196　数学课堂中如何培养提高学生的注意力 …… 王金森
197　如何点燃舞蹈班学生的数学热情 …… 施梅兰
198　浅析高中体育课堂如何激发学生参与热情 …… 刘　颖
199　优化动手操作活动　引导学生“做”数学 …… 邓其灿
200　论如何打造精彩而又高效的高中政治课堂 …… 张云霞
201　把课堂还给学生 …… 张科荣
202　贵在练说　重在交际 …… 陈德长
204　课堂观察 ABC …… 陈淑芳
205　数学课堂中发展学生的思维能力 …… 陈　玲
206　中职英语课堂教学中的“小组合作学习”方法研究 …… 方　云
207　用“情感”优化数学教学
——小学数学教学中情感态度、价值观培养研究 …… 陈乐轩
208　体验式教学中怎样创设教学情景 …… 韩秀霞
209　小学语文综合性学习的问题与对策 …… 靳钟琦
211　师生互动构建和谐的英语课堂 …… 尹　程
212　浅谈高一阶段如何开展英语综合实践活动 …… 胡俊阁

探索与实践

213　生物技术专业本科生科研创新能力培养模式探讨
…… 王雪琴,谭晓蓉,张　璐,张慧茹
214　高中历史教学新探索 …… 陈光远
215　团体心理辅导在中职班级管理中的实践探索 …… 吴小琴
217　精品开放资源共享课程建设探讨 …… 弥　锐
218　高职“岗位情境　产品导向”的“2+1+1”实训教学模式探究 …… 任枫轩
220　《航空发动机自动控制与适航性》实验教学探索与改革 …… 刘晓锋
221　小学数学课堂有效操作现状分析和策略探讨 …… 陈根玉
222　提高医学文献检索教学质量的实践与探析 …… 陈玉琼

阅读与写作

224　初中语文独立创新写作教学的前奏 …… 杨　蓉
225　语文:永远不能“改名换姓” …… 王心凯
226　浅谈高中语文的阅读教学 …… 王全胜
227　“赏析—模仿—独创”式写作教学思路探微 …… 王立新
228　探寻高中语文体验式教学阅读之方法 …… 魏祥波
230　谈语文阅读教学中写作知识的渗透 …… 张晓梅
231　浅谈初中语文现代文阅读教学 …… 陈为信
232　谈听说训练贯穿于阅读教学全过程 …… 陈爱兰
233　浅谈如何让学生感悟语言 …… 刘　杰
234　中国古代诗歌教学方法例谈 …… 梁媛媛
235　浅谈如何培养学生的阅读能力 …… 黄培龙

236　浅谈语文教学的研究性学习方式
——以李白诗歌阅读指导课为例 …… 耿　玮
237　新课改下的作文教学 …… 熊丽华
238　开启文思　主动创新 …… 韩志鸿

信息技术

240　关于教育游戏的发展现状及其发展趋势综述 …… 刘小莹,张秀梅,李　慧
241　多媒体教学给语文教学带来一方亮丽的蓝天 …… 方丽媛
242　信息技术与学科课程整合的有效策略探究 …… 寇　秀
243　浅谈多媒体技术在集成电路工艺教学过程中的利与弊 …… 白晋军,李鸿强
245　运用信息技术优化小学生语文学习 …… 沈　希
246　运用现代教育技术　优化小学作文教学 …… 张芙蓉
247　游戏化展示教学在网页制作这门课中的应用 …… 吴丽丹
248　基于多媒体学习理论的 PPT 的设计 …… 张秀梅,刘小莹,李　慧
250　PPT 课件中使用音视频的方法探讨 …… 曹　平
252　浅谈多媒体技术与语文教学的巧合 …… 任　英
254　以信息网络为平台　开创党建工作新局面 …… 李　荀
255　多媒体辅助生物教学的巧妙应用 …… 吴功如
256　加强探究型学习　提升高中信息技术教学质量 …… 卢兆明
258　大学多媒体英语教学在支架式教学中的优势 …… 梁　岚
259　巧用多媒体辅助英语教学 …… 徐　利
260　游戏化展示教学在 flash 动画设计课中的应用 …… 袁莉娅

实验平台

261　推行免疫学实验教学改革　提高学生科研兴趣
…… 刘白南,罗军敏,杨　鸣,田　丹,郑　静
262　浅谈微生物实验心得 …… 刘叶丹,申屠旭萍,傅小伟,边亚琳
264　课外实验对微生物学教学的作用与意义 …… 陈昳丽,申屠旭萍,傅小伟,边亚琳

学前教育

265　探究幼儿园综合艺术课程的建构与实施策略 …… 徐　丹,余致静
266　幼儿教育小学化影响孩子健康发展 …… 杨志芳
267　组织材料活动　培育幼儿健康人格 …… 郑晓芸,曾昭镇
268　注重情绪激发　增强合作技能
——浅谈幼儿合作教育与情商发展 …… 张　黎
270　浅析幼儿音乐活动教学中的情感教育 …… 郑　娟

快乐课堂

271　创设多种手段　激发小学生学习汉语拼音兴趣 …… 刘和荣
272　兴趣教学在高中生物课堂上的运用 …… 周传萍
273　培智数学的生活化教学 …… 张登龙
274　让小学数学教学走向生活化 …… 林燕香
275　让生物课堂快乐充实 …… 陈宁宁
276　小学低年级数学课堂教学中小组合作学习的探索 …… 秦小荣
277　巧妙设计数学课堂教学 …… 孙文娟
278　让写作贴近学生生活
——我市小学英语作文教学大赛观摩有感 …… 刘玉萍
279　《话说端午节》教学设计 …… 周永胜

学术前沿

280　浅议小学数学探究性学习的教学策略 …… 王　宇
281　基于高校“优待生”现象的教育管理引发的思考
——以“优待学生”三个事件为例 …… 燕红梅,王建鲁

以兴趣培养为核心的植物学教学改革

龚　维，张荣京，谢建光，郝　刚
（华南农业大学　生命科学学院，广东　广州　510642）

摘要：植物学是国内高校生物科学及相关专业的基础学科，传统的植物学教学内容和教学模式已不能满足现代教学体系的要求。学生在课业繁重的压力下逐步失去了对植物学的学习热情和兴趣。本文以学生兴趣培养为核心，以发挥学生主观能动性为目的，从植物学教学现状调查入手，对植物学教学内容、教学形式和考核方式进行探讨，提出相应的教学实践和创新方案。

关键词：植物学；生物科学；兴趣培养
中图分类号：G642.0　　**文献标志码**：A　　**文章编号**：1674-9324(2013)42-0021-02

植物学是生物学的分支学科，是一门综合性学科，历史悠久、内容广博。作为一门历史悠久的学科，其教学内容主要包括植物形态解剖和植物分类两大方面。前者涵盖植物营养器官与生殖器官的解剖结构和生长发育，后者主要介绍植物的分门别类和各科属的代表植物。目前，国内高校的植物学教学多是采取理论课教学与实验课教学相结合的形式。理论课以老师课堂传授植物学基本知识为主，实验课则与理论课同步开展，通过实验观察进一步巩固理论知识，增加感性认识、培养实践能力。随着生命科学的飞速发展，植物学在学科地位、教学理念、教学内容和教学手段等方面都面临着严峻挑战。作为国内高校生物学及相关专业的基础学科，植物学也是必修课程，其传统的教学模式已不能满足现代教学体系的要求。因此，进行植物学教学的创新和改革已成为当务之急。

由于植物学内容繁杂，知识点多，实践性强，许多学生在课业繁重的压力下逐渐丧失了对植物学的学习热情。为了应付考试，许多学生通过死记硬背来达到考核合格的目的。长此以往，植物学教学将违背素质教育和创新型人才培养的要求。只有激发学生的兴趣，调动学生的学习积极性，才能轻松愉快的进行学习，获得良好的教学效果[1]。近年来，我们在植物学教学理念、教学内容、教学方法和手段以及考核方式等多方面，进行了一系列的探索和创新。以学生兴趣培养为核心，其目的在于充分发挥学生的主观能动性，提高教学质量。本文将从植物学教学现状调查入手，揭示现存的教学问题，提出相应的教学实践和创新方案。

使之明白即使我们走了一条我们不喜欢的道路，但是在找到适合的、自己喜欢的道路之前，还得脚踏实地地走好现在的路。只有做好现在，才有可能有未来。

2.明晰教学目标。由于该课程针对的是化工设备维修技术专业的学生，所需的主要是化工设备的维修角度所需的知识。因此，我们把教学重点放在了培养学生运用这些理论知识解决实际问题的能力，弱化了公式的推导过程，强化如何通过公式解决实际问题。例如，把工程力学中杆件受力分析部分与杆件变形融合在一起，只讲需要的，而杆件的几种变形，简化了各公式的推导，重点讲解公式的应用及如何提高杆件强度的措施等；机械传动等教学内容，只做简要的、概述性的介绍，具体内容由学生阅读学习，并提出一些问题供学生分析思考。这样可以将教师的重点讲授与学生的阅读学习相配合，实现教师的“教”与学生的“学”相辅相成，有助于提高学生的学习兴趣[2]。

3.多种教学方式同时采用。在教学方式上，一是为了提高授课的效果，另外也是为了提高学生的学习兴趣。我们采用了多种的教学方式：多媒体教学，这是目前广为使用的一种教学手段。它能以很少的学时尽可能多地给学生展示各种图片、立体模型，增加直观性，弥补黑板教学的不足。我们在网上下载一些运动机构，如带传动、齿轮传动等播放给学生观看，加深学生对机械传动运动特点的理解；下载化工设备内部工作情况，使学生能更好地理解其工作原理，弥补实训车间无法直视设备内部操作情况。其次，实训车间教学，也是我们教学改革的一种方式。例如，在讲解化工设备结构及零部件时，在实训车间学生可以零距离接触这些设备，并且就书本上的标准零部件与实际安装在设备上的零部件进行比对，还可以动手拆装设备，加深设备结构认识。期间，对学生分组，先让学生自己拆装，记下拆卸和装配过程，然后组与组之间进行讨论、评分，最后教师总结归纳。只要动手拆装一遍之后，学生都能很流利地说出该设备的结构及工作原理。我们的学生不太喜欢课堂教学，动手操作却兴趣盎然，这样课堂气氛被调动起来，学生的学习积极性也增加了不少，教学效果也大大提高了。

4.改革考核方式。在考核的方法上，采用过程性考核和期末考核，理论考核和实践考核相结合。每完成一个训练就进行一次考核，考核内容和方式视具体章节内容而定。比如压力容器部分，会有理论考核、也有现场考核，现场考核主要考察学生对压力容器零部件的名称、结构、用途的掌握程度。

四、结语

化工行业是一个国家综合国力和国际竞争力的重要体现。虽然我国近年来化工行业取得了较大发展，但高级操作维修人员始终都有一定缺口。如何培养具有高素质高技能的专业技术人员，是职业技术教育的长期目标。《过程设备机械基础》是一门专业基础课，涵盖诸多行业的基本知识，是进一步培养具有高级技术人才的必备基础。所以，加强《过程设备机械基础》课程的改革探索，对提升教学质量和水平非常重要。我们近几年对“过程设备机械基础”课程教学的一些改革和体会，取得了一些成绩，但还需要不断地探讨和改进，才能与时俱进，才能培养紧跟时代发展的高素质人才。

参考文献：

[1]潘红良.过程设备机械基础[M].上海：华东理工大学出版社，2011.
[2]刘理华，刘书群.化工设备机械基础课程教学改革研究[J].广州化工，2012，(19).

?1994-2015 China Academic Journal Electronic Publishing House. All rights reserved.　http://www.cnki.net

一、丰富教学内容

目前，我们主要使用两本植物学教材，分别作为生命科学学院以及其它学院的专业基础课教材。除此之外，我们几乎没有引入其它教学资源。在国外，许多高校的专业课并非只有一本指定的教材，而是向学生提供一系列参考书籍或文献，从而扩充了教学资源，也在很大程度上培养了学生的自学能力。对比我们的教学内容，仅以课本为基础，使授课内容显得平凡而枯燥，难以调动学生的学习积极性。因此，科学精选教学内容，引入丰富教学资源，对于在有限的学时内提高学生的学习兴趣、拓展学生的知识面显得十分重要。我们通过以下手段来丰富教学内容。

1.引入教学资源。加强教材建设，以本校植物学教材为基础，引入国内外高校优秀的植物学教材，如《Principle of Botany》、《Botany，An Introduction to Plant Biology》、《Plant Systematics》等。此外，提供学生课外阅读资源，包括网络资源、参考图书、植物图片以及生动有趣的教学电影、动画等，实现资源优化配置。其中，网络学习资源如普兰塔网站(www.planta.cn)，教学电影如BBC的《the Private Life of Plant》等。

2.理论结合实际。在植物形态解剖的教学内容上，避免空洞的、照本宣科式的讲解植物根茎叶的形态特征，突出植物形态与功能的适应，如水生植物茎的解剖特征、旱生植物叶的形态特征等，尽可能结合自然现象进行介绍，如"藕断丝连"、"秋风扫落叶"等。在植物分类的教学内容上，减少对植物形态列举式的描述，仅简要介绍代表植物的识别要点，增加植物类群的介绍，包括代表类群、生物学特性、地理分布、利用价值、应用潜力等。将植物学知识与实际生活、自然常识相联系，深入浅出、由近及远的讲解植物学知识，提高学生对植物类群的感性认识、培养学生的实际应用能力。

3.注重科学研究。逐步摆脱传统的知识灌输和应试教育模式，引导学生自主、创新的进行学习，活跃学术思维。针对目前植物学各研究方向的发展，将植物学科与交叉学科近几年来的新进展、新成果充实到教材和课堂，介绍学科发展方向、研究热点，激发学生从事科学研究的兴趣、培养科学研究能力和科学素养。例如，涉及被子植物繁殖器官部分，可向同学们介绍异型花柱、功能性雌雄异株的研究进展，提及被子植物传粉机制和模式的研究案例，如发表于《Nature》杂志的《黄花大苞姜自花传粉机制》一文。讲解裸子植物部分，可具体介绍一些我国特有的第三纪孑遗植物，如银杉、水杉等，对"活化石"植物银杏自末次盛冰期以来的进化历史及其在中国避难所群体等研究结果等，可做简要阐释。基于此，使同学们能够了解学科研究进展，从而丰富教学内容。

二、优化教学方式

植物学教学主要以老师课堂讲解为主，由于植物学知识点多、内容繁杂，学生在课堂上很难长时间保持新鲜感，集中注意力，使得课堂教学质量降低。加上课时数少，学习时间紧，学生们课后复习以死记硬背为主，没有达到理解记忆的目的，不能真正掌握植物学知识。植物学也是一门理论结合实践的学科，除了在课堂上学习理论知识，更需要回到大自然中进行观察和实践。虽然有相应的植物学实验课及野外实习的安排，但是，由于课时数少、经费有限、指导教师不足等问题，学生并没有充足的时间进行野外观察和实验室学习，不能真正的提高实践动手能力[3]。

在植物学理论课程方面，除了传统的课堂讲授方式，我们将采取灵活多变的教学方式，包括学生自学与课堂教学相结合，个别章节以专题讨论形式开展，走出课堂进行野外观察等，增加野外实习及实践，充分发挥学生的自主性和科研性，开阔学生眼界，增加学生对植物学的学习热情和兴趣。我们将采取以下教学方式：①鼓励学生进行专题讨论、制作PPT、轮流进行课程内容讲解和比赛、撰写简单的科研论文；②放映植物学教学图片、电影或动画等。在植物学实践课程方面，增加实验课的学时数，提供学生进行创新性实验以及进入研究室、实验室参观学习的机会，以学生动手实验为主，结合老师一对一辅导，以期达到良好的实验课教学效果，培养学生的动手能力和实践能力。定期进行植物学实习，开展校园、植物以及野外植物学实习，从身边的植物开始，由浅入深、由易入难的讲授植物分类学知识，逐步带领学生进行植物分类学领域，开拓学生视野。

三、改革考核形式

一直以来，植物学以卷面作答的形式进行考核。考核形式单一，且势必导致学生以应试为目的进行学习，限制学生自主性和科研能力的发展。改革传统的考核方式，逐步改变学生以应试为目的复习方式。在掌握基础知识的前提下，另需考核学生对知识的理解程度及实践能力。将卷面考试与实验考试、题目作答与课堂论文以及自学成绩相结合，以提高综合能力为目的进行考核，从而避免传统的、单一的、机械式的考核方式。我们采取多元化、灵活的考核形式，遵循素质教育和创新型人才培养的要求[2]。

植物学成绩评定除了期末考试以外，平时成绩以专题讨论、PPT讲解、论文撰写、随堂测验以及课题考勤等形式进行平时学习的考核。其中，期末成绩占总成绩的50%；课程论文两次，内容分别对应植物形态解剖和植物分类，课程论文占总成绩的15%；课堂演讲则要求学生3~4人为一组，每组依据所写的课程论文制作PPT课件，并选派1名代表进行课堂演讲，其成绩占总成绩的15%；同时，我们在课堂教学中安排4次简单的随堂小测验，检查学生对理论知识的掌握和理解，占总成绩的15%；另外，每个学期将有两次课题考勤，以强化教学管理，其成绩占总成绩的5%。通过上述考评措施，目的在于调动了学生的学习积极性，发挥主观能动性，提高学生的学习兴趣，同时，培养学生在文献资料查阅、论文撰写、语言表达等方面的能力，为将来学生继续深造或就业奠定基础。

综上所述，我们在对植物学教学现状调查的基础上，揭示现存的教学问题和弊端，以学生兴趣培养为核心，以发挥学生主观能动性为目的，针对植物学教学内容、教学形式和考核方式等，提出相应的教学实践和创新方案，最终获得良好的教学效果。

参考文献：

[1]王飞娟，朱诚，蔡冲，孙骏威，郝培应.加强植物学教学改革的基础建设研究[J].出国与就业(就业版)，2011，17(93).

[2]耿世磊.以应用能力培养为目的的植物资源学教学改革[J].教育教学论坛，2012，23(174-175).

[3]胡青，高述民，刘頔，刘忠华，郭惠红，陈瑾，高宏波.植物学实验课程改革与探索[J].生物学通报，2012，47(3)：46-49.

作者简介：龚维，华南农业大学生命科学学院，副研究员，主要从事植物学教学和科研工作。

?1994-2015 China Academic Journal Electronic Publishing House. All rights reserved. http://www.cnki.net

ISSN 1674—9324
CN 13-1399/G4

教育教学论坛

EDUCATION TEACHING FORUM

2014 年 10 月　第 42 期

中国知网
万方数据
维普网 收录本刊全文
龙源期刊网
博看网

ISSN 1674-9324
42>
9 771674 932102

目录 contents

特别关注

1 大学精神与校园文化建设的思考 …… 孙 巍
3 高校自主招生与学生家庭资本:一个社会学视角 …… 王 红
6 文化快餐心理冲击下学生创造力的消解与恢复 …… 林 青

院校发展

9 地方高校特色办学战略思想的探讨与认识 …… 王 璐,田水承,孟凡静
11 构建二级学院教学质量保障体系的实践研究
…… 李 蔚,罗胜利,屠 远
13 加强重点特色专业建设是新升本院校转型发展的当务之急 …… 闫新生
16 高职教育与远程开放教育一体高校发展非学历继续教育的思路探析
——以武汉软件工程职业学院为例 …… 杨 玲

科学管理

18 浅谈大学生班主任如何协助学生自主管理班级 …… 殷金玲,温 青
20 项目管理在实验实训教学管理中的应用 …… 项保连
23 对高职院校学生心理档案建设的思考 …… 姚 萍
25 学校人文管理初探 …… 陶文辉,陈 峥
27 中职学生在校时间管理中存在的问题及对策 …… 王 雯
30 新建本科院校“双师型”教师队伍建设探析 …… 周景伟
32 浅谈如何提高教学秘书工作质量 …… 徐新丽
34 基于因子分析的教学质量评价体系研究 …… 苏 娜
36 中外合作办学外方教师聘任与效益化管理 …… 汤美玲

学校与社会

40 电信诈骗犯罪的法律惩治 …… 杨 鸿,苏剑邦
44 校企合作提高本科教育质量的探索
——以微电子学科为例 …… 王福学
46 如何用社会主义核心价值观构建高职院校生的主体精神
——创新高职院校思想政治工作 …… 刘 瑛
48 毕节试验区职业教育校企合作、产教结合工作思考 …… 彭永贤,熊荣谦

思想政治

51 传统文化视野下的大学生德育教育路径 …… 徐维悦,张 岚
53 巧借数学语言辅助高校思想政治理论课教学 …… 蒋国琴
56 内蒙古化工职业学院思想政治理论课实践教学模式探索项目的
问卷调查报告 …… 杜海燕
58 大学生就业指导中思想政治教育探讨 …… 陈彦合
60 公共课程学习与教学方案的实践和思考
——以《邓小平理论和“三个代表重要思想概论”》课程为例 …… 吴晓辉

教育教学论坛

JIAOYU JIAOXUE LUNTAN

2014年10月 第42期 总第175期

期刊名称 教育教学论坛
主 管 河北出版传媒集团有限责任公司
主 办 河北教育出版社有限责任公司
花山文艺出版社有限责任公司
出 版 教育教学论坛杂志社
印 刷 石家庄市飞达印刷有限公司
发 行 河北省报刊发行局
出版日期 2014年10月15日
主 编 韩新保
发行范围 国内外公开
定 价 40.00元
国内统一连续出版物号 CN 13-1399/G4
国际标准连续出版物号 ISSN 1674-9324
广告许可证号 1301024D00093
广告代理 河北腾博广告有限公司
地 址 石家庄市联盟路705号
邮 编 050061
订 购 处 全国各地邮局
邮发代号 18-219
网 址 http://www.jyjxltzzs.com/
电子信箱 jyjxlt@jyjxltzzs.com
联系电话 0311-87760976

副主编 王瑞婵
编委会 韩新保 王瑞婵 秘云霞 刘春玮 王雪平 郭桂香 张保玉 韩向军 康 薇 张玉玲
社长助理 王越西
市场总监 展建军
责任编辑 汪 瑞 韩向军 张保玉 王 京 陈鑫玉 段月影
美术编辑 张贵新

63　人本主义理论在大学生就业焦虑心理辅导中的运用 …… 曹绍平

学生教育

65　关于提高少数民族大学生人际交往能力的探析与研究
——以大连民族学院为例 …… 王　言,马国艳,朴　晶,杨　琨
67　大学生职业价值观探析 …… 彭仲生
70　大学生网络迷恋引导策略探究 …… 黄先梅

专题研讨

72　民族传统体育专业《体能练习》课程考核内容与评分标准研究
…… 叶　伟,汤铁军
75　理工科女大学生就业价值取向分析与提升就业质量研究
…… 张林立,刘景军,徐建华
78　依法治国与治吏 …… 周志明
80　浅谈高校 CIO 的几大误区
——基于《2013 年高等教育 CIO 角色与效力研究报告》…… 吴延慧,吴寒飞
82　生物医学工程专业中《人体解剖生理学》课程教学模式改革与思考
…… 杨文伟,薛凌云,杨　勇
84　社会转型时期高职女大学生实训课程满意度研究 …… 谭　星
87　民办大学大学生英语学习动机与策略的调查研究 …… 马金贵
89　高等教育国际化维度下的大学全英语教学机制研究 …… 顾志勇
92　破解金字塔建造之谜而创立的“蓄能起重法” …… 侯曾炎
94　基于因子分析法的人机课程实践教学应用研究 …… 陈文颖
96　高校本科复合型人才培养模式现状研究 …… 靖杨萍,亓文涛
98　从认知语用角度解读课堂教学中的非言语行为 …… 崔英杰,王俊红
100　高校临床专业《医学细胞生物学》的教学初探
…… 牛　蓓,辜丽沙,何海蓉,符　佳,伍小飞
102　我国基础教育资源配置优质均衡的设想 …… 范雪梅
104　生物科学双语教学模式与发展 …… 龚　维,郝　刚
106　初探药学有机化合物波谱解析的教学方式
…… 朱玲娟,张　雪,孙博航,陈丽霞,高慧媛,邱　峰

教改创新

109　高校生物统计学课程教学改革与探索 …… 戚文华,蒋雪梅
111　基于 COOP 项目的旅游管理专业本科实践教学的改革与创新
…… 徐文燕,罗　微
113　实现高校金融类课程教学创新改革的途径分析 …… 吴玉菡
115　空中交通管制专业的教学质量调查及改革建议研究 …… 王　超,闫少华
118　基于卓越医师计划的医学免疫学实验教学改革
…… 张忆雄,徐　林,罗军敏,秦娜琳,马　龙
119　基于项目化教学的《化工设备基础》教学改革与实践 …… 闫国伦
122　论应用型人才培养目标下高校《资本论》课程的教学内容改革 …… 王冬梅
124　基于任务与项目混合驱动的 Java 平台课程改革探索 …… 解绍词,代　劲
126　浅议基于知识链的高校教学模式创新 …… 刘小锦,姚　煜
128　广西普通高中新课改实施过程中存在的若干问题与改进途径
…… 陈施然,李　艺,陈超梅

课题项目

131　高职高专机电一体化应用型专门人才培养探究 …… 张义俊,吴慧敏,高　展
133　采矿专业教学活动与班主任管理工作的结合分析 …… 彭洪阁

135　新形势下边疆民族地区的群众工作现状分析
……杨国华,邵维庆,俞群俊,陈　龙,王云洁,杨　睿
137　论地方高等农业院校交通工程专业本科毕业论文质量提高措施
……朱兴琳,李雪莲,唐　茜
140　旅游美学教学相关问题及对策 ……苏　飞
142　基于 WITNESS 仿真软件的《生产运作管理》课程实验教学 ……蒋洪伟
144　“985”高校影响教授为本科生授课的制度思考
——基于“985”高校 2011 年本科教学质量报告的分析
……闫祖书,郭　超,姚军虎,袁伟斌,袁　明
146　地方高校人才创新、创业教育体系研究 ……温长吉,贺珊珊,李　健,王增辉
148　针对地方医学院校留学生教学的思考
……游　咏,李　熠,尹　凯,沈元琼,桂庆军
151　地方高校自动化特色专业建设模式的构建与实践
……胡向东,唐贤伦,向　敏,蔡林沁

探索与实践

154　给水排水工程专业实践教学模式及考核方法探究
……马伟芳,孙德智,伦晓秀,程　翔
157　多元化实践教学对提升特殊教育专业人才培养质量的探索
……侯晓晖,慕雯雯,王　鹏,王　涛
160　素质教育在高职英语课堂中的实施探索 ……贾冬玲
162　五年制临床药学专业课程设置的探索与实践
……赵明沂,惠福海,杨静玉,夏焕章,宫　建,刘袁媛
165　高校计算机硬件基础课程教学探索 ……宋大虎,王　忠,黄百钢
167　教学科研一体化在面向本科素质教育实验教学改革中的探索与思考
……刘　洋,倪　芳,姚　忠,胡永红,张　霞
169　模块化教学在环境艺术设计专业技能课程中的探索与实践
——以《软件应用 AutoCAD》课程设计为例 ……吴　迅
171　“自动控制系统”课程的教学研究与探索
……闻　凯,王　恒,朱海霞,王志凌
173　基于产学研合作的光源与照明专业人才培养的探索与实践
……曹冠英,李　萍,张云翠,房　媛,曹　帆,邹念育
175　控制工程全日制专业学位型硕士研究生培养模式的构建与实践
……张瑞成,陈　波,陈至坤
178　《家禽生产》情境化教学平台运行机制的实践与探索
……张　玲,段修军,袁旭红,顾文婕,李小芬
180　浅谈研究生学籍管理现状、问题及对策 ……熊金革,程捍卫,陶　波
182　新课标下英语试卷讲评课的模式探究 ……张丽芝
184　研究生探究型研讨课教学探析 ……胡奕明,代传金

教法研究

187　探究式教学法在会计课程教学中的应用研究 ……赵茂林,谢　晖
189　“得失观”在模拟电子技术知识点教学中的启迪 ……王文虎,杨　峰,李建奇
191　成人高校会计专科职业教学模式的研究
——以北京市石景山区业余大学会计专业为例
……朱学军,王群建,海占芳,赵秀艳
194　现代化教学手段在高职高专文科高等数学教学中的应用 ……王　平
196　案例式教学在理论力学中的应用 ……高富强,黄　强
198　道路交通安全工程课程教学创新研究 ……肖敏敏,艾辉林
201　高职院校计算机应用基础课教学问题及解决策略 ……沈蓓颖

203　食品包装专业《平面装潢设计》课程教学模式探讨
……智秀娟,杜　斌,伍　军,徐广谦
205　双语小学数学多媒体教学中存在问题的调查研究 …… 阿衣提拉·买买提
208　工科专业应用型课程的课堂教学研究
……曾广根,武莉莉,黎　兵,李　卫,张静全,冯良桓
210　培养师范生使用并制作小学数学教具和学具的能力 …… 童　琳
213　基于编程语言类课程教学方法的探讨 …… 张秀国
215　体育教学游戏化研究 …… 柳　磊,王林钧
217　浅析少儿声乐的多样化教学模式 …… 郑　媛
219　小组合作六步达标教学模式探究 …… 南　华,刘会玲
222　探究兴趣教学路径　构建语文生命课堂 …… 曹宪春

学法指导

224　利用几何、算术均值不等式证明有关数学问题的技巧 …… 王洁琼
225　斐波那契数的标准分解式中因子 19 的指数 …… 严婉琳
228　汉语和日语惯用句之比较
——以与动物有关的成语为例 …… 张　敏,方峥炜

教师观点

230　高职院校高等数学有效课堂构建的研究与探讨 …… 赵　丹
233　浅谈跨文化交际能力的培养 …… 陈媛媛
235　雷夫·艾斯奎斯教育理念在高校英语教学中的可行性 …… 陈清菊
237　提高大气科学专业本科毕业论文质量的思考 …… 曾　刚,李碧兰
240　浅析图论教学中多媒体和板书的结合 …… 杨　帆
242　试析对外汉语教学中的文化教学 …… 刘汉银
244　孔子“德”思想及其现实意义 …… 张　娟

职业教育

246　构建高职院校全过程教学质量监控体系的探索
……邓　敏,沈红梅,王莉平,罗春连,杨林宏
248　高职学生生态意识培育机制的研究与探索 …… 苏锦霞
250　高职院校沟通课程能力训练教学模式初探 …… 邓先丽
253　如何上好仿真实训课 …… 巨红梅,王曼青
255　现代林业技术专业学生生产性(综合)实训效果分析
——以新疆林业学校为例 …… 韩燕燕,任　伟
257　拓展职业教育职能　助力区域经济发展
——数控加工专业为社会培养人才实践研究 …… 王卉娟,赵　璟
260　高职学前教育的钢琴即兴伴奏解析探索 …… 李斌杰,李　婷
263　计算机模拟走入光学理论课堂 …… 吴　艳,张晓波,董文钧,李超荣
265　澳大利亚悉尼大学网络学习特点及其启示 …… 朱乐平
267　基于 matlab 的数字信号处理软件平台在地球物理学科教学中的尝试与探索
……郑　晶,姜天琪,姜　喆
269　QQ 群在诊断学教学互动中的应用 …… 刘惠娜,韦昌法
271　C 语言程序设计教学模式探讨 …… 吴　秦
273　基于 GNS3 与 SecureCRT 的 OSPF 虚拟网络实验平台的设计与实现
……姜　磊
275　管理信息系统案例教学方法探讨 …… 李桃迎,陈　燕
277　面向职业认证的网络工程实验教学改革 …… 费雄伟,欧阳艾嘉,陈伟宏
279　药剂学专业本科生药物动力学实验方法的改进 …… 陈　钧,王建新
281　做好院级教学管理工作的几个抓手 …… 赵志根,吴　军,张　坤
283　新课标下高年级小学习作教学的问题与对策 …… 陈俊竹

生物科学双语教学模式与发展

龚 维,郝 刚
(华南农业大学 生命科学学院,广东 广州 510642)

摘要:生物科学是21世纪蓬勃发展且最受关注的学科之一,在现代科学技术以及高等教育中占有重要地位。国际化建设在全国高校大力推进,生物科学双语教学是高校国际化建设的重要环节。本文阐述了生物科学双语教学的必要性,探讨了生物科学双语教学的模式,提出将中英文授课、英文教学资源、多媒体资源、学生参与以及多样化考核方式等融入生物科学双语教学中,并对生物科学双语教学的发展方向提出了建议。

关键词:生物科学;双语教学;国际化建设
中图分类号:G642.4 **文献标志码:**A **文章编号:**1674-9324(2014)42-0104-03

生物科学是全球范围内最受关注的学科之一,在现代科学技术中占有重要地位,也是21世纪自然科学领域的带头学科。在高校,生命科学的教学与研究迫切需要与国际接轨,顺应国际化发展。生命科学领域的教师及科研人员,均需要具备国际化的视野和教学研究水平。所谓双语教学,即是通过两种语言的结合,通常是将英语与汉语相结合,在课堂上对专业知识就是讲解。加强和推广双语教学是高校国际化建设的重要环节,也是我国教学改革的主流方向。培养具有高水平、国际化复合型人才,与世界一流大学教育接轨,迫切需要进行双语教学。双语教学现已渗透到生物科学各个学科,包括植物生理学、生物化学、植物生态学、保护生物学、动物生物化学、生物化学、分子生物学等。本文将阐述双语教学在生物科学中的重要性,并探讨生物科学双语教学的模式,最后,对生物科学双语教学的发展提出建议,以期通过不断的摸索和实践,对生物科学双语教学理念、教学方案和教学形式进行了完善和创新。

一、生物科学双语教学的必要性

1.双语教学是国际化建设的重要环节。国际化是时代赋予大学的历史使命。在经济全球化的今天,知识和信息对经济增长的贡献举足轻重,只有具备国际竞争力的人才能够推动世界科学、技术和经济的持续发展。目前,国内各大高校都在大力推进国际化进程。大学国际化是将国际的、多元的文化融入到中国大学现有的教学、科研、管理和服务中去,与国际一流大学的教学科研水平接轨。在高校国际化发展进程大力推动的背景下,国际化渗透到高校工作的方方面面。各大高校力图借鉴世界一流大学的教学理念、管理模式和运行机制,通过积极引进高层次人才、加强国际学术交流、培养具有国际视野和经验的学生等方式,来提高自身国际化的效率、水平和层次。由此可见,加强和推广双语教学是高校国际化建设的重要环节,也是我国教学改革的主流方向。

2.生物科学教学和科研迫切需要双语教学。随着生物科学不断给人类生活带来巨大变化,该学科已进

现出该校独有的特色。③目前,我国各地区基础教育呈现出极大的不均衡,优质学校与薄弱学校的差距极度明显。$S_{\triangle MON}-S_{\triangle AOB}$=极差;越是发达的国家,其基础教育综合实力极差对比则越小。④模型左边,各个梯形面积的大小代表基础教育各等级学校的数量情况以及比例,此时,薄弱学校占有相当大的比例,优质学校比例非常小;而当达到最佳优质均衡时(圆弧处),各等级学校的数量中,虽然薄弱学校的数量也在增加,但其比例却大大的减少,中等和良好的学校总和增加迅猛,占整体的比例非常高(由面积计算得知:占70%左右),优质学校的数量也相应的有所增加,和相对薄弱的学校所占整体的比例相当。像这样,在全国所有基础教育学校中,等级优秀与较差学校占总数比例为30%,等级中等与良好学校占总数比例为70%,并且其数量关系满足:优秀≥较差,良好≥中等,我认为这将是最佳的基础教育结构模式,简称三七模式。

根据三七模式分析可知:资源的最佳优质均衡最关键的一步是:找出基础教育中较薄弱的学校具体薄弱的方面(共5个方面),国家、政府再相应地进行大力扶持,使其不断提升,最终进军到中等和良好的学校队伍中,实现70%的目标;其次,原本优秀的学校,则投入一定比例的资金进行协作创新、互利共赢的新型教学模式研发;最后。中等、良好的学校则采用高额奖励制度与一定扶持力度相结合的方式调动学校发展的积极性。

参考文献:

[1]姜丽琼.我国教育不公平的现状分析[J].教育与职业,2007,(33).
[2]李明阳.论教育公平[J].安徽大学学报(哲学社会科学版),2009,(1).

作者简介:范雪梅(1989-),女,四川广安人,南京师范大学教育科学学院硕士,研究方向:教育经济学。

?1994-2014 China Academic Journal Electronic Publishing House. All rights reserved. http://www.cnki.net

入到不断完善的新阶段。现代生物科学在农业科学、医药卫生、粮食与食品安全、生态安全、新能源、资源与环境保护等各领域都发挥着越来越重要的作用,与人类生存、人类健康、经济建设和社会发展等息息相关[5-7]。培养生物科学领域具备国际竞争力的人才,与现代科技、人类生活密切相关。然而,与欧美等发达国家相比,我国的生物科学专业在教学和科研上仍然存在着一定的差距和不足。其中,英语水平成为了限制该专业领域教学和科研的重要因素之一。双语教学促使教师和学生将中英文相结合,在教学和科研的过程中,更高效的使用英语,提高英语听说读写等各方面的能力。通过双语教学,生物科学教师和学生可以更加直接和迅速地了解国际教学和研究动态,时刻保持研究领域的国际化嗅觉,紧跟国际化发展步伐,从而提高该专业的教学和科研水平。

3.双语教学是培养国际化人才和高素质教师的有效手段。通过双语教学,不仅有利于学生快速掌握科研发展趋势和研究前沿,培养具备国际视野和竞争力的人才,也有利于开拓生命科学领域的教师及科研人员的国际化视野,提高教学和科研水平。因此,培养国际化复合型人才,提高师资力量,与世界一流大学教育接轨,均需要进行双语教学。从各大高校的实际情况来看,部分高校已设立国家级生物学理科基地班以及中外合作办学的国际班。基地班和国际班的设立,为生物学研究创新型人才培养提供了一个完善的支撑体系。同时,联合国际班中外双方的教学力量,为培养具有高水平、国际化视野的生命科学领域的专业人才提供了优势。在此情形下,部分专业课程实施双语教学成为了提高教育改革、应对国际竞争、培养扎实专业知识的高层次复合人才的重要措施之一。

二、生物科学双语教学模式

1.中英文授课相结合。与普通的中文授课和全英文式授课不同,双语教学以中英文相结合的方式进行授课。同普通课程类似,双语课教学主要以教师讲台授课为主,但授课的多媒体课件均为英文,上课内容以全英文展示。为避免学生不能及时跟进英文课件的内容,老师将个别生疏的或者专业的词汇或关键概念列出,并附上中文注解,从而帮助同学们理解和记忆。双语教学教师主要通过英文对教学内容进行讲授,同时辅以中文解说,帮助同学们掌握课堂知识。最终,教师通过亦中亦英的教学方式来创造一种双语的教学环境,既能保证学生们理解和掌握知识内容,又能提高学生们的英语理解和应用能力。

2.引用英文教材和教学资源。学生的学习无法离开教材,双语教学既需要优秀的中文教材也需要引进优秀的英文教材。仅靠教师课堂上的英文课件或者英文阐释,尚不足以使学生充分理解和掌握教学内容。要真正体现并实现双语教学,需要充分利用现有的国外教学资源,积极引进国外优质教育资源,让生物科学专业的学生能够较好地掌握本领域专业知识。引进并介绍给学生一本优秀的原版英文教材便是前提之一。此外,双语教学不仅需要将教学信息以英文形式进行传授,为了帮助同学们理解并掌握知识内容,需要将中英文教材相结合。通过中英文教材作为参考,可以使班级内各个层次水平的学生学习并掌握知识,从而达到较好的双语教学效果。同时,双语教学给学生提供课外阅读资源,包括网络资源、参考图书以及生动有趣的教学电影、动画等,实现资源优化配置,完善和加强双语课程的教学,实现教学目标。

3.重视多媒体资源。双语教学注重利用多媒体资源,放映教学图片、电影或动画等。我们从国外有关学校引进了生物科学专业的教学图片、教学电影,这些图片均是彩色的英文图片,制作精美、色彩鲜艳,教学电影形象生动,栩栩如生的将一些抽象的知识点或者复杂的生物动态变化过程呈现出来,化抽象为具体,高度集中学生们的注意力,大大加深了学生对相应知识的了解和记忆,使得原本枯燥乏味的生物学课堂变得生动活泼,不仅增强了学生学习生物科学知识的兴趣,调动了他们的积极性,同时也使得学生在生物科学专业英语的听力、阅读等方面得到培养[9]。

4.鼓励学生参与教学活动。双语教学主要以老师课堂讲解为主,由于教学内容繁杂,学生在课堂上常常很难长时间保持新鲜感,集中注意力,使得课堂教学质量降低。加上课时数少,学习时间紧,学生们课后复习以死记硬背为主,没有达到理解记忆的目的,不能真正掌握生物学知识。同时,生物科学专业注重理论结合实践,除了在课堂上学习理论知识,更需要培养学生的观察能力、动手能力。因此,在双语教学过程中,需采取灵活多变的教学方式,包括学生自学与课堂教学相结合,个别章节以专题讨论形式开展,增加实验课程、野外实习等,充分发挥学生的自主性和创造性,开阔学生眼界,增加学生对生物科学的学习热情和兴趣。双语教学的老师鼓励学生进行专题讨论、制作展示课件、轮流进行课程内容讲解和比赛、撰写简单的科研论文。课程中途安排学生走上讲台,用英文呈现自己的PPT,并用英文对所学知识进行交流和讨论,锻炼学生自主学习的能力以及英文表达能力。在此过程中,使学生能够了解学科发展方向、研究热点,拓展学生国际化研究视野,激发学生科学研究的兴趣、培养科学研究能力和科学素养。

5.课程考核方式多样化。传统的考核方式为卷面作答的形式。考核形式单一,且易导致学生以应试为目的进行学习,限制学生自主性和科研能力的发展。改革传统的考核方式,逐步改变学生以应试为目的的复习方式,也是双语教学的目标之一。多元化、灵活的考核形式才能遵循素质教育和创新型人才培养的要求。在掌握基础知识的前提下,另需考核学生对知识的理解程度及实践能力。将卷面考试与实验考试、题目作答与课堂论文以及自学成绩相结合,以提高综合能力为目的进行考核,从而避免传统的、单一的、机械式的考核方式。双语教学课程的成绩评定除了期末考试以外,平时成绩以专题讨论、PPT讲解、论文撰写、随

?1994-2014 China Academic Journal Electronic Publishing House. All rights reserved. http://www.cnki.net

初探药学有机化合物波谱解析的教学方式

朱玲娟,张　雪,孙博航,陈丽霞,高慧媛,邱　峰
(沈阳药科大学　中药学院,辽宁　沈阳　110016)

摘要:针对目前药学有机化合物波谱解析存在的问题,本文初步探讨了解决问题的教学改革方法,旨在提高学生学习兴趣,培养学生分析问题、解决问题的能力,提高教学质量,取得良好的教学效果。

关键词:药学有机化合物波谱解析;教学改革;药学
中图分类号:G642.4　　**文献标志码:**A　　**文章编号:**1674-9324(2014)42-0106-03

人类社会的发展过程是一个人类征服世界和改造世界的过程,而要达到这个目的,人类必须客观的认识世界。有机化合物波谱解析则是人类认识有机物质世界的重要手段。它在药学、石油化工、环境科学、材料科学、食品科学等科学领域中发挥着毋庸置疑的作用,故成为药学类、中药学类、制药类、化学类、化工类等专业及相关专业本科生及研究生的专业基础课[1]。

药学有机化合物波谱解析主要讲述紫外光谱(UV)、红外光谱(IR)、核磁共振光谱(NMR)和质谱(MS)的基本原理、特征、规律以及图谱解析技术,以及这四大光谱技术的综合应用[2-3]。通过本课程的学习,培养学生掌握解析简单有机化合物的能力,为药学各专业课程,特别是对天然药物化学、中药化学的学习打下良好的基础。我校有机化合物波谱解析课程起步较早,是国内药学类院校开设最早的院校之一,2008年该课程被评为省级精品课程。而且,我校一直是卫生部规划教材、全国高等医药院校教材《有机化合物

堂测验以及课题考勤等形式进行平时学习的考核,目的在于调动了学生的学习积极性,发挥主观能动性,提高学生的学习兴趣,同时,培养学生在文献资料查阅、论文撰写、语言表达等方面的能力,为将来学生继续深造或就业奠定基础。另外,期末考试使用双语试卷对学生进行考核。即部分试题为中文,部分试题为英文。鼓励学生用英文答题,进行英文答题的学生可给予适当的加分鼓励。

三、生物科学双语教学发展方向

双语教学顺应高校国际化建设发展趋势,只有经过不懈努力的探索和创新,总结经验、勇于实践,才能不断完善教学理念、改革教学方式,最终取得良好的教学效果。对此,我们对生物科学双语教学的发展提出了一些建议。

1.培养具有较高学科专业英语水平的学生。通过双语教学,与国际上生物科学专业的人才培养模式接轨,对现有课程进行改革创新,促使人才培养国际化,全面提高生物科学专业的教学质量,从而培养具备国际竞争力的生物科学专业人才,提高学生专业水平、科学素养,开拓学生国际化的视野,为学生将来进一步出国深造或者进行科学研究做好准备。

2.实现部分课程的全英文授课。生物科学专业部分高年级的学生将选择继续从事科研事业,部分学生将出国深造,成为国际化人才。随着生物科学双语教学逐步开展并完善,培养具备生物科学领域竞争力和国际化素质的学生将成为其主要目标。针对双语教学的课程,建议对其进行课程体系的改善以及教学质量的测评,在已有双语课程的基础上,进一步完善和加强双语课程的教学,并逐步实现高年级、部分具备条件的双语课程的全英文授课,尤其是一些国际合作课程、国家重点课程以及具备较好前期基础的双语课程,从而满足生物科学教学的国际化需求,与国际教学理念和教学形式接轨。

参考文献:

[1]李春茂,巫跃凤,刘玉.中国高校双语教学的进展研究[D].高校教育管理,2007,1(5):70-76.
[2]周密,丁仕潮.高校国际化战略:框架和路径研究[D].中国高教研究,2011,(9):16-19.
[3]蒋玉婷.全球经济危机给中国高校国际化带来的新挑战及其思考[D].教育论丛,2010,(2):163-164.
[4]韩立新,于诗卉.高校双语教学改革的若干问题思考[D].教育科学,2013,6(29):35-41.
[5]黄国琼.生命科学发展前沿对高等医学教育的影响与对策研究[D].第三军医大学博士学位论文,2006.
[6]何白玉.生命科学教育的哲学探索[D].东北师范大学硕士学位论文,2011.
[7]邓立红.中美四所研究型大学生命科学学科的发展策略研究[D].上海交通大学硕士学位论文,2009.
[8]赵昶灵,萧凤回.农业院校研究所分子生物学双语教学模式与方法探索[J].云南农业大学学报,2008,2(2):82-87.

作者简介:龚维(1979-),女,汉族,重庆,博士研究生,副研究员,研究方向:植物学。

?1994-2014 China Academic Journal Electronic Publishing House. All rights reserved.　http://www.cnki.net

国家自然科学基金资助项目批准通知

（预算制项目）

龚维　先生/女士：

根据《国家自然科学基金条例》、相关项目管理办法规定和专家评审意见，国家自然科学基金委员会（以下简称自然科学基金委）决定资助您申请的项目。项目批准号：32270218，项目名称：物种多样性空间分布格局形成机制探讨：以洲际间断分布绣球花族历史生物地理学研究为例，直接费用：54.00万元，项目起止年月：2023年01月至 2026年 12月，有关项目的评审意见及修改意见附后。

请您尽快登录科学基金网络信息系统（https://isisn.nsfc.gov.cn），**认真阅读《国家自然科学基金资助项目计划书填报说明》并按要求填写《国家自然科学基金资助项目计划书》（以下简称计划书）**。对于有修改意见的项目，请您按修改意见及时调整计划书相关内容；如您对修改意见有异议，须在电子版计划书报送截止日期前向相关科学处提出。

请您将电子版计划书通过科学基金网络信息系统（https://isisn.nsfc.gov.cn）提交，由依托单位审核后提交至自然科学基金委。自然科学基金委审核未通过者，将退回的电子版计划书修改后再行提交；审核通过者，打印纸质版计划书（一式两份，双面打印）并在项目负责人承诺栏签字，由依托单位科研、财务管理等部门审核、签章并在承诺栏加盖依托单位公章，且将申请书纸质签字盖章页订在其中一份计划书之后，一并报送至自然科学基金委项目材料接收工作组。纸质版计划书应当保证与审核通过的电子版计划书内容一致。**自然科学基金委将对申请书纸质签字盖章页进行审核，对存在问题的，允许依托单位进行一次修改或补齐。**

向自然科学基金委提交电子版计划书、报送纸质版计划书并补交申请书纸质签字盖章页截止时间节点如下：

1. **2022年10月8日16点：**提交电子版计划书的截止时间；
2. **2022年10月14日16点：**提交修改后电子版计划书的截止时间；
3. **2022年10月19日：**报送纸质版计划书（一式两份，其中一份包含申请书纸质签字盖章页）的截止时间。
4. **2022年10月28日：**报送修改后的申请书纸质签字盖章页的截止时间。

请按照以上规定及时提交电子版计划书，并报送纸质版计划书和申请书纸质签字盖章页，逾期不报计划书或申请书纸质签字盖章页且未说明理由的，视为自动放弃接受资助；未按要求修改或逾期提交申请书纸质签字盖章页者，将视情况给予暂缓拨付经费等处理。

附件：项目评审意见及修改意见表

国家自然科学基金委员会

2022年9月7日

附件：项目评审意见及修改意见表

项目批准号	32270218	项目负责人	龚维	申请代码1	C0201
项目名称	物种多样性空间分布格局形成机制探讨：以洲际间断分布绣球花族历史生物地理学研究为例				
资助类别	面上项目		亚类说明		
附注说明					
依托单位	华南农业大学				
直接费用	54.00 万元		起止年月	2023年01月 至 2026年12月	

通讯评审意见:

<1>具体评价意见：

一、该申请项目的研究思想或方案是否具有新颖性和独特性？请详细阐述判断理由。

该项目以分子地理学手段研究绣球花族洲际间断分布规律，探索东亚物种多样性空间分布格局形成机制，对于物种多样性分化与地理分布多样化的基础研究增加了新的内容与资料，有较高的学术价值和一定的创新性。

二、请评述申请项目所关注问题的科学价值以及对相关前沿领域的潜在贡献。

对于物种多样性分化与地理分布多样化的基础研究增加了新的内容与资料。

三、请评述申请人的研究基础与研究方案的可行性。

可行。

四、其他建议

<2>具体评价意见：

一、该申请项目的研究思想或方案是否具有新颖性和独特性？请详细阐述判断理由。

洲际间断分布格局及物种演化历史是生物地理学的重点和热点，东亚植物区系更加令人关注。本项目以间断分布的绣球花族为对象，运用新一代测序和系统发育分析技术，重建该族系统关系和进行物种分化分析，通过阐明分布格局的演化历史，揭示其在东亚形成多样性中心的原因，探讨间断分布格局的形成机制。以绣球族为对象材料特色鲜明，结合物种分化分析综合探讨时空格局与机制，研究思路具有创新性，值得深入开展。

二、请评述申请项目所关注问题的科学价值以及对相关前沿领域的潜在贡献。

绣球花科绣球族是洲际间断分布的典型，同时东亚又是高物种多样性中心，该族起源的时间、地点及演化历史，以及为什么在东亚会形成高物种多样性中心，是实现项目目标的关键。通过该族间断分布格局即机制的探讨，可拓展绣球科植物研究的前沿，为其他分类群的研究提供有益的参考和借鉴，为大洲际间断分布生物地理的进一步深入研究积累资料。

三、请评述申请人的研究基础与研究方案的可行性。

申请人具有较好的学科背景以及良好的科研训练经历，前期准备充分尤其在材料收集整理、技术探索和国际合作方面有较好基础，同时也具有完成相关研究的经历的较好的发表记录。研究方案设计总体上合理、方法新颖，基本可行。

四、其他建议

1.鉴于实验材料是项目的基本前提，如果收集的物种数不够，就可能得出不正确的结果。因此，对于需要收集的物种要有明确目标，不仅需要覆盖全部属和代表性物种以外，物种数量也要达一定量（按常规，至少总种数的80%以上），东亚（尤其是中国的种类）尽可能齐全。2.预算还比较粗放，需要根据有关标准进一步明细化。

<3>具体评价意见：

一、该申请项目的研究思想或方案是否具有新颖性和独特性？请详细阐述判断理由。
以往相关研究针对是绣球花属及属下水平的生物地理学研究，但族及以上水平洲际间断分布格局的生物地理学研究尚属空白，也很少考虑物种分化速率对间断分布的格局影响。因此，该申请项目的研究思想或方案具有一定的创新性。

二、请评述申请项目所关注问题的科学价值以及对相关前沿领域的潜在贡献。
本研究利用二代测序技术，并基于单拷贝核基因和叶绿体基因组重建该族系统发育关系，估算物种分化时间、形成速率，阐明绣球花族洲际间断分布演化历史。对相关族级别系统发育研究方法的建立具有潜在的理论价值。

三、请评述申请人的研究基础与研究方案的可行性。
申请人曾进行过亚热带阔叶林类群如：银杏属、紫荆属的系统发育研究。并对绣球花族的形态分类学和系统发育学有过前期研究基础。因此，相似的理论背景、研究手段和实验方法均可供本项目借鉴和参考。

四、其他建议

修改意见:

生命科学部

2022年9月7日

关于国家自然科学基金资助项目批准及有关事项的通知

华南农业大学　　龚维　　先生/女士：

根据《国家自然科学基金条例》的规定和专家评审意见，国家自然科学基金委员会（以下简称自然科学基金委）决定批准资助您的申请项目。项目批准号：31470312，项目名称：北半球历史生物地理学问题探讨：基于RADtaqs方法的紫荆属亲缘地理学研究，资助金额：85.00万元，项目起止年月：2015年01月至 2018年 12月，有关项目的评审意见及修改意见附后。

请尽早登录科学基金网络信息系统（https://isis.nsfc.gov.cn），获取《国家自然科学基金资助项目计划书》（以下简称计划书）并按要求填写。对于有修改意见的项目，请按修改意见及时调整计划书相关内容；如对修改意见有异议，须在计划书电子版报送截止日期前提出。

计划书电子版通过科学基金网络信息系统（https://isis.nsfc.gov.cn）上传，由依托单位审核后提交至自然科学基金委进行审核。审核未通过者，返回修改后再行提交；审核通过者，打印（建议双面打印）为计划书纸质版（一式两份），由依托单位审核并加盖单位公章后报送至自然科学基金委项目材料接收工作组。计划书电子版和纸质版内容应当保证一致。

向自然科学基金委提交和报送计划书截止时间节点如下：

1、提交计划书电子版截止时间为**2014年9月11日16点**（视为计划书正式提交时间）；

2、提交计划书电子修改版截止时间为**2014年9月18日16点**；

3、报送计划书纸质版截止时间为**2014年9月26日16点**。

请按照以上规定及时提交计划书电子版，并报送计划书纸质版，未说明理由且逾期不报计划书者，视为自动放弃接受资助。

附件：项目评审意见及修改意见

国家自然科学基金委员会

生命科学部

2014年8月15日

附件：项目评审意见及修改意见表

项目批准号	31470312	项目负责人	龚维	申请代码1	C020203
项目名称	北半球历史生物地理学问题探讨：基于RAD taqs方法的紫荆属亲缘地理学研究				
资助类别	面上项目		亚类说明	常规面上项目	
附注说明					
依托单位	华南农业大学				
资助金额	85.00 万元		起止年月	2015年01月 至 2018年12月	

通讯评审意见:

<1>申请人选择苏木科古老类群紫荆属，以第二代测序技术RAD tags方法为主，结合原有的cpDNA单倍型分析和SSR分子标记，检测紫荆属群体遗传多样性、谱系地理结构、分化过程和群体进化历史等，结合生态位模型等，来探讨该属的生物地理进化历史以及地质事件对该属地理格局影响和机制。申请人对学科的发展动态了解全面，对研究的类群较熟悉，提出的科学问题清晰明确，实验设计和技术路线可行，采用的方法全面，且已有了一定的前期工作基础。此外，申请人的也有较好的研究背景，相关领域也有较好的论文发表。团队力量较强（唯不足的是团队成员在项目上投入的时间稍显不足），国外合作者有丰富的研究经验，能给予帮助和指导，保证了项目目标的实验。建议给予优先资助。

<2>该申报书立项依据充分，对北半球分布的紫荆属植物的间断分布问题进行亲缘地理学的研究。研究内容合适，重点突出，关键问题也比较准确，总体研究方案合理，申请人具有较强的研究基础和研究能力。
关于研究内容部分，希望申报人今后按照申报书的要求重点阐述。
不过申请人对紫荆属这个类群已经相当熟悉，具有多年的积累，该项目可行性强，仍然建议予以优先资助。

<3>该项目以第二代测序技术RAD taqs方法为主，结合传统的cpDNA单倍型分析和SSR分子标记，首次开展紫荆属亲缘地理学研究，检测该属群体遗传多样性、谱系地理结构、谱系分化过程和群体进化历史等，检测陆桥变迁、气候波动所带来的隔离分化、迁移扩散等历史事件，探明紫荆属洲际间断分布格局的形成机制及物种进化历史，对于揭示东亚类群在该属洲际间断分布格局形成过程中的作用和释北半球广布类群的历史生物地理学问题，具有较重要的科学意义。研究内容合适，方法先进；研究重点突出，所选择的关键问题准确；研究方案与技术路线简明可行，有较强的创新潜力，预期能达到研究目标。本人建议优先立项资助。

对研究方案的修改意见:

生命科学部

2014年8月15日

关于国家自然科学基金资助项目批准及有关事项的通知

华南农业大学 龚维先生/女士:

根据《国家自然科学基金条例》的规定和专家评审意见，国家自然科学基金委员会（以下简称自然科学基金委）决定批准资助您的申请项目。项目批准号: 31300174 ，项目名称 广布种樾木及其近缘类群的亲缘地理学研究 ，资助金额 23.00 万元，项目起止年月: 2014 年 01 月至 2016 年 12 月，有关项目的评审意见及修改意见附后。

请尽早登录科学基金网络信息系统（https://isis.nsfc.gov.cn），获取《国家自然科学基金资助项目研究计划书》（以下简称计划书）并按要求填写。计划书电子文件通过科学基金网络信息系统（https://isis.nsfc.gov.cn）上传，由依托单位确认后，自然科学基金委进行审核；计划书纸质文件（一式两份）由依托单位审核并加盖单位公章后报送至自然科学基金委项目材料接收工作组。

自然科学基金委接收依托单位提交计划书电子版截止时间为 **2013 年 9 月 11 日 16 点前**，提交计划书电子修改版截止时间为 **2013 年 9 月 18 日 16 点前**；计划书纸质版于计划书电子版通过自然科学基金委审核后再行打印（建议双面打印），自然科学基金委接收计划书纸质版截止时间为 **2013 年 9 月 27 日 16 点前**。

请按照依托单位规定时间，及时将计划书电子版和纸质版先后提交依托单位进行确认审核。对于有修改意见的项目，请按修改意见及时调整计划书相关内容；如对修改意见有异议，须在计划书电子版报送截止日期前提出。计划书电子文件和纸质文件内容应当保证一致。

未说明理由且逾期不报计划书者，视为自动放弃接受资助。

附件: 项目评审意见及修改意见

国家自然科学基金委员会

生命科学部

2013 年 08 月 15 日

附件：项目评审意见及修改意见表

项目批准号	31300174	项目负责人	龚维	申请代码 1	C020203
项目名称	广布种檵木及其近缘类群的亲缘地理学研究				
资助类别	青年科学基金项目	亚类说明			
附注说明					
依托单位	华南农业大学				
资助金额	23.00 万元	起止年月	2014 年 01 月至 2016 年 12 月		

通讯评审意见：

<1>采用亲缘地理学的研究方法探讨植物类群的进化历史是近年来的研究热点。本项目选取檵木及其与之形成单系类群的近缘种为研究对象，在揭示该种的遗传变异的空间分布格局和谱系进化历史的基础上，推测其第四纪冰川避难所、冰期后扩散路线和群体扩张，进而探讨我国甚至东亚地区常绿阔叶林的进化历史。该项目立论依据充分，选题合理，具有一定的科学意义，另外该项目的研究重点突出，实验方案和技术路线可行，拟解决的关键问题明确，经费预算合理。

申请人将檵木的研究结果与常绿阔叶林自冰期以后的变化结合起来，应该是本项目的一个特点，但檵木只是一个常绿灌木，并不是常绿阔叶林中植物群落的建群种，也并非所有的常绿阔叶林群落类型中必须有这个物种，因此的用该种的研究结果来探讨我国甚至东亚地区常绿阔叶林的进化历史是否合适，是值得商榷的，建议申请者只开展檵木的有关研究，不要涉及有关植被进化的内容。

综上所述，建议优先资助该项目。

<2>申请人已经具有谱系生物地理学研究的经历，该申请书立论依据和研究方法及手段均比较合理， 只是在大范围的全分布区取样方面可能会有困难，建议适当聚焦。同意资助。

<3> 在化石和孢粉材料相对缺乏的我国亚热带地区，开展植物谱系地理学研究对于阐明第四纪冰期交替作用下植物分布区的动态演变具有重要的科学意义。檵木属是我国亚热带的广布类群，取样容易且样本量大，同时也是散播能力较弱的代表性类群，该研究对于了解我国亚热带森林植被在第四纪的演化具有重要的潜在价值。项目具有较好的创新性、技术路线设计合理且可行，推荐优先资助！建议：加强对第四纪以来我国亚热带地区古气候和古生态研究成果的收集和总结，在讨论各谱系分支时，将基于分子钟的分化时间与古气候和古环境资料相互参照。

对研究方案的修改意见：

生命科学部

2013 年 08 月 15 日

受理编号：c1730750100002　　项目编号：2017A030303067

文件编号：粤科规财字[2017]120号

广东省省级科技计划项目

合同书

项目名称：南岭山区紫荆属种质资源调查和群体遗传多样性研究

专项资金类别：公益研究与能力建设

计划类别：科技基础条件建设领域

项目起止时间：2017-01-01　至　2019-12-31

管理单位(甲方)：广东省科学技术厅

承担单位(乙方)：华南农业大学

乙方主管部门(丙方)：华南农业大学

通讯地址：广东省广州市天河区五山路483号

邮政编码：510642　　单位电话：020-38632819

项目负责人：龚维　　联系电话：13798169503

项目联系人：龚维　　联系电话：13798169503

2017A030303067

广东省科学技术厅
二〇一七年制

（广东科技微信公众号）　　（受理纸质材料二维码）

一、研发内容和关键技术

1. 主要研究内容

（1）野外调查。在前期研究的基础上，将进一步开展南岭山区紫荆属植物的资源调查，对该属植物群落进行全面、深入的野外调查，统计种群大小，记录其地理分布。

（2）样品采集。在已有样品的基础上，补充采集南岭山区的湖北紫荆、黄山紫荆和广西紫荆群体。

（3）群体遗传学分析。利用改良后的CTAB法进行紫荆属基因组DNA提取。利用GBS方法，对所有紫荆属个体样品进行基因组分析，检测个体多态性SNP位点，计算各项群体遗传学参数，进行群体遗传结构和遗传分化分析。

（4）引种栽培建议。基于群体遗传学证据，为南岭山区紫荆属种质资源的保护提出依据，并为科学、合理的栽培和引种该属植物资源提出建议。

2. 解决的关键问题

拟解决的关键问题是基于GBS方法进行测序，获取多态性SNP位点，分析南岭山区紫荆属3种的群体遗传多样性水平、群体遗传结构以及群体遗传分化程度。技术路线是①南岭山区紫荆属种质资源调查，统计紫荆属3种地理分布情况；②进行群体样品采集；③进行DNA提取，利用GBS方法进行简化基因组测序，获取多态性SNP位点；④比较、分析紫荆属3种在南岭山区的群体遗传多样性水平、群体遗传结构以及群体遗传分化程度；⑤为该地区紫荆属种质资源的保护提出依据，并为科学、合理的栽培和引种该属植物资源提供群体遗传学数据参考。

3. 创新点

（1）南岭山区是生物多样性热点地区，重要的冰期避难所区域，也是是科学家们长期关注的地理区域之一。

（2）紫荆属在群体遗传学研究方面较少，前期研究也存在一定的不足。本研究首次针对南岭山区的紫荆属植物，利用二代测序技术GBS方法，开展群体遗传学分析。本研究将为南岭山区紫荆属植物资源的合理利用和开发提供依据。

（3）本研究的开展可为南岭山区其它植物的种质资源调查和评价提供借鉴。

2017A030303067

二、项目考核指标

<table>
<tr><td colspan="6">1.项目完成后提供的研究开发成果及形式（须明确产品、专利、版权、标准等成果的类型及数量）</td></tr>
<tr><td colspan="2">成果形式</td><td>成果数量</td><td colspan="2">成果形式</td><td>成果数量</td></tr>
<tr><td rowspan="2">发明专利</td><td>申请</td><td></td><td colspan="2">引进人才(人)</td><td></td></tr>
<tr><td>授权</td><td></td><td colspan="2">培养人才(人)</td><td>1</td></tr>
<tr><td rowspan="2">实用新型专利</td><td>申请</td><td></td><td colspan="2">科技人才奖励(人)</td><td></td></tr>
<tr><td>授权</td><td></td><td rowspan="2">技术标准制定</td><td>牵头(个)</td><td></td></tr>
<tr><td rowspan="2">外观设计专利</td><td>申请</td><td></td><td>参与(个)</td><td></td></tr>
<tr><td>授权</td><td></td><td colspan="2">科技报告(篇)</td><td></td></tr>
<tr><td rowspan="2">国外专利</td><td>PCT受理</td><td></td><td colspan="2">软件著作权(项)</td><td></td></tr>
<tr><td>授权</td><td></td><td colspan="2">论文论著(篇)</td><td>1</td></tr>
<tr><td colspan="2">获得国家级奖项(项)</td><td></td><td rowspan="3">其中：被收录论文数(篇)</td><td>SCI</td><td>1</td></tr>
<tr><td colspan="2">获得省级奖项(项)</td><td></td><td>EI</td><td></td></tr>
<tr><td colspan="2">新服务(项)</td><td></td><td>ISTP</td><td></td></tr>
<tr><td colspan="2">新产品（或新材料、新装备、新品种（系））</td><td></td><td colspan="2">新工艺（或新方法、新模式、新技术）</td><td></td></tr>
<tr><td colspan="2" rowspan="2">创新载体项目必填</td><td colspan="3">技术服务数量（项）</td><td></td></tr>
<tr><td colspan="3">服务企业数量（家）</td><td></td></tr>
<tr><td colspan="2" rowspan="4">科技金融项目必填</td><td colspan="3">开展培训宣讲活动场次(次)</td><td></td></tr>
<tr><td colspan="3">服务企业数量(家)</td><td></td></tr>
<tr><td colspan="3">帮助企业融资(万元)</td><td></td></tr>
<tr><td colspan="3">引进专业机构(家)</td><td></td></tr>
<tr><td colspan="2" rowspan="4">院士工作站项目必填</td><td colspan="3">引进院士及其团队科技成果转化数量</td><td></td></tr>
<tr><td colspan="3">院士开展的战略咨询和技术指导次数</td><td></td></tr>
<tr><td colspan="3">院士年进站次数</td><td></td></tr>
<tr><td colspan="3">院士及院士团队年进站时间</td><td></td></tr>
<tr><td colspan="2" rowspan="8">软科学项目必填</td><td colspan="3">决策咨询报告(篇)</td><td></td></tr>
<tr><td colspan="3">研究总报告(篇)</td><td></td></tr>
<tr><td colspan="3">研究中期报告(篇)</td><td></td></tr>
<tr><td colspan="3">研究分报告(篇)</td><td></td></tr>
<tr><td colspan="3">调研报告(篇)</td><td></td></tr>
<tr><td colspan="3">专著(篇)[须注明“广东省软科学研究计划项目(项目编号：)资助”]</td><td></td></tr>
<tr><td colspan="3">核心期刊论文(篇)[以第一作者发表，须注明“广东省软科学研究计划项目(项目编号：)资助”]</td><td></td></tr>
<tr><td colspan="3">培养人才(人)</td><td></td></tr>
</table>

2017A030303067

	获国家级奖项(项)	
	获省级奖项(项)	
	其他	

2.其他成果及形式说明：

3.主要技术经济指标及社会效益

累计新增销售收入（万元）	
累计新增利税（万元）	

4.其他主要技术经济指标及社会效益说明：

项目负责人（签章）：　　年　　月　　日

2017A030303067

三、项目进度和阶段目标

开始日期	结束日期	主要工作内容
2017-01-01	2017-12-31	在已有研究的基础上，进一步开展南岭山区紫荆属植物资源的野外调查工作，统计该地区紫荆属植物群体大小、地理分布情况等。采集南岭山区紫荆属植物叶片材料，利用GBS方法进行预实验。
2018-01-01	2018-12-31	对已采集的南岭山区紫荆属植物进行全部样品的分子实验和数据分析。利用改良的CTAB法，提取基因组DNA，利用GBS方法进行基因组测序。对测序结果进行处理和分析。计算各项群体遗传学参数，比较、分析湖北紫荆、黄山紫荆和广西紫荆在南岭山区的群体遗传多样性水平、群体遗传结构以及群体遗传分化程度。
2019-01-01	2019-12-31	数据处理和分析，论文撰写。

2017A030303067

四、承担、参与单位工作分工及经费分配情况

承担/参与单位名称（盖章）	工作分工	总经费分摊（万元）	省科技厅经费分配（万元）
华南农业大学	野外调查、样品处理、文献资料查阅、分子实验、大型仪器设备的使用等	10.00	10.00
	合计	10.00	10.00

2017A030303067

五、项目总经费及省科技厅经费预算

1.省科技厅经费下达总额： （大写）壹拾万圆整；（小写 ）10万元；						
2.省科技厅经费拨付方式： **一次性拨款**						
3.省科技厅经费年度下达计划： （大写）壹拾万圆整；（小写 ）10万元；						
分期			经费(万元)			
第1期			10			
4.总经费开支预算计划：						
经费筹集情况：						（单位：万元）
总投入经费：10.00						
	省科技厅经费	自筹资金				合计
		自有资金	贷款	地方政府投入	其它	
已投入经费：						
新增经费：	10.00				0.00	10.00
政府部门、境外资金及其他资金投入情况说明：						

2017A030303067

新增经费预算：				（单位：万元）
	新增经费总额		省科技厅经费	
支出经费	经费额	用途说明	经费额	用途说明
基建费：				
1、直接费用：	9.50		9.50	
(1)设备费：				
(2)材料费：	1.00	购置实验耗材，如离心管、枪头等	1.00	购置实验耗材，如离心管、枪头等
(3)测试化验加工外协费：	1.50	测序费用	1.50	测序费用
(4)燃料动力费：				
（5）差旅费/会议费/国际合作与交流费：	3.10	支付野外工作的交通费、住宿费；赴国外进行学术交流、外国专家来华	3.10	支付野外工作的交通费、住宿费；赴国外进行学术交流、外国专家来华
（6）出版/文献/信息传播/知识产权事务费：	0.20	论文发表版面费以及网络资料查阅等	0.20	论文发表版面费以及网络资料查阅等
（7）劳务费：				
（8）人员费：	3.70	临时工、村民、技术人员和学生的费用	3.70	临时工、村民、技术人员和学生的费用
（9）专家咨询费：				
（10）直接费用其他支出：				
（11）科技金融服务体系其他费用：	0.00		0.00	
①信用评级补贴：				
②大赛场租：				
③特派员奖励与补贴：				
2、间接费用：	0.50		0.50	
（1）间接成本：	0.50	单位管理费占5%	0.50	单位管理费占5%
（2）管理成本：				
（3） 绩效支出：				
合计：	10.00		10.00	

特别提醒：2017年3月份，广东省《关于进一步完善省级财政科研项目资金管理等政策的实施意见（试行）》（粤委办〔2017〕13号）出台，对间接费用比例、劳务费开支范围、人员费用安排等进行了调整优化。为及时拨付2017年度科研经费，平台直接提取申报书相关信息生成合同书并进行了预签订，但各项目负责人、承担单位、主管部门须认真领会相关文件精神，在合同书签订完成后2个月内通过平台提请项目经费变更或确认，对相关经费开支进行细化完善，否则，将影响其科研信用评级或申报新的省级科技项目。

2017A030303067

六、人员信息

项目负责人情况								
姓名	**年龄**	**性别**	**职称**	**职务**	**学历**	**在项目中承担的任务**	**所在单位**	**签名**
龚维	38	女	副教授	无	博士研究生	负责整个项目实施，野外调查、数据分析和论文撰写	华南农业大学	

主要研究开发人员								
姓名	**年龄**	**性别**	**职称**	**职务**	**学历**	**在项目中承担的任务**	**所在单位**	**签名**
谢建光	41	男	讲师	无	博士研究生	野外调查和分子数据分析	华南农业大学	
刘婉桢	27	女	未取得	无	博士研究生	野外调查、分子实验	华南农业大学	
周娟	24	女	未取得	无	本科	野外调查、分子实验、论文撰写	华南农业大学	

2017A030303067

七、承担、参与单位合作

本单位独立承担项目

2017A030303067

八、合同条款

第一条	甲方与乙方根据《中华人民共和国合同法》及国家有关法规和规定，为顺利完成（2017）年**南岭山区紫荆属种质资源调查和群体遗传多样性研究** 专项项目（项目编号： 2017A030303067 ）经协商一致，特订立本合同，作为甲乙双方在项目实施管理过程中共同遵守的依据。
第二条	甲方的权利义务： 1.按合同书规定进行经费核拨的有关工作协调。 2.根据甲方需要，在不影响乙方工作的前提下，定期或不定期对乙方项目的实施情况和经费使用情况进行检查或抽查。 3.根据《广东省科技计划项目信用管理办法(试行)》对乙方进行科技计划信用管理。
第三条	乙方的权利义务： 1.确保落实自筹经费及有关保障条件。 2.按合同书规定，对甲方核拨的经费实行专款专用，单独列账，并随时配合甲方进行监督检查。 3.使用财政资金采购设备、原材料等，按照《广东省实施〈中华人民共和国招标投标法〉办法》有关规定，符合招标条件的须进行招标。 4.项目实施完成或实施到一定程度，须按照《广东省省级科技计划项目结题管理的实施细则（试行）》提出验收或终止结题的申请，并按甲方要求做好项目结题工作。 5.在每年1月向甲方如实提交上年度工作情况报告，报告内容包含上年度项目进展情况、经费决算和取得的效果等。 6.按照国家和省有关规定，每年须提交年度科技报告；项目验收时，须提交验收科技报告。
第四条	在履行本合同的过程中，如出现广东省相关政策法规重大改变等不可抗力情况，甲方有权对所核拨经费的数量和时间进行相应调整。
第五条	在履行本合同过程中，需要对项目起止时间、项目经费使用（包括自筹经费、经费分配及经费支出预算等）、项目内容（包括研发内容、技术指标、经济指标及成果指标等）、项目名称、项目承担单位（包括承担单位更名、承担单位替换）、参与单位、项目负责人和成员等进行变更的，甲乙双方按照《广东省省级科技计划项目合同书管理的 实施细则（试行）》有关规定执行。
第六条	在履行本合同的过程中，当事人一方发现可能导致项目整体或部分失败的情形时，应及时通知另一方，并采取适当措施减少损失，没有及时通知并采取适当措施，致使损失扩大的，应当就扩大的损失承担责任。
第七条	本项目技术成果的归属、转让和实施技术成果所产生的经济利益的分享，除双方另有约定外，按国家和广东省有关法规执行。

2017A030303067

第八条	属技术保密的项目，甲乙双方应另行订立技术保密条款，作为本合同正式内容的一部分，与本合同具有同等效力。
第九条	根据项目具体情况，经双方另行协商订立的附加条款，作为本合同正式内容的一部分，与本合同具有同等效力。
第十条	本合同的争议应由双方本着协商一致的原则解决，如双方协商不成的，则应向甲方所在地法院提起诉讼。
第十一条	保密条款： 1.本合同保密内容范围为： / 2.本合同保密期限为： / 3.乙方应与可能知悉保密内容的人员签订技术秘密保护协议。 4.各方应建立技术秘密保护制度。 5.属技术保密的项目必须经省负责技术保密部门审查后，确定可否发表或用于国际合作和交流。
第十二条	甲方可根据具体情况决定乙方是否需要单位担保，若需要保证单位，应订立担保条款，作为本合同正式内容一部分。当乙方不履行或不完全履行本合同，以及没有或没有完全承担违约责任时，乙方的保证单位承担连带保证责任。
第十三条	本合同一式六份，各份具有同等效力。甲方存三份，乙方存二份，丙方存一份，本合同自签字之日起生效，有效期至项目结题后一年内。各方均应负合同的法律责任，不应受机构、人事变动的影响。
说明：本合同书中，凡是当事人约定无需填写的内容，应在空白处划（/）。	

2017A030303067

九、本合同签约各方

管理单位（甲方）：　广东省科学技术厅　（盖章）

单位地址：　连新路171号

法定代表人（或授权代表）：　黄宁生　（签章）

立项责任人：　余亮　（签章）

年　月　日

承担单位（乙方）：　华南农业大学　（盖章）

二级部门：　华南农业大学生命科学学院

单位地址：　五山路483号

法定代表人（或法人代理）：　陈晓阳　（签章）

联系人（项目主管）姓名：　石睿　（签章）

Email：kjcgxk@scau.edu.cn

电话：020-85285390 / 13430350923

开户单位名称：　华南农业大学

开户银行及帐号：　广东广州工行五山支行　3602002609000310520

年　月　日

乙方主管部门（丙方）：　华南农业大学　（盖章）

单位地址：　五山路483号

法定代表人（或法人代理）：　陈晓阳　（签章）

年　月　日

2017A030303067

受理编号：c1630750100041

项目编号：2016A030303048

文件编号：粤科规财字〔2016〕47号

2016A030303048

广东省省级科技计划项目

合同书

项目名称：南雄市银杏种质资源调查及雌雄株性别分子鉴定研究

计划类别：科技基础条件建设领域

项目起止时间：2016-01-01 至 2018-12-31

管理单位(甲方)：广东省科学技术厅

承担单位(乙方)：华南农业大学

乙方主管部门(丙方)：华南农业大学

通讯地址：广东省广州市天河区五山路483号

邮政编码：510642 单位电话：020-38632819

项目负责人：龚维 联系电话：13798169503

项目联系人：龚维 联系电话：13798169503

广东省科学技术厅
二〇一四年制

一、项目实施内容

银杏（Ginkgo biloba L. ），也称白果树，为世界上最著名的“活化石”植物，我国一级保护植物。根据化石资料记载，在早白垩纪银杏广泛分布于现今的亚洲、欧洲和北美地区。第四纪冰期的到来，欧洲和北美洲为冰川所覆盖，银杏仅在中国受冰川作用较小的部分地区存活下来（http://www.xs4all.nl/~kwanten/）。我国具有悠久的银杏栽培历史。其中，广东省南雄市位于南岭山脉，其白果产量占全省的90%以上。该市具备独特气候、土壤条件，境内现存1.3 万多株百年以上银杏树，银杏种质资源丰富，银杏产业已成为继黄烟产业之后的又一支柱产业。

通过鉴定银杏雌雄株个体，根据不同栽培目的，合理取舍和利用银杏种质资源，已成为南雄市银杏产业迫切需要解决的关键技术问题。然而，银杏的性别差异主要表现在花器官上，其实生树定植年限长，从而促使我们开发准确、可靠的早期性别鉴定方法。此外，南雄市银杏资源丰富，对该市银杏种质资源进行野外调查，通过科普宣传，有利于增加社会团体对银杏古树的保护意识，进一步促进南雄市银杏产业的发展。

该项目实施内容如下：

（1）野外调查。

在前期研究的基础上，进一步针对南雄市银杏群落进行全面、深入的野外调查，记录该地区银杏群落生态学特征，统计雌雄株地理分布情况和个体数量，排除嫁接雌株个体。

（2）样品采集。

广泛采集南雄市银杏雌雄株个体叶片材料，硅胶干燥保存，以备用于后续分子实验。

（3）雌雄株性别鉴定分子标记开发。

利用 CTAB 法进行银杏基因组DNA 提取。利用RAD taqs 方法，对所有雌雄株个体样品进行基因组分析，检测雌雄株个体多态性SNP 位点。利用STACKS、VENNDIAGRAM 软件对测序结果进行处理。通过BLAST 对比与似然值检测，整合序列。对RAD taqs 结果进行序列分析，对比获得的最终数据矩阵，比较银杏雌雄株个体基因组序列差异，找出银杏雌雄株个体基因组序列差异位点，进而开发早期雌雄株个体性别鉴定的分子标记。

（4）将所开发的性别特异性分子标记，应用于南雄市银杏种质资源雌雄株个体性别鉴定，检验其准确性，从而保证科学、合理的利用银杏种质资源。

二、项目考核指标

1.项目完成后提供的研究开发成果及形式（须明确产品、专利、版权、标准等成果的类型及数量）

成果形式		成果数量	成果形式		成果数量
发明专利	申请	1	引进人才(人)		
	授权		培养人才(人)		1
实用新型专利	申请		科技人才奖励(人)		
	授权		技术标准制定	牵头(个)	
外观设计专利	申请			参与(个)	
	授权		科技报告(篇)		
国外专利	PCT受理		软件著作权(项)		
	授权		论文论著(篇)		1
获得国家级奖项(项)			其中：被收录论文数(篇)	SCI	1
获得省级奖项(项)				EI	
新服务(项)				ISTP	
新产品（或新材料、新装备、新品种（系））			新工艺（或新方法、新模式、新技术）		
创新载体项目必填	技术服务数量（项）				
	服务企业数量（家）				
科技金融项目必填	开展培训宣讲活动场次(次)				
	服务企业数量(家)				
	帮助企业融资(万元)				
	引进专业机构(家)				
院士工作站项目必填	引进院士及其团队科技成果转化数量				
	院士开展的战略咨询和技术指导次数				
	院士年进站次数				
	院士及院士团队年进站时间				
软科学项目必填	决策咨询报告(篇)(至少1篇)				
	研究总报告(篇)(至少1篇)				
	研究中期报告(篇)				
	研究分报告(篇)				
	调研报告(篇)				
	专著(篇)[须注明“广东省软科学研究计划项目(项目编号：)资助”]				
	核心期刊论文(篇)[以第一作者发表，须注明“广东省软科学研究计划项目(项目编号：)资助”]				
	培养人才(人)				

	获国家级奖项(项)	
	获省级奖项(项)	
	其他（具体形式：用户填)	
其他成果及形式说明：		
2. 主要技术经济指标及社会效益		
累计新增销售收入（万元）		
累计新增利税（万元）		
其他主要技术经济指标及社会效益说明：		
项目负责人（签章）：[illegible] 2016年 9 月 2 日		

2016A030303048

三、项目进度和阶段目标

开始日期	结束日期	主要工作内容
2016-01-01	2016-12-31	广泛开展南雄市银杏群体野外调查和样品采集工作。统计该地银杏地理分布情况以及雌雄株个体分布情况。
2017-01-01	2017-12-31	补充遗漏的银杏个体材料，进行分子实验，提取基因组DNA，利用RAD taqs方法进行基因组测序。对测序结果进行处理和分析。开发雌雄株性别鉴定标记，并对南雄市银杏雌雄株个体进行检验。
2018-01-01	2018-12-31	数据处理和分析，论文撰写、专利申请。

2016A030303048

四、承担、参与单位工作分工及经费分配情况

承担/参与单位名称（盖章）	工作分工	总经费分摊（万元）	省科技厅经费分配（万元）
华南农业大学	样品处理，分子实验，资料查阅，大型仪器的使用等。	20.00	20.00
	合计	20.00	20.00

2016A030303048

五、项目总经费及省科技厅经费预算

1.省科技厅经费下达总额： （大写）贰拾万圆整；（小写 ）20.00万元；						
2.省科技厅经费拨付方式： **一次性拨款**						
3.省科技厅经费年度下达计划：**总额20.00(万元)**						
分期			经费(万元)			
第1期			20			
4.总经费开支预算计划：						
经费筹集情况：						（单位：万元）
总投入经费：20.00						
	省科技厅经费	自筹资金				合计
		自有资金	贷款	地方政府投入	其它	
已投入经费：						
新增经费：	20.00					20.00
政府部门、境外资金及其他资金投入情况说明：						

2016A030303042

新增经费预算：				（单位：万元）
	新增经费总额		省科技厅经费	
支出经费	经费额	用途说明	经费额	用途说明
基建费：				
1、直接费用：	19.00		19.00	
(1)设备费：				
(2)材料费：	3.50	购买实验试剂、耗材等	3.50	购买实验试剂、耗材等
(3)测试化验加工外协费：	3.50	测序	3.50	测序
(4)燃料动力费：	0.50	实验室运作水电费等	0.50	实验室运作水电费等
(5)差旅费：	4.50	野外调查和样品采集，野外工作用车燃料费等	4.50	野外调查和样品采集，野外工作用车燃料费等
(6)会议费：				
(7)国际合作与交流费：	3.00	用于赴国外大学进行数据分析和论文撰写	3.00	用于赴国外大学进行数据分析和论文撰写
(8)出版/文献/信息传播/知识产权事务费：	1.00	专利维护、论文发表和资料查阅	1.00	专利维护、论文发表和资料查阅
(9)租赁费：				
(10)人员费：	3.00	用于野外工作中村民劳务费、向导费	3.00	用于野外工作中村民劳务费、向导费
(11)专家咨询费：				
(12)直接费用其他支出：				
(13)科技金融服务体系其他费用：	0.00		0.00	
①信用评级补贴：				
②大赛场租：				
③特派员奖励与补贴：				
2、间接费用：	1.00		1.00	
管理费：	1.00	单位管理费占5%	1.00	单位管理费占5%
合计：	20.00		20.00	

六、人员信息

项目负责人情况								
姓名	年龄	性别	职称	职务	学历	在项目中承担的任务	所在单位	签名
龚维	37	女	副教授	无	博士研究生	负责整个项目的开展，进行野外调查、样品采集以及后续分子实验、数据分析和文章撰写	华南农业大学	龚维

主要研究开发人员								
姓名	年龄	性别	职称	职务	学历	在项目中承担的任务	所在单位	签名
谢建光	40	男	讲师	无	博士研究生	野外调查和样品采集	华南农业大学	谢建光
张彩云	37	女	助理研究员	无	博士研究生	分子实验	华南农业大学	张彩云
刘婉桢	26	女	未取得	无	硕士研究生	分子实验和数据分析	华南农业大学	刘婉桢

2016A030303048

七、承担、参与单位合作协议（须与申报书中合作协议或意向书相一致）

无

2016A030303048

八、合同条款

第一条 甲方与乙方根据《中华人民共和国合同法》及国家有关法规和规定，为顺利完成（2016）年**南雄市银杏种质资源调查及雌雄株性别分子鉴定研究** 专项项目（项目编号： 2016A030303048 ）经协商一致，特订立本合同，作为甲乙双方在项目实施管理过程中共同遵守的依据。

第二条 甲方的权利义务：

1.按合同书规定进行经费核拨的有关工作协调。

2.根据甲方需要，在不影响乙方工作的前提下，定期或不定期对乙方项目的实施情况和经费使用情况进行检查或抽查。

3.根据《广东省科技计划项目信用管理办法(试行)》对乙方进行科技计划信用管理。

第三条 乙方的权利义务：

1.确保落实自筹经费及有关保障条件。

2.按合同书规定，对甲方核拨的经费实行专款专用，单独列账，并随时配合甲方进行监督检查。

3.使用财政资金采购设备、原材料等，按照《广东省实施〈中华人民共和国招标投标法〉办法》有关规定，符合招标条件的须进行招标。

4.项目实施完成或实施到一定程度，须按照《广东省省级科技计划项目结题管理的实施细则（试行）》提出验收或终止结题的申请，并按甲方要求做好项目结题工作。

5.在每年1月向甲方如实提交上年度工作情况报告，报告内容包含上年度项目进展情况、经费决算和取得的效果等。

6.按照国家和省有关规定，每年须提交年度科技报告；项目验收时，须提交验收科技报告。

第四条 在履行本合同的过程中，如出现广东省相关政策法规重大改变等不可抗力情况，甲方有权对所核拨经费的数量和时间进行相应调整。

第五条 在履行本合同过程中，需要对项目起止时间、项目经费使用（包括自筹经费、经费分配及经费支出预算等）、项目内容（包括研发内容、技术指标、经济指标及成果指标等）、项目名称、项目承担单位（包括承担单位更名、承担单位替换）、参与单位、项目负责人和成员等进行变更的，甲乙双方按照《广东省省级科技计划项目合同书管理的实施细则（试行）》有关规定执行。

第六条 在履行本合同的过程中，当事人一方发现可能导致项目整体或部分失败的情形时，应及时通知另一方，并采取适当措施减少损失，没有及时通知并采取适当措施，致使损失扩大的，应当就扩大的损失承担责任。

第七条 本项目技术成果的归属、转让和实施技术成果所产生的经济利益的分享，除双方另有约定外，按国家和广东省有关法规执行。

第八条 属技术保密的项目，甲乙双方应另行订立技术保密条款，作为本合同正式内容的一部分，与本合同具有同等效力。

第九条 根据项目具体情况，经双方另行协商订立的附加条款，作为本合同正式内容的一部分，与本合同具有同等效力。

第十条 本合同的争议应由双方本着协商一致的原则解决，如双方协商不成的，则应向甲方所在地法院提起诉讼。

第十一条 保密条款：

1. 本合同保密内容范围为：

   无

2. 本合同保密期限为：

   无

3. 乙方应与可能知悉保密内容的人员签订技术秘密保护协议。
4. 各方应建立技术秘密保护制度。
5. 属技术保密的项目必须经省负责技术保密部门审查后，确定可否发表或用于国际合作和交流。

第十二条 甲方可根据具体情况决定乙方是否需要单位担保，若需要保证单位，应订立担保条款，作为本合同正式内容一部分。当乙方不履行或不完全履行本合同，以及没有或没有完全承担违约责任时，乙方的保证单位承担连带保证责任。

第十三条 本合同一式六份，各份具有同等效力。甲方存三份，乙方存二份，丙方存一份，本合同自签字之日起生效，有效期至项目结题后一年内。各方均应负合同的法律责任，不应受机构、人事变动的影响。

说明：本合同书中，凡是当事人约定无需填写的内容，应在空白处划（/）。

2016A030303048

九、本合同签约各方

管理单位（甲方）： 广东省科学技术厅 （盖章）

单位地址： 广东省广州市连新路171号

法定代表人（或授权代表）： 黄宁生 （签章）

联系人（经办人）姓名： 余亮 （签章）

Email： yul@gdstc.gov.cn

电话： 020-83163886

2016年 9月 1日
年 月 日

承担单位（乙方）： 华南农业大学 （盖章）

二级部门： 华南农业大学生命科学学院

单位地址： 广东省广州市天河区五山路483号

法定代表人（或法人代理）： 陈晓阳 （签章）

联系人（项目主管）姓名： 石睿 （签章）

Email： 77909213@qq.com

电话： 020-85283435

开户单位名称： 华南农业大学

开户银行及帐号： 广东广州工行五山支行 3602002609000310520

2016年 9月 1日
年 月 日

乙方主管部门（丙方）： 华南农业大学 （盖章）

单位地址： 广东省广州市天河区五山路483号

法定代表人（或法人代理）： 陈晓阳 （签章）

联系人（项目主管）姓名： 石睿 （签章）

Email： 77909213@qq.com

电话： 020-85283435

开户单位名称： 华南农业大学

开户银行及帐号： 广东广州工行五山支行 3602002609000310520

2016年 9月 1日
年 月 日

SCAULIB202519495

检索证明

根据委托人提供的论文材料，委托人华南农业大生命科学学院 龚维 2 篇论文收录情况如下表。

序号	论文名称	发表刊物及发表的年月卷期/页码等	作者排名	论文等级	作者文中单位	收录情况	影响因子	中科院大类分区
1	The complete plastid genome provides insight into maternal plastid inheritance mode of the living fossil plant Ginkgo biloba	PLANT DIVERSITY 出版年：2023 出版日期：NOV 卷期：45 6 页码：752-756 文献类型：Editorial Material	共同通讯（倒数第一）	T2 类	华南农业大学	SCI	IF2-year=4.6 IF5-year=4.2 （2023）	生物学 1 区 Top 期刊：否 （2023）
2	新时代全英课程《植物学》国际化教学改革思 路探索	教育科学 出版年：2024 出版日期：10 卷期： 页码：- 文献号： 文献类型：	第一	普刊类	华南农业大学	维普	无	无

说明：论文等级和中科院大类分区按《华南农业大学学术论文评价方案（试行）》划分。

报告免责声明:如未盖章,报告无效

检索员：刘汉思

华南农业大学图书馆 二〇

2025 年 1 月

华南农业大学图书馆信息检索专用章

华南农业大学图书馆SCAULIB202519495

SCAULIB202405520

检索证明

根据委托人提供的论文材料，委托人华南农业大学生命科学学院 Wei Gong 18篇论文收录情况如下表。

序号	论文名称	发表刊物及发表的年月卷期/页码等	作者排名	论文等级	作者单位	收录情况	影响因子	中科院大类分区
1	The complete plastid genome provides insight into maternal plastid inheritance mode of the living fossil plant Ginkgo biloba	Plant Diversity 出版年：2023 卷期：2023,45(06) 06 页码：752-756 文献号： 文献类型：期刊论文	共同通讯作者（倒数第二）	T2 类	华南农业大学	已发表，暂未被SCI 收录	IF2-year=4.8 IF5-year=4.1 （2022）	生物学 1区 Top 期刊：否 （2023）
2	Population dynamics linked to glacial cycles in Cercis chuniana F. P. Metcalf (Fabaceae) endemic to the montane regions of subtropical China	EVOLUTIONARY APPLICATIONS 出版年：2021 卷期：14 11 页码：2647-2663 文献号： . 文献类型：Article,Early Access	共同通讯作者（倒数第一）	T2 类	华南农业大学	SCI	IF2-year=4.929 IF5-year=5.453 （2021）	生物学 1区 Top 期刊：是 （2021）
3	The complete chloroplast genome of Philadelphus pekinensis Rupr. (Hydrangeaceae)	MITOCHONDRIAL DNA PART B-RESOURCES 出版年：2020 卷期：5 2 页码：1178-1179	通讯作者	B 类	华南农业大学	SCI	IF2-year=0.658 IF5-year=0.674 （2020）	生物学 4区 Top 期刊：否 （2020）

		文献号： 文献类型：Article						
4	The complete chloroplast genome of Deutzia pilosa Rehd. (Hydrangeaceae)	MITOCHONDRIAL DNA PART B-RESOURCES 出版年：2020 卷期：5 2 页码：1419-1420 文献号： 文献类型：Article	通讯作者	B 类	华南农业大学	SCI	IF2-year=0.658 IF5-year=0.674 （2020）	生物学 4 区 Top 期刊：否 （2020）
5	Complete Chloroplast Genome of Cercis chuniana (Fabaceae) with Structural and Genetic Comparison to Six Species in Caesalpinioideae	INTERNATIONAL JOURNAL OF MOLECULAR SCIENCES 出版年：2018 卷期：19 5 页码： 文献号：1286 文献类型：Article	共同通讯作者（倒数第一）	B 类	华南农业大学	SCI	IF2-year=4.183 IF5-year=4.331 （2018）	化学 3 区 Top 期刊：否 （2018）
6	Identification and characterization of microsatellites in Aconitum reclinatum (Ranunculaceae), a rare species endemic to North America	APPLICATIONS IN PLANT SCIENCES 出版年：2018 卷期：6 6 页码：- 文献号：e1161 文献类型：Article	共同通讯作者（倒数第一）	B 类	华南农业大学	SCI	IF2-year=1.232 IF5-year=1.389 （2018）	生物 4 区 Top 期刊：否 （2018）

华南农业大学图书馆
信息检索专用章
华南农业大学图书馆SCAULIB20240552

7	The complete chloroplast genome of Aristolochia hainanensis Merr. (Aristolochiaceae)	MITOCHONDRIAL DNA PART B-RESOURCES 出版年：2022 卷期：7 9 页码：1650-1652 文献号： 文献类型：Article	共同通讯作者	B 类	华南农业大学	SCI	IF2-year=0.5 IF5-year=0.6 （2022）	生物学 4 区 Top 期刊：否 （2022）
8	Characterization of the whole chloroplast genome of a rare and endangered species Aconitum reclinatum (Ranunculaceae) in the United States	CONSERVATION GENETICS RESOURCES 出版年：2018 卷期：10 2 页码：165-168 文献号： 文献类型：Article	通讯作者	B 类	华南农业大学	SCI	IF2-year=1.154 IF5-year=0.614 （2018）	生物 4 区 Top 期刊：否 （2018）
9	A comparison of chloroplast genome sequences in Aconitum (Ranunculaceae): a traditional herbal medicinal genus	PEERJ 出版年：2017 卷期：5 页码：- 文献号：e4018 文献类型：Article	通讯作者	B 类	华南农业大学	SCI	IF2-year=2.118 IF5-year=2.469 （2017）	生物 3 区 Top 期刊：否 （2017）
10	The complete chloroplast genome of Sedum tricarpum Makino. (Crassulaceae)	MITOCHONDRIAL DNA PART B-RESOURCES 出版年：2022 卷期：7 1 页码：15-16 文献号：	通讯作者	B 类	华南农业大学	SCI	IF2-year=0.5 IF5-year=0.6 （2022）	生物学 4 区 Top 期刊：否 （2022）

华南农业大学图书馆 信息检索专用章
华南农业大学图书馆SCAULIB2024053

		文献类型：Article					
11	The complete chloroplast genome of Hylotelephium erythrostictum (Miq.) H. Ohba (Crassulaceae)	MITOCHONDRIAL DNA PART B-RESOURCES 出版年：2022 卷期：7 2 页码：365-366 文献号： 文献类型：Article	通讯作者	B 类	华南农业大学	SCI	IF2-year=0.5 IF5-year=0.6 （2022）	生物学 4 区 Top 期刊：否 （2022）
12	Evolution of the sex-determining region in Ginkgo biloba	PHILOSOPHICAL TRANSACTIONS OF THE ROYAL SOCIETY B-BIOLOGICAL SCIENCES 出版年：2022 卷期：377 1850 页码：- 文献号：20210229 文献类型：Article	第一作者	T2 类	华南农业大学	SCI	IF2-year=6.3 IF5-year=7.2 （2022）	生物学 1 区 Top 期刊：是 （2022）
13	DNA barcodes identify Chinese medicinal plants and detect geographical patterns of Sinosenecio (Asteraceae)	JOURNAL OF SYSTEMATICS AND EVOLUTION 出版年：2016 卷期：54 1 页码：83-91 文献号： 文献类型：Article	第一作者	B 类	华南农业大学	SCI	IF2-year=2.05 IF5-year=1.768 （2016）	生物 4 区 Top 期刊：否 （2016）

华南农业大学图书馆 信息技术专用章
华南农业大学图书馆SCAULIB20240530

14	珍稀濒危植物伯乐树的潜在适生区预测	华南农业大学学报 出版年：2014 卷期：2015,36(04) 04 页码：98-104 文献号： 文献类型：期刊论文	第一作者	B 类	华南农业大学	北大核心	无	无
15	Phylogenetic Relationships of Tilia (Malvaceae) Inferred from Multiple Nuclear Loci and Plastid Genomes	INTERNATIONAL JOURNAL OF PLANT SCIENCES 出版年：2023 卷期： 页码：- 文献号： 文献类型：Article,Early Access	第七作者	B 类	华南农业大学	SCI	IF2-year=2.3 IF5-year=2.0 （2022）	生物学 3 区 Top 期刊：否 （2023）
16	Leaf adaptations and species boundaries in North American Cercis: implications for the evolution of dry floras	AMERICAN JOURNAL OF BOTANY 出版年：2018 卷期：105 9 页码：1577-1594 文献号： 文献类型：Article	第四作者	B 类	华南农业大学	SCI	IF2-year=2.858 IF5-year=3.414 （2018）	生物 3 区 Top 期刊：否 （2018）
17	以兴趣培养为核心的植物学教学改革	教育教学论坛 出版年：2013 卷期：2013(42) 42 页码：21-22 文献号： 文献类型：期刊论文	第一作者	无	华南农业大学	CNKI	无	无

华南农业大学图书馆 信息检索 SCAULIB2024055202

18	生物科学双语教学模式与发展	教育教学论坛 出版年：2014 卷期：2014(42) 42 页码：104-106 文献号： 文献类型：期刊论文	第一作者	无	华南农业大学	CNKI	无	无

说明：论文等级和中科院大类分区按《华南农业大学学术论文评价方案（试行）》划分。

报告免责声明:如未盖章,报告无效

检索员：张进

华南农业大学图书馆

2024-03-05

华南农业大学图书馆SCAULIB202405520

PHILOSOPHICAL TRANSACTIONS B

royalsocietypublishing.org/journal/rstb

Research

Cite this article: Gong W, Filatov DA. 2022 Evolution of the sex-determining region in *Ginkgo biloba*. *Phil. Trans. R. Soc. B* **377**: 20210229.
https://doi.org/10.1098/rstb.2021.0229

Received: 23 September 2021
Accepted: 6 December 2021

One contribution of 15 to a theme issue 'Sex determination and sex chromosome evolution in land plants'.

Subject Areas:
evolution, genetics, genomics

Keywords:
sex chromosomes, *Ginkgo biloba*, genetic mapping

Author for correspondence:
Dmitry A. Filatov
e-mail: dmitry.filatov@plants.ox.ac.uk

Electronic supplementary material is available online at https://doi.org/10.6084/m9.figshare.c.5887084.

THE ROYAL SOCIETY PUBLISHING

Downloaded from https://royalsocietypublishing.org/ on 21 March 2022

Evolution of the sex-determining region in *Ginkgo biloba*

Wei Gong[1,2] and Dmitry A. Filatov[2]

[1]College of Life Sciences, South China Agricultural University, Guangzhou, Guangdong 510642, People's Republic of China
[2]Department of Plant Sciences, University of Oxford, South Parks Road, Oxford, UK

WG, 0000-0002-0881-6130; DAF, 0000-0001-8077-5452

Sex chromosomes or sex-determining regions (SDR) have been discovered in many dioecious plant species, including the iconic 'living fossil' *Ginkgo biloba*, though the location and size of the SDR in *G. biloba* remain contradictory. Here we resolve these controversies and analyse the evolution of the SDR in this species. Based on transcriptome sequencing data from four genetic crosses we reconstruct male- and female-specific genetic maps and locate the SDR to the middle of chromosome 2. Integration of the genetic maps with the genome sequence reveals that recombination in and around the SDR is suppressed in a region of about 50 Mb in both males and females. However, occasional recombination does occur except a small, less than 5 Mb long region that does not recombine in males. Based on synonymous divergence between homologous X- and Y-linked genes in this region, we infer that the *Ginkgo* SDR is fairly old—at least of Cretaceous origin. The analysis of substitution rates and gene expression reveals only slight Y-degeneration. These results are consistent with findings in other dioecious plants with homomorphic sex chromosomes, where the SDR is typically small and evolves in a region with pre-existing reduced recombination, surrounded by long actively recombining pseudoautosomal regions.

This article is part of the theme issue 'Sex determination and sex chromosome evolution in land plants'.

1. Introduction

Most animal species are comprised of separate male and female individuals, which raises the question: how do separate sexes originate and evolve? Plants provide an excellent opportunity to address this question as separate sexes (dioecy) evolved many times independently and quite recently in different genera [1,2]. Evolution of separate sexes (dioecy) and the diversity of plant mating systems stimulated significant research efforts to understand the drivers of mating system evolution in plants [3–7]. Dioecy is a relatively rare mating system in plants, with only about 5–6% of the species known to be dioecious [1]. On the other hand, dioecy is very common in gymnosperms, where about two thirds of described species (667 of 1033) have separate sexes [8]. The genetic bases of gymnosperm sex determination are not well studied and sex determination in *Ginkgo biloba*, which is the focus of this paper, can serve as a model to start exploring the evolution of mating systems in this interesting and important plant group.

Ginkgo biloba is an iconic gymnosperm tree species that is widely cultivated across the world and is praised for its beauty and medicinal properties. This 'living fossil' is known from fossil data to have existed as a recognizable species at least since the Jurassic [9] and it is a sole representative of Ginkgoales—one of the four extant gymnosperm lineages (cycads, conifers, Ginkgoales and Gnetales). *Ginkgo biloba* is dioecious, with separate male and female individuals, and its sex-determination system is only starting to be explored. Dioecy in *G. biloba* is suggested to have evolved from monoecious ancestors that had

© 2022 The Authors. Published by the Royal Society under the terms of the Creative Commons Attribution License http://creativecommons.org/licenses/by/4.0/, which permits unrestricted use, provided the original author and source are credited.

Downloaded from https://royalsocietypublishing.org/ on 21 March 2022

Table 1. Accession information of the male and female *Ginkgo* trees used in the analyses.

code	sex[a]	location	voucher	latitude	longitude
FG1-NXDLB	♀	Dalingbei, Pingtian, Nanxiong, Guangdong	ZH010	25.22° N	114.63° E
FG2-NXLBT2	♀	Lingbeitang, Pingtian, Nanxiong, Guangdong	ZH011	25.22° N	114.63° E
FG3-NXLBT3	♀	Lingbeitang, Pingtian, Nanxiong, Guangdong	ZH012	25.22° N	114.63° E
MG1-NXAB	♂	Aobei, Pingtian, Nanxiong, Guangdong	ZH013	25.22° N	114.63° E
MG2-NXDLB	♂	Dalingbei, Pingtian, Nanxiong, Guangdong	ZH009	25.22° N	114.63° E
MG3-NXPH	♂	Pinghu, Pingtian, Nanxiong, Guangdong	ZH014	25.22° N	114.63° E
MG4-ZJLKY[b]	♂	Zhejiang Forestry Inst., Hangzhou, Zhejiang	ZH019	30.22° N	120.03° E
MG5-ZJTM	♂	Tianmu Mountain, Lian'an, Zhejiang	ZH020	30.35° N	119.43° E

[a]The sex of the individuals was identified by phenotypic observation.
[b]Male MG4-ZJLKY was not used in the crosses, but it was used in other analyses.

ovulate and pollen cones on different parts of the plant [10–12]. Although no fossil data of *Ginkgo* ancestral reproductive structures are available to support this hypothesis, it is in line with evolution of dioecy in conifers where dioecy has evolved from monoecy at least 10 times [12,13].

Despite the large size of the *G. biloba* genome (approx. 10 Gb), it has been sequenced and assembled twice [14,15] and the recent assembly based on long-read sequencing is 'nearly complete', including 12 large scaffolds corresponding to 12 chromosomes of this species [15]. Based on the previous cytological research, the somatic diploid chromosome number of *G. biloba* is $2n = 24$ [16–18]. The chromosome complement of *G. biloba* is a bimodal and asymmetrical karyotype [17–19], which is not similar to that reported in any other gymnosperm species [20–22]. The karyotype consists of one pair of long submetacentric chromosomes, one pair of short metacentric chromosomes, and 10 pairs of short subtelocentric chromosomes [16–18].

Though dioecy is widespread in gymnosperm plants (64.6%), only six (0.6%) species from three families are reported to possess sex chromosomes, one of which is *G. biloba* [23,24]. Identification of *G. biloba* sex chromosomes was attempted with optical microscopy and fluorescence *in situ* hybridization approaches but reported karyotypic variation was subsequently found not to be related to sex [17,18,25]. The early works studying sex determination in *G. biloba* reported both XY and ZW sex chromosome systems [17–19,25–28], while recent genome sequencing-based studies indicate that this species has male heterogamety [29,30]. Both of these genome-based studies of the *G. biloba* sex chromosomes reported the sex-determining regions (SDR) on chromosome 2 [29,30]. However, the location and size of the SDR remains contradictory, with one study stating that the SDR is small (4 Mb), including only 16 genes and located between megabases 380 and 384.6 [29], while the other study reported much larger (approx. 27 Mb) SDR including over 200 genes and located between megabases 48 and 75 [30]. Our analysis resolves this controversy and verifies the location of the SDR using an independent set of data.

2. Results

(a) Genetic mapping of the sex locus in *Ginkgo biloba*

To locate the *G. biloba* SDR region we created four genetic families by crossing wild and semi-cultivated trees of this species. These crosses involved three female and four male *G. biloba* individuals (table 1 and the electronic supplementary material, table S1). In addition to that, we sequenced the transcriptome of a male MG4-ZJLKY that was not used in the crosses. As the seedlings from the resulting F_1 seeds will not reach reproductive age for at least a quarter of a century, their sex was established using a polymerase chain reaction (PCR)-based approach (electronic supplementary material, figure S1) with a sex-specific marker reported previously [30]. The reliability of the PCR-based sex marker was confirmed on nine unrelated females and five unrelated male individuals with sex known from the phenotype (electronic supplementary material, figure S2). In total, this PCR-based approach identified 50 F_1 females and 51 F_1 males across the four genetic crosses analysed (electronic supplementary material, table S1).

In order to obtain genotypic information for coding regions of the *G. biloba* genome we used Illumina paired-end transcriptome sequencing for parents and F_1 progeny of the four crosses, which in total yielded 379.26 Gb of sequence data across the adult plants and 101 F_1 individuals (electronic supplementary material, table S1). These sequence reads were mapped to coding regions (CDS) annotated in the female reference genome [15], and single nucleotide polymorphisms (SNPs) were called and filtered as described in the methods.

Given the limited size of individual families (19 to 30 F_1-individuals per cross; electronic supplementary material, table S1), we included all four families in a joint analysis to increase resolution of the genetic map. The genetic map was reconstructed with the lepMap3 software [31]. The total length of the resulting female and male maps were 1173 cM and 1225 cM, respectively, and included 12 linkage groups (electronic supplementary material, table S2), which corresponds to the number of chromosomes in this species. The maps were based on 10 016 SNP markers in 4915 protein coding genes. The maps for individual linkage groups included 409 to 1262 SNPs in 206 to 594 genes (electronic supplementary material, table S2). The length of linkage groups ranged from 33 to 122 cM in the female map and from 47 to 143 cM in the male map.

The sex locus is mapped to the central part of chromosome 2. The map of chromosome 2 is based on 789 markers in 392 genes. The female and male maps for this chromosome were 90 and 109 cM long, respectively (figure 1). In the male map, the sex locus co-locates with

Downloaded from https://royalsocietypublishing.org/ on 21 March 2022

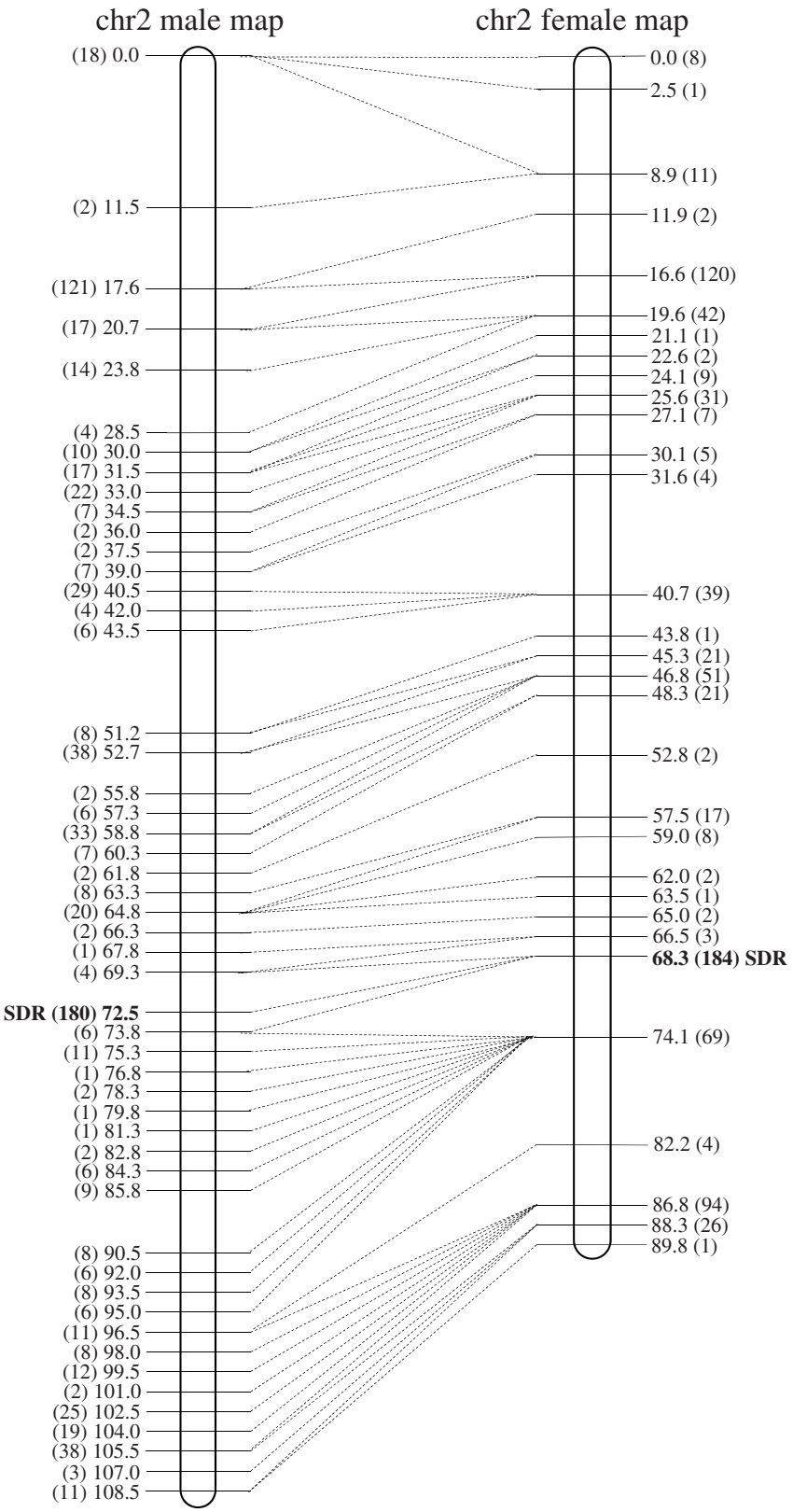

Figure 1. Male and female genetic maps for chromosome 2. Genetic positions (cM) are shown to the left of the male map and to the right of the female map. The numbers in brackets show how many markers co-locate to the same position in the map. The locations of the markers in the male and female maps are connected with a dashed line.

180 markers in 33 genes that all have the same genetic position (72.53 cM). In the female map, it co-locates with 184 markers in 34 genes at genetic position 68.34 cM (figure 1; electronic supplementary material, table S2). Co-location of multiple markers indicates that recombination is suppressed or reduced in the region around the sex locus in both male and female maps. Recombination suppression in the region around the sex locus was confirmed once the genetic maps were integrated with the genome sequence [15].

(b) Integration of the genetic map and the genome sequence

The combined analysis of the genetic map and the female reference genome [15] revealed that the order of genes is

Downloaded from https://royalsocietypublishing.org/ on 21 March 2022

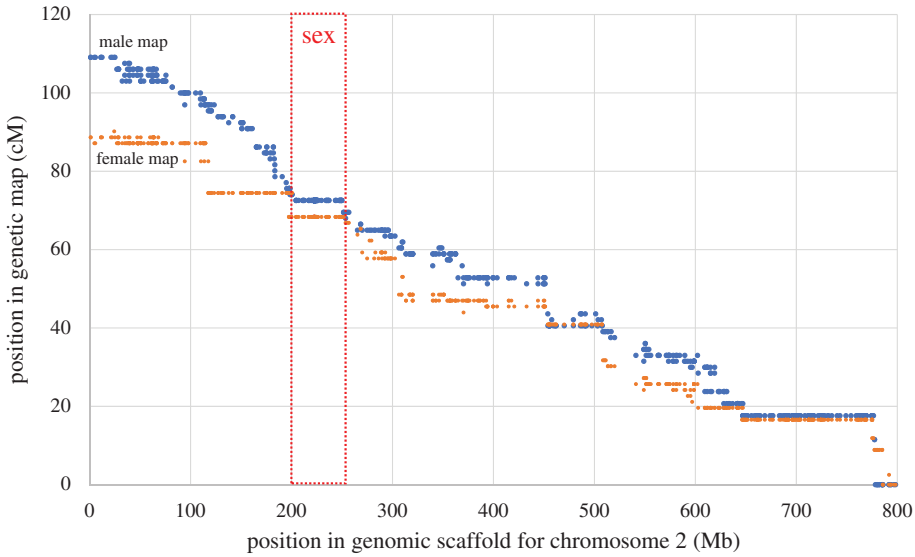

Figure 2. Genetic versus physical positions on chromosome 2 in the female *G. biloba* genome assembly [15] for male (blue) and female (orange) genetic maps. The dotted box shows the genomic location of the sex-determining locus, as located by genetic mapping. For other chromosomes see the electronic supplementary material, figure S3. (Online version in colour.)

mostly colinear for all chromosomes, except chromosomes 1 and 4 (electronic supplementary material, figure S3). According to the genetic map, the first approximately 400 Mb of the scaffold for chromosome 1 is misplaced in the genome assembly—this region should either be on the other side of chromosome 1 or it may belong to a different chromosome, as recombination distance between markers in this region and the rest of the chromosome 1 is over 90 cM (electronic supplementary material, figure S3). A similar problem is present on chromosome 4: the genetic distance between multiple markers in the first 200 Mb and the rest of chromosome 4 is over 90 cM (electronic supplementary material, figure S3), indicating that the first approximately 200 Mb of chromosome 4 should be moved to the other side of chromosome 4 or disconnected from this chromosomal scaffold. As fixing errors in the *G. biloba* genome sequence assembly is beyond the scope of the current paper, we flag these likely errors in the female genome reference [15] and leave their resolution to later studies.

Focusing on chromosome 2 and the SDR, the integrated map and female genome sequence [15] revealed that the region with reduced recombination surrounding the sex locus is approximately 50 Mb long (figure 2). It is flanked by genes *evm.chr2.722* and *evm.chr2.564* (electronic supplementary material, table S3) located at 251.7 and 200.8 Mb on chromosome 2 in the female *G. biloba* genome reference assembly [15]. According to the annotation of the reference sequence, this region contains 159 protein-coding genes, however, we were able to genetically map only 34 of these genes in the genetic map, with other genes probably missing informative markers owing to lack of polymorphic sites and/or low expression in our transcriptome sequence-based genotyping analysis.

(c) The size and age of the non-recombining Y-specific region

The size of the *G. biloba* non-recombing region surrounding the sex locus, obtained from our genetic mapping data is likely an overestimate, as rare recombination events in this region would not be detected with the relatively small number of F1 progeny analysed. To locate the non-recombining Y-specific region (NRY) boundaries more accurately we looked for SNPs that segregated as Y-linked in independent genetic crosses. As the males listed in table 1 are unrelated, the SNPs that are Y-specific in all the crosses are likely to be located in the NRY. Truly Y-linked SNPs are expected to never be found in females, while the SNPs closely linked to the NRY could be separated from the NRY by recombination and occasionally would be found in females. Our analysis of four genetic crosses identified 61 putative NRY SNPs in four adjacent genes (*evm.chr2.642* to *evm.chr2.645*; electronic supplementary material, table S3) located between 222.5 Mb and 223.9 Mb on the chromosome 2 genomic scaffold in the latest genome assembly [15]. None of these SNPs were present in any of the female F_1 or female parents analysed, which is consistent with location of these genes and SNPs in *G. biloba* NRY. It is worth noting that all four of these genes are actively expressed in both sexes (see below), so the presence of Y-SNPs only in males is not owing to male-specific expression of these genes.

The age of *Ginkgo* NRY could be measured from synonymous sequence divergence between the X- and Y-linked gametologues. Prior to NRY formation, recombination should have precluded accumulation of differences between the alleles, so the divergence between the homologous X- and Y-linked genes owing to neutral mutations (e.g. at synonymous codon positions) can serve as the clock measuring the time since recombination cessation. To measure this divergence, we reconstructed the sequences of Y-alleles for the X-linked genes located in the *G. biloba* sex-determining region. As described in the methods, this reconstruction is based on the identification of Y-specific sequence reads containing the Y-linked (male-specific) SNPs. That is why this analysis was done only for the four NRY genes described above, where such Y-SNPs were found.

For all NRY genes, the length of the reconstructed Y-linked sequence covered 100% of the length of the CDS of X-linked gametologues. The reconstructed Y-sequences were nearly

Downloaded from https://royalsocietypublishing.org/ on 21 March 2022

Table 2. Synonymous and non-synonymous divergence between the X- and Y-linked gametologs in the *G. biloba* non-recombining Y-specific region.

gene	CDS length	SynDif[a]	SynPos[b]	K_s[c]	NSynDif[d]	NSynPos[e]	K_a[f]	K_a/K_s
evm.chr2.642	1932	43.50	455.25	0.102	44.50	1476.75	0.031	0.30
evm.chr2.643	331	3.00	80.33	0.038	5.00	249.67	0.020	0.53
evm.chr2.644	1230	9.00	275.75	0.033	8.00	954.25	0.008	0.25
evm.chr2.645	2760	11.00	622.75	0.018	14.00	2137.25	0.007	0.37

[a]Number of synonymous differences.
[b]Number of synonymous positions analysed.
[c]Synonymous divergence.
[d]Number of non-synonymous differences.
[e]Number of non-synonymous positions analysed.
[f]Non-synonymous divergence.

identical to, but longer than the Y-sequences reconstructed for these genes by [30], see the electronic supplementary material, table S3 (sequences *MSTRG.230.1.p1*, *MSTRG.108.1.p1*, *MSTRG.304.2.p1* and *MSTRG.187.1.p1*, which were obtained from [30] by request). The reconstruction of the sequence for Y-linked gametologues allowed us to analyse X:Y divergence based on 80.33 to 622.75 synonymous sites per gene (table 2). Synonymous X:Y divergence (K_s) ranged from 1.8% for gene *evm.chr2.645* to 10.2% for gene *evm.chr2.642* (table 2). An estimate of the NRY age depends on the mutation rate and average generation time, neither of which are known for *G. biloba*. Given that *G. biloba* does not start reproducing until it is at least 25 years old, we can use $g \sim 25$ years as a minimal estimate of generation time. Gymnosperms have been reported to have a slower evolutionary rate compared to angiosperms [32], so we can assume that $m \sim 10^{-8}$ is a maximal estimate of the per nucleotide per generation mutation rate, which allows us to calculate the minimal age of the *G. biloba* NRY as $T = g\ K_s/2\ m = 25{*}0.1/2{*}10^{-8} = 125$ million years. We use the gene with $K_s = 0.1$ (for gene *evm.chr2.642*) in this calculation because the genes with lower K_s may have been added to NRY more recently, so their K_s may not reflect the age of the NRY. Alternatively, the variation in K_s among the NRY genes may reflect local variation in mutation rate, in which case it would be more appropriate to use the average $K_s = 0.048$ across all four NRY genes. This gives the minimal age of the *G. biloba* NRY as $T = g\ K_s/2\ m = 25{*}0.048/2{*}10^{-8} = 60$ million years.

(d) Do *Ginkgo biloba* non-recombining Y-specific region genes undergo degeneration?

In the absence of recombination, the efficacy of natural selection to eliminate deleterious mutations and fix advantageous mutations is reduced, which is expected to lead to genetic degeneration of genes in the non-recombining regions, such as is found in the non-recombining regions of the Y(or W)-chromosomes of many organisms [33,34].

Elevated substitution rate at non-synonymous positions is one of the signs of inefficient purifying selection and ongoing degeneration. In all the NRY genes analysed, non-synonymous divergence between the X- and Y-gametologues (K_a) was lower than synonymous divergence (K_s) (table 2). The K_a/K_s ratio ranged from 0.25 to 0.53, indicating the presence of relatively weak purifying selection eliminating deleterious mutations at non-synonymous sites of these sex-linked genes. To test whether the Y-linked alleles accumulate

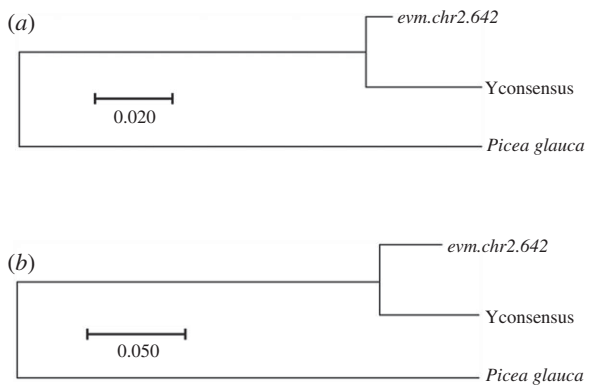

Figure 3. Maximum-likelihood phylogeny for the 1st (*a*) and 3rd (*b*) codon positions in the gene *evm.chr2.642*.

more non-synonymous substitutions compared to the corresponding X-linked alleles, as expected for genes in the non-recombining regions [33,34], we used homologous genes from an outgroup *Picea glauca* [35] to 'polarize' the pairwise X : Y divergence (figure 3), identifying the substitutions that occurred in the X- or Y-linked copies of the sex-linked genes. Tajima's relative rates test [36] revealed a significant excess of substitutions on the Y compared to the X at the 1st codon position of the *evm.chr2.642* gene (table 3 and figure 3). All other comparisons showed no significant difference in the number of substitutions on the X- and the Y-chromosomes.

Reduced expression of the Y- compared to the X-linked gametologues is another sign of ongoing genetic degeneration of Y-linked genes. The analysis of expression of sex-linked genes in males and females revealed that, as expected, expression of Y-alleles is not detectable in females, indicating that the expression of homologous X- and Y-linked genes are accurately distinguished in our expression analysis. Furthermore, comparing expression between the sexes, the X-linked genes in males were expressed at about twice the lower level compared to females (table 4), as expected from the number of copies of X-linked genes present in the two sexes, which is also consistent with accurate quantification of gene expression despite low divergence between homologous X- and Y-linked genes. In three out of four NRY genes in males, expression of X- and Y-linked genes was nearly identical (table 4). On the other hand, expression of the Y-linked copy of the *evm.chr2.643* gene was consistently (across the families) lower compared to its X-linked

Downloaded from https://royalsocietypublishing.org/ on 21 March 2022

Table 3. Tajima's relative rates test [36] comparing substitutions in the X- and Y-linked gametologues.

gene:	*evm.chr2.642*			*evm.chr2.643*			*evm.chr2.644*			*evm chr2.645*		
codon pos:	1st	2nd	3rd	1st	2nd	3rd	1st	2nd	3rd	1st	2nd	3rd
invariable:	515	574	408	100	100	79	317	261	298	198	208	170
substitutions:												
in X-allele	4	6	17	0	1	2	2	3	0	1	1	0
in Y-allele	**14***	6	23	2	2	1	2	6	2	0	1	0
in outgroup	100	49	179	5	4	25	34	86	55	56	45	84
chi^2	**5.56**	0.00	0.90	2.00	0.33	0.33	0.00	0.14	2.00	1.00	0.00	0.00
p	**0.018**	1.00	0.34	0.16	0.56	0.56	1.00	0.71	0.16	0.32	1.00	1.00

Table 4. Gene expression in four *G. biloba* genes on the X-chromosome in males (mX) and females (fXX) and the Y-chromosome in males (mY), shown separately for each of the genetic crosses (PH, DLB, LTM and LAB).

family (sample size)				median FPKMs		
gene_id	mY/mX	mXY/fXX	mX/fXX	fXX	mX	mY
PH (11F, 9M)						
evm.chr2.642	1.077	1.035	0.499	40.92	20.40	21.97
evm.chr2.643	0.829	0.783	0.428	32.99	14.13	11.71
evm.chr2.644	1.061	1.060	0.514	29.22	15.03	15.94
evm.chr2.645	1.246	0.995	0.509	15.75	8.01	9.98
DLB (12F, 14M)						
evm.chr2.642	1.301	1.141	0.496	33.68	16.70	21.72
evm.chr2.643	0.522	0.850	0.559	65.62	36.66	19.14
evm.chr2.644	1.076	1.149	0.554	24.89	13.78	14.83
evm.chr2.645	1.196	1.164	0.616	12.93	7.97	9.53
LTM (11F, 13M)						
evm.chr2.642	1.342	1.397	0.596	34.14	20.36	27.33
evm.chr2.643	0.620	0.620	0.383	54.50	20.86	12.94
evm.chr2.644	0.975	0.892	0.452	30.56	13.80	13.46
evm.chr2.645	1.146	0.988	0.536	14.58	7.82	8.96
LAB (10F, 13M)						
evm.chr2.642	1.087	0.971	0.465	44.91	20.90	22.71
evm.chr2.643	0.492	0.990	0.663	30.37	20.15	9.92
evm.chr2.644	1.168	0.926	0.427	31.42	13.43	15.68
evm.chr2.645	1.382	1.083	0.530	15.06	7.98	11.03

gametologues in males (table 4), suggesting partial degeneration or silencing of this gene on the Y-chromosome. No evidence of elevated expression of the X-linked copy of the *evm.chr2.643* gene to compensate for reduced expression of the Y-linked copy in males was found.

(e) The comparison of sex-linked genes between the studies

The comparison between the studies reveals that our four NRY genes represent reciprocal best blast hits with four out of more than 200 putatively sex-linked (PSL) genes reported by [30] and three of our NRY genes correspond to three of the 16 PSL genes reported by [29]. Furthermore, eight and 12 of the PSL genes reported by [29] and [30], respectively, represent reciprocal best blast hits with some of the genes in the approximately 50 Mb region around the NRY that showed no recombination in the genetic crosses described above (electronic supplementary material, table S3). PSL genes reported in the previous studies [29,30] have reciprocal best blast hits with genes on different chromosomes in the latest female genome assembly [15], though most PSL genes do show close homology with the genes on chromosome 2 (figure 4).

Downloaded from https://royalsocietypublishing.org/ on 21 March 2022

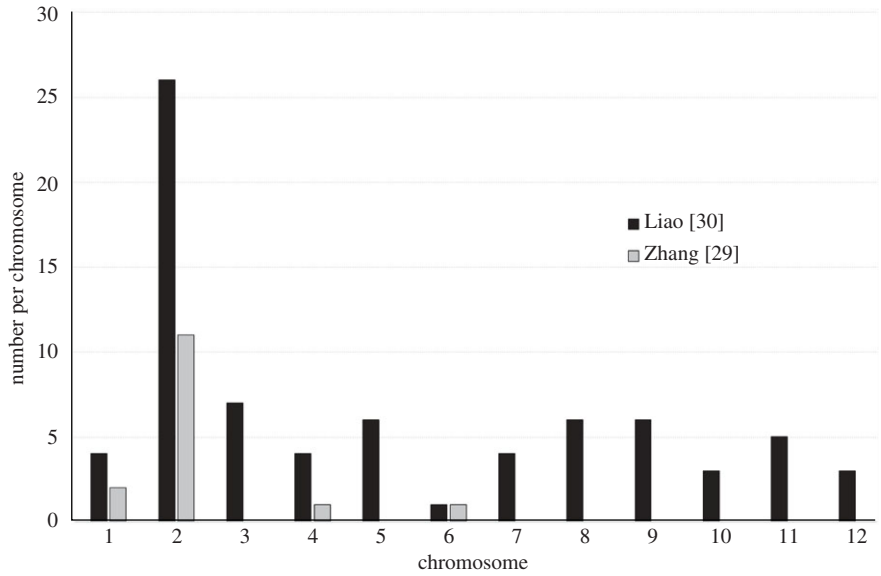

Figure 4. The distribution of best blast hits for putatively sex-linked genes from [29,30] across the 12 chromosomes in the latest *G. biloba* female genome assembly [15].

It is worth noting that the putative *G. biloba* sex-determining gene *GbMADS18* (Genbank accession MN548764.1) reported by [30] shows close homology (96.4% sequence identity) with gene *evm.chr2.641* that is adjacent to our four NRY genes, though the region of homology is quite short—only 137 bases. The absence of a complete *GbMADS18* gene in the female genome reference [15] is probably because the gene is Y-specific and present only in male genomes. No expression of the *GbMADS18* or *evm.chr2.641* genes was detected, hence they could not be used in our transcriptome-based analysis. NRY may include *evm.chr2.641* and a few other adjacent genes that could not be tested in our analysis owing to lack of expression. However, NRY is unlikely to be larger than 5 Mb and extend beyond *evm.chr2.638* and *evm.chr2.649* genes located at 220.99 Mb and 225.22 Mb of chromosome 2, respectively, because no Y-linked SNPs were found in these genes or any of the genes located at positions less than 220 Mb and greater than 225 Mb on the chromosome 2 (table 5; electronic supplementary material, table S3).

3. Discussion

In this paper, we focused on genetic mapping of the SDR in *G. biloba* using a set of four independent genetic crosses. This allowed us to build separate female and male genetic maps, integrating information across the genetic crosses. Overall, the male and female genetic maps are similar, but the male map tends to be slightly longer for most chromosomes, which is consistent with slight male bias in heterochiasmy in gymnosperms (e.g. fig. 1 in [37]). But the length difference between the male and female maps is minor and the rate and distribution of recombination in meiosis do not show large differences between the two sexes. This contrasts with many other species with fairly strong sex differences in overall recombination rate and distribution of crossovers along the chromosomes [38].

The use of SNPs in expressed genes as genetic markers allowed us to integrate the maps with the female genome sequence [15] and to measure the recombination rate in different genomic regions. This revealed several relatively short regions where recombination is reduced in both sexes, with no obvious pattern in the location of such regions in the chromosomes. In particular, we detected no evidence for large regions with reduced recombination in the middle of the chromosomes (presumably in pericentromeric regions), as reported for other plant species [39]. The standard karyotype of *G. biloba* is composed of 12 chromosome pairs with metacentric, submetacentric and subtelocentric chromosomes [17–19,25]. Thus, the lack of extended regions with low recombination in central parts of the chromosomes suggests that pericentromeric suppression of recombination is not extensive in *G. biloba*.

Our genetic mapping of the SDR located it to the central part of chromosome 2. The SDR locates to a region approximately 50 Mb long where recombination is rare or absent in both males and females. This situation contrasts with 'typical' sex chromosomes found in many animals (e.g. mammals, birds) and some plants (*Silene latifolia* [40], *Rumex hastatulus* [41]) where recombination is suppressed only on the sex-specific Y(or W)-chromosome, while the other sex chromosome X(or Z) recombines normally in the homogametic sex. Low recombination around the *G. biloba* SDR in both sexes suggests that in this species sex-determining gene(s) evolved in a region with pre-existing low recombination, as was also hypothesized for papaya [42]. Alternatively, recombination suppression around the SDR may have evolved after the rise of the sex locus in this region, as postulated by the classic 2-locus model of sex chromosome evolution [7], though, in the case of *G. biloba*, recombination suppression evolved in a non-sex-specific manner. In the absence of other *Ginkgo* species with different mating systems and/or sex chromosomes, it is difficult to test these hypotheses.

The location of the SDR on chromosome 2 is consistent with other studies [29,30], though the exact position of the SDR on that chromosome was contradictory. In particular, [29] reported that the SDR is located at 380.00 Mb–384.60 Mb on chromosome 2, while according to [30], it is located at 48 Mb–75 Mb on chromosome 2. This contradiction is partly owing to the use of different genomic references in these studies. The former study used the draft female genome assembly published by [14], while the latter used

Downloaded from https://royalsocietypublishing.org/ on 21 March 2022

Table 5. The comparison of SDR genes between the studies. The genes with male-specific Y-SNPs are highlighted in bold.

gene	Pos. (Mb)	Y-SNPs	Zhang [29]	Liao [30]	putative function
chr2.630	218.69	0			nucleolar GTP-binding protein 1-like
chr2.631	218.91				LURP-one-related 12-like protein
chr2.632	218.91				LURP-one-related 6-like protein
chr2.633	219.24				two-component response regulator-like PRR73
chr2.634	219.66				no homology
chr2.635	220.06			*MSTRG.35.1.p1*	putative disease resistance protein
chr2.636	220.18	0	*Gb_30344 (S3)*	*MSTRG.183.1.p2*	FGGY family of carbohydrate kinases
chr2.637	220.69	0		*MSTRG.399.2.p1*	adenosylmethionine-8-amino-7-oxononanoate aminotransferase
chr2.638	220.99	0	*Gb_30343 (S3)*		DAPA aminotransferase [*Arabidopsis thaliana*]
chr2.639	221.46		*Gb_28587 (S2)*		MADS-box transcription factor GbMADS9
chr2.640	221.71			*MSTRG.305.1.p1*	MADS-box transcription factor GbMADS4
chr2.641	222.14			*MSTRG.480.1.p1*	MADS-box transcription factor GbMADS10
chr2.642	222.55	**32**	*Gb_28585 (S2)*	*MSTRG.230.1.p1*	protein NUCLEAR FUSION DEFECTIVE 4-like
chr2.643	222.97	**5**	*Gb_28589 (S2)*	*MSTRG.108.1.p1*	alpha/beta hydrolase domain-containing protein 17B-like
chr2.644	223.53	**11**		*MSTRG.304.2.p1*	unknown protein
chr2.645	223.87	**13**	*Gb_15883 (S1)*	*MSTRG.187.1.p1*	two-component response regulator ORR24-like protein
chr2.646	224.37		*Gb_15885 (S1)*		lysine-specific demethylase JMJ706-like
chr2.647	224.49				no homology
chr2.648	224.88		*Gb_15886 (S1)*		brassinosteroid-related acyltransferase 1
chr2.649	225.1	0			pentatricopeptide repeat-containing protein At5g10690
chr2.650	225.42	0			calmodulin-binding protein 60C

an unpublished female assembly reported in the form of a PhD thesis [43] and unfortunately that genome assembly is not publicly available. It is possible that the unpublished assembly of [43], which was used as a reference sequence by [30], is the same as the latest 'nearly complete' publicly available *G. biloba* female genome assembly [15], though this is not clear from the papers. The location of the SDR around position 222 Mb in the latest assembly [15] contradicts the SDR location at 48 Mb–75 Mb on chromosome 2 reported by [30], suggesting that the assembly used by [43] and by [30] is different from the genome that is publicly available [15]. This makes it difficult to verify the results of [30] and work out the reasons for the discrepancies in reported SDR location between the papers.

On the X-chromosome, the SDR appears to comprise a fairly small (less than 5 Mb long) region, where recombination is entirely suppressed in males. The size of the corresponding NRY region is less clear. In our analysis, we focused on the genes present in the SDR region on the X-chromosome (in the genome assembly for a female *G. biloba* [15]) and their homologous on the Y-chromosome. Thus, any Y-specific genes that are not present on the X were missed in our analysis. Owing to the accumulation of repetitive DNA, and translocation of genes from other chromosomes to the Y-chromosome, as reported for other species (e.g. [44]), the NRY may be larger than the corresponding SDR region on the X-chromosome, which may partly account for the larger estimate of SDR size reported by [30], as that study reconstructed the Y-linked contigs based on male-specific k-mers. The highly dynamic nature of repetitive DNA in the NRY, with frequent inversions, gains and losses of genetic material owing to recombination between different copies, as described in other species [45], may also affect the NRY in *G. biloba*. This may cause the NRY region to vary in size among males of the same species, which could, at least partly, account for the controversy with cytogenetic reports of hetero- and homo-morphic sex chromosomes in *G. biloba* [17,18,25].

The fairly large size of the SDR (more than 200 genes) reported by [30] may be explained by the fact that they used a single sibling family in their analysis, which limited the number of recombination events detectable in the family of relatively small size (100 individuals). Given the approximately 50 Mb low-recombination region we detected around the SDR, all the genes in that region may appear completely sex-linked in a sibling family of limited size, yet, most of that region may not be fully sex-linked and occasionally recombine, which can be detected only by the analysis of multiple unrelated individuals, or using sibling families of very large size. As such, the more than 200 SDR genes reported by [30] are likely to be an overestimate of the actual size of the fully sex-linked region in *G. biloba*. It is more difficult to explain why reciprocal best blast hits for many of the putatively sex-linked genes identified by [30] are located on other chromosomes (figure 4), according to the latest genome assembly [15]. It is possible that the NRY is larger and contains many more genes than the corresponding region on the X-chromosome, including the genes transferred to the Y from other chromosomes. This may, at least partly, account for the homology of many sex-linked genes reported by [30] to genes on other chromosomes.

Downloaded from https://royalsocietypublishing.org/ on 21 March 2022

The age of the *G. biloba* SDR, as inferred from our analysis of synonymous divergence for X- and Y-linked gametologues, is comparable to ancient sex chromosomes in mammals [46,47] and birds [48], and it is older than in many other plant species analysed, such as *Silene* [49], *Rumex* [50], papaya [42], *Asparagus* [51]. Our estimate of the *G. biloba* SDR age contrasts with the much lower estimate of approximately 14 Myr reported by Zhang *et al.* [29]. The estimate of the SDR age in *G. biloba* critically depends on the assumptions of the per-base per-generation mutation rate and generation time, which are not known for this species. The higher mutation rate and shorter generation time would lead to younger estimates of the SDR age and it is not clear what values for these parameters were used by Zhang *et al.* [29] to estimate the age of SDR. We used a minimal estimate of the generation time (25 years) and a fairly high ad hoc mutation rate (10^{-8} mutations per site per generation) to obtain the minimal age of the non-recombining region on the Y-chromosome (approx. 125 million years). Given that *G. biloba* can live for hundreds of years and it does not start reproducing until it is at least 25 years old, its average generation time is probably much higher than 25 years. Based on the divergence between pine and spruce at synonymous sites of 3723 orthologous, it was reported that the substitution rate in conifers is approximately 0.68×10^{-9} per synonymous site per year [32]. Assuming this substitution rate for *Ginkgo*, we get an estimate $T = K_s/2m = 0.1/0.68{*}10^{-9}{\sim}147$ million years for the age of *G. biloba* sex chromosomes. However, this is also likely to be an underestimate because [32] estimated the substitution rate for fast-growing pine and spruce, while slow-growing *G. biloba* is likely to have a longer generation time and hence a slower per-year substitution rate assuming the same per-generation mutation rate.

The limited number of genes with X- and Y-linked sequences available to calculate X:Y divergence, and variation of synonymous X:Y divergence among the genes (table 2) present additional difficulties for estimation of the SDR age in *G. biloba*. To obtain a conservative minimal estimate for the SDR age one can average synonymous X:Y divergence across the four NRY genes, which gives $K_s = 0.048$, placing the minimal estimate for the sex chromosome age in *Ginkgo* at the Cretaceous–Palaeogene boundary, assuming 25 years as generation time and 10^{-8} as per-nucleotide per generation mutation rate. It is difficult to reliably estimate the age of *G. biloba* sex chromosomes based on so few genes, but it is clear that the *Ginkgo* SDR is at least of Cretaceous origin. This conclusion fits well with the palaeontological evidence: in the 121 Myr old fossil, ovulate organs of *Ginkgo* are similar to those of the present-day *G. biloba*, while the *Ginkgo* plants from the Jurassic appear to have a more primitive type of reproductive organs [9,11]. Furthermore, the depth of the X:Y clade relative to the total depth of the phylogeny (figure 3) is also consistent with Cretaceous origin of the *Ginkgo* SDR, assuming the divergence of Ginkgoales from other gymnosperms back in the Palaeozoic [11]. As such, the SDR age is probably older than the age of the species *G. biloba* that is thought to have originated less than 50 Ma [9].

Our conclusion that *Ginkgo* sex chromosomes are at least of Cretaceous origin goes against the claim of [29] that the SDR originated in the last 14 million years. However, the authors of that paper reconstructed Y-linked alleles only for the genes with low X:Y divergence in the areas of the SDR they called S1 and S3. Y-alleles in the older part of the SDR (called S2 in [29]) were not reconstructed, so they could not estimate the age for the oldest part of the sex chromosomes. Two (*evm.chr2.642* and *evm.chr2.643*) out of four genes with Y-linked SNPs we used for reconstruction of Y-alleles (table 2) are located in the older S2 area of the SDR (table 5). These two genes do show the highest X:Y divergence (table 2), leading to older SDR age inferred in our study.

The variation in synonymous X:Y divergence across the genes (table 2) may reflect an expansion of the NRY over time. The order of genes on the genomic scaffold from *evm.chr2.642* having the highest X:Y divergence ($K_s = 0.1$) to *evm.chr2.645* having the lowest divergence ($K_s = 0.02$) is consistent with such expansion. The model of NRY expansion over time seemingly contradicts our observation that recombination around the SDR in *G. biloba* is reduced in both sexes. However, the recombination suppression in the approximately 50 Mb region around the SDR is incomplete, as indicated by the lack of Y-specific SNPs outside the small NRY region. Thus, pre-existing reduced recombination in the approximately 50 Mb region around the SDR does not contradict the gradual expansion of the small NRY region where recombination is suppressed completely.

Our analysis detected little evidence for genetic degeneration of Y-linked genes. A slight reduction of the Y- compared to X-expression for gene *evm.chr2.643*, and significantly faster non-synonymous substitution rate in the Y- compared to X-linked gametologues of the *evm.chr2.642* gene, were the only signs of ongoing Y-degeneration. This may seem surprising given our conclusion that the *Ginkgo* SDR is fairly ancient [52]. However, the rate of genetic degeneration depends on the number of genes linked together in the NRY. In particular, with relatively few functional genes left on the old Y(or W)-chromosomes in mammals and birds the rate of degeneration is expected to be very slow [53,54]. Thus, in small NRYs, such as the one found in *G. biloba*, genes are not expected to undergo rapid degeneration. Furthermore, the long generation time of *G. biloba* and its (likely) low mutation rate, result in a fairly slow rate of molecular evolution, which is also expected to slow down the process of genetic degeneration.

4. Conclusion

Our paper resolves the ambiguities and contradictions present in the literature [29,30] regarding the location of the sex-determining region in *G. biloba* genome. The results of our analyses indicate that the SDR is located in the central part (around megabase 222) of chromosome 2 in the latest 'nearly complete' assembly of the female *G. biloba* genome [15]. The region of chromosome 2 (the X) around the sex-determining region where recombination in males is suppressed completely is fairly small—it is at least 1.3 Mb and probably less than 5 Mb long. The size of the corresponding NRY region is unclear, but may be larger owing to accumulation of repetitive DNA, which typically occurs in non-recombining regions. The small SDR is embedded into an approximately 50 Mb long genomic region where recombination is reduced in both sexes, but does occur occasionally, which prevents the divergence between the X- and Y-linked alleles of the genes in this region. The NRY appears to have expanded over time, though these expansion(s) were small,

Downloaded from https://royalsocietypublishing.org/ on 21 March 2022

adding only a few genes to the NRY. The divergence between the X- and Y-linked gametologues is modest (K_s less than 10%), which prompted the previous study to claim that *G. biloba* sex chromosomes are of 'recent origin' [29]. However, our analysis shows that *Ginkgo* sex chromosomes are at least of Cretaceous origin and the relatively low rate of synonymous X:Y divergence reflects the slow evolution of this species owing to long generation time and (likely) low mutation rate.

5. Methods

(a) Genetic crosses

Three female and four male trees of *G. biloba* were selected as candidates for genetic crosses. Accession information is listed in the electronic supplementary material, table S1. Artificial pollinations were conducted in the county of Pingtian, Nanxiong, Guangdong Province, in southern China. Large population size and numerous old trees of *G. biloba* have been identified and documented in Nanxiong, which is thought to be one of the glacial refugia of *Ginkgo* as revealed by genetic diversity analysis [55]. To ensure a high seed rate, we chose three female *Ginkgo* trees which are recorded to possess high seed production and documented to have an average age of more than 100 years. Three male *Ginkgo* trees were also selected in the same county of Pingtian. They are recorded as wild trees over 1000 years old, having a diameter at breast height of more than 80 cm and a height of approximately 20 m. One other male *Ginkgo* tree was chosen from Tianmu Mountain, Lin'an, Zhejiang Province, in eastern China. This tree is also growing in a refugium population of *Ginkgo*. In April, 2016, the branches of the female trees were wrapped with parchment paper and the male flowers from the nearby male trees were all removed before flowering to avoid any pollen pollution. Artificial pollinations were conducted for four crosses: LAB (MG1_NXAB × FG3_NXLBT3), DLB (MG2_NXDLB × FG1_NXDLB), PH (MG3_NXPH × FG2_NXLBT2) and LTM (MG5_ZJTM × FG3_NXLBT3). For each cross, more than 100 seeds were collected and germinated. In total, 101 *Ginkgo* F_1 seedlings were grown in the greenhouse. In the spring of 2017, leaves were collected and total RNA extracted using RNA Easy Fast (DP452) according to the manufacturer's instructions (Tiangen Biotech (Beijing) Co., Ltd.).

(b) Sex identification of F_1 progeny

We used the primer pairs of the Y-linked gene *GbMADS18* reported by [30] to identify the sex of the F_1 progeny. The male and female parents and several other *Ginkgo* trees with known sex were also tested as controls for accurate sex identification. The PCR-based marker produced a 1030 bp fragment precisely and robustly only in male leaf samples, while only positive control bands were amplified in female leaf samples. The PCR reactions were carried out in a total volume of 25 µl, containing 12 ng of template DNA, 1.25 units of Taq DNA polymerase, 0.8 µM of forward and reverse primer, 0.2 µM of dNTP, 2 mM of $MgCl_2$, 2.5 µl of 10× PCR buffer and 14.25 µl of sterilized double-distilled water. Thermo cycling conditions were: initial denaturation at 94°C for 5 min; 32 cycles of denaturation at 94°C for 30 s, annealing at 57°C for 30 s and polymerization at 72°C for 45 s; and a final elongation step at 72°C for 5 min. The amplified fragments were visualized via gel documentation Tanon 3500. The upper band shows the positive control and the lower band is the Y-specific marker (electronic supplementary material, figures S1, S2).

(c) Transcriptome sequencing and data processing

Paired-end Illumina transcriptome sequencing was conducted by Novogene Co. Ltd. for parents and F_1 progeny of the four crosses. All sequence reads were submitted to the SRA database under project number PRJNA758727. For the complete list of samples and accession numbers see the electronic supplementary material, table S1.

Quality checking of the sequence reads was done with *FastQC* v. 0.11 (available from http://www.bioinformatics.babraham.ac.uk/projects/fastqc). *CutAdapt* v. 1.4 [56] and *Trimmomatic* v. 0.32 [57] were used to remove Illumina adapters and to trim low-quality bases at the ends of the reads. Trimming was done for leading and trailing bases with quality below 5, as well as for bases with the average quality less than 15 per 4 consecutive bases. Reads shorter than 36 bases after trimming were discarded.

For expression analysis, RNA-seq reads were mapped to the CDS sequences from the reference genome [15] and gene expression measured using *RSEM* v. 1.3.3 [58] with default parameters. As shown in our previous work, this approach is sufficiently accurate to distinguish the expression of X- and Y-linked gametologues with divergence greater than 1% [59].

For SNP calling, RNA-seq reads were mapped to the CDS sequences extracted from the reference genome [15], with *bwa-mem* v. 0.7.17-r1188 [60]. Duplicated reads were removed with *Picard* v. 2.26 (https://broadinstitute.github.io/picard/). The genome analyses toolkit (*GATK*) v. 4.1.2.0 [61] was then used for base quality recalibration, local realignment around insertions/deletions. The resulting bam files were sorted, indexed and used for SNP calling with *samtools* v. 1.7 [62]. The resulting multi-sample vcf file with SNP calls for parents and F_1 progeny of the four crosses was used for reconstruction of the genetic map and location of the sex-determining region.

(d) Construction of genetic maps

For genetic mapping we used *lepMap3* v. 0.2 [31]. Before construction of genetic maps, the relatedness of parents and progeny was checked with the identity by descent (*IBD*) tool in *lepMap3* [31]. For this purpose, we used a subset of 5000 SNPs selected randomly across the genome. As expected, most F_1 individuals had approximately 0.5 identity to each of the parents, while five F_1 individuals in the PH cross (PH203, PH208, PH221, PH224 and PH232) had lower *IBD* (less than 0.35) with their presumed father (MG3) and were excluded from analyses as possible contaminants. The remaining individuals were used to call the parental genotypes with the *ParentCall2* module of *lepMap3*, including parameter halfSibs = 1 to take into account the half-sibling family structure. SNP filtering was done with *Filtering2* module of the *lepMap3*, with parameter dataTolerance = 0.001, to exclude the markers showing distorted segregation. The resulting filtered SNPs were used to define linkage groups with *SeparateChromosomes2* module of *lepMap3*, with default parameters (lodLimit = 10). Additional markers were added to linkage groups with *JoinSingles2All* with lodLimit = 8 and lodDifference = 2. The markers on each of the chromosomes were ordered and recombination distances were measured with *OrderMarkers2* tool in the *lepMap3* software [31].

To locate the position of the sex locus in the genetic map we added a 'sexSNP' to the filtered set of SNPs prior to genetic mapping. The sexSNP was heterozygous in all males and homozygous for the same allele in all females, corresponding to male heterogamety of *G. biloba* reported by the previous studies [29,30]. *OrderMarkers2* placed the sexSNP next to gene *evm.chr2.642* in the non-recombining block of markers on chromosome 2 located at 72.53 and 68.34 cM in the male and female maps, respectively. Consistent with the location of the sexSNP in the genetic map, the same block of markers contained the genes with Y-specific SNPs and was also the hotspot for reciprocal best blast hits for sex-linked genes identified in the previous studies (table 5; electronic supplementary material,

Downloaded from https://royalsocietypublishing.org/ on 21 March 2022

table S3). We reasoned that this block of genes corresponds to, or contains *G. biloba* SDR.

Reconstruction of the Y-linked gametologues for X-linked genes was based on the presence of Y-specific SNPs that were detected in four of the genes in the non-recombining block of markers on chromosome 2. Such Y-SNPs represent SNP positions where all males have the alternative allele in heterozygous configuration and all females have the homozygous reference allele, in the genes transcribed in both sexes. The number of SNPs and Y-SNPs per gene in the non-recombining block of genes on chromosome 2 are listed in the electronic supplementary material, table S3. The reads mapping to the X-linked genes with Y-SNPs were extracted from bam files with a combination of *samtools* and *grep* programs. The resulting gene-specific sam files were processed with the custom-written *filterSAMbyVCF* v. 0.1 program (available at https://filtersambyvcf.sourceforge.io) to separate the sequence reads containing the Y-SNPs, along with their paired reads into a separate Y.sam file. The Y.sam file was subsequently used to call Y-consensus with *ProSeq3* v. 3.994 [63].

(e) Evolutionary genetic analyses

Tajima's relative rates test [36], as implemented in *MEGA* v. 10.1.5 software [64], was conducted separately for three codon positions in each of the four genes with X- and Y-linked sequences available for analysis (table 3). Pairwise sequence divergence at silent and non-silent sites (table 2), as well as the phylogeny reconstruction (figure 3) were conducted with *MEGA* software [64]. The outgroup sequences from *Picea glauca* were found with NCBI *blastn*. The tripartite alignments including X-linked, Y-linked and the outgroup sequence for genes *evm.chr2.642* to *evm.chr2.645* were created and manually checked with *ProSeq3* [63].

Data accessibility. Newly generated transcriptome sequence data were submitted to NCBI under BioProject no. PRJNA758727. The accession numbers for individual samples are listed in the electronic supplementary material, table S1 [65].

Authors' contributions. W.G.: data curation, funding acquisition, investigation, validation, writing—review and editing; D.A.F.: conceptualization, formal analysis, funding acquisition, investigation, methodology, project administration, software, supervision, writing—original draft, writing—review and editing.

All authors gave final approval for publication and agreed to be held accountable for the work performed therein.

Competing interests. We declare we have no competing interests.

Funding. This work was supported by the funding to W.G. from the National Natural Science Foundation of China (31470312), Science and Technology Planning Project of Guangdong Province, China (2016A030303048), and funding to D.A.F. from the BBSRC grant BB/P009808/1.

Acknowledgements. We thank Juan Zhou and Hui Zhou for their assistance in both field and laboratory work, and Fatima Ammar and Niels Müller for careful proofreading of the manuscript. Special thanks goes to Huiyuan Deng for offering help during artificial pollinations and seeds collection.

References

1. Renner SS. 2014 The relative and absolute frequencies of angiosperm sexual systems: dioecy, monoecy, gynodioecy, and an updated online database. *Am. J. Bot.* **101**, 1588–1596. (doi:10.3732/ajb.1400196)
2. Charlesworth D. 2019 Young sex chromosomes in plants and animals. *New Phytol.* **224**, 1095–1107. (doi:10.1111/nph.16002)
3. Lloyd DG. 1979 Parental strategies of angiosperms. *N. Z. J. Bot.* **17**, 595–606. (doi:10.1080/0028825X.1979.10432573)
4. Yakimowski SB, Barrett SC. 2016 The role of hybridization in the evolution of sexual system diversity in a clonal, aquatic plant. *Evolution* **70**, 1200–1211. (doi:10.1111/evo.12941)
5. Renner SS, Ricklefs RE. 1995 Dioecy and its correlates in the flowering plants. *Am. J. Bot.* **82**, 596–606. (doi:10.2307/2445418)
6. Barrett SC. 2010 Understanding plant reproductive diversity. *Phil. Trans. R. Soc.* **365**, 99–109. (doi:10.1098/rstb.2009.0199)
7. Charlesworth B, Charlesworth D. 1978 Model for evolution of dioecy and gynodioecy. *Am. Nat.* **112**, 975–997. (doi:10.1086/283342)
8. Walas Ł, Mandryk W, Thomas PA, Tyrała-Wierucka Ż, Iszkuło G. 2018 Sexual systems in gymnosperms: a review. *Basic Appl. Ecol.* **31**, 1–9. (doi:10.1016/j.baae.2018.05.009)
9. Zhou Z, Zheng S. 2003 The missing link in *Ginkgo* evolution. *Nature* **423**, 821–822. (doi:10.1038/423821a)
10. Crane PR, Manchester SR, Dilcher DL. 1990 A preliminary survey of fossil leaves and well-preserved plant reproductive structures from the Sentinel Butte Formation (Paleocene) near Almont. North Dakota. *Fieldiana Geol.* **20**, 1–63.
11. Zhou ZY. 2009 An overview of fossil Ginkgoales. *Palaeoworld* **18**, 1–22. (doi:10.1016/j.palwor.2009.01.001)
12. Nagataa T, Hasebeb M, Toribab T, Tanedac H, Crane PR. 2016 Sex conversion in *Ginkgo biloba* (Ginkgoaceae). *J. Jpn Bot.* **91**, 120–127.
13. Leslie AB, Beaulieu JM, Crane PR, Donoghue MJ. 2013 Explaining the distribution of breeding and dispersal syndromes in conifers. *Proc. R. Soc. B* **280**, 20131812. (doi:10.1098/rspb.2013.1812)
14. Guan R *et al.* 2016 Draft genome of the living fossil *Ginkgo biloba*. *Gigascience* **5**, s13742-016. (doi:10.1186/s13742-016-0154-1)
15. Liu H *et al.* 2021 The nearly complete genome of *Ginkgo biloba* illuminates gymnosperm evolution. *Nat. Plants* **7**, 748–756. (doi:10.1038/s41477-021-00933-x)
16. Hizume M. 1997 Chromosomes of *Ginkgo biloba*. In *Ginkgo biloba, a global treasure: from biology to medicine* (eds T Hori, RW Ridge, PD Tulecke, J Tredici, J Tremouillaux-Guiller, H Tobe), pp. 109–119. Tokyo, Japan: Springer Verlag.
17. Lee CL. 1954 Sex chromosomes in *Ginkgo biloba*. *Am. J. Bot.* **41**, 545–549. (doi:10.1002/j.1537-2197.1954.tb14376.x)
18. Newcomer EH. 1954 The karyotype and possible sex chromosomes of *Ginkgo biloba*. *Am. J. Bot.* **41**, 542–545. (doi:10.1002/j.1537-2197.1954.tb14375.x)
19. Tanaka N, Takemasa N, Sinoto Y. 1952 Karyotype analysis in gymnospermae. I. Karyotype and chromosome bridge in the young leaf meristem of *Ginkgo biloba* L. *Cytologia (Tokyo)* **17**, 112–123. (doi:10.1508/cytologia.17.112)
20. Mehra PN, Khoshoo TX. 1956 Cytology of conifers. II. *J. Genet.* **54**, 181–185. (doi:10.1007/BF02981709)
21. Mehra PN. 1956 Cytology of conifers. I. *J. Genet.* **54**, 165–180. (doi:10.1007/BF02981708)
22. Sax KC, Sax HJ. 1933 Chromosome number and morphology in the conifers. *J. Arnold Arbor.* **14**, 356–375. (doi:10.5962/bhl.part.9959)
23. Ming R, Bendahmane A, Renner SS. 2011 Sex chromosomes in land plants. *Annu. Rev. Plant Biol.* **62**, 485–514. (doi:10.1146/annurev-arplant-042110-103914)
24. Ohri D, Rastogi S. 2020 Sex determination in gymnosperms. *Nucleus* **63**, 75–80. (doi:10.1007/s13237-019-00297-w)
25. Pollock EG. 1957 The sex chromosomes of the maidenhair tree. *J. Heredity* **48**, 290–294. (doi:10.1093/oxfordjournals.jhered.a106747)
26. Lan TY, Chen R, Li XL, Dong F, Qi Y, Song W. 2008 Microdissection and painting of the W chromosome in *Ginkgo biloba* showed different labelling patterns. *Bot. Stud.* **49**, 33–37.
27. Chen R, Song W, Li X, An Z. 1987 Study on the sex chromosomes of *Ginkgo biloba*. *Cathaya* **5**, 41–48.
28. Ho T. 1963 The nucleolar chromosomes of the maiden-hair tree. *J. Heredity* **54**, 67–74. (doi:10.1093/oxfordjournals.jhered.a107227)

Downloaded from https://royalsocietypublishing.org/ on 21 March 2022

29. Zhang H *et al*. 2019 Recent origin of an XX/XY sex-determination system in the ancient plant lineage *Ginkgo biloba*. *bioRxiv* (doi:10.1101/517946)
30. Liao Q *et al.* 2020 The genomic architecture of the sex-determining region and sex-related metabolic variation in *Ginkgo biloba*. *Plant J.* **104**, 1399–1409. (doi:10.1111/tpj.15009)
31. Rastas P. 2017 Lep-MAP3: robust linkage mapping even for low-coverage whole genome sequencing data. *Bioinformatics* **33**, 3726–3732. (doi:10.1093/bioinformatics/btx494)
32. Buschiazzo E, Ritland C, Bohlmann J, Ritland K. 2012 Slow but not low: genomic comparisons reveal slower evolutionary rate and higher dN/dS in conifers compared to angiosperms. *BMC Evol. Biol.* **12**, 8. (doi:10.1186/1471-2148-12-8)
33. Charlesworth B, Charlesworth D. 2000 The degeneration of Y chromosomes. *Phil. Trans. R. Soc. B* **355**, 1563–1572. (doi:10.1098/rstb.2000.0717)
34. Bachtrog D. 2013 Y-chromosome evolution: emerging insights into processes of Y-chromosome degeneration. *Nat. Rev. Genet.* **14**, 113–124. (doi:10.1038/nrg3366)
35. Nystedt B *et al.* 2013 The Norway spruce genome sequence and conifer genome evolution. *Nature* **497**, 579–584. (doi:10.1038/nature12211)
36. Tajima F. 1993 Simple methods for testing the molecular evolutionary clock hypothesis. *Genetics* **135**, 599–607. (doi:10.1093/genetics/135.2.599)
37. Brandvain Y, Coop G. 2012 Scrambling eggs: meiotic drive and the evolution of female recombination rates. *Genetics* **190**, 709–723. (doi:10.1534/genetics.111.136721)
38. Sardell JM, Kirkpatrick M. 2020 Sex differences in the recombination landscape. *Am. Nat.* **195**, 361–379. (doi:10.1086/704943)
39. Rifkin JL, Beaudry FEG, Humphries Z, Choudhury BI, Barrett SCH, Wright SI. 2021 Widespread recombination suppression facilitates plant sex chromosome evolution. *Mol. Biol. Evol.* **38**, 1018–1030. (doi:10.1093/molbev/msaa271)
40. Filatov DA. 2005 Evolutionary history of *Silene latifolia* sex chromosomes revealed by genetic mapping of four genes. *Genetics* **170**, 975–979. (doi:10.1534/genetics.104.037069)
41. Hough J, Hollister JD, Wang W, Barrett SC, Wright SI. 2014 Genetic degeneration of old and young Y chromosomes in the flowering plant *Rumex hastatulus*. *Proc. Natl Acad. Sci. USA* **111**, 7713–7718. (doi:10.1073/pnas.1319227111)
42. Wang J *et al.* 2012 Sequencing papaya X and Yh chromosomes reveals molecular basis of incipient sex chromosome evolution. *Proc. Natl Acad. Sci. USA* **109**, 13 710–13 715. (doi:10.1073/pnas.1207833109)
43. Liu H. 2018 The whole genome sequencing and analyzing of *Ginkgo biloba*. PhD thesis, Nanjing For. University, Nanjing, People's Republic of China.
44. Tobler R, Nolte V, Schlotterer C. 2017 High rate of translocation-based gene birth on the *Drosophila* Y chromosome. *Proc. Natl Acad. Sci. USA* **114**, 11 721–11 726. (doi:10.1073/pnas.1706502114)
45. Rozen S, Skaletsky H, Marszalek JD, Minx PJ, Cordum HS, Waterston RH, Wilson RK, Page DC. 2003 Abundant gene conversion between arms of palindromes in human and ape Y chromosomes. *Nature* **423**, 873–876. (doi:10.1038/nature01723)
46. Graves JA. 1995 The evolution of mammalian sex chromosomes and the origin of sex determining genes. *Phil. Trans. R. Soc. Lond. B* **350**, 305–311. (doi:10.1098/rstb.1995.0166)
47. Graves JAM. 2015 Weird mammals provide insights into the evolution of mammalian sex chromosomes and dosage compensation. *J. Genet.* **94**, 567–574. (doi:10.1007/s12041-015-0572-3)
48. Zhou Q, Zhang J, Bachtrog D, An N, Huang Q, Jarvis ED, Gilbert MTP, Zhang G. 2014 Complex evolutionary trajectories of sex chromosomes across bird taxa. *Science* **346**, 1332. (doi:10.1126/science.1246338)
49. Krasovec M, Chester M, Ridout K, Filatov DA. 2018 The mutation rate and the age of the sex chromosomes in *Silene latifolia*. *Curr. Biol.* **28**, 1832–1838. (doi:10.1016/j.cub.2018.04.069)
50. Navajas-Perez R, de la Herran R, Gonzalez GL, Jamilena M, Lozano R, Rejon CR, Rejon MR, Garrido-Ramos MA. 2005 The evolution of reproductive systems and sex-determining mechanisms within *Rumex* (Polygonaceae) inferred from nuclear and chloroplastidial sequence data. *Mol. Biol. Evol.* **29**, 1929–1939. (doi:10.1093/molbev/msi186)
51. Harkess A *et al.* 2017 The asparagus genome sheds light on the origin and evolution of a young Y chromosome. *Nat. Commun.* **8**, 1279. (doi:10.1038/s41467-017-01064-8)
52. Renner SS, Müller NA. 2021 Plant sex chromosomes defy evolutionary models of expanding recombination suppression and genetic degeneration. *Nat. Plants* **7**, 392–402. (doi:10.1038/s41477-021-00884-3)
53. Bachtrog D. 2008 The temporal dynamics of processes underlying Y chromosome degeneration. *Genetics* **179**, 1513–1525. (doi:10.1534/genetics.107.084012)
54. Hughes JF *et al.* 2012 Strict evolutionary conservation followed rapid gene loss on human and rhesus Y chromosomes. *Nature* **483**, 82–86. (doi:10.1038/nature10843)
55. Zhao YP *et al.* 2019 Resequencing 545 ginkgo genomes across the world reveals the evolutionary history of the living fossil. *Nat. Commun.* **10**, 4201. (doi:10.1038/s41467-019-12133-5)
56. Martin M. 2011 Cutadapt removes adapter sequences from high-throughput sequencing reads. *EMBnet J.* **17**, 10–12. (doi:10.14806/ej.17.1.200)
57. Bolger AM, Lohse M, Usadel B. 2014 Trimmomatic: a flexible trimmer for Illumina sequence data. *Bioinformatics* **30**, 2114–2120. (doi:10.1093/bioinformatics/btu170)
58. Li B, Dewey CN. 2011 RSEM: accurate transcript quantification from RNA-Seq data with or without a reference genome. *BMC Bioinf.* **12**, 323. (doi:10.1186/1471-2105-12-323)
59. Papadopulos AS, Chester M, Ridout K, Filatov DA. 2015 Rapid Y degeneration and dosage compensation in plant sex chromosomes. *Proc. Natl Acad. Sci. USA* **112**, 13 021–13 026. (doi:10.1073/pnas.1508454112)
60. Li H, Durbin R. 2009 Fast and accurate short read alignment with Burrows-Wheeler transform. *Bioinformatics* **25**, 1754–1760. (doi:10.1093/bioinformatics/btp324)
61. McKenna A *et al.* 2010 The genome analysis toolkit: a MapReduce framework for analyzing next-generation DNA sequencing data. *Genome Res.* **20**, 1297–1303. (doi:10.1101/gr.107524.110)
62. Li H *et al.* 2009 The sequence alignment/map format and SAMtools. *Bioinformatics* **25**, 2078–2079. (doi:10.1093/bioinformatics/btp352)
63. Filatov DA. 2009 Processing and population genetic analysis of multigenic datasets with ProSeq3 software. *Bioinformatics* **25**, 3189–3190. (doi:10.1093/bioinformatics/btp572)
64. Kumar S, Stecher G, Li M, Knyaz C, Tamura K. 2018 MEGA X: molecular evolutionary genetics analysis across computing platforms. *Mol. Biol. Evol.* **35**, 1547–1549. (doi:10.1093/molbev/msy096)
65. Gong W, Filatov DA. 2022 Evolution of the sex-determining region in *Ginkgo biloba*. Figshare.

JSE Journal of Systematics and Evolution

doi: 10.1111/jse.12166

Research Article

DNA barcodes identify Chinese medicinal plants and detect geographical patterns of *Sinosenecio* (Asteraceae)

Wei Gong[1†], Ying Liu[2†], Jing Chen[3], Yu Hong[4,5], and Hang-Hui Kong[4*]

[1]College of Life Sciences, South China Agricultural University, Guangzhou 510642, China
[2]School of Life Sciences, Sun Yat-sen University, Guangzhou 510275, China
[3]College of Life Science, Zhejiang Chinese Medical University, Hangzhou 310053, China
[4]Key Laboratory of Plant Resources Conservation and Sustainable Utilization, South China Botanical Garden, Chinese Academy of Sciences, Guangzhou 510650, China
[5]University of Chinese Academy of Sciences, Beijing 100049, China
[†]These authors contributed equally to this work.
*Author for correspondence. E-mail: konghh@scbg.ac.cn.
Received 8 April 2015; Accepted 3 June 2015; Article first published online 28 July 2015

Abstract DNA barcodes have proved to be efficient for plants species discrimination and identification using short and standardized genomic regions. The genus *Sinosenecio* (Asteraceae) is used for traditional medicinal purposes in China. Most species of the genus occur in restricted geographical regions and exhibit a wide range of morphological variations within species, making them difficult to differentiate in the field. Previously, taxonomic revisions have been made based on morphological and cytological evidence. In the present study, barcoding analysis was performed on 107 individuals representing 38 species in this genus to evaluate the performance of four candidate barcoding loci (*matK*, *rbcL*, *trnH-psbA* and internal transcribed spacer [ITS]) and detect geographical patterns. Three different methods based on genetic distance, sequence similarity, and the phylogenetic tree were used. Comparably high species discrimination power was detected in species-level taxonomic process by the ITS dataset alone or combined with other loci, which was suggested to be the most suitable barcode for *Sinosenecio*. Our results are congruent with previous taxonomic studies concerning the monophyly of the *S. oldhamianus* group. The present study provides an empirical paradigm for the identification of medicinal plant species and their geographical patterns, ascertaining the congruence between taxonomical studies and barcoding analysis in *Sinosenecio*.

Key words: DNA barcoding, geographical patterns, *Sinosenecio*, species identification.

DNA barcoding has developed into a promising approach for species-level discrimination and identification using short and standardized genomic regions (Hebert et al., 2003). It has a broad range of applications, not only providing insights into species-level taxonomy and assisting with the identification and delimitation of medicinal plants, but also in quantifying diversity and creating biodiversity inventories (Ebihara et al., 2010; Kress et al., 2010; Ren et al., 2010; Carr et al., 2011; Hollingsworth et al., 2011; Mao et al., 2014; Yuan et al., 2015). Moreover, barcodes enable investigation and comparison of biogeographic patterns among multiple taxa, which will ultimately contribute to a better understanding of biodiversity, barriers to gene flow, and the process of speciation (Carr et al., 2011). Because of the slow rate of nucleotide evolution and complex evolutionary processes, such as hybridization and polyploidy, in plant species, multilocus barcodes have been suggested as being more useful in plant barcoding systems than single barcode sequences (Rieseberg et al., 2006; Fazekas et al., 2009). The markers *rbcL*, *matK*, *trnH-psbA* and the internal transcribed spacer (ITS) have been proposed as core barcodes in plant, including herbal medicinal species and their adulterants (Li et al., 2011a, 2011b, 2011c; Yan et al., 2011).

Sinosenecio B. Nord. (Asteraceae-Senecioneae) consists of approximately 40 species (Chen et al., 2011). According to Liu (2010), the traditionally circumscribed *Sinosenecio* is polyphyletic, consisting of three groups belonging to different subtribes, namely the *S. oldhamianus* group, the *Sinosenecio* s.s. group, and the *S. hainanensis* group. The *S. hainanensis* group represents a lineage rather distantly related to the other two groups of *Sinosenecio*, and Liu and Yang described it as an independent genus of its own, namely *Hainanecio* Y. Liu & Q. E. Yang (Liu, 2010; Chen et al., 2011; Liu & Yang, 2011a); thus, we excluded it from analysis in the present study. *Sinosenecio* as currently recircumscribed includes the *S. oldhamianus* and *Sinosenecio* s.s. groups, containing 27 and 13 species, respectively (Chen et al., 2011). Most species of *Sinosenecio* occur in China, with only two species, namely *S. euosmus* (Hand.-Mazz.) B. Nord. and *S. oldhamianus* (Maxim.) B. Nord., extending into Myanmar, Thailand, and Vietnam (Chen et al., 2011). The *S. oldhamianus* group extends its ranges from central to southern and

© 2015 Institute of Botany, Chinese Academy of Sciences

eastern China, whereas the *Sinosenecio* s.s. group is geographically restricted to the mountain areas around Sichuan Basin, China. At the species level, except for the widespread *S. oldhamianus*, all other species in both groups exhibit restricted geographical ranges. Some species are geographically restricted to the Western Sichuan Plateau (WSP) at altitudes of 1600–4500 m. Those species include three members from the *S. oldhamianus* group, specifically *S. sungpanensis* (Hand.-Mazz.) B. Nord., *S. fangianus* Y. L. Chen, and *S. euosmus*, and seven from the *Sinosenecio* s.s. group, namely *S. ligularioides* (Hand.-Mazz.) B. Nord., *S. rotundifolius* Y. L. Chen, *S. subrosulatus* (Hand.-Mazz.) B. Nord., *S. sichuanicus* Y. Liu & Q. E. Yang, *S. chienii* (Hand.-Mazz.) B. Nord., *S. yilingii* Y. Liu & Q. E. Yang, and *S. homogyniphyllus* (Cumm.) B. Nord. Six species from the *S. oldhamianus* group are distributed at much lower altitudes than 1600 m in the mountain areas of eastern China (EST), specifically *S. saxatilis* Y. L. Chen, *S. guangxiensis* C. Jeffrey & Y. L. Chen, *S. jiangxiensis* Y. Liu & Q. E. Yang, *S. jiuhuashanicus* C. Jeffrey & Y. L. Chen, *S. wuyiensis* Y. L. Chen, and *S. latouchei* (Jeffrey) B. Nord. The remaining 11 species in both groups are located at an intermediate elevation in central regions (CEN) at altitudes ranging from 400 to 3000 m.

Most species in *Sinosenecio* are used for medicinal purposes (Wu & Wu, 2003; Liang & Ye, 2006; Yang et al., 2014). *Sinosenecio bodinieri* (Vaniot) B. Nord. (Chinese medicine name: *Wugongqi*), *S. dryas* (Dunn) C. Jeffrey & Y. L. Chen (*Yankui*), *S. globigerus* (Chang) B. Nord (*Tuguoqianliguang*), *S. euosmus* (*Ciliehuaqianliguang*), *S. guangxiensis* (*Zoumaxu*), *S. hederifolius* (Dümmer) B. Nord (*Dahancao*), *S. oldhamianus* (*Puergen*), and *S. subcoriaceus* C. Jeffrey & Y. L. Chen (*Zimaohuaqianliguang*) are officially recorded in the Pharmacopoeia-recorded Materia Medica, and are usually collected from the field (Jiangsu Institute of Botany et al., 1990; Chinese Medicine Company, 1994). Like other members of the Asteraceae, *Sinosenecio* shows considerable variety in morphology within and among species, making it difficult to identify especially during collection in the field. For some closely related species in *Sinosenecio*, especially those with overlapping or adjacent distribution ranges, species delimitation is sometimes quite difficult because of the complexity of their inter- and intraspecific morphological variations. The closely related species *S. chienii* and *S. homogyniphyllus*, as well as *S. globigerus* (Chang) B. Nord. var. *adenophyllus* C. Jeffrey & Y. L. Chen, *S. globigerus*, and *S. leiboensis* C. Jeffrey & Y. L. Chen, are among such examples. Recently, several new species have been established by morphological and cytological evidence, such as *S. yilingii* etc., which were further evaluated using DNA barcoding in the present study.

Accordingly, questions regarding genus circumscription, species-level taxonomy, and geographic patterns have been raised for *Sinosenecio*. It is necessary to develop a fast and reliable method for the identification and discrimination of *Sinosenecio* species and their genetic lineages. The aim of the present study was to evaluate the usefulness of DNA barcoding for identifying species and taxonomy. We also investigated the regional specificity and geographical patterns of *Sinosenecio* species using barcoding analysis.

Material and Methods

Taxon sampling and morphological identification

For barcoding analysis, 107 individuals from 38 *Sinosenecio* species were sampled, covering the entire geographic distribution of the genus. Twenty-five species were from the *S. oldhamianus* group and the remaining 13 species were from the *Sinosenecio* s.s. group. There were at least two individuals from each species for barcoding analysis, except the following six species, for which only one individual was collected: *S. nanchuanicus* Z. Y. Liu, Y. Liu & Q. E. Yang, *S. hupingshanensis* Y. Liu & Q. E. Yang, *S. leiboensis*, *S. latouchei*, *S. saxatilis*, and *S. baojingensis* Y. Liu & Q. E. Yang. These species with single individuals exhibited close genetic affinities with other congeneric members. Therefore, we included them in further analyses of our datasets. Corresponding voucher specimens were deposited at the herbarium of the South China Botanical Garden (IBSC; Table S1). Species treatment followed Chen et al. (2011). Voucher information and geographical locations of all the species are given in Table S1 and Fig. 1.

DNA extraction, PCR and sequencing

Total genomic DNA was extracted from silica gel-dried leaf tissue using a modified cetyltrimethylammonium bromide (CTAB) method (Doyle & Doyle, 1987, 1990). The target DNA regions, namely *rbcL*, *matK*, *trnH-psbA* and ITS, were amplified with universal DNA barcoding primers. Two primer pairs of rbcLa_f (Kress & Erickson, 2007) and 724R (Fay et al., 1997) were used for the amplification of the *rbcL* region; 3F-KIM/1R-KIM and 3F-KIM/XF were used to amplify *matK* (Ford et al., 2009; Kim, unpublished data). The universal primers reported by Sang et al. (1997) and Tate & Simpson (2003) were used to amplify *trnH-psbA*. The ITS region was amplified using the ITS4 and ITS 5HP primer pair (Hershkovitz & Zimmer, 1996). For any failed amplification, other unique plant ITS primer sets were used to detect the cause of the failure (Wen & Zimmer, 1996). The PCR was performed using a reaction mixture with a total volume of 50 μL, containing 50 ng genomic DNA, 2 mmol/L $MgCl_2$, 0.2 mmol/L dNTPs, 0.2 μmol/L each primer, and 1.25 U DNA polymerase (Takara Bio Inc., Dalian, China). The amplification program consisted of a 5 min denaturation step at 94 °C, followed by 30 cycles of 1 min denaturation at 94 °C, 1 min annealing at 52 °C, and 90 s elongation at 72 °C. Amplification ended with an elongation phase lasting 8 min at 72 °C and a final hold at 10 °C. Amplification products were checked for length and concentration on 1.5% agarose gels and sent to Shanghai Invitrogen Biotechnology (Shanghai, China) for commercial sequencing. All sequences were deposited in GenBank (Table S1).

Sequence alignment and molecular analyses

The alignments of datasets for all regions were generated online by MUSCLE (Edgar, 2004) and ajusted manually in BioEdit (Hall, 1999). Four single-locus barcodes and all their possible combinations were evaluated using three different methods based on genetic distance, sequence similarity, and phylogenetic tree. First, pairwise genetic distances were calculated based on the Kimura 2-parameter (K2P) distance model (Kimura, 1980) using MEGA 5 (Tamura et al., 2007) in order to evaluate inter- and intraspecific sequence

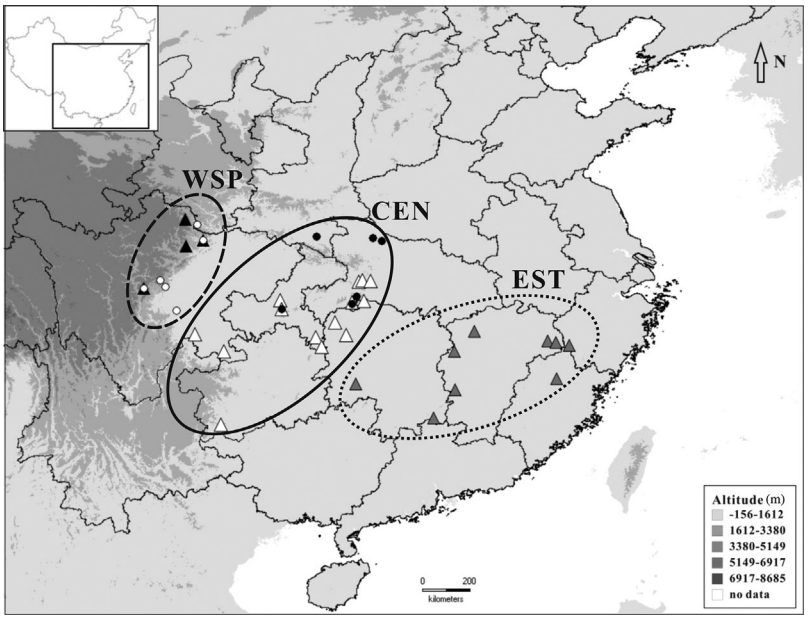

Fig. 1. Map of sample locations of *Sinosenecio* species. Triangles and circles represent the *S. oldhamianus* group and the *Sinosenecio* s.s. group, respectively. Black triangles and white circles represent species restricted to the Western Sichuan Plateau (WSP), white triangles and black circles represent species distributed in the central region (CEN), and gray triangles represent species occurring in the Eastern region (EST). The map is modified from an original map from the National Administration of Surveying, Mapping and Geoinformation of China (http://www.sbsm.gov.cn/article/zxbs/dtfw/, accessed 28 August 2014).

divergence and to estimate the presence of any barcoding gap for each single locus barcode and all possible combinations (CBOL Plant Working Group, 2009; Hollingsworth et al., 2009). Second, to assess the usefulness of DNA barcoding for accurate species assignment, a sequence comparison identification approach was conducted based on K2P distances using the "best match" and the "best close match" functions implemented in TaxonDNA (Meier et al., 2006). In our analysis, species with both single and multiple individuals were included and 38 species were analyzed in total. The tree-building method has been proved to be an efficient way of defining species boundaries in many barcoding studies (Theodoridis et al., 2012; Weigt et al., 2012; Zhou et al., 2012). Third, tree-based methods were used to determine whether sequences in our dataset formed species-specific clusters. Bayesian inference (BI) was conducted for four individual barcodes and all possible barcode combinations in MrBayes v3.1.2 (Huelsenbeck & Ronquist, 2001; Ronquist & Huelsenbeck, 2003) under the General Time Reversible + Gamma (GTR + G) model of nucleotide substitution for all regions. Two independent runs with four Markov chains (one cold and three heated) run for 1×10^7 generations, with trees sampled every 1000 generations, were performed. Each chain used a random tree as a starting point and the default temperature parameter value of 0.2. The first 2500 sampled trees were discarded as "burn in." The remaining trees were used to build a 50% majority rule consensus tree with the sumt option in MrBayes v3.1.2. Species with both single and multiple individuals were included and those forming a monophyletic clade in the BI tree with posterior probabilities higher than 50% were considered to indicate successful identification. In the tree-based analysis, *Petasites tricholobus* was chosen as an outgroup.

Results

PCR amplifications and sequence characteristics

The first step in assessing the usefulness of candidate barcodes was to estimate amplification and sequencing success (universality) across all 107 individuals. In the present study, ITS was revealed to be the best-performing barcode. This target region was successfully amplified and sequenced for all 107 individuals (Table 1). However, multiple attempts at PCR and two primer pairs are required to achieve this level. The three chloroplast (cp) DNA loci *rbcL*, *matK*, and *trnH-psbA* performed well and exhibited comparable amplification success rates (99.07%, 96.26%, and 98.13%, respectively). Altogether 38 species were sequenced with all barcode loci, of which 32 species had multiple individuals. Only one species, *Sinosenecio globigerus*, failed to be amplified for the *rbcL* region. Two species, namely *S. hederifolius* and *S. eriopodus* C. Jeffrey & Y. L. Chen, were missing from the *trnH-psbA* region because of unsuccessful amplification. Four species (*S. hederifolius*, *S. eriopodus*, *S. globigerus*, and *S. subrosulatus*) did not yield clear and unambiguous sequences for the *matK* region even after multiple attempts.

For convenience, the variable characters and mean intra- and interspecific distances of all four regions are given in Table 1. The percentage of variable characters ranged from 1.57% (*rbcL*) to 36.65% (ITS). The highest variation was

Table 1 Success rates for PCR and sequencing, and sequence characteristics of the four candidate barcodes

	rbcL	*matK*	*trnH-psbA*	ITS
Length of candidate barcodes (bp)	701	843–849	332–549	632–724
Alignment length of candidate barcodes (bp)	701	853	662	737
No. test samples	106	103	105	107
Success rate of PCR and sequencing	99.07%	96.26%	98.13%	100%
No. variable/informative nucleotide sites	11/8	52/30	55/43	269/228
Mean intraspecific distance (K2P)	0.0002	0.0006	0.0004	0.0051
Mean interspecific distance (K2P)	0.0022	0.0058	0.0114	0.0660

ITS, internal transcribed spacer; K2P, Kimura 2-parameter.

detected in the ITS region with 31 indels and length variation from 632 to 724 bp. Sequence alignment was reliable and accurate in the *rbcL* region without indels. One indel of 6 bp was revealed in the *matK* region in two individuals of *S. confervifer* (H. Léveillé) Y. Liu & Q. E. Yang. An extra high level of length variation from 332 to 549 bp due to 18 indels was detected and large numbers of poly A/T were discerned in the *trnH-psbA* region, which made it rather difficult in sequencing and correct alignment. To avoid error alignment, careful manual inspection was conducted using BioEdit (Hall, 1999). The mean interspecific distance ranged from 0.0022 to 0.0660, and the mean intraspecific distance ranged from 0.0002 to 0.0051 in the *rbcL* and ITS regions, respectively (Table 1). To evaluate the barcoding gaps, which estimated whether the interspecies distances were larger than intraspecies distances for each pair of regions and for all possible combinations (CBOL Plant Working Group, 2009; Hollingsworth et al., 2009), we checked the distribution of intra- and interspecific divergence. Each distribution graph showed more or less overlapping between intra- and interspecific genetic distances, indicating the absence of any clear DNA barcoding gap.

Species discrimination

The same sample size could not be obtained for all barcoding regions, so each of the single or multilocus barcoding analyses differs in the number of individuals and species examined. Comparison of three different methods revealed that the DNA sequence similarity-based method exhibited the highest level of species discrimination, followed by the BI tree method (Table 2). The method based on genetic distance had the lowest rate of species discrimination (40.63–56.25%) with exclusion of six single individual species (Table 2). Using the BI tree method, the species discrimination power ranged between 65.79% and 71.05% among all 38 species based on ITS data alone or combined. After excluding the single individual species, up to 84.38% of species with multiple individuals could be identified on the basis of ITS data alone or combined (Table 2). The discrimination power showed by the cpDNA loci was extremely low, mostly lower than 50% (Table 2). Therefore, ITS exhibits sufficient variations to discriminate most of the species, alone or combined with cpDNA loci. Any single or combined barcodes without the ITS region always exhibited a relatively low rate of species discrimination.

The BI tree method generated a graphical representation and is useful in determining the power of a given locus combination to discriminating between *Sinosenecio* species. A total of 107 sequences and one outgroup sequence for the four candidate barcodes individually or combined were aligned and used for BI tree construction. Using the ITS barcode alone or combined, the *S. oldhamianus* group was successfully identified in the BI tree. Any of the three cpDNA loci (alone or combined) were not sufficient for discriminating this group. The *Sinosenecio* s.s. group was revealed to be a polyphyly. Using the ITS barcode alone, 25 species with multiple individuals could be accurately distinguished, almost all posterior probabilities being 100% based on the BI tree. If combined with the cpDNA loci, two more species (*S. palmatisectus* C. Jeffrey & Y. L. Chen and *S. albonervius* Y. Liu & Q. E. Yang) could be distinguished in the BI tree derived from the combination of the four barcodes. Although it was missing from the *trnH-psbA* region and has only one individual in the BI tree based on the four combined barcodes, *S. hederifolius* was suggested to be successfully identified, as it was identified based on ITS data. Five species with multiple sequences failed to be detected using any of the single or combined candidate barcodes, including *S. confervifer*, *S. fanjingshanicus* C. Jeffrey & Y. L. Chen, *S. globiger*, *S. chienii*, and *S. homogyniphyllus* (Fig. 2). The three newly published species (Liu & Yang, 2010, 2011b, 2012), namely *S. jiangxiensis*, *S. yilingii* and *S. sichuanicus*, were all successfully identified based on ITS alone or combined.

Regional specificity and geographical patterns

The association between species clusters and geographic distributions was strongly discerned in the BI tree. In general, barcodes divided all the species into three geographical regions in the *S. oldhamianus* group, namely WSP, CEN, and EST. Species from each of the three geographical regions formed a distinct monophyly with high posterior probability (94%, 100%, and 99%, respectively). Within the CEN region of the *S. oldhamianus* group, three clusters were formed by the species with different distributions in the western, central, or eastern CEN region. The clade of *S. oldhamianus* did not show any distinct geographical specificity because of its wide distribution, but it did exhibit close phylogenetic relationships with the WSP region. In the *Sinosenecio* s.s. group, seven species occurring in the WSP region were discerned as a monophyly with a high posterior probability of 100%, whereas the remaining six species forming a polyphyly were geographically distributed in the CEN region. Even at the individual level, associations between phylogenetic and geographical patterns could be detected. In the *S. oldhamianus* group, *S. confervifer*, occurring in the central CEN region, had individuals clustered with *S. nanchuanicus*, both of

Table 2 Identification success rates for single locus and multilocus combinations of the four candidate barcodes (individually and in combination) based on three different methods based on sequence similarity, genetic distance, and phylogenetic tree

Candidate barcodes	N	Best match			Best close match			No match (%)	Threshold %	Distance method*	BI tree method*
		Correct (%)	Ambiguous (%)	Incorrect (%)	Correct (%)	Ambiguous (%)	Incorrect (%)				
rbcL	106	10	95	0	9	92	0	4	0.14	50.00% (16/32)	12.50% (4/32)
matK	103	27	69	6	27	66	5	4	0.35	43.75% (14/32)	28.13% (9/32)
trnH-psbA	105	32	72	0	32	72	0	0	0.81	50.00% (16/32)	25.00% (8/32)
ITS	107	84	10	12	84	10	12	0	5.71	50.00% (16/32)	78.13% (25/32)
trnH-psbA + ITS	105	89	3	12	89	3	10	2	2.60	53.13% (17/32)	84.38% (27/32)
trnH-psbA + *matK*	103	51	44	7	50	44	6	2	0.29	40.63% (13/32)	50.00% (16/32)
trnH-psbA + *rbcL*	105	40	62	1	40	61	1	1	0.41	46.88% (15/32)	46.88% (15/32)
ITS + *matK*	103	91	2	9	91	2	7	2	1.56	53.13% (17/32)	81.25% (26/32)
ITS + *rbcL*	106	87	6	12	87	6	12	0	2.66	46.88% (15/32)	81.25% (26/32)
matK + *rbcL*	103	36	59	6	36	55	6	4	0.25	40.63% (13/32)	34.38% (11/32)
trnH-psbA + ITS + *matK*	103	91	1	10	91	1	8	2	1.16	56.25% (18/32)	84.38% (27/32)
trnH-psbA + ITS + *rbcL*	105	89	2	12	89	2	10	2	1.65	53.13% (17/32)	81.25% (26/32)
ITS + *matK* + *rbcL*	103	89	2	10	89	2	8	2	1.15	50.00% (16/32)	78.13% (25/32)
trnH-psbA + *matK* + *rbcL*	103	59	35	7	58	34	6	3	0.24	40.63% (13/32)	53.13% (17/32)
trnH-psbA + ITS + *matK* + *rbcL*	103	89	3	9	89	3	7	2	1.05	50.00% (16/32)	81.25% (26/32)

*Excluding single sequence species. ITS, internal transcribed spacer; N, No. of individuals surveyed.

which were present at Mt. Jinfo. In the *Sinosenecio* s.s. group, individuals of *S. yilingii* and *S. homogyniphyllus* from the same locations formed a monophyly in the phylogenetic tree.

Discussion

Suggested barcoding regions in *Sinosenecio*

An ideal DNA barcode should be selected based on several criteria as follows: (i) appropriately short sequence length (300–800 bp) suitable for PCR amplification with universal primers; (ii) sequencing routinely and reliably in very large and diverse sample sets; (iii) easily comparable data; and (iv) high inter- but low intraspecific divergence for the purpose of species discrimination (Cowan et al., 2006; CBOL Plant Working Group, 2009; Ford et al., 2009; Hollingsworth et al., 2011). In the present study, all cpDNA regions had high amplification and sequencing efficiency (>95%), and exhibited higher inter- than intraspecific divergence by all single or combined loci (Table 1). However, the species discrimination power revealed by any cpDNA barcodes (alone or combined) was very low. In comparison, ITS had an extraordinarily high success rate (100%) of PCR amplification and sequencing (Table 1). It possessed the most variation, showing greater intra- and interspecific divergence, and demonstrated high effectiveness in discriminating closely related species (>80% of the 32 multiple individual species based on alone or combined barcodes). Meanwhile, ITS has high universality of primers, suitable length (<800 bp), direct sequencing and quick alignment. For all these reasons, ITS is the best choice as a DNA barcode in *Sinosenecio*. In previous studies, some obstacles have been reported to the use of ITS as a universal barcode, such as the presence of homopolymers, multiple copies in the genome, and contamination with fungi (Álvarez & Wendel, 2003; Sass et al., 2007; Spooner, 2009). In *Sinosenecio*, no contamination was found after nuclear blasting with the GenBank database. Several poly-C stretches were detected and made sequencing difficult at times. As the most well-known marker, ITS has long been used in phylogenetics of plant species because of its faster nuclear substitution rate than plastid genes (Chase et al., 2007; Calonje et al., 2009). It has also shown applicability in the phylogenetic and barcoding analyses of the Asteraceae family (Liu et al., 2006; Wang et al., 2009; Gao et al., 2010). Therefore, even with its recognized limitations, ITS is considered to be an effective candidate DNA barcode in *Sinosenecio*, which is also one of core barcodes for seed plants (Li et al., 2011a).

DNA barcoding can complement morphological taxonomy

A strong taxonomic framework ensures correct tests and effective establishment of DNA barcodes (Carr et al., 2011). Conversely, suitable and efficient DNA barcodes could provide assistance with species-level taxonomic processes of defining and delimiting species (Hajibabaei et al., 2007; Hollingsworth et al., 2011). The results obtained in the present study provide further insights into both genus- and species-level taxonomy. First, based on the BI tree, the *S. oldhamianus* group was successfully identified as a monophyly, showing independence from the *Sinosenecio* s.s. group. This result is consistent with previous taxonomic studies and phylogenetic analyses (Liu et al., 2006; Liu, 2010; Wang et al., 2009). The

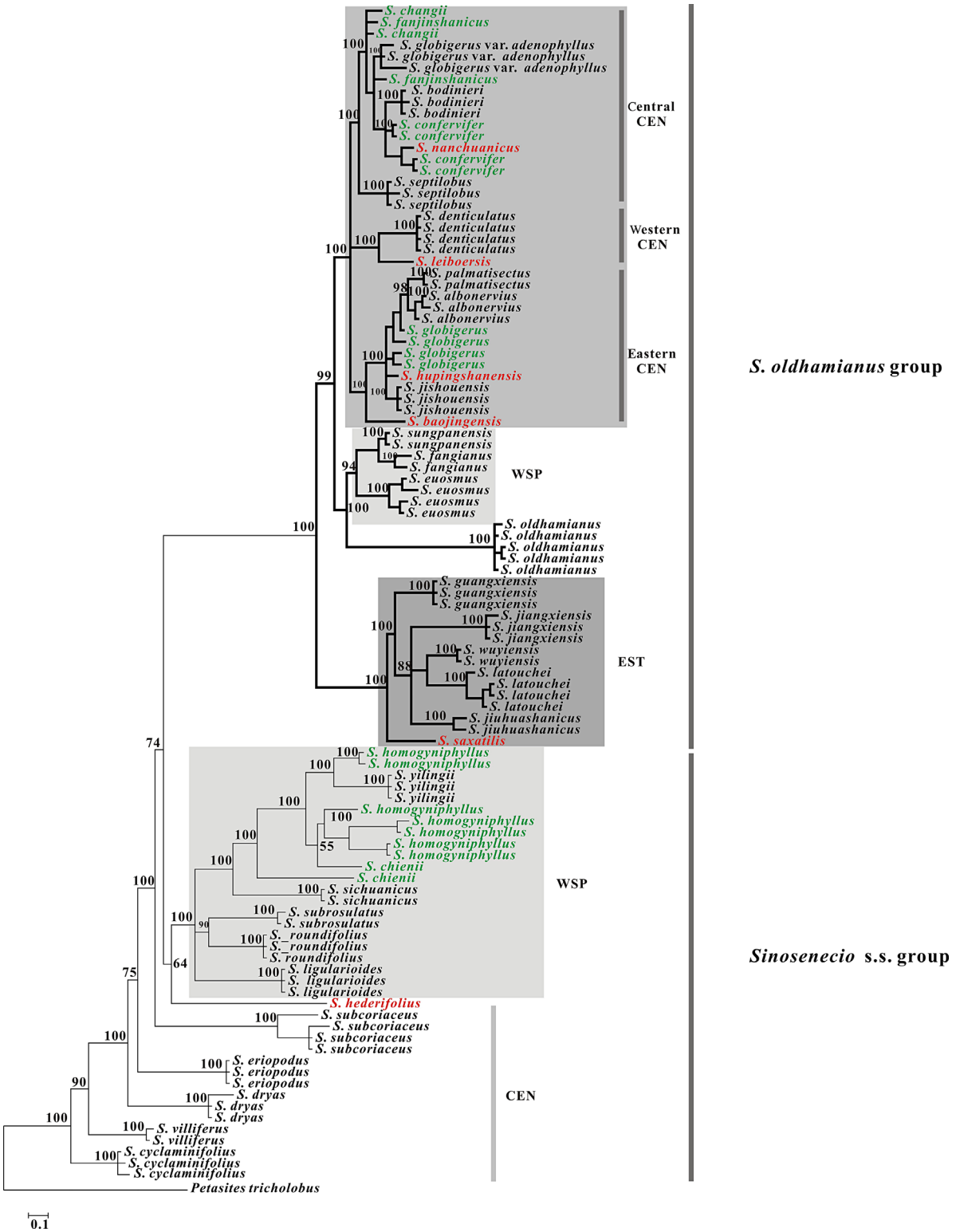

Fig. 2. Fifty percent majority rule consensus cladogram inferred by Bayesian analysis of the combined data set of internal transcribed spacer (ITS) and chloroplast (cp) DNA loci based on the General Time Reversible + Gamma (GTR + G) model of nucleotide substitution. Numbers above branches indicate posterior probabilities. The monophyletic *Sinosenecio oldhamianus* group is displayed by the clade with bold branch lines. Species that possess single individuals or failed to form species-specific clusters are indicated by red and green colors, respectively. The geographical regions of the Western Sichuan Plateau (WSP) and Eastern region (EST) are highlighted in grey boxes, and the geographical region of central region (CEN) is denoted by the right side bars.

Sinosenecio s.s. group was also suggested to be potentially circumscribed as a new genus given more molecular data provided (Liu, 2010). Second, nearly 72% of species or more than 80% of species could be distinguished including or excluding six species of one individual only, respectively, based on the ITS barcode alone or combined, showing a good performance with comparably high species discriminatory power and proving the application for defining and delimiting species in a species-level taxonomic process. Those species with similar morphologies but different distributions were efficiently discriminated by DNA barcoding analysis. For example, *S. bodinieri* was successfully distinguished from closely related *S. confervifer*, and *S. globigerus* var. *adenophyllus* was distinguished from *S. globigerus* and *S. leiboensis*. Third, new species were successfully identified. Two newly published species, namely *S. sichuanicus* and *S. yilingii*, which exhibit similar morphologies to *S. chienii* and *S. homogyniphyllus*, respectively, were correctly detected to be a monophyly. Another three newly published species, namely *S. jiangxiensis*, *S. albonervius* and *S. jishouensis*, with multiple individuals, were also successfully identified, which further demonstrates the usefulness of DNA barcodes for assisting with the definition of species and ascertaining the congruence between taxonomical studies and barcoding analysis in *Sinosenecio*.

DNA barcoding can reveal geographical patterns

DNA barcoding has been proven to complement population genetics, detecting members of species with distinct geographical origins, investigating habitat continuity, genetic structure etc. (Hajibabaei et al., 2007; Carr et al., 2011). As is known, most *Sinosenecio* species have restricted geographical distributions, except for the widespread *S. oldhamianus*. Those geographically restricted species, if sympatrically occurring, tend to share the same genetic lineages based on the phylogenetic tree. Barcodes identified those species as three geographically distinct regions of WSP, EST, or CEN within each group. The highest species diversity was revealed within the CEN region based on phylogenetic analysis. Complex geographical topography and comparably stable ecological conditions during periods of environmental fluctuations are suggested to contribute to the endemism and richness in plant species of this region (Wen et al., 2014). Within the *S. oldhamianus* group, the two regions of WSP and EST were distinctly separate on the basis of the BI tree.

Compared with the classification system of Liu (2010), the three geographical regions reflect the systematic arrangement of *Sinosenecio* in principle. For example, species located in the WSP and CEN regions in the genus *Sinosenecio* group were separated into two sections, as indicated by Liu (2010), which differ morphologically in floret and receptacle with or without hair. The closely related and morphologically intermediate species were inferred to possess the same genetic and geographical regions based on both taxonomic and phylogenetic studies. Not only at a species level, but also at the individual level, species or individuals tend to cluster according to their geographical locations. For example, *S. yilingii* individuals clustered with *S. homogyniphyllus* with exactly the same geographical locations in Baoxing, Sichuan. *Sinosenecio confervifer* individuals clustered with *S. nanchuanicus* with sympatric distribution in Mt. Jinfo. As stated earlier, those sympatric species were hard to discriminate because of their intermediate morphologies. Interspecific hybridization always underlies phenotypic variability (i.e., intermediate phenotypes). However, no susceptible hybrids were detected in the field and significant disjunction in flowering time was found among species. Rapid differentiation is inferred for the evolutionary history of *Sinosenecio* (Liu et al., unpublished data), which has also been considered in other species of the Asteraceae family (Wagstaff & Breitwieser, 2004; Knope et al., 2012). However, more morphological and molecular evidence is needed for further elucidation of the mechanism and process of evolutionary history of these species.

Acknowledgements

The authors thank Dr. Haifei Yan (from South China Botanical Garden, CAS) for his considerable assistance with data analysis and writing of the manuscript. This study was supported financially by the National Natural Science Foundation of China (Grant Nos. 31470319, 31300174, and 31100160).

References

Álvarez I, Wendel JF. 2003. Ribosomal ITS sequences and plant phylogenetic inference. *Molecular Phylogenetics and Evolution* 29: 417–434.

Calonje M, Martin-Bravo S, Dobes C, Gong W, Jordon-Thaden I, Kiefer C, Kiefer M, Paule J, Schmickl R, Koch MA. 2009. Non-coding nuclear DNA markers in phylogenetic reconstruction. *Plant Systematics and Evolution* 282: 257–280.

Carr CM, Hardy SM, Brown TM, Macdonald TA, Hebert PDN. 2011. A tri-oceanic perspective: DNA barcoding reveals geographic structure and cryptic diversity in Canadian polychaetes. *PLoS ONE* 6: e62232.

CBOL Plant Working Group. 2009. DNA barcoding in land plants. *Proceedings of the National Academy of Sciences USA* 105: 6350–6355.

Chase MW, Cowan RS, Hollingsworth PM, van der Berg C, Madriñán S, Petersen G, Seberg O, Jørgsensen T, Cameron KM, Carine M, Pedersen N, Hedderson TAJ, Conrad F, Salazar GA, Richardson JE, Hollingsworth ML, Barraclough TG, Kelly L, Wilkinson M. 2007. A proposal for a standardised protocol to barcode all land plants. *Taxon* 56: 295–299.

Chen YL, Liu Y, Yang QE, Nordenstam B, Jeffrey C. 2011. *Sinosenecio* B. Nord. In: Wu ZY, Raven PH, Hong DY eds. *Flora of China*. Beijing: Science Press; St. Louis: Missouri Botanical Garden Press. 20–21: 464–481.

Chinese Medicine Company. 1994. *The Chinese traditional medicine resource records*. Beijing: Science Press. 1341–1342.

Cowan RS, Chase MW, Kress WJ, Savolainen V. 2006. 300 000 species to identify: Problems, progress, and prospects in DNA barcoding of land plants. *Taxon* 55: 611–616.

Doyle JJ, Doyle JL. 1987. A rapid DNA isolation procedure for small quantities of fresh leaf tissue. *Phytochemical Bulletin* 19: 11–15.

Doyle JJ, Doyle JL. 1990. Isolation of plant DNA from fresh tissue. *Focus* 12: 13–15.

Ebihara A, Nitta JH, Ito M. 2010. Molecular species identification with rich floristic sampling: DNA barcoding the pteridophyte flora of Japan. *PLoS ONE* 5: e15136.

Edgar RC. 2004. MUSCLE: Multiple sequence alignment with high accuracy and high throughput. *Nucleic Acids Research* 32: 1792–1797.

Fay MF, Swensen SM, Chase MW. 1997. Taxonomic affinities of *Medusagyne oppositifolia* (Medusagynaceae). *Kew Bulletin* 2: 111–120.

Fazekas AJ, Kesanakurti PR, Burgess KS, Percy DM, Graham SW, Barrett SCH, Newmaster SG, Hajibabaei M, Husband BC. 2009. Are plant species inherently harder to discriminate than animal species using DNA barcoding markers? *Molecular Ecology Resources* 9 (Suppl. 1): S130–S139.

Ford CS, Ayres KL, Toomey N, Haider N, Van Alphen Stahl J, Kelly LJ, Wikström N, Hollingsworth PM, Duff RJ, Hoot SB, Cowan RS, Chase MW, Wilkinson MJ. 2009. Selection of candidate coding DNA barcoding regions for use on land plants. *Botanical Journal of the Linnean Society* 159: 1–11.

Gao T, Yao H, Song JY, Zhu YJ, Liu C, Chen S. 2010. Evaluating the feasibility of using candidate DNA barcodes in discriminating species of the large Asteraceae family. *BMC Evolutionary Biology* 10: 324.

Hajibabaei M, Singer GAC, Hebert PDN, Hickey DA. 2007. DNA barcoding: How it complements taxonomy, molecular phylogenetics and population genetics. *Trends in Genetics* 23: 167–172.

Hall TA. 1999. BioEdit: A user-friendly biological sequence alignment editor and analysis program for Windows 95/98/NT. *Nucleic Acids Symposium Series* 41: 95–98.

Hebert PDN, Cywinska A, Ball SL, deWaard JR. 2003. Biological identifications through DNA barcodes. *Proceedings of the Royal Society B: Biological Sciences* 270: 313–321.

Hershkovitz MA, Zimmer EA. 1996. Conservation patterns in angiosperm rDNA ITS2 sequences. *Nucleic Acids Research* 24: 2857–2867.

Hollingsworth ML, Clark AA, Forrest LL, Richardson J, Pennington RT, Long DG, Cowan R, Chase MW, Gaudeul M, Hollingsworth PM. 2009. Selecting barcoding loci for plants: Evaluation of seven candidate loci with species-level sampling in three divergent groups of land plants. *Molecular Ecology Resources* 9: 439–457.

Hollingsworth PM, Graham SW, Little DP. 2011. Choosing and using a plant DNA barcode. *PLoS ONE* 6: e19254.

Huelsenbeck JP, Ronquist F. 2001. MrBayes: Bayesian inference of phylogenetic trees. *Bioinformatics* 17: 754–755.

Jiangsu IOB, IMPLAD, Kunming IOB, IMM. 1990. *Xinhua materia medica outline*. Shanghai: Shanghai Science and Technology Press. 3: 458–461.

Kimura M. 1980. A simple method for estimating evolutionary rates of base substitutions through comparative studies of nucleotide sequences. *Journal of Molecular Evolution* 16: 111–120.

Knope ML, Morden CW, Funk VA, Fukami T. 2012. Area and the rapid radiation of *Hawaiian bidens* (Asteraceae). *Journal of Biogeography* 39: 1206–1216.

Kress WJ, Erickson DL. 2007. A two-locus global DNA barcode for land plants: The coding *rbcL* gene complements the non-coding *trnH-psbA* spacer region. *PLoS ONE* 2: e508.

Kress WJ, Erickson DL, Swenson NG, Thompson J, Uriarte M, Zimmerman JK. 2010. Advances in the use of DNA barcodes to build a community phylogeny for tropical trees in a Puerto Rican Forest Dynamics Plot. *PLoS ONE* 5: e15409.

Li DZ, Gao LM, Li HT, Wang H, Ge XJ, Liu JQ, Chen ZD, Zhou SL, Chen SL, Yang JB, Fu CX, Zeng CX, Yan HF, Zhu YJ, Sun YS, Chen SY, Zhao L, Wang K, Yang T, Duan GW. 2011a. Comparative analysis of a large dataset indicates that internal transcribed spacer (ITS) should be incorporated into the core barcode for seed plants. *Proceedings of the National Academy of Sciences USA* 108: 19 641–19 646.

Li DZ, Liu JQ, Chen ZD, Wang H, Ge XJ, Zhou SL, Gao LM, Fu CX, Chen SL. 2011b. Plant DNA barcoding in China. *Journal of Systematics and Evolution* 49: 165–168.

Li M, Cao H, But PPH, Shaw PC. 2011c. Identification of herbal medicinal materials using DNA barcodes. *Journal of Systematics and Evolution* 49: 271–283.

Liang AH, Ye ZG. 2006. General situation of the toxicity researches on *Senecio*. *China Journal of Chinese Materia Mediea* 31: 93–97.

Liu JQ, Wang YJ, Wang AL, Hideaki O, Abbott R. 2006. Radiation and diversification within the *Ligularia–Cremanthodium–Parasenecio* complex (Asteraceae) triggered by uplift of the Qinghai–Tibetan Plateau. *Molecular Phylogenetics and Evolution* 38: 31–39.

Liu Y. 2010. *A systematic study of the genus* Sinosenecio *B. Nord. (Compositae)*. Ph.D. Dissertation. Beijing: Institute of Botany, Chinese Academy of Sciences.

Liu Y, Yang QE. 2010. *Sinosenecio yilingii* (Asteraceae), a new species from Sichuan, China. *Botanical Studies* 51: 269–275.

Liu Y, Yang QE. 2011a. *Hainanecio*, a new genus of the Senecioneae, Asteraceae from China. *Botanical Studies* 52: 115–120.

Liu Y, Yang QE. 2011b. *Sinosenecio sichuanicus* (Asteraceae), a new species from Sichuan, China. *Botanical Studies* 52: 219–223.

Liu Y, Yang QE. 2012. *Sinosenecio jiangxiensis* (Asteraceae), a new species from Jiangxi, China. *Botanical Studies* 53: 401–414.

Mao YR, Zhang YH, Nakamura K, Guan BC, Qiu YX. 2014. Developing DNA barcodes for species identification in Podophylloideae (Berberidaceae). *Journal of Systematics and Evolution* 52: 487–499.

Meier R, Shiyang K, Vaidya G, Ng PKL. 2006. DNA barcoding and taxonomy in Diptera: A tale of high intraspecific variability and low identification success. *Systematic Biology* 55: 715–728.

Ren BQ, Xiang XG, Chen ZD. 2010. Species identification of *Alnus* (Betulaceae) using nrDNA and cpDNA genetic markers. *Molecular Ecology Resources* 10: 594–605.

Rieseberg LH, Wood TE, Baack EJ. 2006. The nature of plant species. *Nature* 440: 524–527.

Ronquist F, Huelsenbeck JP. 2003. MrBayes 3: Bayesian phylogenetic inference under mixed models. *Bioinformatics* 19: 1572–1574.

Sang T, Crawford DJ, Stuessy TF. 1997. Chloroplast DNA phylogeny, reticulate evolution, and biogeography of *Paeonia* (Paeoniaceae). *American Journal of Botany* 84: 1120–1136.

Sass C, Little DP, Stevenson DW, Specht CD. 2007. DNA barcoding in the cycadales: Testing the potential of proposed barcoding markers for species identification of Cycads. *PLoS ONE* 2: e1154.

Spooner DM. 2009. DNA barcoding will frequently fail in complicated groups: An example in wild potatoes. *American Journal of Botany* 96: 1177–1189.

Tamura K, Dudley J, Nei M, Kumar S. 2007. MEG A4: Molecular Evolutionary Genetics Analysis (MEGA) software version 4.0. *Molecular Biology and Evolution* 24: 1596–1599.

Tate JA, Simpson BB. 2003. Paraphyly of *Tarasa* (Malvaceae) and diverse origins of the polyploid species. *Systematic Botany* 28: 723–737.

Theodoridis S, Stefanaki A, Tezcan M, Aki C, Kokkini S, Vlachonasios KE. 2012. DNA barcoding in native plants of the Labiatae (Lamiaceae) family from Chios Island (Greece) and the adjacent Çeşme-Karaburun Peninsula (Turkey). *Molecular Ecology Resources* 12: 620–633.

華南農業大學学报
JOURNAL OF SOUTH CHINA AGRICULTURAL UNIVERSITY

华南农业大学学报
Huanan Nongye Daxue Xuebao
（双月刊，1959 年创刊，1980 年复刊）
第 36 卷　第 4 期　2015 年 7 月

Journal of South China
Agricultural University
(Bimonthly, Started 1959, Resumed 1980)
Vol.36 No.4 Jul. 2015

主管单位：华南农业大学
主办单位：华南农业大学
主　　编：陈晓阳
编辑出版：华南农业大学学报编辑部
（广州五山，邮政编码: 510642）
网　　址：http://xuebao.scau.edu.cn
电子邮箱：journal@scau.edu.cn
电　　话：(020)85280069/38746672
印刷单位：暨南大学印刷厂
发行订购：华南农业大学学报编辑部
国外发行：中国国际图书贸易总公司
（中国国际书店）北京399信箱

Responsible Institution: South China Agricultural University
Sponsor: South China Agricultural University
Chief Editor: CHEN Xiaoyang
Edited and Published by Editorial Department, Journal of South China Agricultural University
Address: Wushan, Guangzhou, 510642, China
Website: http://xuebao.scau.edu.cn
E-mail: journal@scau.edu.cn
Tel: (86-20)85280069/38746672
Distributed by China International Book Trading Corporation(P.O.Box 399 Beijing, China)

国内外公开发行
国内定价：15.00 元/册

刊号：ISSN 1001-411X
CN 44-1110/S

ISSN 1001-411X
9 771001 411157 07>

华南农业大学学报

第三十六卷　第四期

二〇一五年七月

華南農業大學 学报

JOURNAL OF SOUTH CHINA AGRICULTURAL UNIVERSITY

ISSN 1001-411X
CODEN HNDXBH
中国・广州
GUANGZHOU CHINA

全国中文核心期刊

2015

7月　第36卷　第4期
Jul.　Vol.36　No.4

Wagstaff SJ, Breitwieser I. 2004. Phylogeny and classification of *Brachyglottis* (Senecioneae, Asteraceae): An example of a rapid species radiation in New Zealand. *Systematic Botany* 29: 1003–1010.

Wang LY, Pelser PB, Nordenstam B, Liu JQ. 2009. Strong incongruence between the ITS phylogeny and generic delimitation in the *Nemosenecio-Sinosenecio -Tephroseris* assemblage (Asteraceae: Senecioneae). *Botanical Studies* 50: 435–442.

Weigt LA, Baldwin CC, Driskell A, Smith DG, Ormos A, Reyier EA. 2012. Using DNA barcoding to assess Caribbean reef fish biodeversity: Expanding taxonomic and geographic coverage. *PLoS ONE* 7: e41059.

Wen J, Zimmer EA. 1996. Phylogeny and biogeography of *Panax* L. (the Ginseng Genus, Araliaceae): Inferences from ITS sequences of nuclear ribosomal DNA. *Molecular Phylogenetics and Evolution* 6: 167–177.

Wen J, Zhang JQ, Nie ZL, Zhong Y, Sun H. 2014. Evolutionary diversifications of plants on the Qinghai-Tibetan Plateau. *Frontiers in Genetics* 5: 4.

Wu B, Wu LJ. 2003. Advances in studies on chemical constituents of *Senecio*. *China Journal of Chinese Materia Medica* 28: 97–100.

Yan HF, Hao G, Hu CM, Ge XJ. 2011. DNA barcoding in closely related species: A case study of *Primula* L. sect. *Proliferae* Pax (Primulaceae) in China. *Journal of Systematics and Evolution* 49: 225–236.

Yang R, Zeng XL, Wang CF. 2014. NMR characterization of 2-methyl-6-(2-methylphenyl)-2-heptene. *Chinese Journal of Magnetic Resonance* 31: 262–267.

Yuan QJ, Zhang B, Jiang D, Zhang WJ, Lin TY, Wang NH, Chiou SJ, Huang LQ. 2015. Identification of species and materia medica within *Angelica* L. (Umbelliferae) based on phylogeny inferred from DNA barcodes. *Molecular Ecology Resources* 15: 358–371.

Zhou MJ, Xiao JH, Bian SN, Li YW, Niu LM, Hu HY, Wu WS, Murphy RW, Huang DW. 2012. Molecular approaches identify known species, reveal cryptic species and verify host specificity of Chinese *Philotrypesis* (Hymenoptera: Pteromalidae). *Molecular Ecology Resources* 12: 598–606.

Supplementary Material

The following supplementary material is available online for this article at http://onlinelibrary.wiley.com/doi/10.1111/jse.12166/suppinfo:

Table S1. Taxon, voucher, locations, and Genbank accession numbers (*rbcL*, *matK*, *trnH-psbA*, and ITS).

华南农业大学学报

第 36 卷　第 4 期　2015 年 7 月

目　　次

葡萄糖醛酸木聚糖生物合成研究进展(综述) …… 吴蔼民，赵先海，解巧丽，解新明(1)
伪狂犬病病毒 *gE* 基因主要抗原表位区的原核表达及间接 ELISA 方法的建立
…… 吉艺宽，王　雨，程　艺，张宝石，向柯宇，琚春梅(11)
猪流行性腹泻病毒抗体间接 ELISA 检测方法的建立与应用
…… 曾喜多，魏钟艳，李智丽，孙宝丽，谢青梅，毕英佐，马静云(16)
猪流行性腹泻病毒 GD-A 株的分离鉴定及 *S* 基因序列分析
…… 朱　俊，高又文，张　杰，叶　昱，廖　明，樊惠英(21)
截短侧耳素衍生物 BC-7013 在鸡体内的药物动力学和生物利用度研究
…… 杨德学，陈良柱，赖丽虹，任妙贤，张桂君，潘志坤，方炳虎(26)
二甲氧苄啶在猪体内的残留消除 …… 郭红燕，周连根，钟佳莲，孙美珍，梁超平，黄显会，曾振灵(32)
饲料必需氨基酸平衡关联度对框镜鲤生长、蛋白质消化和代谢的影响
…… 陈秀梅，申　斌，李　萌，于桂玲，王桂芹，芦洪梅(36)
水稻单片段代换聚合系的产量比较试验
…… 朱海涛，刘桂富，曾瑞珍，刘自强，傅雪琳，代资举，王少奎，张桂权(43)
沼液中挥发性有机物去除技术及肥效验证 …… 王　宇，金生威，鞠天琛，栾晓晨，冯连双，王玉军(50)
福寿螺和田螺的纤维素酶反应体系对不同 pH 和温度的响应
…… 罗明珠，章家恩，胡九龙，赵本良，邓智心(55)
2 种萱草对铅、镉的吸收累积及其在亚细胞的分布和化学形态特征 …… 李红婷，董　然(59)
^{60}Coγ 射线对海滨雀稗成活率及生长特性的影响 …… 谢新春，刘天增，解新明，张巨明(65)
华南地区推广应用大豆品种对疫霉根腐病的抗性评价
…… 程艳波，马启彬，牟英辉，谭志远，吴　鸿，年　海(69)
华南地区瓜实蝇田间种群的抗药性监测 …… 谷世伟，曾　玲，梁广文(76)
基于线粒体 *COI* 序列对云南地区柚喀木虱单倍型的鉴定
…… 王妍晶，岑伊静，江宏燕，罗孝竹，邓晓玲，XIA Yulu(81)
象耳豆根结线虫对 7 个品种番茄生长的影响 …… 张怀军，赵志祥，陈绵才(87)
原生质体融合选育高产多糖的罗尔阿太菌菌株
…… 李鸿梅，赵　慧，魏　明，闵伟红，张桂弘，刘景圣(91)
珍稀濒危植物伯乐树的潜在适生区预测 …… 龚　维，夏　青，陈红锋，俞新华，伍　菲(98)
基于“高分一号”遥感影像反演华南地区亚热带典型作物冠层 SPAD
…… 黄汝根，刘振华，胡月明，肖北生(105)
四川黑茶渥堆过程中主要品质成分及酶类活性变化 …… 刘婷婷，齐桂年，邹　瑶，李　伟，黄亚芳(112)
1-甲基环丙烯对无核黄皮贮藏品质和生理的影响 …… 陈丽晖，黄雪梅，张昭其，黄水生(117)
羊草 *CDPK* 基因全长 cDNA 的克隆及原核表达
…… 崔喜艳，秦思余，刘忠野，高　瑜，蒋载阳，郭继勋(123)
5-氯甲基水杨醛缩 *L*-酪氨酸锰(II)配合物的合成及生物活性的研究
…… 熊亚红，黄显才，何金锋，钟志伟，王子芫，黄嘉琪，郑嘉雯(129)
征订启事 …… (20)

期刊基本参数：CN44-1110/S * 1959 * b * A4 * 136 * zh + en * P * ¥15.00 * 1600 * 23 * 2015-07　　**封面设计**：林　敏

JOURNAL OF SOUTH CHINA AGRICULTURAL UNIVERSITY

Vol. 36 No. 4 Jul 2015

CONTENTS

Research progress in glucuronoxylan biosynthesis(review)
…… WU Aimin, ZHAO Xianhai, XIE Qiaoli, XIE Xinming(1)

Prokaryotic expression of main antigen epitope of pseudorabies virus *gE* gene in *Escherichia coli* and establishment of indirect ELISA
…… JI Yikuan, WANG Yu, CHENG Yi, ZHANG Baoshi, XIANG Keyu, JU Chunmei(11)

Development and application of indirect ELISA for porcine epidemic diarrhea virus antibody detection
…… ZENG Xiduo, WEI Zhongyan, LI Zhili, SUN Baoli, XIE Qingmei, BI Yingzuo, MA Jingyun(16)

Isolation and identification of GD-A strain of porcine epidemic diarrhea virus and phylogenetic tree analyses based on *S* gene
…… ZHU Jun, GAO Youwen, ZHANG Jie, YE Yu, LIAO Ming, FAN Huiying(21)

Research on pharmacokinetics and bioavailability of pleuromutilin derivative BC-7013 in chickens
…… YANG Dexue, CHEN Liangzhu, LAI Lihong, REN Miaoxian, ZHANG Guijun, PAN Zhikun, FANG Binghu(26)

Residue depletion of diaveridine in pigs …… GUO Hongyan, ZHOU Liangen, ZHONG Jialian, SUN Meizhen, LIANG Chaoping, HUANG Xianhui, ZENG Zhenling(32)

Effects of dietary essential amino acid balance relativity on growth, digestion and metabolism of protein of *Cyprinus carp*
…… CHEN Xiumei, SHEN Bin, LI Meng, YU Guiling, WANG Guiqin, LU Hongmei(36)

Comparative trial on grain yield for pyramiding lines of single segment substitution lines in rice
…… ZHU Haitao, LIU Guifu, ZENG Ruizhen, LIU Ziqiang, FU Xuelin, DAI Ziju, WANG Shaokui, ZHANG Guiquan(43)

Removal technology of volatile organic compounds from biogas slurry and fertilizer efficiency test
…… WANG Yu, JIN Shengwei, JU Tianchen, LUAN Xiaochen, FENG Lianshuang, WANG Yujun(50)

Responses of cellulase reaction systems of *Pomacea canaliculata* and *Cipangopaludina chinensis* to different pH and temperature
…… LUO Mingzhu, ZHANG Jiaen, HU Jiulong, ZHAO Benliang, DENG Zhixin(55)

Pb & Cd adsorption and accumulation characteristics, subcellular distribution and chemical forms in two types of *Hemerocallis* plants ····· LI Hongting, DONG Ran(59)

Effects of ^{60}Coγ ray irradiation on survival rates and growth characteristics of seashore paspalum ····· XIE Xinchun, LIU Tianzeng, XIE Xinming, ZHANG Juming(65)

Resistance evaluation of soybean varieties to phytophthora root rot in South China ····· CHENG Yanbo, MA Qibin, MU Yinghui, TAN Zhiyuan, WU Hong, NIAN Hai(69)

Monitoring for insecticide resistance of melon fly populations in the field of Southern China ····· GU Shiwei, ZENG Ling, LIANG Guangwen(76)

Identification of haplotypes of *Cacopsylla citrisuga* from Yunnan Province based on mitochondria *COI* sequence ····· WANG Yanjing, CEN Yijing, JIANG Hongyan, LUO Xiaozhu, DENG Xiaoling, XIA Yulu(81)

The effects of *Meloidogyne enterolobii* on the growth of seven tomato varieties ····· ZHANG Huaijun, ZHAO Zhixiang, CHEN Miancai(87)

Breeding of *Athelia rolfsii* strain with high polysaccharide yield by protoplast fusion ····· LI Hongmei, ZHAO Hui, WEI Ming, MIN Weihong, ZHANG Guihong, LIU Jingsheng(91)

Prediction of potential distributions of *Bretschneidera sinensis*, an rare and endangered plant species in China ····· GONG Wei, XIA Qing, CHEN Hongfeng, YU Xinhua, WU Fei(98)

Retrieval of typical subtropical crop canopy SPAD value in South China using GF-1 remote sensing image ····· HUANG Rugen, LIU Zhenhua, HU Yueming, XIAO Beisheng(105)

Variations in quality ingredients and primary enzymes activities of Sichuan dark tea during post-fermentation ····· LIU Tingting, QI Guinian, ZOU Yao, LI Wei, HUANG Yafang(112)

Effects of 1-methylcyclopropene on the storage quality and the postharvest physiology of seedless wampee fruit ····· CHEN Lihui, HUANG Xuemei, ZHANG Zhaoqi, HUANG Shuisheng(117)

Cloning and prokaryotic expression of the full-length cDNA of *CDPK* gene from *Leymus chinensis* ····· CUI Xiyan, QIN Siyu, LIU Zhongye, GAO Yu, JIANG Zaiyang, GUO Jixun(123)

Synthesis and biological activities of maganesium(II) complex with 5-(chloromethyl) salicylaldehyde-tyrosine ····· XIONG Yahong, HUANG Xiancai, HE Jinfeng, ZHONG Zhiwei, WANG Ziyuan, HUANG Jiaqi, ZHENG Jiawen(129)

华南农业大学学报 2015,36(4):98-104
Journal of South China Agricultural University
http://xuebao.scau.edu.cn
doi:10.7671/j.issn.1001-411X.2015.04.018

龚 维,夏 青,陈红锋,等.珍稀濒危植物伯乐树的潜在适生区预测[J].华南农业大学学报,2015,36(4):98-104.

珍稀濒危植物伯乐树的潜在适生区预测

龚 维[1],夏 青[1],陈红锋[2],俞新华[3],伍 菲[4]

(1 华南农业大学 生命科学学院,广东 广州 510642;2 中国科学院 华南植物园/中国科学院 植物资源保护和可持续利用重点实验室,广东 广州 510650;3 华南农业大学公共基础课实验教学中心,广东 广州 510642;4 21 世纪空间技术应用股份有限公司,北京 100096)

摘要:【目的】揭示伯乐树 *Bretschneidera sinensis* 地理分布格局,预测其潜在适生区,探讨环境和气候因子对其地理分布格局的影响.【方法】基于 1950—2000 年期间及 21 世纪 70 年代的 19 个气候因子数据以及中国 13 个省区、110 个有记录的地理分布点,利用最大熵算法模型(Maxent),结合地理软件 DIVA-GIS 和 ARCGIS,预测伯乐树的潜在适生区.结合野外调查和标本数据,以海拔图层和植被覆盖图层为底图绘制该种地理分布.【结果和结论】伯乐树潜在适生区位于华南地区,最适分布区位于南岭地区以及罗霄山和幕阜山.该种常见于海拔 500 ~ 2 000 m 的山地常绿阔叶林、常绿针叶林和落叶阔叶林,适宜气候条件为最暖季度平均雨量 500 ~ 2 750 mm,昼夜温差 7.8 ~ 9.8 ℃.随着全球气候变化,该种潜在适生区北移,最适分布区面积减少.基于此,还分析了主导环境和气候因子对该种地理分布格局的影响,并对其保护策略提出了建议.

关键词:伯乐树;最大熵算法模型;潜在适生区;环境和气候因子;保护策略

中图分类号:Q94 **文献标志码:**A **文章编号:**1001-411X(2015)04-0098-07

Prediction of potential distributions of *Bretschneidera sinensis*, an rare and endangered plant species in China

GONG Wei[1], XIA Qing[1], CHEN Hongfeng[2], YU Xinhua[3], WU Fei[4]

(1 College of Life Sciences, South China Agricultural University, Guangzhou 510642, China; 2 Key Laboratory of Plant Resources Conservation and Sustainable Utilization, South China Botanical Garden, Chinese Academy of Sciences, Guangzhou 510650, China; 3 Center of Experimental Teaching for Common Basic Courses, South China Agricultural University, Guangzhou 510642, China; 4 Twenty First Century Acrospace Technology Co., Ltd., Beijing 100096, China)

Abstract:【Objective】The present study aimed to investigate the geographical distribution pattern and predict the potential distribution range of *Bretschneidera sinensis*, a rare Tertiary tree species in China.【Method】A maximum entropy algorithm modelling program (Maxent) and GIS software systems of DIVA-GIS 7.4.0 and ARCGIS 9.1 were used to construct ENM based on 110 occurrences in 13 provinces or regions and 19 climatic factors in 1950—2000 and the 2070s.【Result and conclusion】*Bretschneidera sinensis* exists in subtropical evergreen broadleaved forests, evergreen needle-leaved forests or deciduous broadleaved forests in middle mountain regions at an altitude between 500 to 2 000 m, with a warm temperature and abundant precipitation. The most suitable habitat was predicted to be located in the ranges of Mts. Nanling, Mts. Luoxiaoshan and Mts. Mufushan. The most suitable environmental conditions for

收稿日期:2014-04-24 **优先出版时间:**2015-06-10

优先出版网址:http://www.cnki.net/kcms/detail/44.1110.s.20150610.1630.017.html

作者简介:龚 维(1979—),女,副研究员,博士,E-mail:wgong@scau.edu.cn

基金项目:国家自然科学基金(31300174,31170196,31470312);教育部博士点基金(20124404120014)

B. sinensis were revealed to be characterized by the precipitation of the warmest quarter with an average rainfull between 500 and 2 750 mm and a day-night temperature difference between 7.8 – 9.8 ℃. With the global climate change, the potential distribution range of *B. sinensis* shows a trend to move northwards in response to global warming. Therefore, environmental and climatic factors involved in the geographical distribution and endangered status of *B. sinensis* have been analyzed. Accordingly, conservation strategies are suggested for *in situ* and *ex situ* conservation of *B. sinensis*.

Key words: *Bretschneidera sinensis*; Maxent; potential distribution range; environmental and climatic factors; conservation strategy

物种地理分布格局对于研究生物多样性保护具有重要意义,也是制定物种保护策略的重要依据. 亚热带常绿阔叶林是我国最重要的森林群落类型之一,蕴藏着丰富的植物类群,其地理分布格局对于探讨我国常绿阔叶林植物响应全球气候变化具有重要意义. 物种分布模型常用于物种潜在分布区预测,基于气候匹配法的物种分布模型已得到了不断的完善和发展. 目前,最大熵算法模型(Maximum entropy algorithm modeling program, Maxent)在珍稀濒危动植物的潜在分布区预测中得到了广泛应用[1-6].

伯乐树 *Bretschneidera sinensis* 是伯乐树科唯一的一个种,也是我国的特有种,以我国为分布中心[7-9]. 该种在我国主要分布于长江流域各省,多生于亚热带常绿阔叶林山地[9-10]. 长期以来,伯乐树生境破坏严重,现存母树资源极为稀少. 加上结实率低,天然更新困难,该种已处于珍稀濒危状态,被评估为濒危等级[11],是我国一级重点保护野生植物,世界自然保护联盟(the International Union for Conservation of Nature,IUCN)红皮书已将其列为濒危种[12]. 作为第三纪古热带植物区系的濒危孑遗种[13],探讨其地理分布格局对气候变化的响应有利于开展该种的保护生物学研究. 本研究对伯乐树进行生态位模型(Ecological niche modelling)构建和分析,根据该种已知地理分布点数据,基于气候相似性原理,利用 Maxent 模型,结合地理分析软件,预测伯乐树当代及 21 世纪 70 年代的潜在适生区. 同时,结合该种野外调查资料、地理分布区海拔和植被数据,分析其地理分布格局及生态和气候影响因子,以期为将来进一步开展该种保护生物学研究、野外资源调查等积累数据、提供依据.

1　材料与方法

1.1　数据收集

伯乐树的物种分布数据主要来源于中国数字标本馆的记录(CVH),包括中国科学院成都生物研究所、中国科学院西双版纳热带植物园、中国科学院广西植物研究所、中国科学院华南植物园、中国科学院昆明植物研究所、中国科学院庐山植物园以及西北农林科技大学等. 同时,结合《中国植物红皮书:稀有濒危植物(第一册)》[13]、《中国植物志》[9]及各地方植物志. 另外,查阅伯乐树野外调查数据、研究成果和文献资料[14-17]. 最终,获得了全面的伯乐树地理分布数据,共 13 个省份(地区)、114 个分布点. 对于部分采集记录或相关文献资料中缺乏具体地理坐标的分布记录,根据百度地图,并借助 Google Earth 软件,查找出相应的经纬度.

在伯乐树地理分布数据收集的基础上,利用 DIVA-GIS 7.4.0 软件和 ARCGIS 9.1 软件分别以海拔图层和植被覆盖图层作为底图绘制该种的地理分布图. 海拔图层来自于 DIVA-GIS 软件自带的地理信息数据库,植被覆盖图层来自于网站 www.iscgm.org. 所采用气候数据共包括 19 个气候因子(表 1),来源于世界气候数据网站(http://www.worldclim.org). 当代气候数据为 Worldclim 数据库 1950—2000 年的来自世界各地气象站的气候信息,21 世纪 70 年代气候数据为 Worldclim 数据库校准后的 GCMs 气候投影数据[18]. 应用 2.5 arcminutes 数据库,每个栅格单元大致相当于 22 km^2(表 1). 分析用的底层地图是 1∶400 万中国行政区划图,从国家基础地理信息系统网站(http://nfgis.nsdi.gov.cn/nfgis/chinese/c_xz.htm)下载.

1.2　数据处理

根据所获得的伯乐树经纬度数据,借助 ARCGIS 9.1 软件,生成该种在中国境内的地理分布图,每个分布点至少有 1 个标本采集或者文献的确切记录. 分别以海拔图层和植被覆盖图层为底图,整合伯乐树地理分布点,利用 ARCGIS 9.1 软件绘制该种的地理分布图.

表1 利用 Maxent 进行伯乐树地理分布区预测的19个气候因子及相对贡献率

Tab. 1 Nineteen climatic factors used in the prediction of distributions and relative contributions of the main climatic factors to the Maxent model for *Bretschneidera sinensis*

气候因子	相对贡献率/%
年平均温	0.4
昼夜温差月均值	10.1
昼夜温差与年温差比值	6.5
温度季节变化	9.8
最热月份最高温	1.0
最冷月份最低温	7.6
年温度变化范围	0
最湿季度平均温度	4.9
最干季度平均温度	6.5
最暖季度平均温度	0.1
最冷季度平均温度	0.2
年平均雨量	0
最湿月份雨量	1.1
最干月份雨量	0.1
雨量变化方差	0.6
最湿季度雨量	4.4
最干季度雨量	0.9
最暖季度平均雨量	45.5
最冷季度平均雨量	0.3

将 Worldclim 下载的气候数据通过 DIVA-GIS 7.4.0软件转换成ASCII格式,应用Maxent模型对伯乐树的潜在适生区进行预测. 将地理分布点的经纬度数据和环境数据导入 Maxent v3.3.3 软件,随机选取 75% 的数据作为训练集(Sample file),用于建模,剩余 25% 的分布点作为测试集(Test sample file),用于验证. 选择启发式估测和刀切法(Jackknife),设置 10 次重复,产生 10 个预测随机模型,其它参数均为软件默认值. 采取常用的 ROC 曲线(Reciever operating characteristic curve)分析法预测精度,以 AUC(Area under roc curve)值作为模型预测准确性的衡量指标,选择具有最高 AUC 值的图层进行分布区预测分析. AUC 值越大,模型的预测能力越好. 相应的标准是:AUC <0.5,模型的预测能力低于随机模型的预测能力;AUC =0.5~0.7,模型的诊断价值低;AUC =0.7~0.9,模型的诊断价值中等;AUC =0.9~1.0,模型的诊断价值较高[1, 19-20].

模拟结果的输出选择 ASCII 格式,在 ARCGIS 9.1 软件中加载 Maxent 运行结果,将结果转换成 RASTER 格式. 根据重分类程序将生境适应性按照自然划分法(Natural break)分成6个等级(Ⅰ~Ⅵ),其中第Ⅵ级为最适分布区. 对各等级的图层进行统计分析,得到所研究的 13 个省份或地区在各适生等级下的适生面积. 另外,根据模拟结果中各气候因子的相对贡献率,筛选出影响伯乐树地理分布的主导气候因子.

2 结果与分析

2.1 伯乐树在中国的地理分布情况及潜在适生区预测

根据现有的伯乐树分布点数据,江西省(18个)、湖南省(18个)、广东省(20个)和贵州省(16个)的分布点最多. 另外,福建省和广西壮族自治区分别有 11 和 10 个分布点,云南省和浙江省分别有 6 和 7 个分布点,分布点最少的是四川省(4个)、重庆市(1个)、湖北省(1个)、海南省(1个)和台湾(1个). 其中,海南省的鹦哥岭是伯乐树在热带地区的唯一分布点. 以海拔图层为底图绘制的伯乐树地理分布图(图1)表明,该种主要沿南岭山脉、罗霄山、武夷山分布,最常见于亚热带地区海拔 500~2 000 m的中山地带,在海拔低于500 m或近2 000 m的地区也有少量分布. 以植被图层为底图绘制伯乐树地理分布图(图2),结合野外调查数据,结果显示该种主要分布于常绿阔叶林、常绿针叶林和落叶阔叶林中,常散生在湿润沟谷、溪旁坡地的林丛和灌丛. 部分群体出现在耕地边缘及其他自然植被的镶嵌区. 根据 Maxent 的输出结果,基于 1950—2000 年及 21 世纪 70 年代的气候数据,训练集数据和测试集数据的 AUC 值分别为 0.994 和 0.993. 由图 3 显示,基于 1950—2000 年气候数据,该种潜在适生区位于亚热带地区,20.0°~32.5°N、105.0°~122.5°E. 其最适分布区位于长江以南山地,如广西猫儿山、大瑶山,广东北部山地,以及江西九连山等,沿南岭山脉以及罗霄山和幕阜山呈东西走向分布,在中国的总面积约为337 551 km^2(表2). 基于 21 世纪 70 年代气候数据,该种潜在适生区北移至35°N,在中国的最适分布区总面积减少为 228 109 km^2,川渝交界处新增为其最适分布区(表2和图3).

基于1950—2000年气候数据,该种在广西壮族自治区的最适分布区面积最大(74 592 km^2),其次是江西省(66 100 km^2),但是该种在广西壮族自治区现

有地理分布点较少(10 个). 该种在广东省、贵州省、湖南省和福建省的最适分布区面积相当(25 336 ~ 37 161 km^2),在四川省、重庆市、浙江省、湖北省和云南省的最适分布区面积均低于 10 000 km^2,在海南省以及台湾均无最适分布区. 基于 21 世纪 70 年代气候数据,该种在江西省的最适分布区面积最大(78 680 km^2),其次是广西壮族自治区(66 488 km^2). 该种在贵州省和福建省的最适分布区面积明显减小,低于 10 000 km^2,在浙江省、湖北省和云南省减少更为显著,均低于 1 000 km^2,但是,该种在川渝地区最适分布区面积均明显增加.

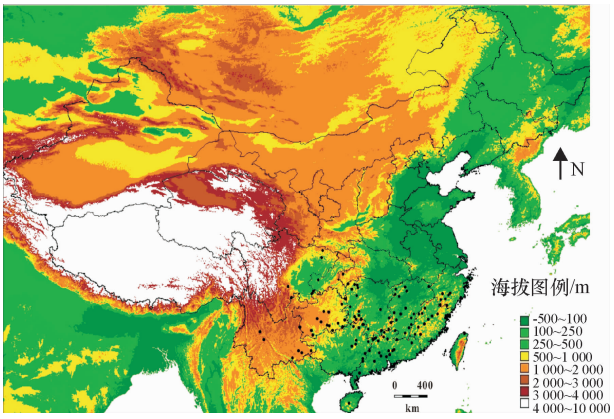

图 1　伯乐树地理分布点海拔图

Fig. 1　Altitudes in the geographical distribution of *Bretschneidera sinensis*

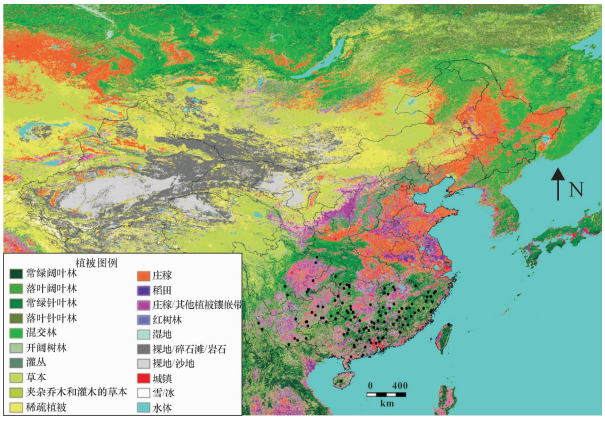

图 2　伯乐树地理分布的植被覆盖情况

Fig. 2　A landcover type in the geographical distribution of *Bretschneidera sinensis*

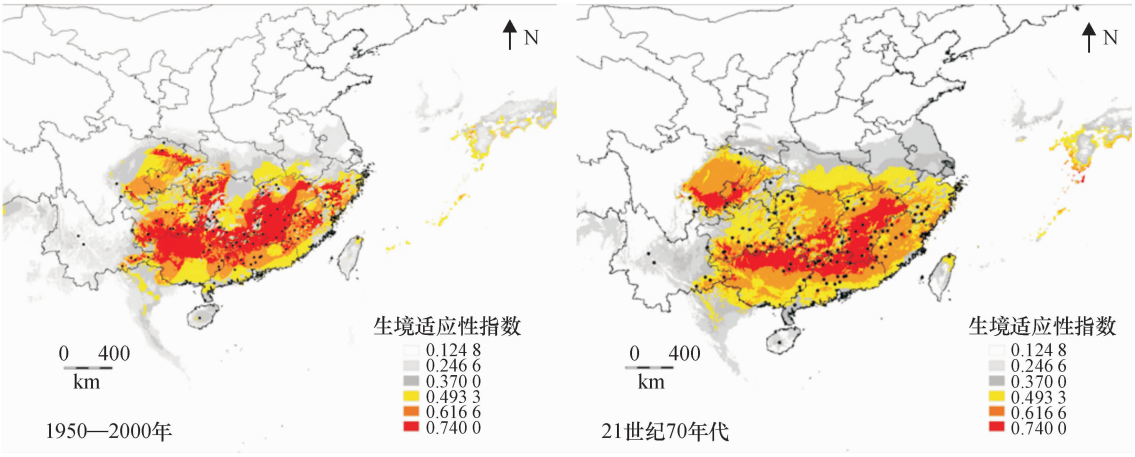

图 3　基于 Maxent 模型与 19 个气候因子预测的伯乐树 1950—2000 年及 21 世纪 70 年代的潜在适生区

Fig. 3　A prediction of the potential distribution range of *Bretschneidera sinensis* in 1950—2000 and the 2070s based on 19 climatic factors using Maxent model

2.2　主导气候因子及其对伯乐树地理分布区的影响

从表 1 可见,基于 1950—2000 年气候数据,最暖季度平均雨量对伯乐树潜在适生区影响最大,贡献率为 45.5%. 此外,温度条件也对该种潜在适生区产生了一定影响,如昼夜温差月均值的影响居第 2 位,其贡献率为 10.1%. 相对贡献率接近或大于 5% 的气候因子为温度季度化、最冷月份最低气温、昼夜温差与年温差比值、最干季度平均温度和最湿季节平均温度. 相对贡献率大于 10% 的气候因子(主导因子)对伯乐树分布概率的影响见图 4. 当最暖季度平均雨量低于 500 mm 时,伯乐树的分布概率随着降雨量的上升而迅速增加;当降雨量超过 500 mm 时,其分布概率仍随着降雨量的增加而缓慢上升;当降雨量在 2 750 mm 时,其分布概率达到平衡(图 4A). 因此,最暖季度平均雨量 >2 750 mm 后将不利于伯乐树生长. 图 4B 显示,昼夜温差月均值在 7.8 ~ 9.8 ℃ 范围内,伯乐树的分布概率达到最高,低于 7.8 ℃ 或高于 9.8 ℃ 均不利于伯乐树生长.

表2 伯乐树在中国13个省(地区)6个等级的分布区面积

Tab. 2 Distribution areas of *Bretschneidera sinensis* in 13 provinces (regions) of China based on 6 classes km^2

省(区)	年代	Ⅰ	Ⅱ	Ⅲ	Ⅳ	Ⅴ	Ⅵ[1)]
江西	1950—2000年	4 595	12 726	14 360	24 501	44 619	66 100
	21世纪70年代	38	873	4 173	18 835	64 302	78 680↑
广西	1950—2000年	2 806	9 336	30 615	42 058	77 294	74 592
	21世纪70年代	39	1 099	5 317	57 032	106 726	66 488
广东	1950—2000年	549	10 874	39 965	48 969	48 958	35 485
	21世纪70年代	248	1 903	20 929	58 670	62 021	41 030↑
福建	1950—2000年	4 690	14 033	21 007	20 988	33 946	25 336
	21世纪70年代	38	2 044	5 922	25 062	83 477	3 457
贵州	1950—2000年	6 639	16 934	27 220	43 300	44 662	31 245
	21世纪70年代	5 540	13 149	31 082	71 029	40 685	8 514
湖南	1950—2000年	9 659	34 288	44 676	41 621	44 423	37 161
	21世纪70年代	190	4 511	14 765	50 588	117 021	24 754
重庆	1950—2000年	5 590	10 587	13 526	25 291	20 705	6 701
	21世纪70年代	5 460	8 884	12 900	17 953	27 171	10 032↑
四川	1950—2000年	170 182	200 760	41 646	36 988	31 892	6 531
	21世纪70年代	300 865	26 250	21 167	28 763	90 459	20 497↑
浙江	1950—2000年	10 079	23 171	23 980	21 475	15 707	9 730
	21世纪70年代	312	4 851	20 205	46 313	31 914	546
湖北	1950—2000年	49 932	72 336	35 421	20 250	8 217	1 244
	21世纪70年代	9 982	47 240	44 586	68 800	16 792	0
台湾	1950—2000年	6 743	21 378	6 324	1 476	128	0
	21世纪70年代	12 585	12 329	5 661	5 148	276	0
海南	1950—2000年	8 364	16 618	8 626	382	10	0
	21世纪70年代	15 346	17 193	1 421	41	0	0
云南	1950—2000年	166 308	182 663	22 519	9 921	8 173	4 416
	21世纪70年代	203 273	123 607	39 893	15 478	11 629	120
中国	1950—2000年	7 682 228	516 074	335 807	357 047	371 674	337 551
	21世纪70年代	7 908 652	430 014	288 167	449 576	595 481	228 109

1)↑表示分布区面积增加.

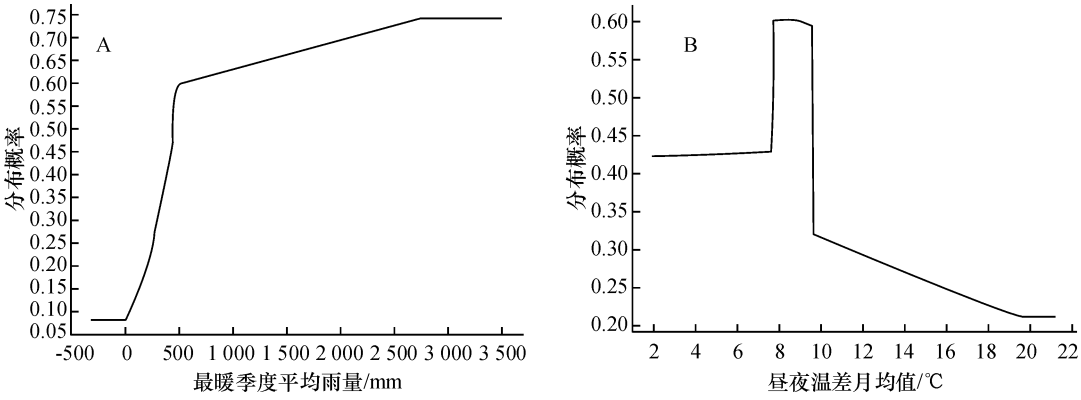

图4 主导气候因子对伯乐树分布概率影响的曲线

Fig. 4 Response curves of distribution probability of *Bretschneidera sinensis* to two important climatic factors of the Maxent model

3 讨论与结论

3.1 Maxent模型的适用性

基于本研究结果,利用气候因子和最大熵模型构建的伯乐树地理分布与气候关系模型的AUC值高达0.993($P=0.01$),表明预测结果非常好,能够较为准确地反映该种的潜在适生区.越来越多的研究证明,Maxent模型简单易操作,与物种的拟合度较

高,能准确反映物种的潜在适生区. 该模型运算已知物种的地理分布点和环境因子数据,已知物种分布点数据越多、越准确,对模型的构建越有利,精确度也越高[21-22]. 本研究通过各个渠道尽可能多地获得该种的地理分布信息,包括 CVH 标本数据库、各地植物志、已报道文献等,并加以实地考察,最大限度地保证数据来源全面、可靠,这是本研究具有较高 AUC 值的前提之一. 此外,本研究利用 ARCGIS 软件进行数据处理和分析,使物种分布数据和气候数据在每栅格单元上相对应,进一步提高了数据的准确性,降低了误差.

3.2　环境因子和气候因子对伯乐树潜在适生区的影响

根据本研究结果,伯乐树最适宜分布在中海拔(500 ~ 2 000 m)山地的林中. 部分群体位于耕地边、林缘,这些地区更容易遭受人为干扰,生境破坏严重,生态条件恶劣,致使伯乐树在这些地区的群体小,个体少,从而濒临危险,部分群体甚至灭绝. 从各气候因子对伯乐树地理分布的影响来看,最暖季度降雨量的影响最为明显,充沛的降水和潮湿的环境有利于其生长. 根据野外调查资料,该种大多生长于湿润沟谷、溪旁坡地,尤其是华南地区的一些群体,多生长于相对湿度在 80% 以上的环境. 同时,该树种幼树耐荫,环境中的高大乔木可为其遮挡阳光. 而在耕地或林缘的群体,缺乏遮光条件,极不利于伯乐树幼苗成长. 另外,一些高海拔地区往往高寒、干燥,且昼夜温差较大,也不利于伯乐树的生长. 因此,亚热带中海拔山地气候温暖湿润,为伯乐树生长提供了有利条件.

3.3　伯乐树潜在适生区特征及其对气候变化的响应

本研究显示,伯乐树潜在适生区位于我国亚热带常绿阔叶林、海拔 500 ~ 2 000 m 的中山地带,分布区位于南岭地区以及幕阜山、罗霄山和大娄山地区. 伯乐树为第三纪古热带植物区系的孑遗种,同其他古老孑遗植物类似,其地理分布区不可避免地会受到第四纪冰期气候波动的影响. 通常,冰期气候剧烈波动的情况下,一些地形复杂多样的山区仍然保持相对稳定的生态环境和地质条件,从而成为一些物种冰期时的适合生境[23]. 我国的西南山地和南岭山地,地形复杂多样,没有直接受到第四纪冰川的影响,富集植物物种多样性,是许多第三纪孑遗植物的冰期避难所,分布着许多第四纪气候性地理残遗种. 位于我国中部地区的幕阜山和罗霄山在一定程度上阻挡了第四纪冰川的影响,也为一些物种的生存提供了适合的生境条件,独特的地形地貌和地质条件使得这些地区成为了伯乐树的潜在适生区. 对其他常绿阔叶林植物进行最大熵模型的潜在适生区预测,同样表明这些地区为冰期避难所,如杜鹃、鄂报春等[24-25]. 此外,有研究指出,随着 CO_2 浓度增加,全球气候变暖,北半球植被带有向北方高纬度迁移的趋势[26-27]. 本研究获得了相似的预测结果. 基于 21 世纪 70 年代的气候数据,伯乐树未来的潜在适生区将由南向北迁移和扩张. 同时,该种最适分布区面积将减少,说明全球气候变暖一定程度上将导致该种生境适应性降低.

3.4　伯乐树保护策略的建议

近年来,生态位模型在生物多样性保护研究中的作用和意义日益突出. 在自然保护区的选择和设计过程中,构建相应的生态位模型常常具有重要的价值和意义[28-30]. 根据本研究结果,我们对伯乐树群体就地保护和迁地保护工作提出几点建议. 南岭地区以及幕阜山、罗霄山和大娄山地区具有较高的生物多样性,也是伯乐树在 1950—2000 年期间及 21 世纪 70 年代的最适分布区,建议对这些地区的伯乐树群体进行就地保护. 盲目开荒、乱砍滥伐和过度放牧是造成伯乐树原有生境破坏的重要原因. 针对伯乐树最适分布区群体,建议选择这些地区建立自然保护小区,进行规范管理,避免人为干扰和破坏. 在自然保护小区内,收集伯乐树种子,培育异龄幼苗. 通过人工授粉,加强个体及群体间的交流,增加个体数量和群体规模. 同时,对最适分布区群体的自然演替过程进行长期跟踪和监测,以保证最大限度地保护现有群体. 生态位模型可以帮助我们判断未知群体的实际分布地[28-30]. 广西壮族自治区虽为最适分布区,但其现有地理分布点却很少. 我们建议核查该地区是否存在一些记录空缺的分布点,并对该地区进行全面的野外调查,发现未知群体,及时对这些群体进行生态学研究和种质资源保护. 此外,迁地保护可以使物种占据新的分布点,是特有珍稀濒危植物保护策略中一个十分重要的环节. 位于伯乐树最适分布区以外的群体,尤其是一些边缘群体,个体数量少,群体小,存在生境片断化和地理隔离的风险,建议采取迁地保护策略. 根据该种生物学特性和生态学特性以及适宜的气候因子数据,结合已有的迁地保护成功实例,选择适宜地区建立规范的迁地保护基地,如南岭地区. 在迁地保护区域内,建立种质资源库和种苗基地,进行长期的管理和监测,保证湿度和温度,同时进行野外回归实验,最大限度地保护伯乐树的种质资源.

致谢:感谢中国科学院华南植物园罗中莱博士和黄惠润博

士在数据分析和文章撰写中提供的帮助和支持!

参考文献:

[1] ELITH J, GRAHAM C H, ANDERSON R P, et al. Novel methods improve prediction of species' distributions from occurrence data [J]. Ecography, 2006, 29 (2): 129-151.

[2] PHILLIPS S J, ANDERSON R P, SCHAPIRE R E. Maximum entropy modeling of species geographic distributions [J]. Ecol Model, 2006, 190 (3/4): 231-259.

[3] KUMAR S, STOHLGREN T J. Maxent modeling for predicting suitable habitat for threatened and endangered tree *Canacomyrica monticola* in New Caledonia [J]. J Ecol Nat Environ, 2009, 1(4): 94-98.

[4] KREMEN C, CAMERON A, MOILANEN A, et al. Aligning conservation priorities across taxa in Madagascar with high-resolution planning tools [J]. Science, 2008, 5873 (320): 222-226.

[5] 罗翀,徐卫华,周志翔,等. 基于生态位模型的秦岭山系林麝生境预测 [J]. 生态学报, 2011,31(5): 1221-1229.

[6] 张蓝月,叶向斌,刘念,等. 白花油麻藤的地理分布及适生区预测 [J]. 广西植物,2012,32(1): 27-32.

[7] 吴征镒. 中国种子植物属的分布区类型 [J]. 云南植物研究,1991,13(S4): 1-139.

[8] 吴征镒,周浙昆,李德铢,等. 世界种子植物科的分布区类型系统 [J]. 云南植物研究, 2003,25(3): 245-257.

[9] 中国科学院中国植物志编辑委员会. 中国植物志:第34卷[M]. 北京: 科学出版社,2013.

[10] 中国科学院华南植物园. 广东植物志 [M]. 广州: 广东科技出版社,2009:1-4406.

[11] 汪松,解焱. 中国物种红色名录 [M]. 北京: 高等教育出版社,2004:1-365.

[12] 于永福. 国家重点保护野生植物名录:第一批[J]. 植物杂志,1999,5: 4-11.

[13] 傅立国. 中国植物红皮书:稀有濒危植物:第1册 [M]. 北京: 科学出版社,1991:94-195.

[14] 陈建民. 贵州省珍惜濒危植物信息系统 [D]. 重庆: 西南师范大学,2003.

[15] 何克军,李意德. 广东省国家I级重点保护野生植物资源现状及保护策略 [J]. 热带亚热带植物学报,2005, 13(6):519-525.

[16] 乔琦. 珍稀植物伯乐树的濒危机制和保育技术研究 [D]. 广州:中国科学院华南植物园,2010.

[17] 张荣京,邢福武,萧丽萍,等. 海南鹦哥岭的种子植物区系 [J]. 生物多样性,2007,15(4): 382-392.

[18] VAN VUUREN D P, EDMONDS J A, KAINUMA M, et al. The representative concentration pathways: An overview[J]. Climatic Change, 2011, 109(1/2): 5-31.

[19] FIELDING A H, BELL J F. A review of methods for the assessment of prediction errors in conservation presence / absence models [J]. Environ Conserv, 1997, 24(1): 38-49.

[20] SWETS J A. Measuring the accuracy of diagnostic systems [J]. Science, 1988, 240 (4857): 1285-1293.

[21] LOZIER J D, ANIELLO P, HICKERSON M J. Predicting the distribution of Sasquatch in western north America: Anything goes with ecological niche modeling [J]. J Biogeogr, 2009,36(9): 1623-1627.

[22] 曹向锋,钱国良,胡白石,等. 采用生态位模型预测黄顶菊在中国的潜在适生区 [J]. 应用生态学报,2010,21 (12): 3063-3069.

[23] HEWITT G M. Some genetic consequences of ice ages, and their role, in divergence and speciation [J]. Biol J Linn Soc, 1996, 58(3):247-276.

[24] YAN Haifei, ZHANG Caiyun, WANG Fengying, et al. Population expanding with the phalanx model and lineages split by environmental heterogeneity: A case study of *Primula obconica* in subtropical China [J]. PLoS One, 2012, 7(9): e41315.

[25] LI Yong, YAN Haifei, GE Xuejun. Phylogeographic analysis and environmental niche modeling of widespread shrub Rhododendron simsii in China reveals multiple glacial refugia during the last glacial maximum [J]. J Syst Evol, 2012, 50(4):362-373.

[26] LUCHT W, PRENTICE I C, MYNENTR B, et al. Climatic control of the high-latitude vegetation greening trend and pinatubo effect [J]. Science, 2002, 296 (5573): 1687-1689.

[27] 冯彩云,许新桥,马月萍,等. 植物对气候变化生理反应研究进展 [J]. 世界林业研究, 2012,25(4): 16-21.

[28] 朱耿平,刘国卿,卜文俊,等. 生态位模型的基本原理及其在生物多样性保护中的应用[J]. 生物多样性, 2013,21(1): 90-98.

[29] BOURG N A, MCSHEA W J, GILL D E. Putting a CART before the search: Successful habitat prediction for a rare forest herb [J]. Ecology, 2005, 86(10), 2793-2804.

[30] MENON S, CHOUDHURY B I, KHAN M L, et al. Ecological niche modeling and local knowledge predict new populations of *Gymnocladus assamicus*, a critically endangered tree species [J]. Endanger Species Res, 2010, 11 (2): 175-181.

【责任编辑 李晓卉】

Plant Diversity 45 (2023) 752–756

Contents lists available at ScienceDirect

Plant Diversity

journal homepage: http://www.keaipublishing.com/en/journals/plant-diversity/
http://journal.kib.ac.cn

Report

The complete plastid genome provides insight into maternal plastid inheritance mode of the living fossil plant *Ginkgo biloba*

Mengxue Feng [a, 1], Hanghui Kong [b, 1], Meixiu Lin [a], Rongjing Zhang [a, **], Wei Gong [a, *]

[a] College of Life Sciences, South China Agricultural University, Guangzhou 510614, China
[b] Key Laboratory of Plant Resources Conservation and Sustainable Utilization, South China Botanical Garden, Chinese Academy of Sciences, Guangzhou 510650, China

ARTICLE INFO

Article history:
Received 16 March 2023
Received in revised form
6 September 2023
Accepted 19 September 2023
Available online 4 October 2023

The plastid is widely present in algae and plants with important functions in the process of photosynthesis, carbon fixation, and stress response (Shi et al., 2022). Despite the consistency between plastid genomes in plants, size variation of the plastid genome, gene loss, structure changes, and pseudogenes have been frequently observed (Ivanova et al., 2017). Plastid genome has currently shown a wide application in research of phylogeny, populations and biogeography in combination with nucleus genome (Wang et al., 2021). As is known, the plastid originates from cyanobacteria through two independent secondary endosymbiosis and has its own genetic replication mechanism (Howe et al., 2003). Thus, plastids have been suggested not to be transmitted according to the rules of Mendelian genetics, but generally demonstrate uniparental inheritance mode (Birky, 1995). Concerning the uniparental inheritance of plastids, research have been mainly conducted on species of angiosperms, but few on gymnosperms or ferns (Kita et al., 2005; Li et al., 2013).

Uniparental inheritance potentially evolved from relaxed organelle inheritance patterns because it mitigates the spread of cytoplasmic components. Three possible patterns were suggested for plastid inheritance, including maternally, paternally and biparentally (Reboud and Zeyl, 1994; Kormutak et al., 2018). Angiosperms seem to display mainly a maternal transmission of its plastids (Greiner et al., 2015). In most gymnosperms, the plastid transmission is considered to occur exclusively by paternal inheritance. *Cryptomeria japonica* was the first gymnosperm known to inherit its plastid genome from its male parent (Ohba et al., 1971). Most conifers exhibit exclusively or predominantly paternal inheritance of both plastids and mitochondrias (Mogensen, 1996; Jansen and Ruhlman 2012; Lubna et al., 2021). However, there are a few exceptions. Several gymnosperms, including *Ginkgo*, are supposed to probably exhibit maternal inheritance of both plastids and mitochondrias. A few of studies have been carried out for plastid inheritance of gymnosperm species, most of which are based on cytological analysis (Mogensen, 1996; Guo et al., 2005; Zhong et al., 2011). So far, the information seems to be fragmentary and no strong evidence is available specifically for *Ginkgo*.

Ginkgo biloba L. is a sole representative of Ginkgoales - one of the eight extant gymnosperm orders (Yang et al., 2022). This species shows a geographical distribution range in broadleaved forest of both subtropical and temperate zones in Eastern Asia. It is widely cultivated all over the world due to its highly horticultural, medicinal and ecological values. Several glacial refugial of *G. biloba* were identified in subtropical evergreen broad forest in China (Gong et al., 2008; Zhao et al., 2019). This species is a dioecious tree plant, with separate male and female individuals. The characteristics of separate male and female individuals produced by dioecy could rule out the possibility of self-pollination and show advantages in studying plastid genetic research (Zhai and Sun, 2015). During genetic crosses, different parents were selected for artificial pollination to produce hybrid offsprings, then genetic similarities and differences between the parents and offsprings were compared to explore their organelle inheritance more distinctively. A few of research have been conducted on *G. biloba* since its first plastid genome was assembled and annotated (Lin et al., 2012; Zhou et al., 2020; Yang et al., 2021). However, previous research only focused on structural comparison and gene composition of the plastid genome, which aimed to develop molecular markers, analyze plant phylogeny, or compare genomics. So far, no molecular evidence is available to reveal the inheritance mode of the plastid genome of *G. biloba*.

Traditional methods to investigate organelle inheritance involve hybridization experiment, using electron microscopy or DAPI

* Corresponding author.
** Corresponding author.
E-mail addresses: zhangrongj@scau.edu.cn (R. Zhang), wgong@scau.edu.cn (W. Gong).
Peer review under responsibility of Editorial Office of Plant Diversity.
[1] These authors contributed equally to the work.

https://doi.org/10.1016/j.pld.2023.09.001
2468-2659/Copyright © 2023 Kunming Institute of Botany, Chinese Academy of Sciences. Publishing services by Elsevier B.V. on behalf of KeAi Communications Co. Ltd. This is an open access article under the CC BY-NC-ND license (http://creativecommons.org/licenses/by-nc-nd/4.0/).

fluorescence microscopy, as well as molecular markers, such as restriction fragment length polymorphism (RFLPs), and simple sequence repeats (SSRs) (Zhong et al., 2011). Most recently, the development of next-generation sequencing technologies has stimulated a rapid and successful achievement in the database of plastid genomes (Wang et al., 2018). Thus, genomic data demonstrates a strong potentiality to explore the molecular mechanism of organelle inheritance mode (Villanueva-Corrales et al., 2021). In the current study, we conducted artificial pollination for three crosses of *Ginkgo biloba*. Using next generation sequencing, plastid genomes of all the parents and offsprings were investigated and compared, showing strong genomic evidence on maternal inheritance mode.

Two female and three male trees of *Ginkgo biloba* were selected as candidates for genetic crosses. Artificial pollinations were conducted in the county of Pingtian, Nanxiong, Guangdong Province, in southern China, which is suggested as one of the glacial refugia with a large population of *Ginkgo* trees (Zhao et al., 2019). Two female *Ginkgo* trees over 100 years, showing an average diameter at breast height (DBH) more than 80 cm and an average height of ~20 m, are recorded to possess high seed production. Thus, they were chosen as maternal origin. Three old male *Ginkgo* trees, estimated to be over 100 years, showing an average DBH more than 80 cm and an average height of ~20 m, were selected as paternal origin. In April, 2016, the branches of the female trees were wrapped with parchment paper and the male flowers from the nearby male trees were all removed before flowering in order to avoid any pollen pollution. Artificial pollinations were conducted for three crosses. For each cross, seeds were collected and germinated. The accession information for each cross and the corresponding offsprings in the current study were listed in Table S1.

Fresh leaves were collected from the seedlings in the spring. Leaf tissue was ground in tubes with glass beads with the tissue homogenizer Tissuelyser-96 (Shanghai Jingxin Industrial Development Co., Ltd). Total genomic DNA was extracted with modified cetyl trimethyl ammonium bromide (CTAB) method (Doyle and Doyle, 1987). An Illumina HiSeq2000 sequencer was used to sequence paired-end (PE) sequencing libraries with an average 300 bp insert length. Over 10 million clean reads were passed through quality control with a 150 bp each read length.

We assembled the plastid genome using GetOrganelle pipeline (https://github.com/Kinggerm/GetOrganelle) and editing *de novo* assembly graph using Bandage (Coil et al., 2015). The plastid genome of *Ginkgo biloba* (MN443423.1) (Yang et al., 2021) was downloaded from NCBI and used as the reference sequence. PGA (https://github.com/quxiaojian/PGA) (Qu et al., 2019), Geneious 9.1.4 (Biomatters Ltd., Auckland, New Zealand), and ARAGORN program were jointly used for annotating the plastid genome in comparison with references. The circular genome map of *G. biloba* was illustrated with the Organellar Genome DRAW tool (OGDRAW, available online: http://ogdraw.mpimp-golm.mpg.de/) (Lohse et al., 2013).

The plastid genome sequences from the finalized data set of all parents and F1 individuals were aligned with MAFFT v.7.0.0 (Katoh and Standley, 2013) with manual adjustment when necessary. Using DnaSP 6 (Rozas et al. al., 2017), we determined the substitutions numbers and types of the sequences, and also performed comparative analyses of the nucleotide diversity (*Pi*) among the complete plastid genomes of the parents and offsprings based on a sliding window analysis. All the protein coding genes (PCGs) were extracted and aligned using MAFFT v.7.0.0. Using DnaSP 6 and MEGA v.11.0 (Tamura et al., 2021), we estimated the genetic distance between the parents and offsprings based on Kimura 2-parameter (*K2–P's*) model.

The original reads were mapped to plastid genome references using BWA-0.7.17-R1188 (Li, 2013) to detect the SNPs between the parents and the offsprings. The generated bam files were sorted and variant calls were performed by Samtools-1.7 and Bcftools v.1.9, respectively (Danecek et al., 2021; Li, 2009, 2011). Sequence similarities between the parents and offsprings were used as reference indicators. To identify SNPs among parents and F1 individuals, we inspected the alignment results in Geneious and generated haplotype files using DnaSP 6. All the SNPs were statistic to identify the polymorphism between the parents and offsprings.

All parents and F1 individuals were used to reconstruct phylogenetic relationships in order to trace plastid genome inheritance. *Cycas revoluta* (JN867588) was used as outgroup. Maximum parsimony (MP) method was applied for phylogenetic analyses by PAUP* v.4.0 (Swofford, 2002). Bootstrap values were calculated in PAUP* with 1000 bootstrap replicates. Neighbor-Joining (NJ) method was also used to conduct phylogenetic analysis among all parents and F1 individuals by MEGA v.11.0 (Tamura et al., 2021). Additionally, using GetOrganelle pipeline, we assembled nuclear ribosomal RNA sequences (18S-ITS1-5.8S-ITS2-26S) and extracted the ITS regions, which were further used to reconstruct phylogenetic trees as a control.

A total number of 2 × 150 bp pair-end reads of 6,504,575–35,285,882 were produced with 1.95–10.59 Gb of clean data. All reads data were deposited in the NCBI Sequence Read Archive (SRA) (Table S3). The size of the complete plastid genome is from 156,970 bp to 156,999 bp, which is supposed to be smaller than cycads ranging from 161,815 to 166,341 bp (Wu and Chaw, 2015). The plastid genome displays a typical quadripartite structure, including a pair of IRs of 17,733 bp each in length, separated by LSC region ranging from 99,248 bp to 99,267 bp and SSC region from 22,257 bp to 22,266 bp (Fig. 1 and Table S2). The GC content of the plastid genome is 39.6%, within that range of gymnosperms from 34.3% to 40.11% (Wu and Chaw, 2015). The plastid genome encodes 134 predicted functional genes when duplicated genes in the IR regions were only counted once. A total of 85 PCGs, 41 tRNA genes and eight rRNA genes are identified among all the individuals (Table S2). The remaining non-coding regions include introns, intergenic spacers, and pseudogenes. Each of the four genes (two PCGs and two tRNA genes) contains only one intron.

The IRs can be normally identified by a central unit of eight rRNA genes including *rrn*4.5, *rrn*5, *rrn*16 and *rrn*23. In *Ginkgo biloba*, the IRs were detected to be composed of 13 genes, including three PCGs, six tRNA genes, and four rRNA genes. In comparison with other gymnosperms, the length of IRs in *G. biloba* is shorter than *Cycas revoluta* (25,066 bp; JN867588), *Nothotsuga longibracteata* (25,918 bp) and *Ephedra sinica* (20,743 bp), but longer than *Cycas taitungensis* (15,830 bp) and some conifers that lost IRs. Due to the lack of *ycf*2 gene, the IRs in *G. biloba* are relatively shorter than that of the most angiosperms. Consequently, the LSC/IR junction region, which is supposed to retain the complete *ycf*2 gene and the adjoining *psb*A or *rpl*23-*rps*3 gene cluster in order, has been changed and produces a pseudolized *Ψrpl*23 gene.

The average nucleotide variability (*Pi*) value was estimated to be 0.75×10^{-5} among parents and offsprings based on the comparative analysis with DnaSP 6 (Fig. S2). The nucleotide variability (*Pi*) is overall low with only eight genes displaying relatively high values ($Pi > 0.0001$), which are *psbK-I, trnG-R, infA-rps8, ycf2, trnL-ndhB, ndhA* intron, *ycf*1, and *ndhB-trnL*. The first four loci are present in the LSC, while two genes *ndhA* intron and *ycf*1 in SSC. Therefore, the highest variation was found in the LSC region with *Pi* ranging from 0.0001 to 0.0014, followed by the SSC region (Fig. S2). The IRs had much lower nucleotide diversity, each of which possesses only one gene showing $Pi > 0.0001$. Those eight highly variable loci are thus

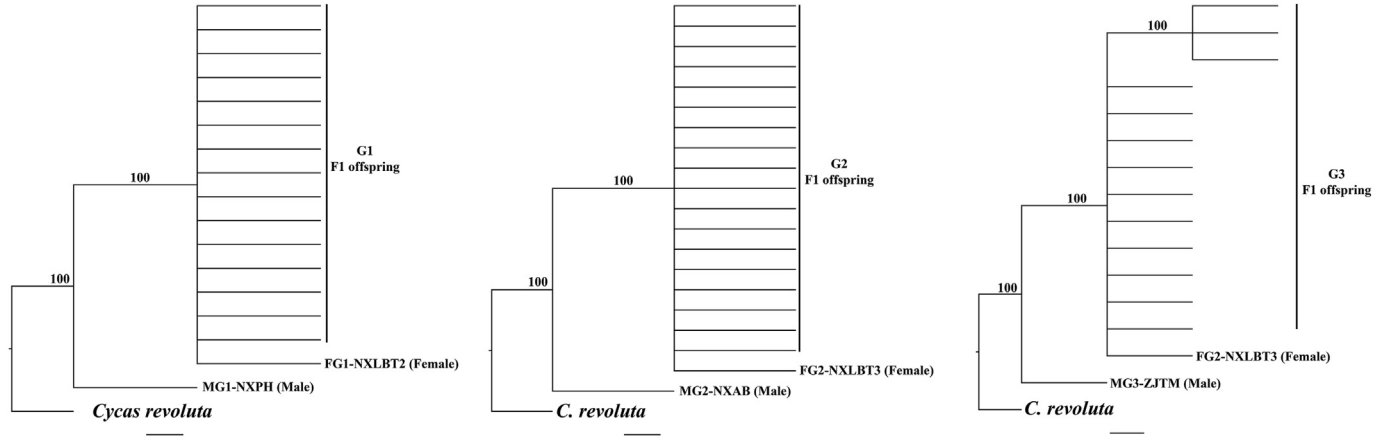

Fig. 1. Phylogenomic analysis for all parents and F1 offsprings in three genetic crosses (G1, G2 and G3) of *Ginkgo bilboa* based on Maximum Parsimony (MP) method. *Cycas revoluta* was used as an outgroup. Numbers above the branches represent bootstrap values.

suggested as phylogenetic informative markers for population research of *Ginkgo biloba*.

Based on the *K2–P's* parameter model, we calculated the genetic distance among the parents and offsprings using 86 PCGs. The *K2–P's* genetic distance is major generated by that between male parent and offsprings, with the value of $(0.06–1.27) \times 10^{-4}$ among the three genetic crosses (Table 1). The *K2–P's* genetic distance between female parent and offsprings is extremely weak with overall values to be 0. We aligned the plastid genome sequences for all *Ginkgo* parents and off springs to detect the SNPs and check the numbers of offsprings that are consistent with female or male parent. Notably, all offsprings show SNPs identical to their female parent (Table 1). Consequently, all offsprings possess the same haplotypes with female parent based on three genetic crosses (Table S4).

We performed phylogenetic analyses for each cross, in order to detect the evolutionary relationship of the parent and offsprings based on MP and NJ trees (Figs. 1, S3 and S4). In each cross, all F1 individuals grouped with their female parent, forming a monophyly with a high bootstrap value, while the male parent was divergent from them based on MP and NJ analysis (Fig. 1). As for the control based on ITS data in G1 and G2 crosses, some individuals of the F1 individuals grouped with female parent, while others with male parents. No result was shown for G3 cross as there is no variation detected in ITS among the individuals.

The plastid genome of *Ginkgo biloba* is revealed to be a circular molecule about 156,978 bp with a pair of IRs (35,466 bp) separated by large single-copy (LSC: 99,254 bp) and small single-copy (SSC: 22,258 bp) regions with GC content 39.6% (Fig. S1), which is consistent with the result given by Lin et al. (2012) and Lubna et al. (2021), although the total lengths differ slightly. The plastid genome of *G. biloba* is characterized by the shortened IR region due to the complete loss of *ycf*2, which is about 7,269 bp in length (Lin et al., 2012; Lubna et al., 2021). This gene is detected to be informative at population level with relatively high nucleotide diversity ($Pi > 0.0001$). It is also suggested to be an information phylogenetic marker for ferns and gymnosperms, as it shows two copies in the IR regions in *Cycas* and *Genetum*, but only one copy in LSC or SSC region in *G. biloba* and *Pinus*, respectively (Lin et al., 2012). Therefore, the evolution of *ycf*2 gene demonstrates to be potential in phylogenetic analysis and speciation of plant species.

In the current study, altogether 134 genes were identified including 85 PCGs, 41 tRNAs and four rRNAs. The total number of the genes is consistent with the previous research (Lin et al., 2012). However, when we compared with the data set in GenBank deposited by Lin et al. (2012), about ten genes were missing in the annotations of the plastid genome. After annotations for all genes, the gene *rpl*23 was also revealed to be pseudolized. This gene is detected to be pseudo due to the truncated 5' region as in comparison with *Cycas* (Lin et al., 2012; Lubna et al., 2021). The gene *rpl*23 is commonly found in angiosperms, but lost in some gymnosperms, therefore, the pseudo *rpl*23 demonstrates strong evolutionary implications in plant species as well.

As is known, the inheritance of plastid genome differs from that of the nuclear genome. Maternal inheritance, which is the most common form of seed plant organelle transmission, demonstrates the transfer of chloroplasts from the female parent to the progeny. Maternal inheritance of chloroplast occurs when the organelles are only present in the cytoplasm of the egg cells during the fertilization of eggs in seed plants (Vaughn et al., 1980). Though paternal inheritance of plastid genome is widely distributed in gymnosperms, several species have been reported to show maternal

Table 1
K2–P's genetic distance and the number of SNPs among all parents and offsprings.

Crosses	Parents (F)	Parents (M)	*K2–P's* genetic distance ($\times 10^{-4}$)		No. of SNPs					
			F1 *vs.* F	F1 *vs.* M	M	F	Introns	Exon	Intergenic	Total
G1	FG1-NXLBT2	MG1-NXPH	0	0.57	0	9	1	4	4	9
G2	FG2-NXLBT3	MG2-NXAB	0	1.27	0	20	0	1	19	20
G3	FG2-NXLBT3	MG3-ZJTM	0	0.06	0	1	1	0	0	1
Average			0	0.63	0	30	2	5	23	30

M: male; F: female; F1: offsprings.

inheritance, including *Ginkgo*, *Gnetum*, and *Cycas* (Neale et al., 1989; Mogensen, 1996). However, the evidence for uniparental inheritance of gymnosperms is mostly based on cytological method previously. The current study is further confirmed plastid genome inheritance in *Ginkgo* based on genomic data using next generation sequencing.

Concerning the investigations of organelle inheritance of plant species, traditional methods including hybridization experiment, electron microscopy, DAPI fluorescence microscopy or genetic markers demonstrate several disadvantages. First, the cytological methods only show the process of the transfer of chloroplasts without any further investigation in the offsprings. No molecular evidence is available to prove the phylogenetic relationship among the parents and offsprings. Second, the traditional molecular markers, such as PCR-RFLP or SSRs, are less informative and effective than SNPs based on genomic data. With the development of next-generation sequencing technologies, a rapid and successful achievement has been promoted in the database of genomic data, among which is plastid genome (Wang et al., 2018). Genomic data shows a strong potentiality to be applied in the exploration of molecular mechanism of organelle inheritance (Villanueva-Corrales et al., 2021). Additionally, artificial crosses help to control the origins of male and female parents, which make possible to compare the genomic constituent among parents and offsprings. The combination of manually genetic crosses and chloroplast genomic data is an efficient way to investigate the inheritance mode of the chloroplasts in land plants. In our study, strong molecular evidence has been provided for maternal inheritance mode of its plastid genomes. Therefore, we suggested artificial crosses together with subsequent verification of SNPs among parents and progenies to be a recommendable way to directly infer organelle genome inheritance in land plants.

Data availability

The high-quality sequencing data of current study were deposited in the NCBI under Bioproject accession number PRJNA866875. Other supporting data were provided within the article.

Author contributions

W.G. was the principal investigator and wrote the manuscript. R.Z. contributed mainly to field work, including sample collections and artificial pollinations. M.F. and H.K. contributed equally to lab work, data analysis, and figures. M.F. edited the manuscript and had discussion with H.K. and M.L.

Declaration of competing interest

The authors declared no conflict of interest.

Acknowledgements

We are very grateful to Miss Juan Zhou and Dr. Wanzhen Liu for their assistance in field work. This work is supported by the National Natural Science Foundation of China (32270218 and 31970231).

Appendix A. Supplementary data

Supplementary data to this article can be found online at https://doi.org/10.1016/j.pld.2023.09.001.

References

Birky, C.J., 1995. Uniparental inheritance of mitochondrial and chloroplast genes: mechanisms and evolution. Proc. Natl. Acad. Sci. U.S.A. 92, 11331–11338.
Coil, D., Jospin, G., Darling, A.E., 2015. A5-miseq: an updated pipeline to assemble microbial genomes from Illumina MiSeq data. Bioinformatics 31, 587–589.
Danecek, P., Bonfield, J.K., Liddle, J., et al., 2021. Twelve years of SAMtools and BCFtools. GigaScience 10, 1–4.
Doyle, J.J., Doyle, J.L., 1987. A rapid DNA isolation procedure for small quantities of fresh leaf tissue. Phyto. Chem. Bull. 19, 11–15.
Gong, W., Zeng, Z., Chen, Y., et al., 2008. Glacial refugia of *Ginkgo biloba* and human impact on its genetic diversity: evidence from chloroplast DNA. J. Integr. Plant Biol. 50, 368–374.
Greiner, S., Sobanski, J., Bock, R., 2015. Why are most organelle genomes transmitted maternally? Bioessays 37, 80–94.
Guo, F., Hu, S., Yuan, Z., et al., 2005. Paternal cytoplasmic transmission in Chinese pine (*Pinus tabulaeformis*). Protoplasma 225, 5–14.
Howe, C.J., Barbrook, A.C., Koumandou, V.L., et al., 2003. Evolution of the chloroplast genome. Phil. Trans. Roy. Soc. Lond. B 358, 99–107.
Ivanova, Z., Sablok, G., Daskalova, E., et al., 2017. Chloroplast genome analysis of resurrection Tertiary relict *Haberlea rhodopensis* highlights genes important for desiccation stress response. Front. Plant Sci. 8, 204.
Jansen, R.K., Ruhlman, T.A., 2012. Plastid genomes of seed plants. In: Genomics of Chloroplasts and Mitochondria, Advances in Photosynthesis and Respiration. Springer, Dordrecht, The Netherlands, pp. 103–126.
Katoh, K., Standley, D.M., 2013. MAFFT multiple sequence alignment software version 7: improvements in performance and usability. Mol. Biol. Evol. 30, 772–780.
Kita, K., Kurashige, Y., Yukawa, K., et al., 2005. Plastid inheritance and plastome-genome incompatibility of intergeneric hybrids between *Menziesia* and *Rhododendron*. J. Jpn. Soc. Hortic. Sci. 74, 318–323.
Kormutak, A., Galgoci, M., Sukenikova, D., et al., 2018. Maternal inheritance of chloroplast DNA in *Pinus mugo* Turra: a case study of *Pinus mugo* × *Pinus sylvestris* crossing. Plant Syst. Evol. 304, 71–76.
Li, H., 2011. A statistical framework for SNP calling, mutation discovery, association mapping and population genetical parameter estimation from sequencing data. Bioinformatics 27, 2987–2993.
Li, H., 2013. Aligning sequence reads, clone sequences and assembly contigs with BWA-MEM. arXiv: Genomics. https://ui.adsabs.harvard.edu/abs/2013arXiv1303.
Li, H., Handsaker, B., Wysoker, A., et al., 2009. The sequence alignment/map format and SAMtools. Bioinformatics 25, 2078–2079.
Lin, C., Wu, C., Huang, Y., et al., 2012. The complete chloroplast genome of *Ginkgo biloba* reveals the mechanism of inverted repeat contraction. Genome Biol. Evol. 4, 374–381.
Lohse, M., Drechsel, O., Kahlau, S., et al., 2013. OrganellarGenomeDRAW—a suite of tools for generating physical maps of plastid and mitochondrial genomes and visualizing expression data sets. Nucleic Acids Res. 41, 575–581.
Lubna, A.S., Khan, A.L., Jan, R., et al., 2021. The dynamic history of gymnosperm plastomes: insights from structural characterization, comparative analysis, phylogenomics, and time divergence. Plant Genome 14, e20130.
Mogensen, H.L., 1996. The hows and whys of cytoplasmic inheritance in seed plants. Am. J. Bot. 83, 383–404.
Neale, D.B., Marshall, K.A., Sederoff, R.R., 1989. Chloroplast and mitochondrial DNA are paternally inherited in *Sequoia sempervirens* D. Don Endl. Proc. Natl. Acad. Sci. U.S.A. 86, 9347–9349.
Ohba, K., Iwakawa, M., Okada, Y., et al., 1971. Paternal transmission of a plastid anomaly in some reciprocal crosses of Sugi, *Cryptomeria japonica* D. Don. Silvae Genet. 20, 101–107.
Qu, X., Moore, M.J., Li, D., et al., 2019. PGA: a software package for rapid, accurate, and flexible batch annotation of plastomes. Plant Methods 15, 50.
Reboud, X., Zeyl, C., 1994. Organelle inheritance in plants. Heredity 72, 132–140.
Rozas, J., Ferrer-Mata, A., Sánchez-DelBarrio, J.C., et al., 2017. DnaSP 6: DNA sequence polymorphism analysis of large data sets. Mol. Biol. Evol. 34, 3299–3302.
Shi, Y., Ke, X., Yang, X., et al., 2022. Plants response to light stress. J. Genet. Genomics 49, 735–747.
Swofford, D.L., 2002. PAUP*: Phylogenetic Analysis Using Parsimony (*and Other Methods). version 4.
Tamura, K., Stecher, G., Kumar, S., 2021. MEGA11: molecular evolutionary genetics analysis version 11. Mol. Biol. Evol. 38, 3022–3027.
Vaughn, K.C., Debonte, L.R., Wilson, K.G., et al., 1980. Organelle alteration as a mechanism for maternal inheritance. Science 208, 196–198.
Villanueva-Corrales, S., García-Botero, C., Garcés-Cardona, F., et al., 2021. The complete chloroplast genome of *Plukenetia volubilis* provides insights into the organelle inheritance. Front. Plant Sci. 12, 667060.
Wang, H., Park, S.Y., Lee, A.R., et al., 2018. Next-generation sequencing yields the complete chloroplast genome of *C. goeringii* acc. smg222 and phylogenetic analysis. Mitochondrial DNA B Resour. 3, 215–216.
Wang, Y., Wang, S., Liu, Y., et al., 2021. Chloroplast genome variation and phylogenetic relationships of *Atractylodes* species. BMC Genomics 22, 103.
Wu, C., Chaw, S., 2015. Evolutionary stasis in *Cycad* plastomes and the first case of plastome GC-biased gene conversion. Genome Biol. Evol. 7, 2000–2009.

Yang, X., Zhou, T., Su, X., et al., 2021. Structural characterization and comparative analysis of the chloroplast genome of *Ginkgo biloba* and other gymnosperms. J. For. Res. 32, 765–778.
Yang, Y., Ferguson, D.K., Liu, B., et al., 2022. Recent advances on phylogenomics of gymnosperms and a new classification. Plant Divers. 44, 340–350.
Zhai, F., Sun, Z., 2015. Progress in study on sexual differences of woody dioecious plants. Sci. Silvae Sin. 51, 110–116.
Zhao, Y., Fan, G., Yin, P., et al., 2019. Resequencing 545 ginkgo genomes across the world reveals the evolutionary history of the living fossil. Nat. Commun. 10, 4201.
Zhong, Z., Li, N., Qian, D., et al., 2011. Maternal inheritance of plastids and mitochondria in *Cycas* L. (Cycadaceae). Mol. Genet. Genom. 286, 411–416.
Zhou, X., Liao, Y., Kim, S., et al., 2020. Genome-wide identification and characterization of *bHLH* family genes from *Ginkgo biloba*. Sci. Rep. 10, 13723.

Check for updates

Received: 20 September 2020 | Revised: 19 August 2021 | Accepted: 1 September 2021

DOI: 10.1111/eva.13301

ORIGINAL ARTICLE

Evolutionary Applications Open Access WILEY

Population dynamics linked to glacial cycles in *Cercis chuniana* F. P. Metcalf (Fabaceae) endemic to the montane regions of subtropical China

Wanzhen Liu[1] | Jianguang Xie[1] | Hui Zhou[1] | Hanghui Kong[2,3] | Gang Hao[1] | Peter W. Fritsch[4] | Wei Gong[1]

[1]Guangdong Laboratory for Lingnan Modern Agriculture, & College of Life Sciences, South China Agricultural University, Guangzhou, China

[2]Key Laboratory of Plant Resources Conservation and Sustainable Utilization, South China Botanical Garden, Chinese Academy of Sciences, Guangzhou, China

[3]Center of Conservation Biology, Core Botanical Gardens, Chinese Academy of Sciences, Guangzhou, China

[4]Botanical Research Institute of Texas, Fort Worth, Texas, USA

Correspondence
Wei Gong, Guangdong Laboratory for Lingnan Modern Agriculture, & College of Life Sciences, South China Agricultural University, Guangzhou 510614, China.
Email: wgong@scau.edu.cn

Peter W. Fritsch, Botanical Research Institute of Texas, 1700 University Drive, Fort Worth, TX 76107, USA.
Email: pfritsch@brit.org

Funding information
Science and Technology Planning Project of Guangdong Province, China, Grant/Award Number: 2016A030303048; National Natural Science Foundation of China, Grant/Award Number: 31470312, 31470319 and 31970231

Abstract

The mountains of subtropical China are an excellent system for investigating the processes driving the geographical distribution of biodiversity and radiation of plant populations in response to Pleistocene climate fluctuations. How the major mountain ranges in subtropical China have affected the evolution of plant species in the subtropical evergreen broadleaved forest is an issue with long-term concern. Here, we focused on *Cercis chuniana*, a woody species endemic to the southern mountain ranges in subtropical China, to elucidate its population dynamics. We used genotyping by sequencing (GBS) to investigate the spatial pattern of genetic variation among 11 populations. Geographical isolation was detected between the populations located in adjacent mountain ranges, thought to function as geographical barriers due to their complex physiography. Bayesian time estimation revealed that population divergence occurred in the middle Pleistocene, when populations in the Nanling Mts. separated from those to the east. The orientation and physiography of the mountain ranges of subtropical China appear to have contributed to the geographical pattern of genetic variation between the eastern and western populations of *C. chuniana*. Complex physiography plus long-term stable ecological conditions across glacial cycles facilitated the demographic expansion in the Nanling Mts., from which contemporary migration began. The Nanling Mts. are thus considered as a suitable area for preserving population diversity and large population sizes of *C. chuniana* compared with other regions. As inferred by ecological niche modeling and coalescent simulations, secondary contact occurred during the warm Lushan–Tali Interglacial period, with intensified East Asia summer monsoon and continuous habitat available for occupation. Our data support the strong influence of both climatic history and topographic characteristics on the high regional phytodiversity of the subtropical evergreen broadleaved forest in subtropical China.

KEYWORDS
Cercis chuniana, demographic modeling, geographical isolation, mountains, Pleistocene glacial cycles, secondary contact, subtropical China

This is an open access article under the terms of the Creative Commons Attribution License, which permits use, distribution and reproduction in any medium, provided the original work is properly cited.
© 2021 The Authors. *Evolutionary Applications* published by John Wiley & Sons Ltd.

1 | INTRODUCTION

High physiographical heterogeneity is suggested to prompt rapid diversification in montane habitats because of the increased ecological opportunities afforded by frequent episodes of geographical isolation (Colin & Ruth, 2006; Muellner-Riehl, 2019; Simpson, 1964). Subtropical China comprises a geographically and climatically heterogeneous mid-elevation montane region bordered by the Qinling Mountains–Huai River (~34°N) in the north, the tropical region (~22°N) in the south, the Qinghai–Tibetan Plateau in the west, and the coastline in the east (Wu, 1980; Wu et al., 1987). Many studies have identified the mountains of subtropical China as one of the main centers of phytodiversity and endemism in the country and globally, with much higher diversity than the other regions in the Northern Hemisphere (López-Pujol et al., 2011; Qian et al., 2005). The high biodiversity of subtropical China is due in large part to the extreme physiographical heterogeneity of its mountain ranges (Fan et al., 2018; Xu et al., 2017; Yang et al., 2016). Generally oriented in north–south or northeast–southwest directions (Hou, 1983; Wang, 1992a, 1992b; Ying, 2001), these topographically diverse ranges have been suggested to serve as either geographical barriers or colonization corridors for various plant species (Gong et al., 2016; Tian et al., 2018; Xiong et al., 2019). The uniqueness of their local habitats has been attributed to complex topography correlated with longitudinal or steep elevational gradients (Qiu et al., 2013; Wang et al., 2012). The primary vegetation type of these mountains is subtropical evergreen broadleaved forest (STEBF), one of the largest continuous such forests in the world and well known for harboring ancient relictual elements of the north temperate biota (Qiu et al., 2011; Wang et al., 2012). Many of their plant species, predominantly endemics, exhibit high rates of local and rapid radiation (Hou et al., 2017; López-Pujol et al., 2011) presumably arising within the last 5 million years, in line with both orogenic events and Pleistocene glacial cycles (Li et al., 1979; Liu et al., 2013; Shi et al., 1998; Wang et al., 2010). These characteristics make subtropical China an excellent system for investigating the processes driving the geographical distribution of biodiversity and radiation of plant populations in response to Pleistocene climate fluctuations.

Climatic oscillations associated with glacial cycles during the Pleistocene are also considered an important factor driving the distribution pattern of biodiversity and shaping the demographic history of populations, particularly in montane regions (Bueno de Mesquita et al., 2018; Hewitt, 2004; Li, Kong, et al., 2019; Li, Zhang, et al., 2019; Svenning et al., 2009). Although still under debate, considerable data are now available to support four glacial periods in eastern China (east to 105°E) during the Pleistocene, that is, the Poyang, Dagu, Lushan and Tali glacials (Duan et al., 1980). In subtropical China, the degree of habitat connectivity is thought to have decreased during glacial periods, with vegetation belts lowering in latitude and contracted geographical ranges, allowing geographical isolation and genetic divergence to occur (Harrison et al., 2001; Shi et al., 2006). Multiple glacial refugia correlated with centers of genetic diversity have been identified in subtropical China, out of which subsequent localized or rapid range expansions have been inferred (Chen et al., 2012; Gong et al., 2008; Li et al., 2012; Qiu et al., 2011; Tian et al., 2015). Previous research has elucidated the scenarios involved with the evolutionary history of plant species thought to be affected by glacial and postglacial cycles in subtropical China (Gong et al., 2016; Liu et al., 2012; Tian et al., 2020). This research suggests that climate change is considered the main driver in triggering genetic differentiation and population divergence in subtropical China (Chen et al., 2020; Qiu et al., 2011; Wang et al., 2015, 2017). However, the extent to which topographic heterogeneity and the major mountain ranges of subtropical China may have affected the evolution of endemic species has been less studied. The studies that have been done on this issue suggest that topographic heterogeneity is as important as climate fluctuations in driving the evolution of species diversity in subtropical China (Li, Kong, et al., 2019; Li, Zhang, et al., 2019; Liu et al., 2014; Zhang et al., 2018; Zhu et al., 2019).

Cercis chuniana F.P. Metcalf (Fabaceae: Cercidoideae; Azani et al., 2017) is a small tree or shrub endemic to the STEBF of southern China. In comparison with its congeners, including *C. canadensis* L., *C. glabra* Pamp. and *C. siliquastrum* L., which have wide-ranging distributions with large population sizes, *C. chuniana* has a relatively narrow geographical distribution. It occurs in the major mountain ranges in subtropical China, extending from the Wuyi and Eastern China Mountains westward to the Nanling Mountains. As with its congeners in China, it exhibits an adaptation to mesic environments by its acuminate leaf blade apex (Fritsch & Cruz, 2012; Fritsch et al., 2018; Isely, 1975; Wunderlin et al., 1981). Unique among *Cercis* species, it has an asymmetrical leaf blade (Chen et al., 2010; Metcalf, 1940), which makes it easily identifiable morphologically. The species is resolved near the base of the *Cercis* phylogenetic tree, and the species diversification time is estimated to be 2.40 Ma based on fossil-calibrated divergence time analysis in *Cercis* (Fritsch et al., 2018; Liu et al., unpublished data, 2020). Therefore, we considered *C. chuniana* as a strong candidate for investigating the influence of both climatic history and topographic characteristics on the high regional phytodiversity of the subtropical evergreen broadleaved forest in southern China.

Genotyping by sequencing (GBS) is a streamlined workflow for generating reduced representation libraries for Illumina sequencing (Heffelfinger et al., 2014; Ilut et al., 2014; Melo et al., 2016) and has been widely used as a genomic approach for investigating genetic diversity and population structure (Chen et al., 2017; Metzker, 2010; Niu et al., 2019). Because it is based on genomic reduction with restriction enzymes, GBS does not require a reference genome to detect single nucleotide polymorphisms (SNPs). In combination with marker discovery and genotyping, GBS provides a rapid, high-throughput, and cost-effective tool for a genome-wide analysis for nonmodel species (Andrews et al., 2016; Davey et al., 2011; Scheben et al., 2017). Here, we used GBS and collected genome-wide SNPs for population genetic analyses of *C. chuniana*. We aimed to (1) investigate genetic diversity and population structure of the species, (2) elucidate its demographic history, and (3) use the data to test the

relative influence of topographic heterogeneity versus Pleistocene climatic fluctuations in driving population diversification and geographical distribution within the STEBF in subtropical China.

2 | MATERIALS AND METHODS

2.1 | Population sampling

We collected 11 populations and 112 individuals of *C. chuniana* from throughout the current geographical distribution of the species (Figure 1, Table 1). Anywhere from one to five populations were collected from each of the mountain ranges in subtropical China. The sampled populations are located in the southern Yandang Mts. (YDS), the northern Wuyi Mts. (WYS), the southern Luoxiao Mts. (LXS1 and LXS2), the eastern Nanling Mts. (NLE1 and NLE2), and the western Nanling Mts. (NLW1 through NLW5; Figure 1, Table 1). Some population sizes are very small with limited numbers of living individuals because of the destruction of habitat. Therefore, less than ten individuals were collected in five small populations, including YDS, WYS, LXS1, NLW2, and NLW5. We also collected 20 individuals from one population of *C. chingii* Chun located in Chichengshan, Zhejiang Province (CCS), which were used as the outgroup. The reason that we chose *C. chingii* as the outgroup is mainly based on the ML tree constructed for *Cercis* based on GBS data, which shows that *C. chuniana* is at the basal branch followed by *C. chingii*. Therefore, we chose *C. chingii* as the outgroup as the other congeneric species are phylogenetically much most distant. Additionally, we tested the result of the ML tree by randomly choosing one individual of *C. chingii*, which did not change the final topology.

2.2 | Ecological niche modeling

We used ecological niche modeling (ENM; Soberón & Peterson, 2005) to characterize the spatial distribution of suitable conditions for *C. chuniana* and locate potential distributional areas in conjunction with historical biological inferences. We based the analysis on high-resolution paleoclimate data inferred for the Last Interglacial (LIG, 0.14~0.12 Ma), Last Glacial Maximum (LGM, ≈ 0.02 Ma), Middle Holocene (MH, ≈ 0.006 Ma), and current. Bioclimatic variables were downloaded from the WorldClim database (http://worldclim.org/download; Fick & Hijmans, 2017) for the four different stages with 2.5-minute spatial resolution. The LIG, LGM, and MH data were obtained from circulation model simulation of the Community Climate System Model (CCSM; Collins et al., 2006), which provides downscaled high-resolution estimates of the climate parameters (Hijmans et al., 2005). We used the maximum entropy modeling method with Maxent v3.3.2 (Phillips et al., 2006). Herbarium specimen records of *C. chuniana* from nine herbaria (A, IBEC, IBK, IBSC, KUN, LBG, NMNH, PE, and SCFI) and our sample collection locations were used to determine the locations of populations considered to occur at present. The analysis pipelines and parameter settings, including the occurrence points, current/past bioclimatic variables and the convergence threshold and maximum number of iterations, were all as in Dai et al. (2011) and Gong et al. (2016). Model accuracy was assessed by evaluating the area under the curve (AUC) of the receiver operating characteristic (ROC) plot (Phillips et al., 2006), where scores higher than 0.70 were considered to show good model performance (Fielding & Bell, 1997). This approach is thus conservative, identifying the minimum predicted area possible while maintaining zero omission error in the training dataset (Pearson et al., 2007). We added a layer of GIS-based vegetation map for comparison in each period of LIG, MH, LGM and current (Allen et al., 2020; Ray & Adams, 2001). The most influential climate factors were also compared, including precipitation and temperature in each month or on average.

2.3 | DNA extraction, genotyping by sequencing (GBS), SNP calling, and quality filtering

Fresh leaves of *C. chuniana* and *C. chingii* were sampled and placed into centrifuge tubes, which were instantly immersed in liquid nitrogen and stored at −80°C. Leaf tissue was ground in tubes with glass beads with the tissue homogenizer TissueLyser-96 (Shanghai Jingxin Industrial Development Co., Ltd). Total genomic DNA was extracted with the modified cetyl trimethyl ammonium bromide (CTAB) method (Doyle & Doyle, 1986). DNA concentration was quantified with a NanoDrop spectrophotometer (Thermo Scientific), and a final DNA concentration of >30 ng/μl was used.

The genomic DNA was digested with a combination of *Mse*I and *Nla*III enzymes. Subsequent ligation to barcodes after multiplex amplification was constructed, and the desired fragments were selected for GBS library construction in Novogene Co., Ltd. The Illumina HiSeq sequencing platform (Illumina) was used for paired-end (PE) 150 sequencing. Further analyses and DNA library assembly were performed to remove low-quality reads. Reads in fastq format were assembled by using STACKS v2.2 (Catchen et al., 2013) with one individual of *Cercis glabra* as reference and up to six base mismatches allowed. BWA v0.7.8 (Li & Durbin, 2009) was used for sequence mapping and sorting with the following settings: mem -t 4 -k 32 -M. The alignment files were converted to bam files with SAMtools v1.3.1 (Li et al., 2009). We used 132 individuals for SNP calling with Stacks. For population analysis, we extracted SNPs with a minor allele frequency (MAF) of at least 0.05 and a genotyping rate of at least 80% of individuals within populations. We also specified a maximum observed heterozygosity of 50% and a minimum number of five populations per locus.

2.4 | Phylogenetic analysis and divergence time estimation

Using the SNPs extracted from the GBS dataset, we employed maximum likelihood (ML) to reconstruct phylogenetic relationships among the 11 populations of *C. chuniana*. We used *C. chingii*

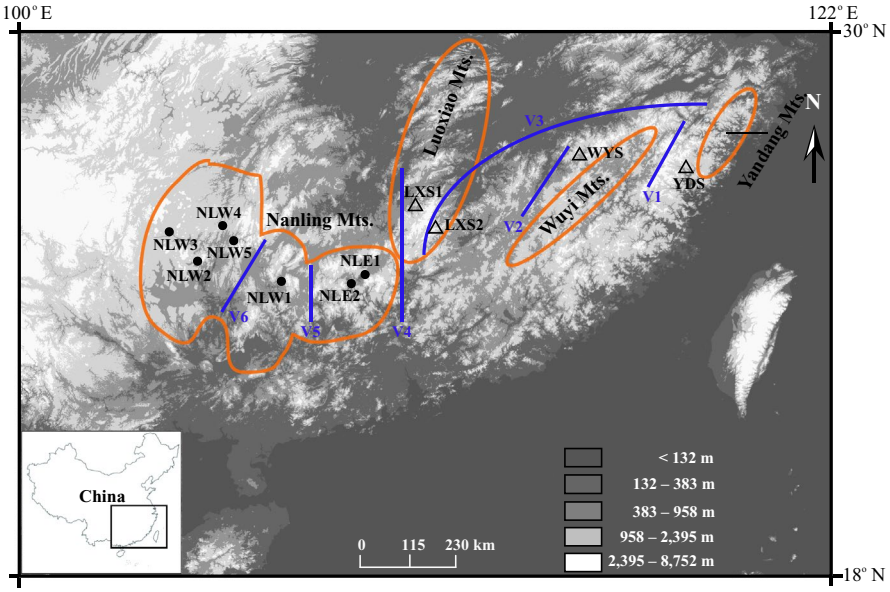

FIGURE 1 Map of subtropical China, showing the sampling locations of *Cercis chuniana* populations used in this study. The mountain ranges involved in the study are shown in orange frames. Populations sampled in the Nanling Mts. are indicated with black circles; populations in the east are indicated with triangles. Vicariance events detected with S-DIVA are shown with blue lines. The key at bottom right indicates elevational ranges. Latitudes and longitudes are shown on the right side and top side, respectively. Additional accession information is given in Table 1

to root the trees based on FastStructure analysis showing a close relationship between *C. chuniana* and *C. chingii* (Figure 4) and Mega analysis showing no remarkable differences in genetic distances between *C. chuniana* and other species. Therefore, we consider that *C. chingii* is sufficiently close to the ingroup for the purpose of rooting the tree in the ML analysis. Analyses were performed on the high-performance computer cluster available in the CIPRES Science Gateway 3.3 (www.phylo.org; Miller et al., 2015). The ML analyses were performed simultaneously with 1000 ML bootstrap pseudoreplicates in RAxML v8 (Alexandros, 2014). The model of nucleotide substitution was selected with the Akaike information criteria (AIC; Akaike, 1974) in PhyML-SMS (http://www.atgc-montpellier.fr/phymL/; Lefort et al., 2017).

We used fossil calibrations for the estimation of divergence time in *Cercis*. The fossil age of *Cercis* was originally estimated as 34 Ma (Lavin et al., 2005), but recently updated to 36 Ma (Fritsch et al., 2018). We conducted divergence time estimation based on all *Cercis* species using the fossil calibration of 36 Ma at the crown node of the genus. The result indicated that the root age for *Cercis* is 33.53 Ma and the crown age for *C. chuniana* is 2.39 (Figure S2; Liu et al., unpublished data, 2020), the latter of which was used for further analysis of time divergence for all the *C. chuniana* populations. Therefore, to estimate the divergence time within *C. chuniana*, we used BEAST v2.4.7 (Bouckaert et al., 2014) and applied the age of 2.4 Ma as the secondary calibration point with a normal prior distribution and standard deviation of 0.2 Ma, which covered the 95% HPD range. The divergence time analyses were conducted with the GTR + G + I model and four rate categories, a Coalescent Constant Population prior, and the Strict Clock setting with uncorrelated and log-normal-distributed rate variation across the branches. We ran the MCMC simulations in BEAST for 10 million generations with parameters sampled every 1000th generation. We used Tracer v1.6 (Rambaut et al., 2014) to assess convergence and to check that the effective sample size (ESS) was >200 for each parameter. We discarded the first 10% of trees as burn-in with the mean node heights option, and then generated the maximum clade credibility (MCC) chronogram from the remaining trees with nodal mean heights and 95% confidence time intervals with TreeAnnotator v2.4.7 (Bouckaert et al., 2014) in BEAST. The final trees were edited with FigTree v.1.4.3 (http://tree.bio.ed.ac.uk/software/figtree/; Rambaut, 2014).

2.5 | Genetic diversity, population assignment, and admixture

The number of alleles and allele frequencies for the selected SNPs were calculated with vcftools 0.1.16 (Danecek et al., 2011). To measure genetic diversity, we estimated expected heterozygosity (He) and observed heterozygosity (Ho). We used Arlequin v3.5 (Excoffier & Lischer, 2010) to estimate genetic differentiation by calculating pairwise values of differences among populations (Fst). To compare molecular diversity between and within populations, we used analysis of molecular variance (AMOVA) and a hierarchical analysis of subdivision (Excoffier et al., 1992; Weir, 1996; Weir & Cockerham, 1984). Altogether, seven groups were defined on the basis of FastStructure analysis.

We estimated population genetic structure with a Bayesian Markov chain Monte Carlo (MCMC) model implemented in FastStructure v1.0 (Raj et al., 2014). We used the default setting with 10-fold cross-validation on the 112 individuals of *C. chuniana*, testing for subpopulations (*K*) ranging from 1 to 11. The python script Choose K in FastStructure was used to choose the optimal *K*, that is, the value that maximizes the marginal likelihood. Results were graphically represented and edited with Adobe Illustrator. We performed principal component analysis (PCA) using the PCA function in SNPRelate (Zheng et al., 2012) and visualized the results using the scripts of Tanya Lama (https://github.com/ECOtlama/SNPRelate.git) in the R package.

TABLE 1 Accession information and genetic diversity parameters of observed heterozygosity (Ho) and expected heterozygosity (He) for the 11 *Cercis chuniana* populations and the outgroup *C. chingii*

No.	Population	Location	Mountain range	*N*	Latitude	Longitude	Elevation range (m)	He/Ho	Pi
	C. chuniana								
1	YDS	Tonglingshan, Wenzhou, Zhejiang	Southern Yandang Mts.	8	27.82°N	119.85°E	264–727	0.32/0.31	15.90
2	WYS	Wuyi Mts., Nanping, Fujian	Western Wuyi Mts.	9	27.94°N	117.77°E	460–712	0.34/0.28	8.17
3	LXS1	Jinggangshan, Ji'an, Jiangxi	Southern Luoxiao Mts.	9	26.78°N	113.90°E	264–509	0.32/0.30	2.44
4	LXS2	Wuzhifeng, Ganzhou, Jiangxi	Southern Luoxiao Mts.	14	26.00°N	114.15°E	369–722	0.31/0.19	5.77
5	NLE1	Mangshan Nature Reserve, Chenzhou, Hunan	Eastern Nanling Mts.	12	24.98°N	112.89°E	716	0.32/0.21	3.53
6	NLE2	Dadongshan Nature Reserve, Qingyuan, Guangdong	Eastern Nanling Mts.	10	24.92°N	112.72°E	774	0.32/0.32	1.36
7	NLW1	Yindianshan Nature Reserve, Guilin, Guangxi	Western Nanling Mts.	11	24.91°N	110.96°E	700	0.33/0.34	1.75
8	NLW2	Tianpingshan, Huaping Nature Reserve, Guilin, Guangxi	Western Nanling Mts.	5	25.61°N	109.90°E	852	0.38/0.33	8.60
9	NLW3	Dupoxiang, Huaihua, Hunan	Western Nanling Mts.	13	26.07°N	109.47°E	612–657	0.32/0.30	1.54
10	NLW4	Nanshan Log Yard, Shaoyang, Hunan	Western Nanling Mts.	14	26.18°N	110.19°E	611–703	0.32/0.30	1.03
11	NLW5	Mao'ershan National Nature Reserve, Guilin, Guangxi	Western Nanling Mts.	7	25.89°N	110.38°E	700–852	0.35/0.25	4.48
	C. chingii								
12	CCS	Chichenshan, Tiantai, Taizhou, Zhejiang	Xianxia Mts.	20	29.17°N	121.03°E	167–236		

2.6 | Inference of demographic history

For ancestral area reconstruction, we used seven groups of *C. chuniana* for S-DIVA (statistical dispersal–vicariance analysis) analysis implemented in RASP v3.2 (Ronquist, 1997; Yu et al., 2015). The analysis was based on the BEAST MCMC trees and the maximum clade credibility tree derived from the Bayesian analysis with BEAST and TreeAnnotator (Matuszak et al., 2016). With this method, the frequencies of an ancestral area at a node in the ancestral reconstructions are averaged over all trees. Dispersal or vicariance events were also detected with S-DIVA.

We applied coalescent simulations with the program fastsimcoal2 (FSC2; Excoffier et al., 2013) to provide model evidence of divergence, secondary contact, bottleneck effects, and demographic expansion. The populations in the Nanling Mts. (NL), which formed a monophyletic group and were distinct geographically, were delimited as one group, and the remaining populations as another, that is, the eastern populations (ES). We used easySFS (https://github.com/isaacovercast/easySFS) to transform SNPs into a folded site frequency spectrum (SFS) based on the construction of 10 demographic models with the two groups (Figure S3). The models are as follows: without isolation (NIS), isolation only (IS), isolation followed by migration (MIG), bottleneck effect (BOT) or secondary contact (SEC). Models including ancient (AMIG) or recent migration (RMIG), bidirectional or one-way migration, and demographic expansion (EXP) were also applied. In each model, NL or ES were alternatively used as the split source that was subjected to each scenario. We estimated effective population size (*Ne*), time (*T*) and migration rates in individual migrants per generation ($M_{NL\text{-}ES}$ *and* $M_{ES\text{-}NL}$) for the two groups in each model from posterior distributions. To scale parameter estimates into real values, we calculated the substitution/site/generation mutation rate based on phylogenetic analysis and divergence time estimate of *Cercis* (Liu et al., unpublished data, 2020), because the genomic mutation rate has not been calculated for this genus. The clock rate was firstly estimated as 2.32×10^{-8} substitutions/site/year for nine species and 241 individuals of *Cercis* with Tracer v1.6 (Rambaut et al., 2014). With a generation time of five years as based on congeners (Aldworth, 1998; Chen & Mao, 1999), the mutation rate was calculated as 1.16×10^{-7} substitutions/site/generation. As compared to some other plants such as *Arabidopsis*, *Prunus*, and *Silene* that show ~7×10^{-9} substitutions/site/year, the substitution rate for *C. chuniana* appears to be faster. However, the substitution/mutation rates vary in a wide range among different plant species and are strongly associated with the life history traits and generation time (Smith & Donoghue, 2008). We ran 100 replicate FSC2 analyses under each model with 10,000 simulations for optimal parameters and composite likelihood estimation. All 10 demographic models were compared (Figure S3, Tables S2–S4). The composite likelihood of arbitrarily complex demographic models under the given SFS was calculated by using best-fit models based on the Akaike information criterion (AIC). The models with the lowest AIC were chosen as the best fit of the data (Akaike, 1974).

3 | RESULTS

3.1 | Ecological niche modeling

Evaluation of model performance based on both training and test sample data indicated that the models had high predictive power (AUC = 0.9976 and 0.9966, respectively). Results yielded a continuous geographical distribution of *C. chuniana* across several mountain ranges in subtropical China during the Last Interglacial (LIG) period, under higher temperature than current (Figure 2a). In contrast, during the Last Glacial Maximum (LGM) the geographical distribution contracted into three fragmented areas, when the temperature was ~5–10°C lower than current (Figure 2b). We compared these data with a vegetation map of the LGM (http://intarch.ac.uk/journal/issue11/2/map/download_page_js.htm), finding that the three fragmented distribution areas were located mainly inside forest steppe (number 7) and partially in semi-arid temperate woodland or scrub (number 3; Ray & Adams, 2001). The geographical distribution of *C. chuniana* was inferred to have expanded widely during the Middle Holocene (MH), occupying most of the Chinese subtropical region. No changes in the geographical distribution were evident between MH and current. Precipitation in April, May, and June was revealed to be the most influential climate factor for the suitable distribution range of *C. chuniana* (Table S1).

3.2 | Characterization and distribution of SNPs

GBS produced 200 Gb clean reads after filtration. High-quality tags were identified from 10,761,958 Gb-PE reads. The sequence data were high quality with Q20 ≥ 92.23% and Q30 ≥ 85.00%. The mean G + C content was 37.84%. We detected 61,748 SNPs for *C. chuniana* with *C. chingii* as outgroup, among which 32,890 SNPs agreed with the SNP extraction criteria. The data have been deposited in Figshare (https://doi.org/10.6084/m9.figshare.15283395).

3.3 | Phylogenetic relationships and divergence times

The phylogenetic analysis yielded monophyly for most populations with mostly high bootstrap values, except YDS (Figure 3 and Figure S1). YDS was revealed to be positioned at the first-diverging branch, followed by the populations WYS, LXS2, and LXS1. The populations in the Nanling Mts. formed a monophyletic group, with NLE2 and NLE1 in the eastern Nanling Mts. forming a clade separate from the others in the western Nanling Mts. The time of origin for *C. chuniana* was estimated as 2.39 (95% HPD = 1.97–2.74) Ma during the early Pleistocene (Figure S2). YDS was first divergent from the remaining populations, followed by WYS diverging from the rest ca.

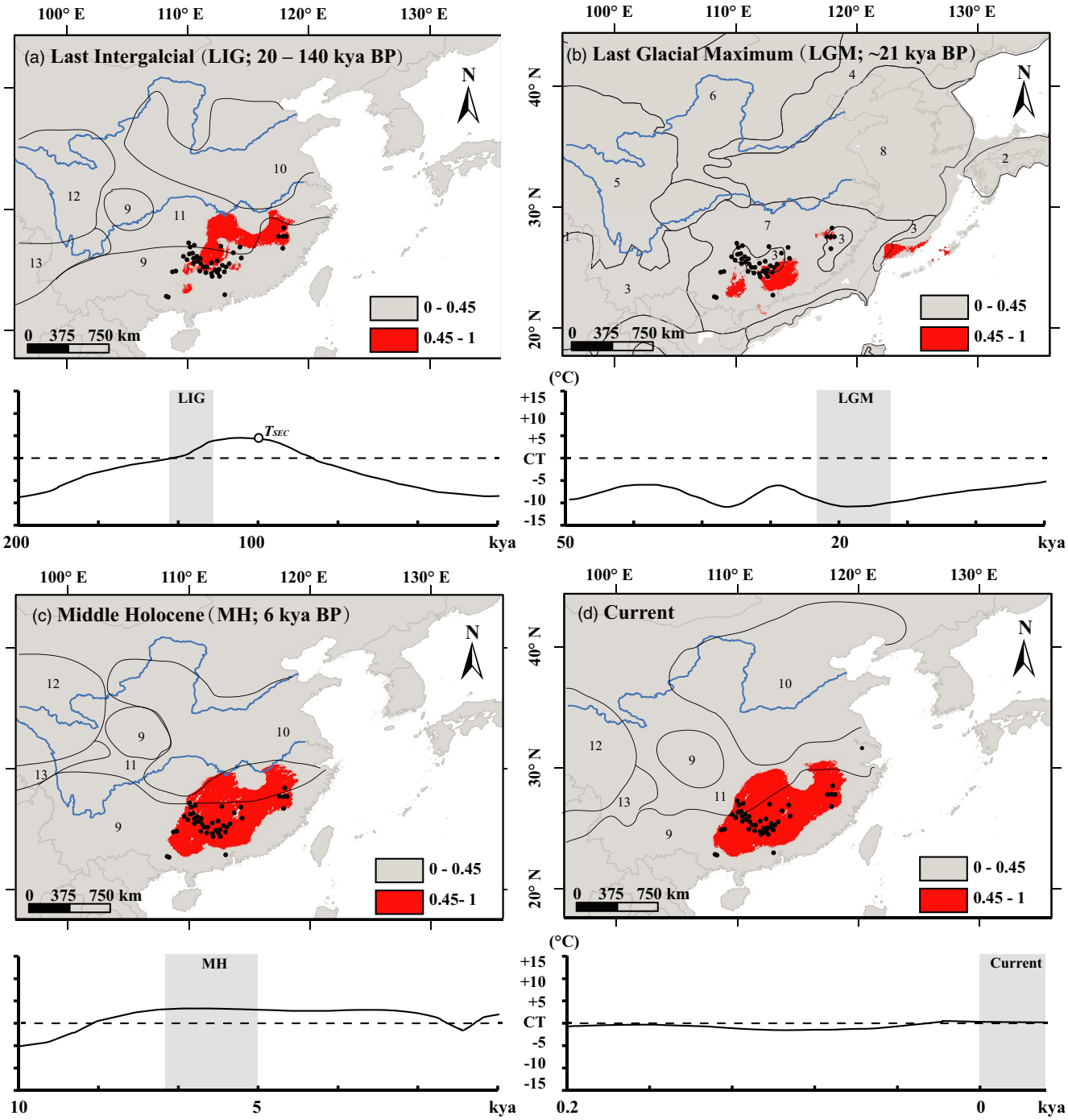

FIGURE 2 Potentially suitable areas for *Cercis chuniana* predicted by ecological niche modeling (ENM) and corresponding variation in temperature for four different periods of LIG (a), LGM (b), MH (c), and Current (d). Suitable and unsuitable habitats are indicated in red and gray, respectively, where red represents the habitat suitability (occurrence probability) higher than 44.93%. Each map is shown in comparison with a layer of GIS-based vegetation map for each period. Numbers 1–13 represent different vegetation types: 1, tropical thorn scrub and scrub woodland; 2, open boreal woodland; 3, semi-arid temperate woodland or scrub; 4, steppe-tundra; 5, polar and alpine desert; 6, temperate desert; 7, forest steppe; 8, dry steppe; 9, temperate broadleaved evergreen forest; 10, warm temperate woodland; 11, temperate mixed forest; 12, shrub tundra, and 13, boreal evergreen coniferous forest. Gray boxes enclose the temperatures for that time interval. The *y*-axis shows the temperatures compared with the current one (CT). The temperature during secondary contact (T_{SEC}) is indicated in LIG (a). The most influential factors are listed in Table S1

0.78 Ma during the end of the Poyang Interglacial period. The divergence occurring between LXS2 and the remaining populations was estimated as ca. 0.74 Ma, and the divergence between LSX1 and the populations in the Nanling Mts. as ca. 0.65 Ma. Both divergence times arose within the third glacial period in China in the Middle Pleistocene, although the exact glacial and interglacial time

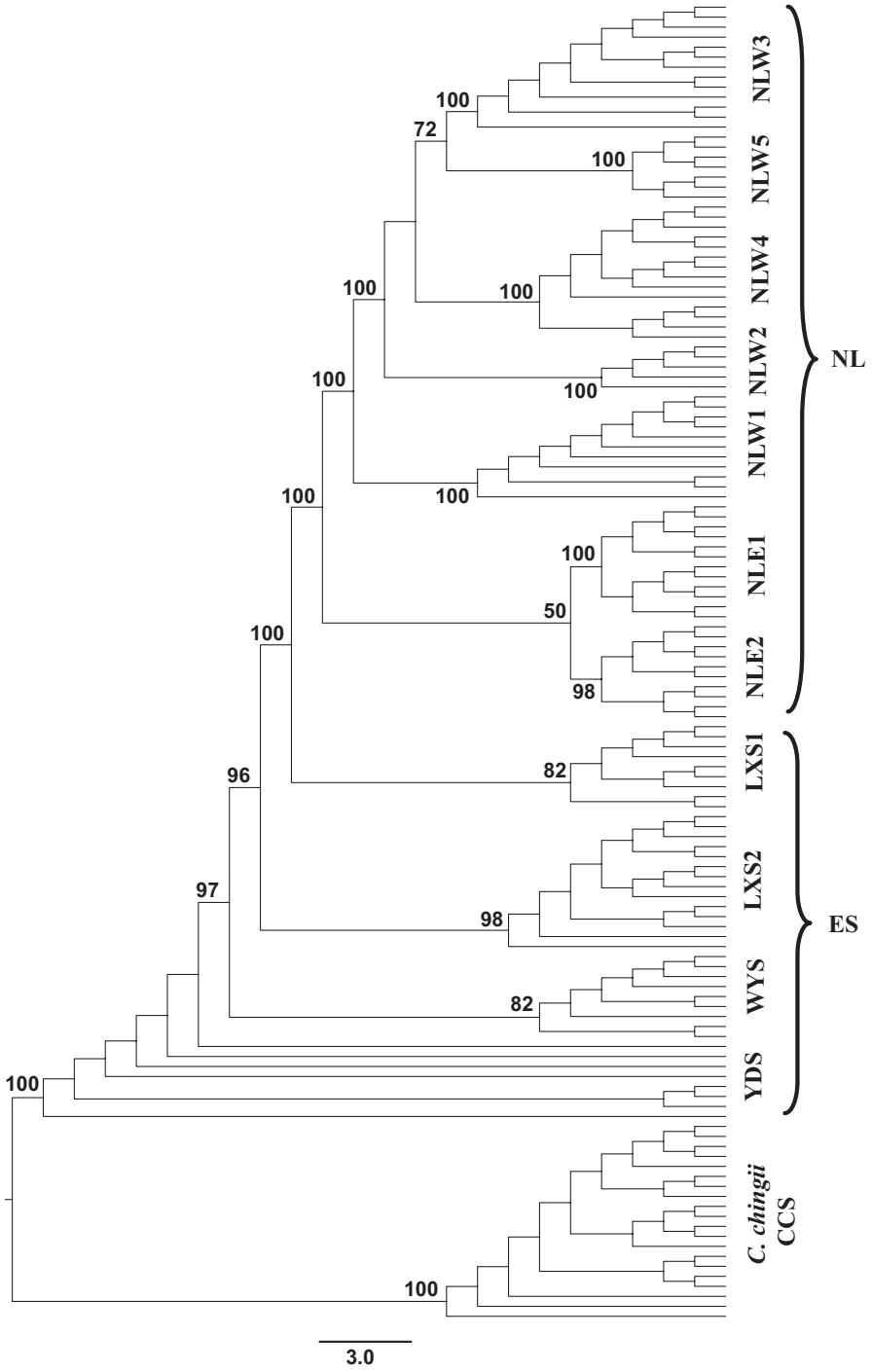

FIGURE 3 Phylogenetic tree of *Cercis chuniana* populations based on maximum-likelihood (ML) analysis. Bootstrap percentages (>50) in the ML tree are indicated above the branches. NL refers to the populations in Nanling Mts., whereas ES refers to the populations in the east. All other abbreviations are population abbreviations from Table 1. *Cercis chingii* was used as the outgroup

ranges are still under debate (Figure 4). Within the Nanling Mts., the eastern NLE1/NLE2 populations diverged from the western NLW1–NLW5 populations ca. 0.55 Ma, and NLW1 from the rest of the western populations ca. 0.48 Ma, both during the Dagu Glacial period (Figure 4). Population diversification within the Nanling Mts. ranges from 0.19 to 0.27 Ma in the western populations and from 0.33 to 0.35 Ma in the eastern populations, the former during the Lushan Glacial period and the latter during the Dagu–Lushan Interglacial period. Population diversifications in the east (YDS, WYS, LXS1 and LXS2) range from 0.34 to 0.47 Ma, spanning the Dagu–Lushan Glacial and Interglacial periods (Figure 4).

3.4 | Genetic diversity and differentiation

The highest He was detected in NLW2 (0.38) followed by NLW5 (0.35); the lowest was detected in LXS2 (0.31; Table 1). The highest H_0 was detected in NLW1 (0.34) followed by NLW2 (0.33); the lowest was detected in LXS2 (0.19). On average, He and Ho in the Nanling Mts. (He = 0.33; Ho = 0.29) were comparable to those of the other populations in the east (He = 0.32; Ho = 0.27). In the FastStructure analysis, YDS separated from the remaining populations when $K = 2$. When $K = 3$, WYS and LXS2 clustered as one group and this group was separated from the remaining groups.

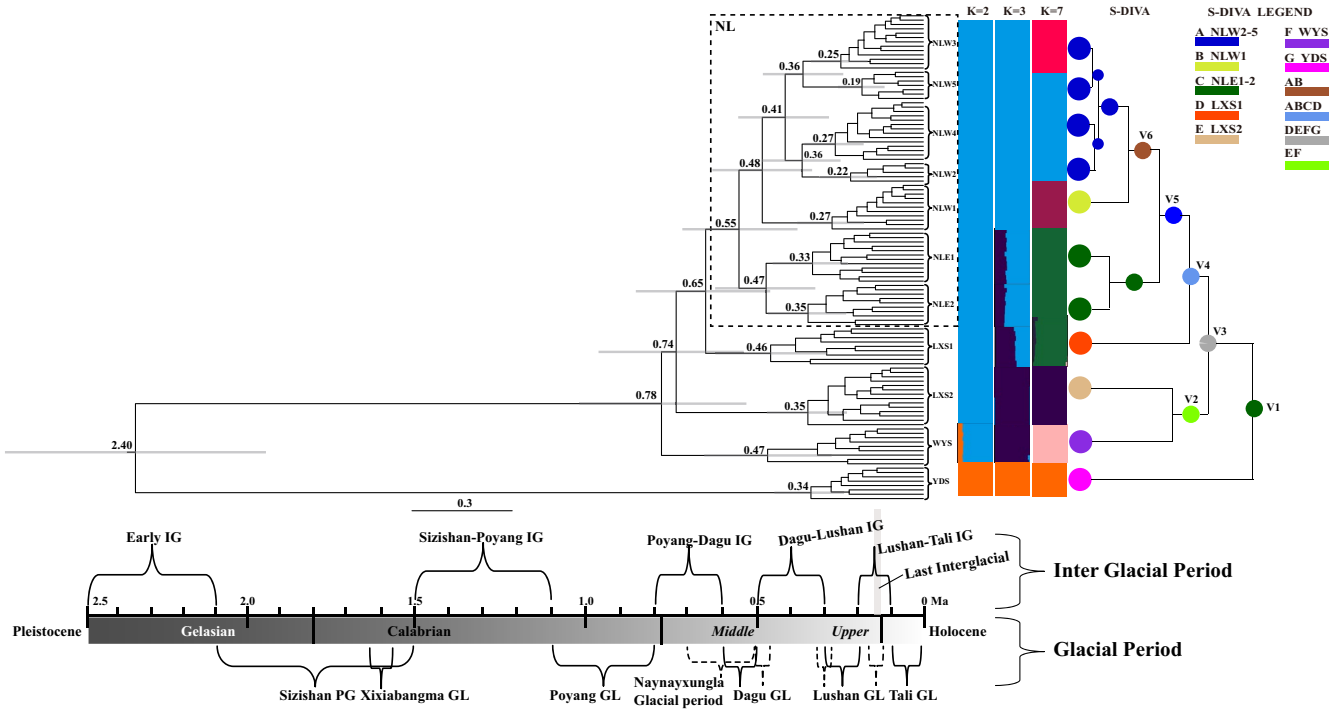

FIGURE 4 Chronogram of the Bayesian tree for divergence time estimates, population structural clustering and ancestral area reconstruction. Branch lengths were transformed via Markov chain Monte Carlo (MCMC) simulations in the Bayesian time estimation. The light gray bars indicate 95% confidence intervals. The key glacial and interglacial periods are indicated by the braces, with GL standing for glacial period, IG for interglacial period, and PG for periglacial period. Individuals assigned to different clusters in FastStructure are shown in corresponding colors with $K = 2$, 3, and 7, with 7 as the optimal value. In the S-DIVA analysis, color legends indicate different geographical regions and ancestral areas. The individuals from the same population are represented in one colored circle. Vicariance events (V1–V6) with high probabilities ($p \geq 0.70$) are shown for nodes. Populations in the Nanling Mts. are distinguished within the dotted line frame. Timescale bar is shown at the bottom. The population abbreviations are from Table 1

Seven subpopulations ($K = 7$) were determined as the optimal clustering for *C. chuniana* (Figure 4). PCA results showed similar groupings except that LXS1 and LXS2 clustered together, and were distinct from WYS and from the Nanling Mts. populations (Figure 5). Considering the FastStructure, PCA, and phylogenetic results together with the geographical locations of populations, we ultimately circumscribed seven groups of *C. chuniana* populations for further analyses: YDS, WYS, LXS1, LXS2, [NLE1 + NLE2], NLW1, and [NLW2 through NLW5]. Analysis of the molecular variance based on the GBS data indicated significant genetic differentiation among populations (Fst = 0.99, $p = 0.00$), of which the variation among the seven groups accounted for 96.28% of the total variation (Table 2).

3.5 | Geographical isolation, secondary contact and demographic expansion

Six vicariance events (V1–V6) among the geographical regions were inferred from the S-DIVA analysis (Figure 1). V1 is between YDS and the rest of the populations. V2 is between WYS and LXS2, located in the western Wuyi Mts. and southern Luoxiao Mts., respectively. V3 is between WYS/LXS2 and the rest of the populations, including LXS1 and the populations in the Nanling Mts. V4 is between LXS1 and the rest of the populations. V5 is between the eastern and western Nanling Mts., separating [NLE1 + NLE2] and [NLW1 through NLW5], whereas V6 is between NLW1 and [NLW2 through NLW5]. Across the six vicariance events, the eastern populations diverged from the rest of the species first, and the western populations later.

The best-fit model for the demographic analysis with FSC2 is SECEXP, indicating isolation followed by secondary contact (SEC) and demographic expansion (EXP; Figure 6 and Figure S3, Tables S2–S4). In combination with the time tree given by BEAST, the timescale of 548,000 generations (2.74 Ma) was confirmed by the program fastsimcoal2 from the lowest AIC value. Based on the mutation rate, we converted the genome-wide estimates of nucleotide diversity into effective population sizes. Nucleotide diversity per population is listed in Table 1. The current effective population sizes of the Nanling Mts. (NL) and eastern regions (ES) are $Ne_{NL} = 57{,}495$ and $Ne_{ES} = 14{,}955$, respectively. From the current effective population size, the ancestral effective population size was calculated as $Ne_{ANC} = 755{,}955$ (Figure 6, Table S3). Using the ancestral effective population size, we converted the divergence time between NL and ES into the number of generation times, $T_{DIV} = 319{,}472$ generations ago, that is, about 1.6 Ma. Secondary contact (SEC) was estimated at ca. $T_{SEC} = 0.10$ Ma. This date is within the Lushan–Tali Interglacial period in China (Duan et al., 1980; Zhu et al., 2004), when temperature increased and was ca. 5°C higher than at present (Figure 2). The

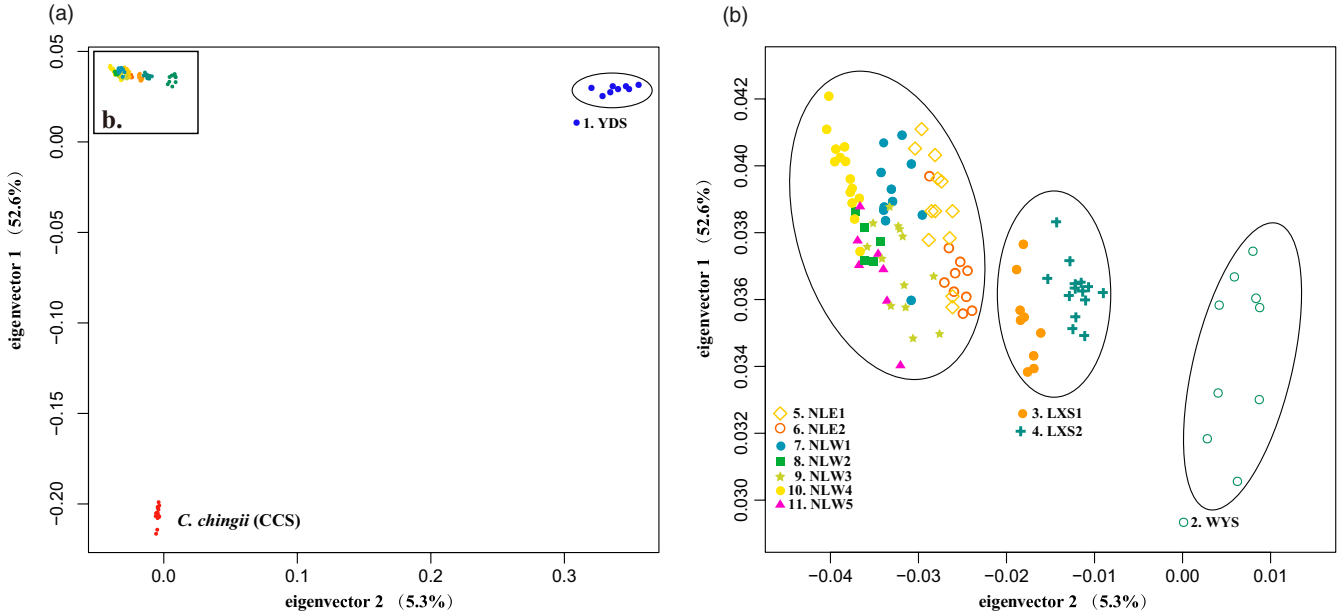

FIGURE 5 Principal component analysis (PCA) of *Cercis chuniana* populations. Different colors and shapes refer to each of the 11 populations of *C. chuniana* and one outgroup population of *C. chingii*

TABLE 2 Analysis of molecular variance (AMOVA) results for global Fst statistics of *Cercis chuniana*

Source of variation	*df*	Sum of squares	Variance components	Percentage of variation
Among groups	6	3367.488	37.06608	96.28%
Among populations within groups	4	36.908	0.89979**	2.34%
Within populations	101	53.747	0.53215**	1.38%
Total	111	3458.143	38.49802	
Fixation indices	Fsc: 0.6284**	Fst: 0.9862**	Fct: 0.9628	

Abbreviations: *df*, degrees of freedom; Fct, difference among groups; Fsc, differences among populations within groups; Fst, differences among all populations.
**$p < 0.001$.

ancestral effective population size of NL was estimated to be much smaller ($N_{e\text{-}pre\text{-}exp} = 866$) than at present. In contrast, the ES population sizes remained more or less constant (Figure 6). The migration rate $M_{NL\text{-}ES}$ (2.14) was much higher than $M_{ES\text{-}NL}$ (0.33), with migration occurring after NL and ES divergence.

4 | DISCUSSION

4.1 | Geographical isolation associated with Pleistocene climatic oscillations and mountain ranges

As based on ML analysis (Figures 1, 3), populations of *C. chuniana* are mostly monophyletic and closely aligned with geographical regions except YDS suggesting that they evolved mostly via local diversification. This is thought to occur especially when geographical isolation plays a dominant role (Harrington et al., 2018; Hughes, 2017; Hughes & Atchison, 2015; Kadereit, 2017; Nevado et al., 2018; Xing & Ree, 2017). Analysis of the molecular variance with significantly high population divergence (Fst = 0.99, $p = 0.00$) also indicates low inter-population gene flow (Table 2). Mountain ranges sometimes are considered as poorly conducive for facilitating long-distance dispersal, thus contributing to limited gene flow and geographical isolation (Oyama et al., 2018). In our study, isolation between YDS and WYS (V1) was attributed to the Wuyi Mts. acting as geographical barrier to separate the populations from each other (Figures 1, 4). The rise of the Wuyi Mts. during the early Pleistocene is thought to have caused geographical isolation and genetic divergence for many species in subtropical China (Liu, 1984; Yan et al., 2013). Notably, the central Luoxiao Mts., with a north–south orientation, are assumed to have served as a geographical barrier particularly for east–west colonization. This appears to apply to LXS1 and LXS2 in the Luoxiao Mts., which are currently isolated from each of their eastern or western populations (V2 and V3; Figures 1, 4). We infer that the geographical isolation between the populations of the Nanling Mts. and those to the east (V4) has arisen through the lack of geographical corridors. Vicariance events also exist between the western and eastern (V5) and the middle and northwest

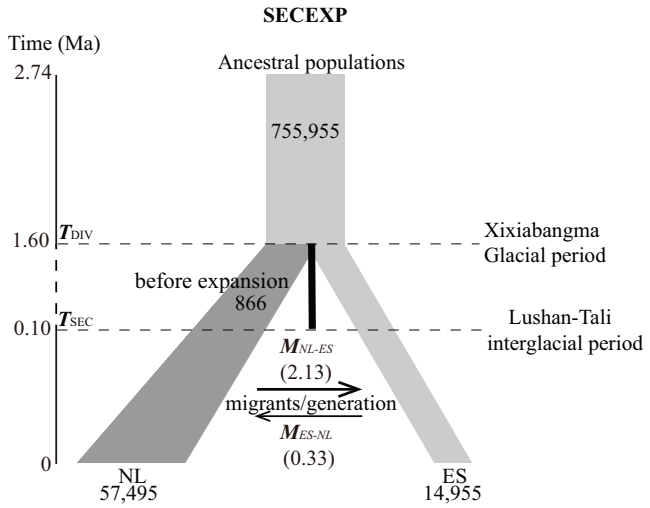

FIGURE 6 Schematic representation of the best-fit demographic model investigated in our study. Model parameters correspond to those in Tables S2 and S3, respectively. The left vertical line shows time (Ma), which progresses from top to bottom (current time). Time of divergence (T_{DIV}) and secondary contact (T_{SEC}) are indicated as dashed lines, with the corresponding glacial or interglacial periods shown on the right. Vertical black bar represents a period of isolation of lineages before migration initiates at the secondary contact. The spanning time of this period is shown in dashed line on the left vertical timeline, which is shortened for visual purposes. The migration directions and corresponding rates (M_{ES}) in individual migrants per generation are shown between NL and ES. Demographic expansion is indicated by the increasing areas of the gray ladder shapes. The current effective population sizes are shown at the bottom after the split between the Nanling Mts. (NL) and the eastern mountains (ES)

(V6) populations within the Nanling Mts. The Nanling Mts. present a general north–south orientation, which we infer as disadvantageous for east–west colonization, thus contributing to vicariance involving V5. Unlike the populations NLW2~5, NLW1 is isolated on one ridge of the Nanling Mts. and geographically distant from the remaining populations, thus resulting in the vicariance involving V6. Therefore, the geographical barriers formed by the associated mountain ranges including the Wuyi, Luoxiao, and Nanling Mts. have directly limited long-distance colonization and are considered a major factor contributing to the historical isolation of *C. chuniana* populations (Jiang et al., 2019; Li, Kong, et al., 2019; Li, Zhang, et al., 2019; Yang et al., 2019). Similar patterns have been found in many other plant species with a wide distribution range in subtropical China, such as *Machilus pauhoi* (Zhu et al., 2017), *Loropetalum chinense* (Gong et al., 2016), and *Liriodendron chinense* (Shen et al., 2019).

Our study suggests that population divergence of *C. chuniana* occurred in the Pleistocene and has been affected by the glacial cycles. These cycles periodically changed suitable habitat and are thought to have promoted range contraction and expansion coupled with geographical isolation (Knowles, 2001; Qu et al., 2011). Based on Bayesian estimation, the time of divergence (0.65 Ma) between the populations in the Nanling Mts. and those of the east coincides with the third (last) glacial period in China in the Middle Pleistocene (Figure 4). The time may fall in the Naynayxungla Glacial period (0.5–0.7 Ma; Zheng et al., 2002; Zhou & Li, 1998) or Poyang–Dagu Interglacial period (0.6–0.8 Ma; Duan et al., 1980). Although the precise time for the glaciations is under debate, it is at least clear that primarily the third (last) glaciation drove the genetic divergence between populations in the Nanling Mts. and those to the east, and shaped the geographical patterns of genetic variation. The estimated divergence time of the best-fit model in FSC2 is older, that is, 1.60 Ma (Figure 6), which overlaps with the earliest known Quaternary glacial of the Xixiabangma Glacial period ca. 1.6 Ma (Wan et al., 2016), or the Sizishan Periglacial period (1.5–2.1 Ma; Duan et al., 1980), when the temperature was 10°C lower than at present. The discrepancy between the results of Bayesian time estimation and FSC2 may be partially attributed to the wider time range under the log-uniform setting in FSC2. The secondary calibration used in BEAST is thought to generate smaller time estimates (Foster et al., 2017; Kong, Condamine, et al., 2017; Kong, Zhang, et al., 2017). The climate during glacial periods tended to be dry and cool, which would favor the populations shifting to lower elevations or latitudes with contracted distribution ranges due to the reduced subtropical evergreen broadleaved forest during the glacial period. The glacial period in the Middle Pleistocene has been shown to have driven spruce fir forests to lowlands in northern China (Liu, 1988). In our study, the geographical distribution of *C. chuniana* in subtropical China is also associated with the Pleistocene glacial cycles (Figure 4). The Dagu Glacial period (0.5–0.6 Ma; Duan et al., 1980) primarily affected the population divergence between the east and west, whereas the Dagu–Lushan Interglacial period (0.3–0.5 Ma; Duan et al., 1980) and Lushan Glacial period (0.2–0.3 Ma; Duan et al., 1980) primarily affected population diversification. The dominant role for Pleistocene glacial cycles affecting the geographical distribution of populations is also apparent in ecological niche modeling (ENM), where several isolated glacial refugia were identified during the LGM, although the climatic conditions may not be analogous to those of other glacial cycles.

4.2 | Genetic divergence between eastern and western populations

The population divergence in the eastern portion of the geographical range of *C. chuniana* is estimated to be older (0.47–0.34 Ma) and with smaller population sizes than within the Nanling Mts., where more recent and rapid population diversification occurred (0.35–0.19 Ma) with larger population sizes (Figure 4). The phylogenetic analysis also revealed that populations of the Nanling Mts. formed a monophyletic group and were distinctly separated from the eastern populations. This pattern agrees with the general pattern of genetic divergence observed between eastern and western China in other plant species with wide distributions (Chen et al., 2018; Gong et al., 2008; Ha et al., 2018; Hohmann et al., 2018; Lu et al., 2018;

Qiu et al., 2009). One main factor contributing to the differences in population divergence time and level of diversification between the east and west is likely to be the different orientations of mountain ranges (Chen et al., 2018). The southwest–northeast orientation of the Wuyi Mts. and East China Mts. is thought to present geographical barriers that blocked southward migrations in times of cooler climate or northward postglacial population expansion, which is disadvantageous for increasing population size and diversification, and may have contributed to an older divergence as is seen in the eastern populations (YDS, WYS, LXS1 and LXS2). Conversely, the north–south orientation of the Nanling Mts., allowing various elevational shifts of plant species, can facilitate gradual retreat from north to south and short-distance migrations during glacial and interglacial periods, thus promoting population diversification, larger population size and younger divergence as is seen in the populations of the Nanling Mts. (NLE1 and NLE2, and NLW1 through NLW5). The Nanling Mts. form a geographical boundary between the south- and the mid-subtropical regions and possess complex topography and diverse habitats favoring population diversification. The orientation and physiography of the mountain ranges appear to have critically contributed to the geographical pattern of genetic variation between the eastern and western populations of *C. chuniana*.

4.3 | Postglacial demographic expansion from the Nanling Mts. and secondary contact

FSC2 analyses yield a best-fit model of isolation followed by demographic expansion and secondary contact (Table S4, Figure 6). Demographic expansion in the Nanling Mts. was inferred with notably increased effective population size (Table S4, Figure 6), indicating high local population diversification as is seen in Figure 3. The Nanling Mts., which are composed of five distinct ridges, has a long history of subtropical evergreen broadleaved forest (STEBF) in southern China (Fan et al., 2018; Xu et al., 2017). Its vegetation is characterized by highly varied elevational or longitudinal shifts, varying aspects of slope directions, high heterogeneity of soils, and abundant microhabitats (Huang et al., 2012; Qiu et al., 2011; Shen et al., 2019; Tang et al., 2006; Zhu et al., 2017), which together served as a buffer from climatic change and thus helped to confer relatively stable ecological conditions to these mountains during glacial periods. The Nanling Mts. are suggested to never have been glaciated and have maintained a nearly constant level of annual precipitation during the last glacial period as current (Xiao et al., 2007), making it more suitable for *C. chuniana* than other regions of subtropical China. Therefore, complex physiography plus long-term stable ecological conditions in the Nanling Mts. across glacial cycles are thought to have preserved population genetic diversity, ultimately resulting in population size increase and opportunity for demographic expansion. Similar cases have been documented in widespread species in subtropical China, such as *Eurycorymbus cavaleriei*, *Loropetalum chinense*, and *Eomecon chionantha* (Gong et al., 2016; Tian et al., 2018; Wang et al., 2009).

The estimated time of secondary contact from our analysis (0.10 Ma) coincides with the Lushan–Tali Interglacial period in China (0.10–0.20 Ma; Duan et al., 1980), when a continuous geographical distribution of *C. chuniana* along the mountain ranges in subtropical China was detected by ecological niche modeling (ENM; Figure 2a). Because the Lushan–Tali Interglacial period somewhat overlaps with the last interglacial period (LIG; 0.12~0.14 Ma), its climate and environment was similar to that of the last interglacial period in China, when temperature increased and was estimated to be even higher than the present (Duan et al., 1980; Zhu et al., 2004). This suggests that the secondary contact may have occurred during this warmer time. Moreover, it is thought that the East Asia summer monsoon intensified during that time (Liu et al., 2018; Meng et al., 2018; Wang et al., 1999, 2007, 2012), thus providing more suitable habitat, especially considering that *C. chuniana* is adapted to mesic environments and most influenced by precipitation (Table S1).

Subtropical China has been long known as an area preserving higher species diversity than other regions of the Northern Hemisphere (Qian et al., 2005; Xiang et al., 2004). Such regional diversity bias is thought to be attributable to the high physiographical heterogeneity and diverse climate in the montane regions of subtropical China, which are advantageous for population colonization accompanied by repeated coalescence of populations through glacial cycles and postglacial increase. Our data may provide an explanation for higher species diversity of *Cercis* in subtropical China relative to any other part of its range in the Northern Hemisphere.

Additionally, our FSC2 analysis indicated bidirectional migrations occurring after the divergence of populations between the Nanling (NL) and eastern (ES) mountains, with the migration rate $M_{NL\text{-}ES}$ (2.13) higher than $M_{ES\text{-}NL}$ (0.33; Table S3, Figure 6). The migrations in *C. chuniana* appear to have proceeded primarily from the Nanling Mts. to the east. Many examples of plant species in East Asia exhibit a similar distribution pattern and migration route, such as *Tetrastigma hemsleyanum* and *Eomecon chionantha* (Tian et al., 2018; Wang, 1992a, 1992b; Wang et al., 2015). The question arises as to why the direction of contemporary migration is inferred from the Nanling Mts. toward the east, whereas the populations from the Nanling Mts. diverged more recently than those to the east. The Nanling Mts., with distinct phytogeography and long-term stable ecological condition, are thought to be one of the glacial refugia for *C. chuniana*. Populations of *C. chuniana* are present at relatively higher elevations in the Nanling Mts. (>600 m) than the eastern ones (from 264–727 m). Seeds of *Cercis* are supposedly dispersed primarily by wind during the fall and winter (Dickson, 1990; Robertson, 1976). The mountains' close proximity to each other may have facilitated west-to-east migration when the wind periodically blows most of the fruits from the branches straight across to the next mountain ranges from higher elevations to lower ones via closely adjacent stepping-stone areas.

5 | CONCLUSIONS

We aimed to advance understanding of the roles of mountain ranges and glacial cycles on the geographical distribution pattern of genetic variation for the plant species within the subtropical evergreen broadleaved forest (STEBF) in southern China. The orientation and physiography of the mountain ranges and the climate fluctuations across glacial cycles in this region appear to correlate with the geographical pattern of genetic variation in *C. chuniana*. The Nanling Mts. are considered an important glacial refugium for the preservation of genetic diversity during the glacial periods because of its complex physiography and long-term stable ecological conditions. Our study provides molecular evidence on how topography and climate change affect the phylogeographic history of the representative species within STEBF of southern China. Study of additional plant groups with similar geographical distribution patterns is further required to assess whether the patterns from *Cercis* observed here apply more generally to the evolutionary history and past vegetation changes in the STEBF associated with physiography and climate fluctuation.

ACKNOWLEDGEMENTS

This work was supported by the National Natural Science Foundation of China (31470312; 31470319; 31970231), Science and Technology Planning Project of Guangdong Province, China (2016A030303048). We thank Xiaolan Wang, Juan Zhou, Bo Li, Yemei Huang, and Zhong Zhang for help with sampling and field trips. We thank Zhixia Sun, Mark Ravinet, Joana Meier, Tongjian Liu, Huiqin Yi, and Haifei Yan for data analyses. Special thank goes to Prof. Qi Wang for providing fossil information.

CONFLICT OF INTEREST

The authors declare no conflict of interest to this work.

DATA AVAILABILITY STATEMENT

The vcf files containing SNPs and the model scripts of this study are openly available in Figshare at http://dx.doi.org/10.6084/m9.figshare.15283395 and http://dx.doi.org/10.6084/m9.figshare.15097872, respectively.

ORCID

Wei Gong https://orcid.org/0000-0002-0881-6130

REFERENCES

Akaike, H. (1974). A new look at the statistical model identification. *IEEE Transactions on Automatic Control*, *19*(6), 716–723. https://doi.org/10.1109/TAC.1974.1100705

Aldworth, S. J. (1998). *Trees and Shrubs of the Campus of Iowa State University: A Walking Tour of One Hundred Species*: Iowa State University, Department of Botany.

Alexandros, S. (2014). RAxML version 8: A tool for phylogenetic analysis and post-analysis of large phylogenies. *Bioinformatics*, *30*(9), 1312–1313. https://doi.org/10.1093/bioinformatics/btu033

Allen, J. R. M., Forrest, M., Hickler, T., Singarayer, J. S., Valdes, P. J., & Huntley, B. (2020). Global vegetation patterns of the past 140,000 years. *Journal of Biogeography*, *47*, 2073–2090. https://doi.org/10.1111/jbi.13930

Andrews, K. R., Good, J. M., Miller, M. R., Luikart, G., & Hohenlohe, P. A. (2016). Harnessing the power of RADseq for ecological and evolutionary genomics. *Nature Reviews Genetics*, *17*(2), 81–92. https://doi.org/10.1038/nrg.2015.28

Azani, N., Babineau, M., Bailey, C. D., Banks, H., Barbosa, A. R., Pinto, R. B., & Zimmerman, E. (2017). A new subfamily classification of the Leguminosae based on a taxonomically comprehensive phylogeny. *Taxon*, *66*(1), 44–77. https://doi.org/10.12705/661.3

Bouckaert, R., Heled, J., Kühnert, D., Vaughan, T., Wu, C.-H., Xie, D., Suchard, M. A., Rambaut, A., & Drummond, A. J. (2014). BEAST 2: A software platform for Bayesian evolutionary analysis. *PLoS Computational Biology*, *10*(4), e1003537. https://doi.org/10.1371/journal.pcbi.1003537

Bueno de Mesquita, C. P., Tillmann, L. S., Bernard, C. D., Rosemond, K. C., Molotch, N. P., & Suding, K. N. (2018). Topographic heterogeneity explains patterns of vegetation response to climate change (1972–2008) across a mountain landscape, Niwot Ridge, Colorado. *Arctic Antarctic and Alpine Research*, *50*(1), e1504492. https://doi.org/10.1080/15230430.2018.1504492

Catchen, J., Hohenlohe, P. A., Bassham, S., Amores, A., & Cresko, W. A. (2013). Stacks: An analysis tool set for population genomics. *Molecular Ecology*, *22*(11), 3124–3140. https://doi.org/10.1111/mec.12354

Chen, D., Zhang, D., Larsen, S. S., & Vincent, M. A. (2010). Cercis. In Z. Y. Wu, P. H. Raven, & D. Y. Hong (Eds.), *Flora of China*. Vol. *10*, (pp. 5–6). Science Press.

Chen, S. C., Zhang, L., Zeng, J., Shi, F., Yang, H., Mao, Y. R., & Fu, C. X. (2012). Geographic variation of chloroplast DNA in *Platycarya strobilacea* (Juglandaceae). *Journal of Systematics and Evolution*, *50*(4), 374–385. https://doi.org/10.1111/j.1759-6831.2012.00210.x

Chen, W., Hou, L., Zhang, Z. Y., Pang, X. M., & Li, Y. Y. (2017). Genetic diversity, population structure, and linkage disequilibrium of a core collection of *Ziziphus jujuba* assessed with genome-wide SNPs developed by genotyping-by-sequencing and SSR markers. *Frontiers in Plant Science*, *8*, 575. https://doi.org/10.3389/fpls.2017.00575

Chen, X.-D., Yang, J., Feng, L. I., Zhou, T., Zhang, H., Li, H.-M., Bai, G.-Q., Meng, X. U., Li, Z.-H., & Zhao, G.-F. (2020). Phylogeography and population dynamics of an endemic oak (*Quercus fabri Hance*) in subtropical China revealed by molecular data and ecological niche modeling. *Tree Genetics & Genomes*, *16*, 2. https://doi.org/10.1007/s11295-019-1383-0

Chen, Y. S., Deng, T., Zhou, Z., & Sun, H. (2018). Is the East Asian flora ancient or not? *National Science Review*, *5*(6), 920–932. https://doi.org/10.1093/nsr/nwx156

Chen, Z., & Mao, F. (1999). Plant composition and ecological characteristics of *Cercis yunnanensis* Coppice. *Yunnan Forestryence & Technology*, *1*, 01.

Colin, H., & Ruth, E. (2006). Island radiation on a continental scale: Exceptional rates of plant diversification after uplift of the Andes. *Proceedings of the National Academy of Sciences of the United States of America*, *103*(27), 10334–10339. https://doi.org/10.1073/pnas.0601928103

Collins, W. D., Bitz, C. M., Blackmon, M. L., Bonan, G. B., Bretherton, C. S., Carton, J. A., Chang, P., Doney, S. C., Hack, J. J., Henderson, T. B., Kiehl, J. T., Large, W. G., McKenna, D. S., Santer, B. D., & Smith, R. D. (2006). The community climate system Model Version 3 (CCSM3). *Journal of Climate*, *19*(11), 2122–2143. https://doi.org/10.1175/JCLI3761.1

Dai, C., Zhao, N. A., Wang, W., Lin, C., Gao, B., Yang, X., Zhang, Z., & Lei, F. (2011). Profound climatic effects on two East Asian black-throated tits (Ave: Aegithalidae), revealed by ecological niche models and phylogeographic analysis. *PLoS One*, *6*(12), e29359. https://doi.org/10.1371/journal.pone.0029329

Danecek, P., Auton, A., Abecasis, G., Albers, C. A., Banks, E., DePristo, M. A., Handsaker, R. E., Lunter, G., Marth, G. T., Sherry, S. T., McVean, G., & Durbin, R. (2011). The variant call format and VCFtools. *Bioinformatics*, *27*(15), 2156–2158. https://doi.org/10.1093/bioinformatics/btr330

Davey, J. W., Hohenlohe, P. A., Etter, P. D., Boone, J. Q., Catchen, J. M., & Blaxter, M. L. (2011). Genome-wide genetic marker discovery and genotyping using next-generation sequencing. *Nature Reviews Genetics*, *12*(7), 499–510. https://doi.org/10.1038/nrg3012

Dickson, J. G. (1990). *Cercis canadensis* L. Eastern redbud. In R. M. Burns & B. H. Honkala (Eds.), *Silvics of North America. Vol. 2. Hardwoods. Agriculture Handbook 654* (pp. 266–269). US Department of Agriculture.

Doyle, J., & Doyle, J. (1986). A rapid DNA isolation procedure from small quantities of fresh leaf tissues. *Phytochemical Bulletin*, *19*(1), 11–15.

Duan, W., Pu, Q., & Wu, X. (1980). Climatic variations in China during the quaternary. *GeoJournal*, *4*, 515–524. https://doi.org/10.1007/BF00214217

Excoffier, L., Dupanloup, I., Huerta-Sanchez, E., Sousa, V. C., & Foll, M. (2013). Robust demographic inference from genomic and SNP data. *PLoS Genetics*, *9*(10), e1003905. https://doi.org/10.1371/journal.pgen.1003905

Excoffier, L., & Lischer, H. E. L. (2010). Arlequin suite ver 3.5: A new series of programs to perform population genetics analyses under Linux and Windows. *Molecular Ecology Resources*, *10*(3), 564–567. https://doi.org/10.1111/j.1755-0998.2010.02847.x

Excoffier, L., Smouse, P. E., & Quattro, J. M. (1992). Analysis of molecular variance inferred from metric distances among DNA haplotypes: Application to human mitochondrial DNA restriction data. *Genetics*, *131*(2), 479–491. https://doi.org/10.1093/genetics/131.2.479

Fan, D. M., Huang, J. H., Hu, H. L., Sun, Z. X., Cheng, S. M., Kou, Y. X., & Zhang, Z. Y. (2018). Evolutionary hotspots of seed plants in subtropical China: A comparison with species diversity hotspots of woody seed plants. *Frontiers in Genetics*, *9*, 333. https://doi.org/10.3389/fgene.2018.00333

Fick, S. E., & Hijmans, R. J. (2017). WorldClim 2: New 1-km spatial resolution climate surfaces for global land areas. *International Journal of Climatology*, *37*(12), 4302–4315. https://doi.org/10.1002/joc.5086

Fielding, A. H., & Bell, J. F. (1997). A review of methods for the assessment of prediction errors in conservation presence/absence models. *Environmental Conservation*, *24*(1), 38–49. https://doi.org/10.1017/s0376892997000088

Foster, C. S. P., Sauquet, H., Van der Merwe, M., McPherson, H., Rossetto, M., & Ho, S. Y. W. (2017). Evaluating the impact of genomic data and priors on Bayesian estimates of the angiosperm evolutionary timescale. *Systematic Biology*, *66*(3), 338–351. https://doi.org/10.1093/sysbio/syw086

Fritsch, P. W., & Cruz, B. C. (2012). Phylogeny of *Cercis* based on DNA sequences of nuclear ITS and four plastid regions: Implications for transatlantic historical biogeography. *Molecular Phylogenetics and Evolution*, *62*(3), 816–825. https://doi.org/10.1016/j.ympev.2011.11.016

Fritsch, P. W., Nowell, C. F., Leatherman, L. S. T., Gong, W., Cruz, B. C., Burge, D. O., & Delgado-Salinas, A. (2018). Leaf adaptations and species boundaries in North American Cercis: Implications for the evolution of dry floras. *American Journal of Botany*, *105*(9), 1577–1594. https://doi.org/10.1002/ajb2.1155

Gong, W., Chen, C., Dobes, C., Fu, C. X., & Koch, M. A. (2008). Phylogeography of a living fossil: Pleistocene glaciations forced *Ginkgo biloba* L. (Ginkgoaceae) into two refuge areas in China with limited subsequent postglacial expansion. *Molecular Phylogenetics and Evolution*, *48*(3), 1094–1105. https://doi.org/10.1016/j.ympev.2008.05.003

Gong, W., Liu, W. Z., Gu, L., Kaneko, S., Koch, M. A., & Zhang, D. X. (2016). From glacial refugia to wide distribution range: Demographic expansion of *Loropetalum chinense* (Hamamelidaceae) in Chinese subtropical evergreen broadleaved forest. *Organisms Diversity & Evolution*, *16*(1), 23–38. https://doi.org/10.1007/s13127-015-0252-4

Ha, Y. H., Kim, C., Choi, K., & Kim, J. H. (2018). Molecular phylogeny and dating of Forsythieae (Oleaceae) provide insight into the Miocene history of Eurasian temperate shrubs. *Frontiers in Plant Science*, *9*, 99. https://doi.org/10.3389/fpls.2018.00099

Harrington, S. M., Hollingsworth, B. D., Higham, T. E., & Reeder, T. W. (2018). Pleistocene climatic fluctuations drive isolation and secondary contact in the red diamond rattlesnake (*Crotalus ruber*) in Baja California. *Journal of Biogeography*, *45*(1), 64–75. https://doi.org/10.1111/jbi.13114

Harrison, S. P., Yu, G., Takahar, H., & Prentice, I. C. (2001). Diversity of temperate plants in East Asia. *Nature*, *413*, 129–130. https://doi.org/10.1038/35093166

Heffelfinger, C., Fragoso, C. A., Moreno, M. A., Overton, J. D., Mottinger, J. P., Zhao, H., Tohme, J., & Dellaporta, S. L. (2014). Flexible and scalable genotyping-by-sequencing strategies for population studies. *BMC Genomics*, *15*(1), 979. https://doi.org/10.1186/1471-2164-15-979

Hewitt, G. M. (2004). Genetic consequences of climatic oscillations in the Quaternary. *Philosophical Transactions of the Royal Society of London Series B-Biological Sciences*, *359*(1442), 183–195. https://doi.org/10.1098/rstb.2003.1388

Hijmans, R. J., Cameron, S. E., Parra, J. L., Jones, P. G., & Jarvis, A. (2005). Very high resolution interpolated climate surfaces for global land areas. *International Journal of Climatology*, *25*(15), 1965–1978. https://doi.org/10.1002/joc.1276

Hohmann, N., Wolf, E. M., Rigault, P., Zhou, W. B., Kiefer, M., Zhao, Y. P., & Koch, M. A. (2018). *Ginkgo biloba*'s footprint of dynamic Pleistocene history dates back only 390,000 years ago. *BMC Genomics*, *19*(1), 299. https://doi.org/10.1186/s12864-018-4673-2

Hou, B. W., Luo, J., Zhang, Y. S., Niu, Z. T., Xue, Q. Y., & Ding, X. Y. (2017). Iteration expansion and regional evolution: Phylogeography of *Dendrobium officinale* and four related taxa in southern China. *Scientific Reports*, *7*(1), 43525. https://doi.org/10.1038/srep43525

Hou, H. Y. (1983). Vegetation of China with reference to its geographical distribution. *Annals of the Missouri Botanical Garden*, *70*(3), 509–549. https://doi.org/10.2307/2992085

Huang, J. H., Chen, B., Liu, C., Lai, J. S., Zhang, J. L., & Ma, K. P. (2012). Identifying hotspots of endemic woody seed plant diversity in China. *Diversity and Distributions*, *18*, 673–688. https://doi.org/10.1111/j.1472-4642.2011.00845.x

Hughes, C. E. (2017). Are there many different routes to becoming a global biodiversity hotspot? *Proceedings of the National Academy of Sciences*, *114*(17), 4275–4277. https://doi.org/10.1073/pnas.1703798114

Hughes, C. E., & Atchison, G. W. (2015). The ubiquity of alpine plant radiations: From the Andes to the Hengduan Mountains. *New Phytologist*, *207*(2), 275–282. https://doi.org/10.1111/nph.13230

Ilut, D. C., Nydam, M. L., & Hare, M. P. (2014). Defining loci in restriction-based reduced representation genomic data from nonmodel species: Sources of bias and diagnostics for optimal clustering. *Biomed Research International*, *2014*, 1–9. https://doi.org/10.1155/2014/675158

Isely, D. (1975). Leguminosae of the United States. II. Subfamily Caesalpinioideae. *Memoirs of the New York Botanical Garden*.

Jiang, X. L., Xu, G. B., & Deng, M. (2019). Spatial genetic patterns and distribution dynamics of the rare Oak *Quercus chungii*: Implications for biodiversity conservation in Southeast China. *Forests*, *10*(9), 821. https://doi.org/10.3390/f10090821

Kadereit, J. W. (2017). The role of in situ species diversification for the evolution of high vascular plant species diversity in the European Alps-A review and interpretation of phylogenetic studies of the endemic flora of the Alps. *Perspectives in Plant Ecology*

Evolution and Systematics, *26*, 28–38. https://doi.org/10.1016/j.ppees.2017.03.002

Knowles, L. L. (2001). Did the Pleistocene glaciations promote divergence? Tests of explicit refugial models in montane grasshoppers. *Molecular Ecology*, *10*(3), 691–701. https://doi.org/10.1046/j.1365-294x.2001.01206.x

Kong, H., Condamine, F. L., Harris, A. J., Chen, J., Pan, B. O., Möller, M., Hoang, V. S., & Kang, M. (2017). Both temperature fluctuations and East Asian monsoons have driven plant diversification in the karst ecosystems from southern China. *Molecular Ecology*, *26*(22), 6414–6429. https://doi.org/10.1111/mec.14367

Kong, H. H., Zhang, Y., Hong, Y., & Barker, M. S. (2017). Multilocus phylogenetic reconstruction informing polyploid relationships of *Aconitum* subgenus *Lycoctonum* (Ranunculaceae) in China. *Plant Systematics and Evolution*, *303*(6), 727–744. https://doi.org/10.1007/s00606-017-1406-y

Lavin, M., Herendeen, P. S., & Wojciechowski, M. F. (2005). Evolutionary ratesanalysis of Leguminosae implicates a rapid diversification of lineages during the Tertiary. *Systematic Biology*, *54*(4), 575–594. https://doi.org/10.1080/10635150590947131

Lefort, V., Longueville, J. E., & Gascuel, O. (2017). SMS: smart model selection in PhyML. *Molecular Biology and Evolution*, *34*(9), 2422–2424. https://doi.org/10.1093/molbev/msx149.

Li, H., & Durbin, R. (2009). Fast and accurate short read alignment with Burrows-Wheeler transform. *Bioinformatics*, *25*(14), 1754–1760. https://doi.org/10.1093/bioinformatics/btp324

Li, H., Handsaker, B., Wysoker, A., Fennell, T., Ruan, J., Homer, N., Marth, G., Abecasis, G., & Durbin, R. (2009). Genome project data processing S: The sequence alignment/map format and SAMtools. *Bioinformatics*, *25*(16), 2078–2079. https://doi.org/10.1093/bioinformatics/btp352

Li, H., Kong, L., Wang, K., Zhang, S., Motokawa, M., Wu, Y., & Li, Y. (2019). Molecular phylogeographic analyses and species delimitations reveal that *Leopoldamys edwardsi* (Rodentia: Muridae) is a species complex. *Integrative Zoology*, *14*(5), 494–505. https://doi.org/10.1111/1749-4877.12378

Li, J., Wen, S., Zhang, Q., Wang, F., Zheng, B., & Li, B. (1979). A discussion on the period, amplitude and type of the uplift of the Qinghai-Xizang plateau. *Scientia Sinica*, *22*, 1314–1328.

Li, X. H., Shao, J. W., Lu, C., Zhang, X. P., & Qiu, Y. X. (2012). Chloroplast phylogeography of a temperate tree *Pteroceltis tatarinowii* (Ulmaceae) in China. *Journal of Systematics and Evolution*, *50*(4), 325–333. https://doi.org/10.1111/j.1759-6831.2012.00203.x

Li, Y., Zhang, X., & Fang, Y. (2019). Landscape features and climatic forces shape the genetic structure and evolutionary history of an oak species (*Quercus chenii*) in East China. *Frontiers in Plant Science*, *10*, 1060. https://doi.org/10.3389/fpls.2019.01060

Liu, H. T., Wang, W. J., Song, G., Qu, Y. H., Li, S. H., Fjeldsa, J., & Lei, F. M. (2012). Interpreting the process behind endemism in China by integrating the phylogeography and ecological niche models of the *Stachyridopsis ruficeps*. *PLoS One*, *7*(10), e46761. https://doi.org/10.1371/journal.pone.0046761

Liu, J. S., Algeo, T. J., Yang, H., Pan, J. J., Tang, C. Y., Huang, J. H., & Xie, S. C. (2018). Changes in vegetation type on the Chinese Loess Plateau since 75 ka related to East Asian Summer Monsoon variation. *Palaeogeography*, *Palaeoclimatology*, *Palaeoecology*, *510*, 124–139. https://doi.org/10.1016/j.palaeo.2018.02.030

Liu, J., Moller, M., Provan, J., Gao, L. M., Poudel, R. C., & Li, D. Z. (2013). Geological and ecological factors drive cryptic speciation of yews in a biodiversity hotspot. *New Phytologist*, *199*(4), 1093–1108. https://doi.org/10.1111/nph.12336

Liu, K. (1988). Quaternary history of the temperate forests of China. *Quaternary Science Reviews*, *7*(1), 1–20. https://doi.org/10.1016/0277-3791(88)90089-3

Liu, L., Hao, Z. Z., Liu, Y. Y., Wei, X. X., Cun, Y. Z., & Wang, X. Q. (2014). Phylogeography of *Pinus armandii* and its relatives: Heterogeneous contributions of geography and climate changes to the genetic differentiation and diversification of Chinese white pines. *PLoS One*, *9*, e85920. https://doi.org/10.1371/journal.pone.0085920

Liu, Z. Z. (1984). The origin and morphological characteristics of the Wuyi Mountains, Fujian Province. *Journal of Nanjing University Natural Science*, *3*, 567–578.

López-Pujol, J., Zhang, F. M., Sun, H. Q., Ying, T. S., & Ge, S. (2011). Centres of plant endemism in China: Places for survival or for speciation? *Journal of Biogeography*, *38*(7), 1267–1280. https://doi.org/10.1111/j.1365-2699.2011.02504.x

Lu, L.-M., Mao, L.-F., Yang, T., Ye, J.-F., Liu, B., Li, H.-L., Sun, M., Miller, J. T., Mathews, S., Hu, H.-H., Niu, Y.-T., Peng, D.-X., Chen, Y.-H., Smith, S. A., Chen, M., Xiang, K.-L., Le, C.-T., Dang, V.-C., Lu, A.-M., … Chen, Z.-D. (2018). Evolutionary history of the angiosperm flora of China. *Nature*, *554*(7691), 234–238. https://doi.org/10.1038/nature25485

Matuszak, S., Muellner-Riehl, A. N., Sun, H., & Favre, A. (2016). Dispersal routes between biodiversity hotspots in Asia: The case of the mountain genus *Tripterospermum* (Gentianinae, Gentianaceae) and its close relatives. *Journal of Biogeography*, *43*(3), 580–590. https://doi.org/10.1111/jbi.12617

Melo, A. T. O., Bartaula, R., & Hale, I. (2016). GBS-SNP-CROP: A reference-optional pipeline for SNP discovery and plant germplasm characterization using variable length, paired-end genotyping-by-sequencing data. *BMC Bioinformatics*, *17*(1), 29. https://doi.org/10.1186/s12859-016-0879-y

Meng, X. Q., Liu, L. W., Wang, X. C. T., Balsam, W., Chen, J., & Ji, J. F. (2018). Mineralogical evidence of reduced East Asian summer monsoon rainfall on the Chinese loess plateau during the early Pleistocene interglacials. *Earth and Planetary Science Letters*, *486*, 61–69. https://doi.org/10.1016/j.epsl.2017.12.048

Metcalf, F. P. (1940). Eight new species of Leguminosae from Southeastern China. *Lingnan Science Journal*, *19*, 549–563.

Metzker, M. L. (2010). Applications of next-generation sequencing. Sequencing technologies-the next generation. *Nature Reviews Genetics*, *11*(1), 31–46. https://doi.org/10.1038/nrg2626

Miller, M. A., Schwartz, T., Pickett, B. E., He, S., Klem, E. B., Scheuermann, R. H., Passarotti, M., Kaufman, S., & O'Leary, M. A. (2015). A RESTful API for access to phylogenetic tools via the CIPRES science gateway. *Evolutionary Bioinformatics*, *11*(11), 43–48. https://doi.org/10.4137/EBO.S21501

Muellner-Riehl, A. N. (2019). Mountains as evolutionary arenas: Patterns, emerging approaches, paradigm shifts, and their implications for plant phylogeographic research in the Tibeto-Himalayan region. *Frontiers in Plant Science*, *10*, 195. https://doi.org/10.3389/fpls.2019.00195

Nevado, B., Contreras-Ortiz, N., Hughes, C., & Filatov, D. A. (2018). Pleistocene glacial cycles drive isolation, gene flow and speciation in the high-elevation Andes. *New Phytologist*, *219*(2), 779–793. https://doi.org/10.1111/nph.15243

Niu, S., Song, Q., Koiwa, H., Qiao, D., Zhao, D., Chen, Z., Liu, X., & Wen, X. (2019). Genetic diversity, linkage disequilibrium, and population structure analysis of the tea plant (*Camellia sinensis*) from an origin center, Guizhou plateau, using genome-wide SNPs developed by genotyping-by-sequencing. *BMC Plant Biology*, *19*(1), 328. https://doi.org/10.1186/s12870-019-1917-5

Oyama, K., Ramirez-Toro, W., Penaloza-Ramirez, J. M., Pedraza, A. E. P., Torres-Miranda, C. A., Ruiz-Sanchez, E., & Gonzalez-Rodriguez, A. (2018). High genetic diversity and connectivity among populations of *Quercus candicans*, *Quercus crassifolia*, and *Quercus castanea* in a heterogeneous landscape in Mexico. *Tropical Conservation Science*, *11*, 1940082918766195. https://doi.org/10.1177/1940082918766195

Pearson, R. G., Raxworthy, C. J., Nakamura, M., & Peterson, A. T. (2007). Predicting species distributions from small numbers of occurrence records: A test case using cryptic geckos in

Madagascar. *Journal of Biogeography*, *34*(1), 102–117. https://doi.org/10.1111/j.1365-2699.2006.01594.x

Phillips, S. J., Anderson, R. P., & Schapire, R. E. (2006). Maximum entropy modeling of species geographic distributions. *Ecological Modelling*, *190*(3–4), 231–259. https://doi.org/10.1016/j.ecolmodel.2005.03.026

Qian, H., Ricklefs, E., & White, P. S. (2005). Beta diversity of angiosperms in temperate floras of eastern Asia and eastern North America. *Ecology Letters*, *8*, 15–22. https://doi.org/10.1111/j.1461-0248.2004.00682.x

Qiu, B. W., Zeng, C. Y., Chen, C. C., Zhang, C. G., & Zhong, M. (2013). Vegetation distribution pattern along altitudinal gradient in subtropical mountainous and hilly river basin China. *Journal of Geographical Sciences*, *23*(2), 247–257. https://doi.org/10.1007/s11442-013-1007-9

Qiu, Y. X., Fu, C. X., & Comes, H. P. (2011). Plant molecular phylogeography in China and adjacent regions: Tracing the genetic imprints of Quaternary climate and environmental change in the world's most diverse temperate flora. *Molecular Phylogenetics and Evolution*, *59*(1), 225–244. https://doi.org/10.1016/j.ympev.2011.01.012

Qiu, Y. X., Guan, B. C., Fu, C. X., & Comes, H. (2009). Did glacials and/or interglacials promote allopatric incipient speciation in East Asian temperate plants? Phylogeographic and coalescent analyses on refugial isolation and divergence in *Dysosma versipellis*. *Molecular Phylogenetics and Evolution*, *51*, 281–293. https://doi.org/10.1016/j.ympev.2009.01.016

Qu, Y. H., Luo, X., Zhang, R. Y., Song, G., Zou, F. S., & Lei, F. M. (2011). Lineage diversification and historical demography of a montane bird *Garrulax elliotii* – Implications for the Pleistocene evolutionary history of the eastern Himalayas. *BMC Evolutionary Biology*, *11*(1), 174. https://doi.org/10.1111/j.1365-294X.2008.03998.x

Raj, A., Stephens, M., & Pritchard, J. K. (2014). fastSTRUCTURE: Variational inference of population structure in large SNP data sets. *Genetics*, *197*(2), 573–589. https://doi.org/10.1534/genetics.114.164350

Rambaut, A. (2014). FigTree 1.4.3 software. *Institute of Evolutionary Biology, Univ. Edinburgh*. http://tree.bio.ed.ac.uk/software/figtree/

Rambaut, A., Suchard, M. A., Xie, D., & Drummond, A. J. (2014). Tracer v1. 6. http://beast.bio.ed.ac.uk/Tracer

Ray, N., & Adams, J. M. (2001). A GIS-based vegetation map of the world at the last glacial maximum (25,000–15,000 BP). *Internet Archaeology*, *11*. https://doi.org/10.11141/ia.11.2

Robertson, K. R. (1976). *Cercis*: The redbuds. *Arnoldia*, *36*, 37–49.

Ronquist, F. (1997). Dispersal-vicariance analysis: A new approach to the quantification of historical biogeography. *Systematic Biology*, *46*(1), 195–203. https://doi.org/10.2307/2413643

Scheben, A., Batley, J., & Edwards, D. (2017). Genotyping-by-sequencing approaches to characterize crop genomes: Choosing the right tool for the right application. *Plant Biotechnology Journal*, *15*(2), 149–161. https://doi.org/10.1111/pbi.12645

Shen, Y. F., Cheng, Y. L., Li, K. Q., & Li, H. G. (2019). Integrating phylogeographic analysis and geospatial methods to infer historical dispersal routes and glacial refugia of Liriodendron chinense. *Forests*, *10*(7), 565. https://doi.org/10.3390/f10070565

Shi, Y. F., Cui, Z. J., & Su, Z. (2006). *The Quaternary glaciations and environmental variations in China*. Hebei Science and Technology Press.

Shi, Y. F., Li, J. J., & Li, B. Y. (1998). *Uplift and environmental changes of Qinghai-Tibetan Plateau in the Late Cenozoic*. Guangdong Science and Technology Press.

Simpson, G. (1964). Species density of North American recent mammals. *Systematic Zoology*, *13*(2), 57–73. https://doi.org/10.2307/2411825

Smith, S. A., & Donoghue, M. J. (2008). Rates of molecular evolution are linked to life history in flowering plants. *Science*, *322*(5898), 86–89. https://doi.org/10.1126/science.1163197

Soberón, J., & Peterson, A. (2005). Interpretation of models of fundamental ecological niches and species' distributional areas. *Biodiversity Informatics*, *2*, 1–10. https://doi.org/10.17161/bi.v2i0.4

Svenning, J. C., Normand, S., & Skov, F. (2009). Plio-Pleistocene climate change and geographic heterogeneity in plant diversity-environment relationships. *Ecography*, *32*(1), 13–21. https://doi.org/10.1111/j.1600-0587.2008.05732.x

Tang, Z. Y., Wang, Z. H., Zheng, C. Y., & Fang, J. Y. (2006). Biodiversity in China's mountains. *Frontiers in Ecology and the Environment*, *4*, 347–352.

Tian, S., Kou, Y., Zhang, Z., Yuan, L., Li, D., López-Pujol, J., Fan, D., & Zhang, Z. (2018). Phylogeography of *Eomecon chionantha* in subtropical China: The dual roles of the Nanling Mountains as a glacial refugium and a dispersal corridor. *BMC Evolutionary Biology*, *18*(1), 20. https://doi.org/10.1186/s12862-017-1093-x

Tian, S., Lei, S.-Q., Hu, W., Deng, L.-L., Li, B. O., Meng, Q.-L., Soltis, D. E., Soltis, P. S., Fan, D.-M., & Zhang, Z.-Y. (2015). Repeated range expansions and inter-/postglacial recolonization routes of *Sargentodoxa cuneata* (Oliv.) Rehd. et Wils. (Lardizabalaceae) in subtropical China revealed by chloroplast phylogeography. *Molecular Phylogenetics and Evolution*, *85*, 238–246. https://doi.org/10.1016/j.ympev.2015.02.016

Tian, X. Y., Ye, J. W., Wang, T. M., Bao, L., & Wang, H. F. (2020). Different processes shape the patterns of divergence in the nuclear and chloroplast genomes of a relict tree species in East Asia. *Ecology and Evolution*, *10*(10), 4331–4342. https://doi.org/10.1002/ece3.6200

Wan, D. S., Feng, J. J., Jiang, D. C., Mao, K. S., Duan, Y. W., Miehe, G., & Opgenoorth, L. (2016). The Quaternary evolutionary history, potential distribution dynamics, and conservation implications for a Qinghai-Tibet Plateau endemic herbaceous perennial, *Anisodus tanguticus* (Solanaceae). *Ecology and Evolution*, *6*(7), 1977–1995. https://doi.org/10.1002/ece3.2019

Wang, H., Qiong, L. A., Sun, K., Lu, F., Wang, Y., Song, Z., Wu, Q., Chen, J., & Zhang, W. (2010). Phylogeographic structure of *Hippophae tibetana* (Elaeagnaceae) highlights the highest microrefugia and the rapid uplift of the Qinghai-Tibetan Plateau. *Molecular Ecology*, *19*(14), 2964–2979. https://doi.org/10.1111/j.1365-294x.2010.04729.x

Wang, J., Gao, P. X., Kang, M., Lowe, A. J., & Huang, H. W. (2009). Refugia within refugia: The case study of a canopy tree (*Eurycorymbus cavaleriei*) in subtropical China. *Journal of Biogeography*, *36*(11), 2156–2164. https://doi.org/10.1111/j.1365-2699.2009.02165.x

Wang, L., Sarnthein, M., Erlenkeuser, H., Grimalt, J., Grootes, P., Heilig, S., Ivanova, E., Kienast, M., Pelejero, C., & Pflaumann, U. (1999). East Asian monsoon climate during the Late Pleistocene: High-resolution sediment records from the South China Sea. *Marine Geology*, *156*(1–4), 245–284. https://doi.org/10.1016/S0025-3227(98)00182-0

Wang, R. J., Jian, Z. M., Xiao, W. S., Tian, J., Li, J. R., Chen, R. H., Zheng, Y. L., & Chen, J. F. (2007). Quaternary biogenic opal records in the South China Sea: Linkages to East Asian monsoon, global ice volume and orbital forcing. *Science in China Series D-Earth Sciences*, *50*(5), 710–724. https://doi.org/10.1007/s11430-007-0041-9

Wang, W. T. (1992a). On some distribution patterns and some migration routes found in the eastern Asiatic region. *Acta Phytotaxonomica Sinica*, *30*(1), 1–24.

Wang, W. T. (1992b). On some distribution patterns and some migration routes found in the eastern Asiatic region (Cont.). *Acta Phytotaxonomica Sinica (China)*, *30*(2), 97–117.

Wang, Y., Comes, H. P., Cao, Y., Guo, R., Mao, Y. R., & Qiu, Y. X. (2017). Quaternary climate change drives allo-peripatric speciation and refugial divergence in the *Dysosma versipellis-pleiantha* complex from different forest types in China. *Scientific Reports*, *7*, 40261. https://doi.org/10.1038/srep40261

Wang, Y. H., Jiang, W. M., Comes, H. P., Hu, F. S., Qiu, Y. X., & Fu, C. X. (2015). Molecular phylogeography and ecological niche modelling of a widespread herbaceous climber, *Tetrastigma hemsleyanum* (Vitaceae): Insights into Plio-Pleistocene range dynamics of

evergreen forest in subtropical China. *New Phytologist*, *206*(2), 852–867. https://doi.org/10.1111/nph.13261

Wang, Z. H., Fang, J. Y., Tang, Z. Y., & Shi, L. (2012). Geographical patterns in the beta diversity of China's woody plants: The influence of space, environment and range size. *Ecography*, *35*(12), 1092–1102. https://doi.org/10.1111/j.1600-0587.2012.06988.x

Weir, B. (1996). *Genetic data analysis. Methods for discrete population genetic data*. Sinauer Associates, Inc. Publishers.

Weir, B., & Cockerham, C. (1984). Estimating F-statistics for the analysis of population structure. *Evolution*, *38*, 1358–1370. https://doi.org/10.1111/j.1558-5646.1984.tb05657.x

Wu, Z. (1980). *Vegetation of China* (pp. 825). Science Press.

Wu, Z. Y., Zhu, Y. C., & Jiang, H. Q. (1987). *The vegetation of Yunnan*. Science.

Wunderlin, R. P., Larsen, K., & Larsen, S. S. (1981). Tribe 3. Cercideae Bronn. In R. M. Polhill & P. H. Raven (Eds.), *Advances in legume systematics*, *Part 1* (pp. 107–116). Royal Botanical Garden, Kew.

Xiang, Q. Y., Zhang, W. H., Ricklefs, R. E., Qian, H., Chen, Z. D., Wen, J., & Li, J. H. (2004). Regional differences in rates of plant speciation and molecular evolution: A comparison between eastern Asia and eastern North America. *Evolution*, *58*, 2175–2184. https://doi.org/10.1554/03-712

Xiao, J. Y., Lu, H. B., Zhou, W. J., Zhao, Z. J., & Hao, R. H. (2007). Evolution of vegetation and climate since the last glacial maximum recorded at Dahu peat site, South China. *Science in China Series D: Earth Sciences*, *50*(8), 1209–1217. https://doi.org/10.1007/s11430-007-0068-y

Xing, Y. W., & Ree, R. H. (2017). Uplift-driven diversification in the Hengduan Mountains, a temperate biodiversity hotspot. *Proceedings of the National Academy of Sciences of the United States of America*, *114*(17), E3444–E3451. https://doi.org/10.1073/pnas.1616063114

Xiong, L. F., Wu, S. C., & Zhang, S. H. (2019). Mechanical behavior of a granite from Wuyi Mountain: Insights from Strain-Based Approaches. *Rock Mechanics and Rock Engineering*, *52*(3), 719–736. https://doi.org/10.1007/s00603-018-1617-8

Xu, Y., Shen, Z. H., Ying, L. X., Wang, Z. H., Huang, J. H., Zang, R. G., & Jiang, Y. X. (2017). Hotspot analyses indicate significant conservation gaps for evergreen broadleaved woody plants in China. *Scientific Reports*, *7*(1), 1–10. https://doi.org/10.1038/s41598-017-02098-0

Yan, F., Zhou, W., Zhao, H., Yuan, Z., Wang, Y., Jiang, K., Jin, J., Murphy, R. W., Che, J., & Zhang, Y. (2013). Geological events play a larger role than Pleistocene climatic fluctuations in driving the genetic structure of *Quasipaa boulengeri* (Anura: Dicroglossidae). *Molecular Ecology*, *22*(4), 1120–1133. https://doi.org/10.1111/mec.12153

Yang, A. H., Dick, C. W., Yao, X. H., & Huang, H. W. (2016). Impacts of biogeographic history and marginal population genetics on species range limits: A case study of *Liriodendron chinense*. *Scientific Reports*, *6*(1), 25632. https://doi.org/10.1038/srep25632

Yang, A. H., Zhong, Y. D., Liu, S. J., Liu, L. P., Liu, T. Y., Li, Y. Q., & Yu, F. X. (2019). New insight into the phylogeographic pattern of *Liriodendron chinense* (Magnoliaceae) revealed by chloroplast DNA: East-west lineage split and genetic mixture within western subtropical China. *PeerJ*, *7*, e6355. https://doi.org/10.7717/peerj.6355

Ying, J. (2001). Species diversity and distribution pattern of seed plants in China. *Chinese Biodiversity*, *9*(4), 393–398.

Yu, Y., Harris, A. J., Blair, C., & He, X. J. (2015). RASP (Reconstruct Ancestral State in Phylogenies): A tool for historical biogeography. *Molecular Phylogenetics and Evolution*, *87*, 46–49. https://doi.org/10.1016/j.ympev.2015.03.008

Zhang, X., Li, Y., Zhang, Q., & Fang, Y. (2018). Ancient east-west divergence, recent admixture, and multiple marginal refugia shape genetic structure of a widespread oak species (*Quercus acutissima*) in China. *Tree Genetics & Genomes*, *14*, 88. https://doi.org/10.1007/s11295-018-1302-9

Zheng, B., Xu, Q., & Shen, Y. (2002). The relationship between climate change and Quaternary glacial cycles on the Qinghai-Tibetan Plateau: Review and speculation. *Quaternary International*, *97*, 93–101. https://doi.org/10.1016/s1040-6182(02)00054-x

Zheng, X., Levine, D., Shen, J., Gogarten, S., Laurie, C., & Weir, B. (2012). A high-performance computing toolset for relatedness and principal component analysis of SNP data. *Bioinformatics (Oxford, England)*, *28*(24), 3326–3328. https://doi.org/10.1093/bioinformatics/bts606

Zhou, S., & Li, J. (1998). The sequence of Quaternary glaciation in the Bayan Har Mountains. *Quaternary International*, *45*, 135–142. https://doi.org/10.1016/s1040-6182(97)00011-6

Zhu, H., Yi, X. G., Li, Y., Zhu, S. X., Li, M., Duan, Y. F., & Wang, X. R. (2019). Phylogeography and population genetic structure of flowering cherry species *Cerasus dielsiana* in subtropical China. *Systematics and Biodiversity*, *17*, 622–633.

Zhu, Q., Liao, B. Y., Li, P., Li, J. C., Deng, X. M., Hu, X. S., & Chen, X. Y. (2017). Phylogeographic pattern suggests a general northeastward dispersal in the distribution of *Machilus pauhoi* in South China. *PLoS One*, *12*(9), e0184456. https://doi.org/10.1371/journal.pone.0184456

Zhu, R., Liu, Q., & Jackson, M. (2004). Paleoenvironmental significance of the magnetic fabrics in Chinese loess-paleosols since the last interglacial (<130 ka). *Earth and Planetary Science Letters*, *221*(1–4), 55–69. https://doi.org/10.1016/S0012-821X(04)00103-7

SUPPORTING INFORMATION

Additional supporting information may be found in the online version of the article at the publisher's website.

How to cite this article: Liu, W., Xie, J., Zhou, H., Kong, H., Hao, G., Fritsch, P. W., & Gong, W. (2021). Population dynamics linked to glacial cycles in *Cercis chuniana* F. P. Metcalf (Fabaceae) endemic to the montane regions of subtropical China. *Evolutionary Applications*, 00, 1–17. https://doi.org/10.1111/eva.13301

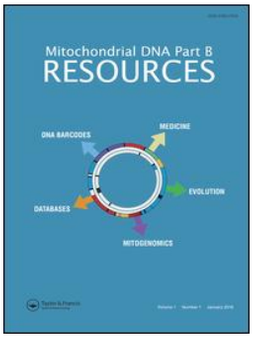

Taylor & Francis
Taylor & Francis Group

Mitochondrial DNA Part B
Resources

ISSN: (Print) 2380-2359 (Online) Journal homepage: https://www.tandfonline.com/loi/tmdn20

The complete chloroplast genome of *Philadelphus pekinensis* Rupr. (Hydrangeaceae)

Qin Fan, Mimi Li, Hui Zhou, Wanzhen Liu & Wei Gong

To cite this article: Qin Fan, Mimi Li, Hui Zhou, Wanzhen Liu & Wei Gong (2020) The complete chloroplast genome of *Philadelphus pekinensis* Rupr. (Hydrangeaceae), Mitochondrial DNA Part B, 5:2, 1178-1179, DOI: 10.1080/23802359.2020.1730725

To link to this article: https://doi.org/10.1080/23802359.2020.1730725

© 2020 The Author(s). Published by Informa UK Limited, trading as Taylor & Francis Group.

Published online: 27 Feb 2020.

Submit your article to this journal

Article views: 41

View related articles

View Crossmark data

Full Terms & Conditions of access and use can be found at
https://www.tandfonline.com/action/journalInformation?journalCode=tmdn20

MITOCHONDRIAL DNA PART B
2020, VOL. 5, NO. 2, 1178–1179
https://doi.org/10.1080/23802359.2020.1730725

Taylor & Francis
Taylor & Francis Group

MITOGENOME ANNOUNCEMENT

OPEN ACCESS Check for updates

The complete chloroplast genome of *Philadelphus pekinensis* Rupr. (Hydrangeaceae)

Qin Fan[a], Mimi Li[b], Hui Zhou[a], Wanzhen Liu[a] and Wei Gong[a]

[a]College of Life Sciences, South China Agricultural University, Guangzhou, China; [b]Institute of Botany, Jiangsu Province and Chinese Academy of Sciences, Nanjing, China

ABSTRACT

Philadelphus pekinensis Rupr. is a common perennial deciduous shrub distributed in temperate China. Here, we report the complete chloroplast genome of *P. pekinensis*. The cp genome is totally 157,308 bp in length, including large single-copy (LSC) region of 86,457 bp, small single-copy (SSC) region of 18,735 bp, and two separated inverted regions (IRs) of 26,058 bp, respectively. It contains 134 genes, including 85 protein-coding genes, 8 rRNA genes, and 37 tRNA genes. The overall GC content is 43.1%. The phylogenetic analysis reveals the monophyly of *P. pekinensis* and *P. calvescens*, which is more related with *Carpenteria californica* than other species in the Hydrangeaceae family.

ARTICLE HISTORY
Received 29 January 2020
Accepted 11 February 2020

KEYWORDS
Philadelphus pekinensis; chloroplast genome; ornamental plant; Illumina sequencing

Philadelphus pekinensis Rupr. is famous for its beautiful, fragrantand long term flowers, making it as an ornamental shrub commonly cultivated in the botanical gardens. It grows in temperate China, Inner Mongolia, Korea, as well as Europe and North America. Here, we report the first chloroplast (cp) genome of *P. pekinensis* for further research on the phylogenetic and biogeographic study among its related species in the future.

Samples of *P. pekinensis* were collected from Yunmeng Mountain National Forest Park in Miyun District, Beijing (Voucher No.: LP161571). Total genomic DNA was extracted from silica gel dried leaves using a modified CTAB method (Doyle and Doyle 1987). The paired-end (2 × 150 bp) library was constructed by Illumina PE150 in Novogene Co. Ltd (Beijing, China). Totally, 2.64 Gb clean data were obtained after removing low-quality reads and adaptor sequences. The complete cp genome of *P. pekinensis* was assembled via GetOrganelle pipeline (available online: https://github.com/Kinggerm/GetOrganelle, JianJun et al. 2018), which implements four steps of recruiting plastid-like reads: (i) conducting *de novo* assembly using SPAdes (Anton et al. 2012), (ii) filtering plastid-like contigs, (iii) visualizing and editing *de novo* assembly graph using Bandage (Ryan et al. 2015), and (iv) checking and adjusting the annotations using Geneious 11.0.3 (http://www.geneious.com, Kearse et al. 2012). The tRNA genes were annotated with ARAGORN (Laslett and Canback 2004). For phylogenetic reconstruction, we downloaded the cp genomes of 10 species in the Hydrangeaceae family, including *Hydrangea densifolia* (MN380652), *Decumaria barbara* (MN380684), *D. sinensis* (MN380685), *Schizophragma hydrangeoides* (KY412467), *Deutzia crassifolia* (MG524993), *D. compacta* (MN380704), *Philadelphus calvescens* (MN380700), *Kirengeshoma palmata* (MN380656), *Carpenteria californica* (MN380687), and *Whipplea modesta* (MN380692). *Mukdenia rossii* (MG470844) from Saxifragaceae was used as an outgroup. The aligned matrix was implemented in MAFFT (Katoh and Standley 2013). Phylogenetic analysis was performed with maximum likelihood (ML) method, using RAxML (Stamatakis 2006; 2014) with 1000 bootstrap replicates.

The annotated cp genomic sequences of *P. pekinensis* were deposited in GenBank (MN938497). The whole cp genome is 156,876 bp in length and has the typical quadripartite structure, including large single-copy (LSC) region of 86,457 bp, small single-copy (SSC) region of 18,735 bp, and two separated inverted region (IRs) of 26,058 bp. A total of 134 genes are identified consisting of 85 protein-coding genes (PCGs), 8 rRNA genes, and 37 tRNA genes. Among these genes, 61 PCGs and 22 tRNA genes are located in the LSC region (including one interregional gene *rps19*), while 12 PCGs and 1 tRNA gene occur in the SSC region (including one interregional gene *ycf1*). All the eight rRNA genes are duplicated in the IR regions. Each of the IR regions contains six PCGs and seven tRNA genes. Each of the 19 genes contains one intron, while the remaining three (*ycf3*, *clpP,* and *rps12*) possess two introns each. The overall GC content is 43.1%. A well supported phylogenetic tree is reconstructed, suggesting a monophyly formed by *P. pekinensis* and *P. calvescens* (Figure 1). The two species demonstrate a comparably closer phylogenetic relationship with *Carpenteria californica* than other species.

CONTACT Wei Gong wgong@scau.edu.cn College of Life Sciences, South China Agricultural University, Guangzhou, China

© 2020 The Author(s). Published by Informa UK Limited, trading as Taylor & Francis Group.
This is an Open Access article distributed under the terms of the Creative Commons Attribution License (http://creativecommons.org/licenses/by/4.0/), which permits unrestricted use, distribution, and reproduction in any medium, provided the original work is properly cited.

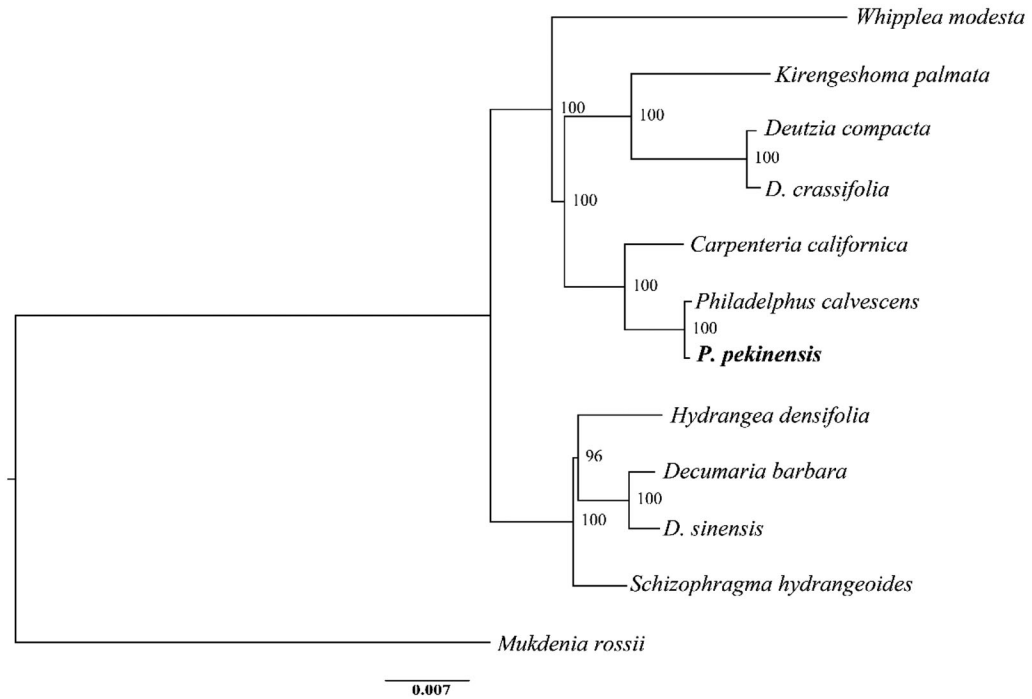

Figure 1. Maximum likelihood tree based on 11 complete chloroplast genomes of Hydrangeaceae and one outgroup species. Numbers in the nodes are bootstrap support values based on 1000 replicates. *Philadelphus pekinensis* is displayed in bold.

Disclosure statement

No potential conflict of interest was reported by the author(s).

Funding

This research was supported by the National Natural Science Foundation of China under [grant number 31570193].

ORCID

Mimi Li http://orcid.org/0000-0002-7883-0325

References

Anton B, Sergey N, Dmitry A, Alexey AG, Mikhail D, Alexander SK, Valery ML, Sergey IN, Son P, Andrey DP, et al. 2012. SPAdes: a new genome assembly algorithm and its applications to single-cell sequencing. J Comput Biol. 19:455–477.

Doyle JJ, Doyle JL. 1987. A rapid DNA isolation procedure for small quantities of fresh leaf tissue. Phytochemic Bullet. 19:11–15.

JianJun J, WenBin Y, JunBo Y, Yu S, TingShuang Y, De-Zhu L. 2018. GetOrganelle: a fast and versatile toolkit for accurate de novo assembly of organelle genomes. bioRxiv. 256479.

Katoh K, Standley DM. 2013. MAFFT multiple sequence alignment software version 7: improvements in performance and usability. Mol Biol Evol. 30(4):772–780.

Kearse M, Moir R, Wilson A, Stones-Havas S, Cheung M, Sturrock S, Buxton S, Cooper A, Markowitz S, Duran C, et al. 2012. Geneious basic: an integrated and extendable desktop software platform for the organization and analysis of sequence data. Bioinformatics. 28(12): 1647–1649.

Laslett D, Canback B. 2004. ARAGORN, a program to the detection of transfer RNA and transfer-messenger RNA genes in nucleotide sequences. Nucleic Acids Res. 32(1):11–16.

Ryan RW, Mark BS, Justin Z, Kathryn EH. 2015. Bandage: interactive visualization of de novo genome assemblies. Bioinformatics. 31: 3350–3352.

Stamatakis A. 2006. RAxML-VI-HPC: maximum likelihood-based phylogenetic analyses with thousands of taxa and mixed models. Bioinformatics. 22(21):2688–2690.

Stamatakis A. 2014. RAxML version 8: A tool for phylogenetic analysis and post-analysis of large phylogenies. Bioinformatics. 30(9): 1312–1313.

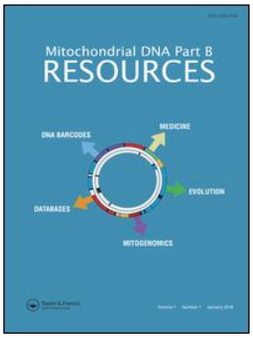

Taylor & Francis
Taylor & Francis Group

Mitochondrial DNA Part B
Resources

ISSN: (Print) 2380-2359 (Online) Journal homepage: https://www.tandfonline.com/loi/tmdn20

The complete chloroplast genome of *Deutzia pilosa* Rehd. (Hydrangeaceae)

Hui Zhou, Qin Fan, Wanzhen Liu & Wei Gong

To cite this article: Hui Zhou, Qin Fan, Wanzhen Liu & Wei Gong (2020) The complete chloroplast genome of *Deutzia pilosa* Rehd. (Hydrangeaceae), Mitochondrial DNA Part B, 5:2, 1419-1420, DOI: 10.1080/23802359.2020.1735969

To link to this article: https://doi.org/10.1080/23802359.2020.1735969

© 2020 The Author(s). Published by Informa UK Limited, trading as Taylor & Francis Group.

Published online: 13 Mar 2020.

Submit your article to this journal

Article views: 38

View related articles

View Crossmark data

Full Terms & Conditions of access and use can be found at
https://www.tandfonline.com/action/journalInformation?journalCode=tmdn20

MITOCHONDRIAL DNA PART B
2020, VOL. 5, NO. 2, 1419–1420
https://doi.org/10.1080/23802359.2020.1735969

Taylor & Francis
Taylor & Francis Group

MITOGENOME ANNOUNCEMENT

OPEN ACCESS Check for updates

The complete chloroplast genome of *Deutzia pilosa* Rehd. (Hydrangeaceae)

Hui Zhou, Qin Fan, Wanzhen Liu and Wei Gong

College of Life Sciences, South China Agricultural University, Guangzhou, China

ABSTRACT

The species *Deutzia pilosa* is well known as a commonly cultivated shrub and traditional Chinese herbal medicine. Here, we report the complete chloroplast genome of *D. pilosa*. It shows a total length of 156,983 bp with typical quadripartite structure, including the large single copy region (LSC) of 86,598 bp, the small single copy region (SSC) of 18,725 bp, and two separated inverted regions (IRs) of 25,830 bp, respectively. It contains 134 genes, including 89 protein-coding genes, 37 rRNA genes, and 8 tRNA genes. The overall GC content of the cp genome is 43.0%.

ARTICLE HISTORY
Received 18 February 2020
Accepted 20 February 2020

KEYWORDS
Deutzia pilosa; chloroplast genome; cultivated shrub; Illumina sequencing

The genus *Deutzia*, with more than 60 species, belongs to the Trib. Philadelpheae of Hydrangeaceae and shows a distribution in East Asia, Mexico and Central America (Shumei 1993). *Deutzia pilosa* Rehd. is often cultivated as ornamental shrub in South China for their spotless, flawless and fascinating flowers. In the current study, we report the first complete chloroplast (cp) genome of *D. pilosa*, on the purpose of further phylogenetic reconstruction or biogeographic study of the Hydrangeaceae family.

One individual was collected from Emei Mts., Sichuan Province (Voucher No. FQ190401). Tender leaves were sampled and instantly put into the silica gel for drying and preservation. Total genomic DNA was extracted using a modified CTAB method (Doyle and Doyle 1987). The paired-end (2 × 150 bp) library was sequenced by Illumina PE150 at Novogene Co. Ltd (Beijing, China). A total of 1.51 Gb clean reads were obtained after removing low-quality reads and adaptor sequences. The complete cp genome of *D. pilosa* was assembled using GetOrganelle and SPAdes (Bankevich et al. 2012), with manual adjustment and annotation using Geneious v8.0.2. The tRNA genes were annotated on ARAGORN (Laslett and Canback 2004). The cp genomes of ten species of Hydrangeaceae were downloaded from GenBank database, including *Cardiandra moellendorffii* (MN380653), *Decumaria barbara* (MN380684), *D. sinensis* (MN380685), *Deinanthe caerulea* (MN380658), *Deutzia compacta* (MN380704), *Dichroa febrifuga* (MN380702), *Hydrangea aspera* (MG524992), *H. luteovenosa* (MF370556), *Philadelphus calvescens* (MN380700) and *Schizophragma hydrangeoides* (KY412467). *Paeonia lactiflora* (MG897127) of

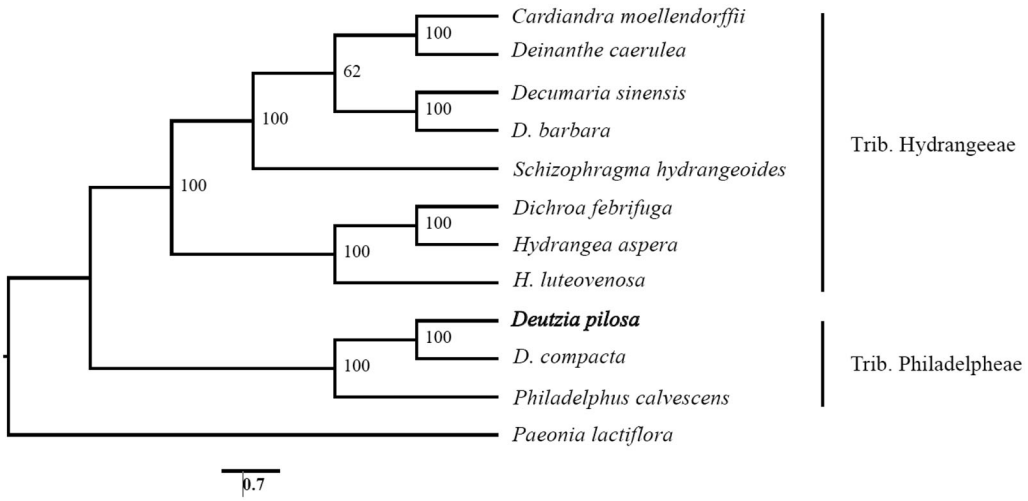

Figure 1. ML tree based on eleven complete chloroplast genomes of Hydrangeaceae and one outgroup species. Numbers at the nodes are bootstrap support values based on 1000 replicates. The species *D. pilosa* is highlighted in bold.

CONTACT Wei Gong wgong@scau.edu.cn College of Life Sciences, South China Agricultural University, Guangzhou, China

© 2020 The Author(s). Published by Informa UK Limited, trading as Taylor & Francis Group.
This is an Open Access article distributed under the terms of the Creative Commons Attribution License (http://creativecommons.org/licenses/by/4.0/), which permits unrestricted use, distribution, and reproduction in any medium, provided the original work is properly cited.

Paeoniaceae was used as an outgroup. Totally, twelve cp genomes were aligned with online software MAFFT on CIPRES (https://www.phylo.org., Miller et al. 2015). Maximum likelihood (ML) analyses were performed using RAxML-HPC v.8 on XSEDE (https://www.phylo.org) with 1000 bootstrap replicates and the substitution GTR + I + G model (Stamatakis et al. 2008), the latter of which was determined by the Akaike information criterion (AIC) in jModeltest v2.1.10 (Darriba et al. 2012).

The *D. pilosa* cp genome has been deposited in GenBank (Accession No.: MN954672). The total length is 156,983 bp with the typical quadripartite structure. It consists of a pair of inverted regions (IRs) of 25,830 bp separated by large single-copy region (LSC) of 86,598 bp and small single copy region (SSC) of 18,725 bp, respectively. The overall GC content of the cp genome is 43.0%. The whole cp genome of *D. pilosa* contains 134 genes with 89 protein-coding genes (PCGs), 37 tRNA genes, and eight rRNA genes. Among these genes, 63 PCGs and 22 tRNA genes are located in the LSC region, while 12 PCGs and one tRNA genes occur in the SSC region. All these eight rRNA genes are duplicated in the IR regions. IR regions contain seven PCGs and seven tRNA genes, if counting only once. Among the annotated genes, eleven genes (*atpF, ndhA, petB, petD, rpl16, rpoC1, rps16, trnaK-UUU, trnG-UCC, trnL-UAA,* and *trnV-UAC)* contain one intron, while seven genes (*clpP, ndhB, rpl2, rps12, trnA-UGC, trnL-GAU,* and *ycf13*) possess two introns. The species *D. pilosa* together with *D. compacta* form a monophyly that is closely related with *Philadelphus calvescens* in the Trib. Philadelpheae (Figure 1).

Disclosure statement

No potential conflict of interest was reported by the author(s).

Funding

This research was supported by the National Natural Science Foundation of China under [grant number 31470319].

References

Bankevich A, Nurk S, Antipov D, Gurevich AA, Dvorkin M, Kulikov AS, Lesin VM, Nikolenko SI, Pham S, Prjibelski AD, et al. 2012. SPAdes: a new genome assembly algorithm and its applications to single-cell sequencing. J Comput Biol. 19(5):455–477.

Darriba D, Taboada GL, Doallo R, Posada D. 2012. jModelTest 2: more models, new heuristics and parallel computing. Nat Methods. 9(8): 772–772

Doyle JJ, Doyle JL. 1987. A rapid DNA isolation procedure for small quantities of fresh leaf tissue. Phytochem Bullet. 19:11–15.

Laslett D, Canback B. 2004. ARAGORN, a program to the detection of transfer RNA and transfer-messenger RNA genes in nucleotide sequences. Nucleic Acids Res. 32(1):11–16.

Miller MA, Schwartz T, Pickett BE, He S, Klem EB, Scheuermann RH, Passarotti M, Kaufman S, O'Leary MA. 2015. A RESTful API for access to phylogenetic tools via the CIPRES Science Gateway. Evol Bioinform Online. 11:EBO.S21501–48.

Shumei H. 1993. The classification and distribution of genus *Deutzia* in China. J Chin Acad Sci. 31(2):105–126.

Stamatakis A, Hoover P, Rougemont J. 2008. A rapid bootstrap algorithm for the RAxML web servers. System Biol. 57(5):758–771.

International Journal of
Molecular Sciences

MDPI

Article

Complete Chloroplast Genome of *Cercis chuniana* (Fabaceae) with Structural and Genetic Comparison to Six Species in Caesalpinioideae

Wanzhen Liu [1], Hanghui Kong [2,3], Juan Zhou [1], Peter W. Fritsch [4], Gang Hao [1,*] and Wei Gong [1,*]

1 College of Life Sciences, South China Agricultural University, Guangzhou 510614, China; xixuegui17@163.com (W.L.); zj13808847221@126.com (J.Z.)
2 Key Laboratory of Plant Resources Conservation and Sustainable Utilization, South China Botanical Garden, Chinese Academy of Sciences, Guangzhou 510650, China; konghh@scbg.ac.cn
3 Guangdong Provincial Key Laboratory of Applied Botany, South China Botanical Garden, Chinese Academy of Sciences, Guangzhou 510650, China
4 Botanical Research Institute of Texas, 1700 University Drive, Fort Worth, TX 76107, USA; pfritsch@brit.org
* Correspondence: haogang@scau.edu.cn (G.H.); wgong@scau.edu.cn (W.G.); Tel.: +86-3829-7712 (G.H.)

Received: 3 April 2018; Accepted: 19 April 2018; Published: 25 April 2018

Abstract: The subfamily Caesalpinioideae of the Fabaceae has long been recognized as non-monophyletic due to its controversial phylogenetic relationships. *Cercis chuniana*, endemic to China, is a representative species of *Cercis* L. placed within Caesalpinioideae in the older sense. Here, we report the whole chloroplast (cp) genome of *C. chuniana* and compare it to six other species from the Caesalpinioideae. Comparative analyses of gene synteny and simple sequence repeats (SSRs), as well as estimation of nucleotide diversity, the relative ratios of synonymous and nonsynonymous substitutions (dn/ds), and Kimura 2-parameter (K2P) interspecific genetic distances, were all conducted. The whole cp genome of *C. chuniana* was found to be 158,433 bp long with a total of 114 genes, 81 of which code for proteins. Nucleotide substitutions and length variation are present, particularly at the boundaries among large single copy (LSC), inverted repeat (IR) and small single copy (SSC) regions. Nucleotide diversity among all species was estimated to be 0.03, the average dn/ds ratio 0.3177, and the average K2P value 0.0372. Ninety-one SSRs were identified in *C. chuniana*, with the highest proportion in the LSC region. Ninety-seven species from the old Caesalpinioideae were selected for phylogenetic reconstruction, the analysis of which strongly supports the monophyly of Cercidoideae based on the new classification of the Fabaceae. Our study provides genomic information for further phylogenetic reconstruction and biogeographic inference of *Cercis* and other legume species.

Keywords: *Cercis chuniana*; Cercidoideae; Caesalpinioideae; chloroplast genome; legume; next-generation sequencing

1. Introduction

The chloroplast (cp) is widely present in algae and plants with important functions in photosynthesis, carbon fixation, and stress response [1,2]. The cp genome in most angiosperms is a circular molecule with a typically quadripartite structure, comprising a large single copy (LSC) region and a small single copy (SSC) region separated by two copies of a large inverted repeat (IR) region [3–6]. Although the cp genome is highly conserved, some differences in gene synteny, simple sequence repeats (SSRs) and pseudogenes have been observed [7–9] and an accelerated rate of evolution has been observed in some cp regions at different taxonomic levels [10,11]. A complete cp genome

is a valuable resource of information for studying plant taxonomy, phylogenetic reconstruction, and historical biogeographic inference. Next-generation sequencing (NGS) technologies have enabled a rapid expansion in the database of whole cp genomes [12,13].

Fabaceae (legumes) are the third largest angiosperm family, with an estimated 727 genera and 20,000 species [14]. The family has been traditionally classified into three well-known and widely accepted subfamilies, i.e., Caesalpinioideae DC., Mimosoideae DC. and Papilionoideae DC. However, the subfamily Caesalpinioideae has been long considered to be non-monophyletic and not reflective of accurate phylogenetic relationships among the species [15–20]. As based on recent phylogenetic analyses, a new classification of six subfamilies has been recognized in Leguminosae: Cercidoideae, Detarioideae, Dialioideae, Duparquetioideae, Papilionoideae and a recircumscribed Caesalpinioideae [21].

The genus *Cercis* L. is removed from Caesalpinioideae and currently placed within Cercidoideae [21]. This genus comprises a clade of about nine species, with a disjunct distribution across the warm temperate zones of Eastern Asia, Europe and North America [22–26]. In China, five species are recognized, i.e., *C. chinensis*, *C. chingii*, *C. chuniana*, *C. glabra* and *C. racemosa* [26,27]. *Cercis chuniana*, a small tree or shrub, occurs mainly in subtropical evergreen broadleaf forest with a relatively narrow geographic distribution in southern China. Unique among *Cercis* species, it has an asymmetrical leaf blade [27,28].

Previous research has been focused on plant anatomy, phylogenetic reconstruction, and historical biogeography of *Cercis* [24–26,29,30]. However, *C. chuniana* has frequently failed to be analyzed in most phylogenetic research, resulting in an unclear phylogenetic position within the genus. Because *Cercis* has been removed to Cercidoideae, it would also be useful to detect additional genomic evidence that might support the new classification system of Fabaceae. Moreover, Sanger-based and whole-cp genome DNA barcoding can been used for phylogenetic reconstruction. Here we present and characterize the complete cp genome of *C. chuniana*. The structural variation, gene arrangement, and distribution of SSRs are compared with previously published cp genome of *C. canadensis* and five species from various genera in Caesalpinioideae. Our results provide cp information for *Cercis* and other legumes for use in comparative genomics, phylogenetic reconstruction, and biogeographic inference.

2. Results and Discussion

2.1. Genome Organization and Features of C. chuniana

A total number of 2 × 250 bp pair-end reads of 1,917,920 were produced with 1.17 Gb of clean data. All reads data were deposited in the NCBI Sequence Read Archive (SRA) under accession number SRP118607. In total, 102 contigs (N50 = 8438 bp) were generated for *C. chuniana*. The size of the complete cp genome is 158,433 bp (Figure 1; Table 1). The cp genome displays a typical quadripartite structure, including a pair of IR regions (25,505 bp) separated by the LSC (88,063 bp) and SSC (19,360 bp) regions (Figure 1 and Table 1). The G + C content of the cp genome is 36.10% for *C. chuniana*, demonstrating congruence with that of *C. canadensis* (36.20%) (Table 1). When duplicated genes in the IR regions were counted only once, the cp genome of *C. chuniana* were found to encode 114 predicted functional genes, including 81 protein-coding genes (PCGs), 29 tRNA genes, and four rRNA genes, all of which are comparable to the numbers in *C. canadensis* and other related species (Table 1). The remaining non-coding regions include introns, intergenic spacers, and pseudogenes. Nineteen genes are duplicated in the IR regions, including eight PCGs, seven tRNA genes, and four rRNA genes (Figure 1 and Table S1). Fifteen genes (nine PCGs and six tRNA genes) contain one intron, and two PCGs (*clpP* and *ycf3*) have two introns each (Table S1). The maturase K (*matK*) gene in the cp genome is located within the *trnK* intron, consistent with the location in *C. canadensis* and similar to most other plant species [31]. In the IR regions of *C. chuniana*, the four rRNA genes and two tRNA genes (*trnE* and *trnA*) are clustered as

16S-*trnE*-*trnA*-23S-4.5S-5S. This differs from the cp genomes of *C. canadensis* and most legumes, which show a cluster of 16S-*trnI*-*trnA*-23S-4.5S-5S [32–37].

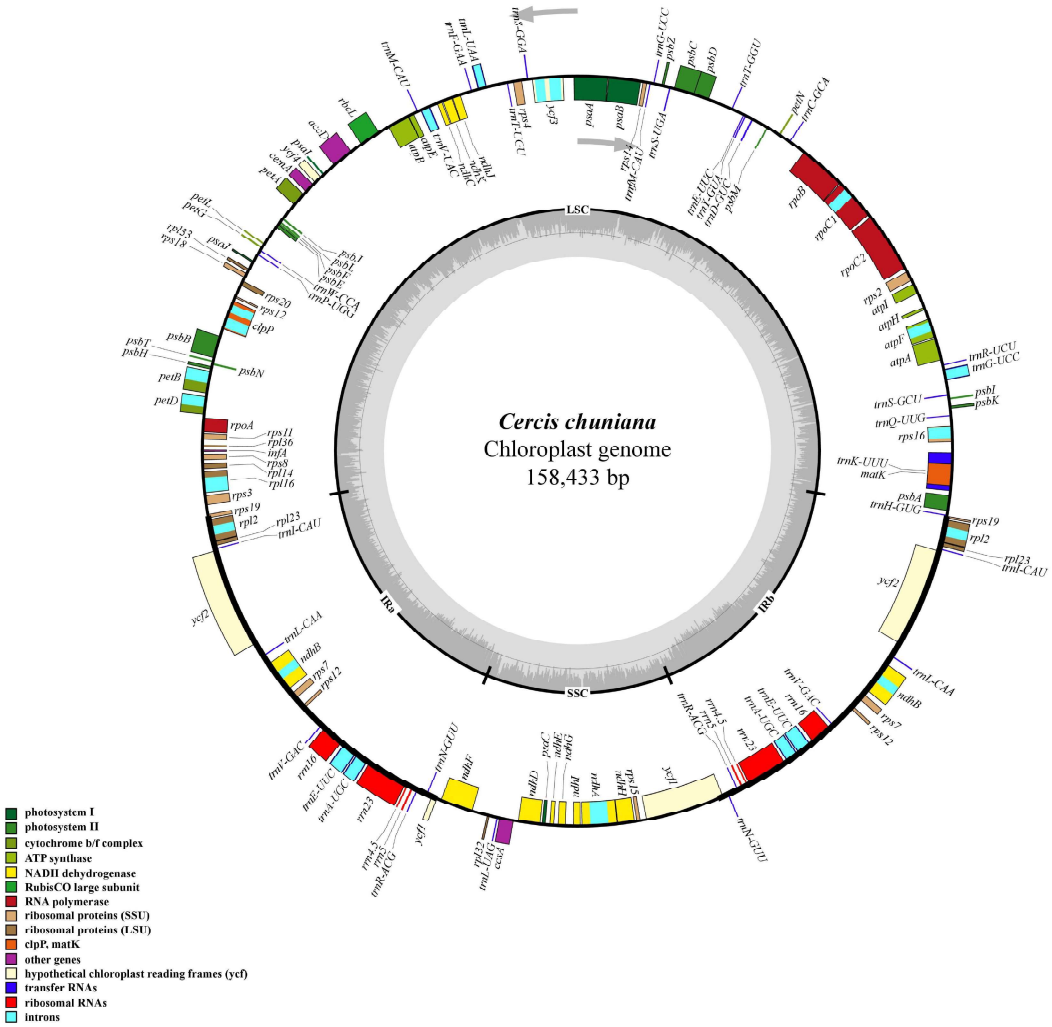

Figure 1. Gene map of the *Cercis chuniana* cp genome. The genes lying inside and outside the outer circle are transcribed in clockwise and counterclockwise direction, respectively (as indicated by arrows). Colors denote the genes belonging to different functional groups. The hatch marks on the inner circle indicate the extent of the inverted repeats (IRa and IRb) that separate the small single copy (SSC) region from the large single copy (LSC) region. The dark gray and light gray shading within the inner circle correspond to percentage G + C and A + T content, respectively.

Table 1. Summary of characteristics in cp genome sequences of *Cercis chuniana* and six other species of caesalpinioid legumes compared in this study.

Genome Features	*C. chuniana*	*C. canadensis*	*T. indica*	*Cera. siliqua*	*L. coriaria*	*M. cucullatum*	*H. brasiletto*
GenBank Accession No.	MF741770	KF856619	KJ468103	KJ468096	KJ468095	KU569489	KJ468097
Size (bp)	158,433	158,995	159,551	156,367	158,045	158,357	157,728
LSC length (bp)	88,063	88,118	87,967	85,801	87,581	87,663	87,465
SSC length (bp)	19,360	19,621	19,546	18,492	18,160	18,091	18,185
IR length (bp)	25,505	25,628	26,019	26,037	26,152	26,294	26,039
Number of genes	114	113	113	112	113	114	113
PCGs	81	79	79	78	80	80	79
tRNA genes	29	30	30	30	29	30	30
rRNA genes	4	4	4	4	4	4	4
G + C content (%)	36.10	36.20	36.20	36.70	36.50	36.40	36.70

2.2. Comparative Analysis of Genomic Structure

Synteny analysis identified a lack of genome rearrangement and inversions in the cp genome sequences among the seven species (Figure S1). Therefore, genomic structure, including gene number and gene order, is highly conserved among the seven species. However, some nucleotide substitutions and indels as well as length variation are still present, particularly in the LSC/IR/SSC boundaries (Figure 2 and Figure S2).

Pseudogenes are frequently identified in cp genomes [38,39]. Four pseudogenes were identified in the current study, i.e., Ψrps19, Ψ*ycf1*, Ψ*infA* and Ψ*accD* (Table 2). Ψrps19 and *ycf1* are partially repeated in the IR regions and were generally found to be pseudogenized. The *rps19* gene is 279 bp in all species (Figure 2) with length variation in the IR regions, from 73 bp in *Tamarindus indica* to 107 bp in *Libidibia coriaria*. It has the same length (152 bp) in both *C. chuniana* and *C. canadensis* in the IR regions (Figure 2). Because it is partially duplicated in the IR regions, the Ψ*rps19* gene has lost its protein-coding ability, thus producing the pseudogenized Ψrps 19 gene. Two nonsynonymous substitutions were detected in the Ψ*rps19* gene between *C. chuniana* and *C. canadensis*. Among the seven species, 28 substitutions (seven in the IRb region and 21 in the LSC region, respectively) and 4 indels with length variation from 4 to 47 bp were identified (Figure 2; Table 2). The same was found with the Ψycf1 gene, as the IRb/SSC junction region is located within the Ψ*ycf1* CDS region and only a partial gene is duplicated in the IRa region, thus producing the pseudogene Ψ*ycf1*. This is generally the case in the dicots. The length of the Ψ*ycf1* pseudogene in the IR regions ranges from 385 bp in *C. chuniana* to 899 bp in *Mezoneruon cucullatum*. Four nonsynonymous substitutions were detected between *C. chuniana* and *C. canadensis*. Altogether 20 substitutions (19 in the IRa region and one in the SSC region) and 7 indels with length variation ranging from 1 to 33 bp are present among the seven species (Figure 2; Table 2). The Ψ*infA* gene is pseudogenized in all species except *Ceratonia siliqua*, with a length of 135 bp in both *C. chuniana* and *C. canadensis* and with length ranging from 192 to 252 bp among the other four species. A total of 23 substitutions and 6 indels ranging from 1 to 13 bp in length occurs in Ψ*infA* (Figure 2; Table 2). The pseudogenized Ψ*infA* gene has also been frequently found in other angiosperm chloroplast genomes as well [40–42]. The pseudogenized Ψ*accD* gene is present in all species except *T. indica* and *M. cucullatum*, with a length of 1473 bp in both *C. chuniana* and *C. canadensis* and with length ranging from 1395 to 1500 bp in the other three species. Six indels ranging from 3 to 36 bp in length, and 101 substitutions were detected in Ψ*accD* (Table 2).

Table 2. The location and characteristics of the four pseudogenes in the seven species of caesalpinioid legumes compared in this study.

Species	IRa	IRb	LSC	LSC
	Ψycf1	**Ψrps19**	**ΨinfA**	**ΨaccD**
C. chuniana	385 bp *	152 bp *	1 indel, 91-bp SV *	5 indels *
C. canadensis	418 bp *	152 bp *	1 indel, 91-bp SV *	5 indels *
T. indica	644 bp *	73 bp *	71-bp SV *	-
Cera. siliqua	776 bp *	85 bp *	-	4 indels, 63-bp SV *
L. coriaria	819 bp *	107 bp *	-	4 indels *
M. cucullatum	899 bp *	103 bp *	4 indels *	3 indels *
H. brasiletto	697 bp *	96 bp *	4 indels *	4 indels *

* Pseudogene present; SV: structural variation with indels ≥ 50 bp.

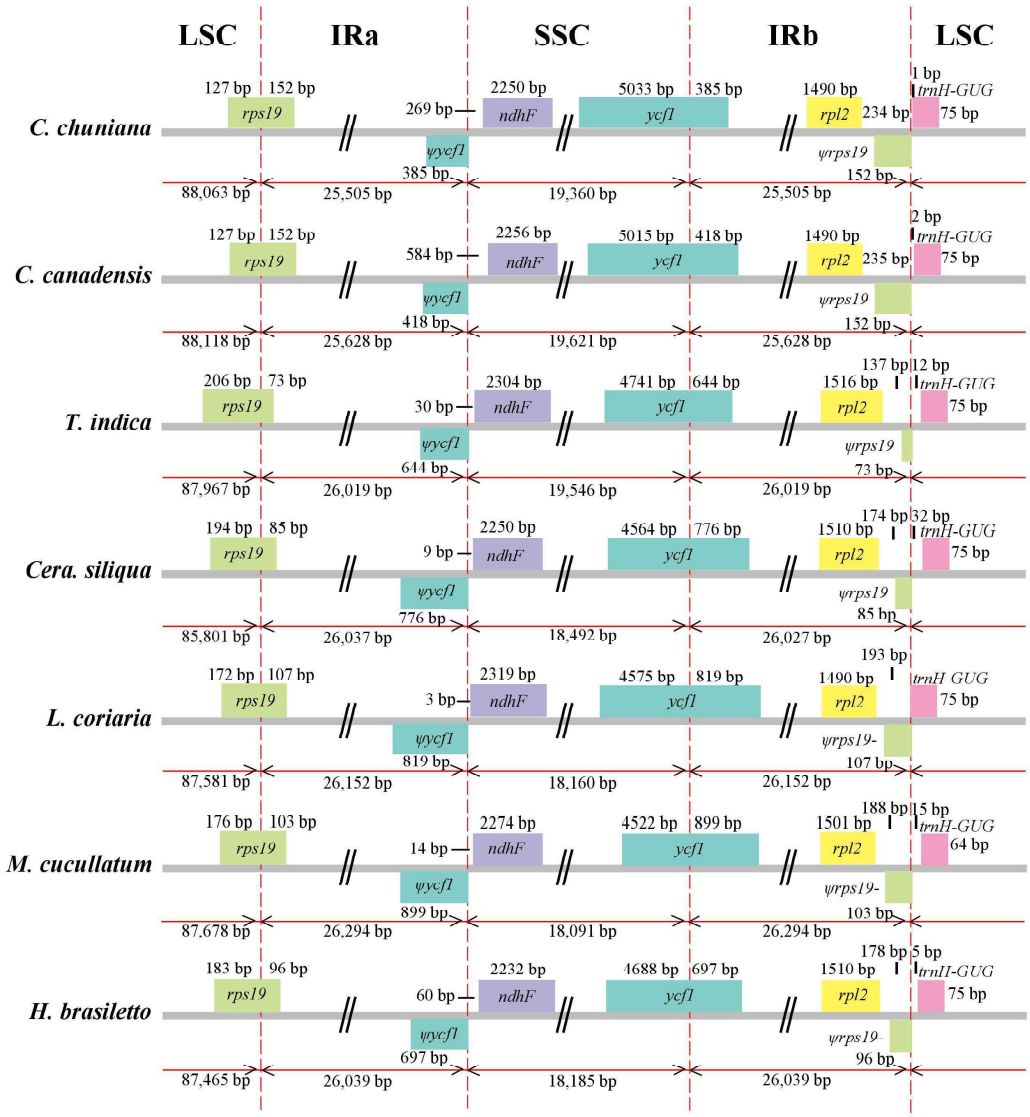

Figure 2. Comparison of the border positions of LSC, SSC and IR regions among the seven species of caesalpinioid legumes compared in this study. Genes are denoted by colored boxes. The gaps between the genes and the boundaries are indicated by the base lengths (bp). Extensions of the genes are indicated above the boxes.

2.3. Characterization of Simple Sequence Repeats

Variable copy numbers and resulting length variation have impelled the wide use of cp SSRs in plant population genetics and biogeographic studies, especially at lower taxonomic levels [43,44]. A total of 91 SSRs of ≥10 bp in length were found in both *C. chuniana* and *C. canadensis*. These two species exhibit the highest number of SSRs among the seven species (Table 3). The lowest number of SSRs was detected in *Haematoxylum brasiletto*, with only 38 SSRs in total (Table 3). Most SSRs are present in the LSC regions, accounting for an average of 75.00% of the total SSRs in each species. Among all of the SSRs, the mononucleotide A or T repeat units were found in highest proportion, with an average of 78.10% of the total SSRs in each species. The SSRs have a remarkably high A + T content, with only 15 compound SSRs containing the nucleotides C or G in *C. chuniana* (Table S2). The lengths of SSRs in the seven species range from 10 to 20 bp, whereas the compound SSRs range from 21 to 275 bp. The copy lengths of 10 to 13 bp are most common, with an average of 77.00% among all species (Figure 3). No pentanucleotide or hexanucleotide SSRs were detected among the seven species.

The shared interspecific SSRs were identified among species, with identical repeats and locations in homologous regions (Table 4). *Cercis chuniana* and *C. canadensis* demonstrated the highest number of 19 common SSRs. Conversely, *Tamarindus indica* has the lowest number of shared SSRs (≤3). Altogether 13 SSRs were isolated and corresponding primer pairs were designed for each di-, tri- and tetranucleotide SSRs of *C. chuniana* (Table S3). These SSRs are expected to be useful in the assessment of genetic diversity and population structure as well as the investigations of biogeographic patterns among the species of *Cercis*.

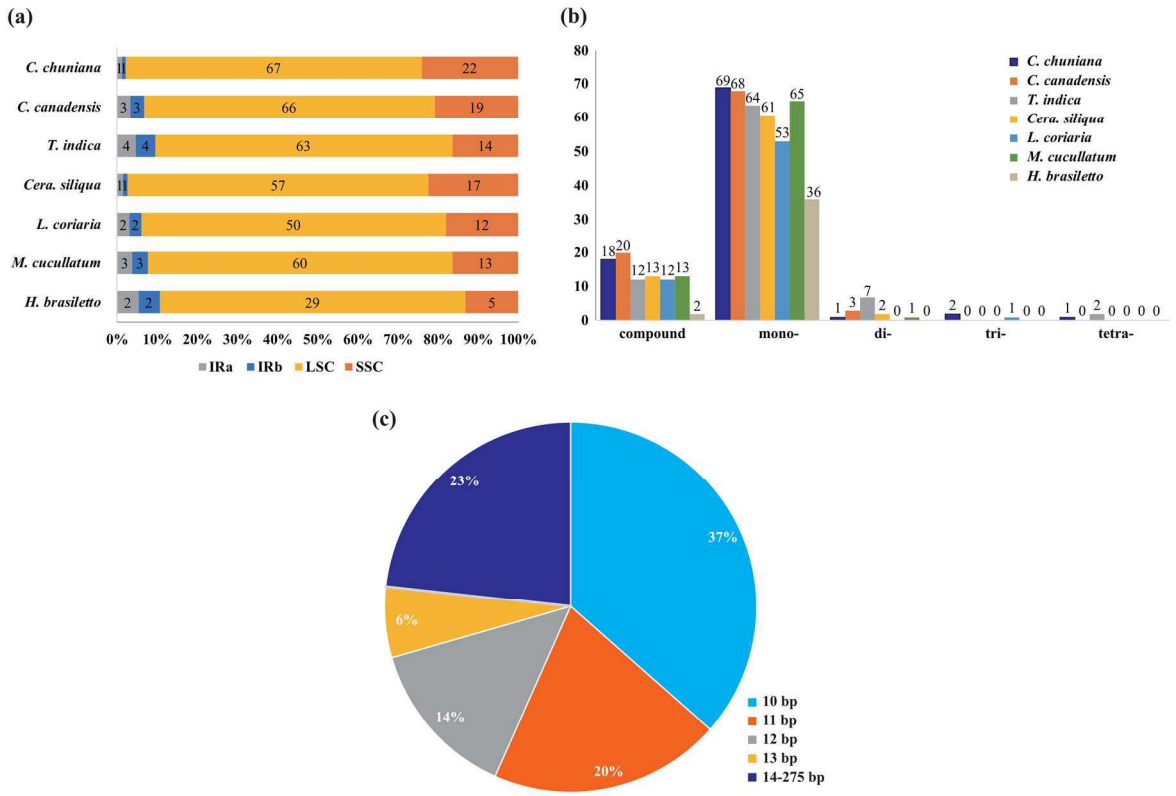

Figure 3. Analysis of repeated sequences of the seven species compared in this study. (**a**) The number of SSRs distributed in different regions; (**b**) The number of SSRs with different types, including compound, mono-, di-, tri-, and tetranucleotides; (**c**) The proportion of SSRs with different lengths.

2.4. Sequence Divergence and Nucleotide Diversity

A complete cp genome is valuable for plant taxonomic analyses, phylogenetic reconstruction, speciation processes, and biogeographical inferences at different taxonomic levels [45–49]. Highly variable regions among cp genomes can provide useful data for phylogenetic reconstruction. In the current study, the average nucleotide variability (*Pi*) was estimated to be 0.006 between *C. chuniana* and *C. canadensis* as based on the comparative analysis with DnaSP (Figure 4a). The highest variation was found in the LSC and SSC regions. The IR regions had a much lower nucleotide diversity with $Pi < 0.006$. Eight regions (*trnS-trnT*, *atpF-atpH*, *trnT-psbD*, *trnL-trnF-ndhJ*, *accD-psaI*, *rps3-rps19*, *ycf1-ndhF* and the *ndhA* intron) were highly variable, with *Pi* values >0.030. The first five loci are present in the LSC, whereas the remaining two are present in the SSC region. In contrast, much higher nucleotide diversity with $Pi = 0.038$ was detected among the seven species (Figure 4b). Five regions (*psbZ-trnG*, *trnT-trnL*, *rps3-rps19*, *rpl32*, and *ycf1*) exhibit the highest nucleotide diversity, all with *Pi* >0.12. These loci are thus suggested as useful regions for phylogenetic analysis at higher taxonomic levels in the Fabaceae.

Table 3. Number of chloroplast SSRs in different regions or different types present in the seven species from caesalpinioid legumes.

Species	N	LSC	SSC	IRa	IRb	Compound	Mono- (≥10)	Di- (≥6)	Tri- (≥5)	Tetra- (≥5)
C. chuniana	91	67 (73.63)	22 (24.18)	1 (1.10)	1 (1.10)	18 (19.78)	69 (75.82)	1 (1.10)	2 (2.20)	1 (1.10)
C. canadensis	91	66 (72.53)	19 (20.88)	3 (3.30)	3 (3.30)	20 (21.98)	68 (74.73)	3 (3.30)	0 (0.00)	0 (0.00)
T. indica	85	63 (74.12)	14 (16.47)	4 (4.71)	4 (4.71)	12 (14.12)	64 (75.29)	7 (8.24)	0 (0.00)	2 (2.35)
Cera. siliqua	76	57 (75.00)	17 (22.37)	1 (1.32)	1 (1.32)	13 (17.11)	61 (80.26)	2 (2.63)	0 (0.00)	0 (0.00)
L. coriaria	66	50 (75.76)	12 (18.18)	2 (3.03)	2 (3.03)	12 (18.18)	53 (80.30)	0 (0.00)	1 (1.52)	0 (0.00)
M. cucullatum	79	60 (75.95)	13 (16.46)	3 (3.80)	3 (3.80)	13 (16.46)	65 (82.28)	1 (1.27)	0 (0.00)	0 (0.00)
H. brasiletto	38	29 (76.32)	5 (13.16)	2 (5.26)	2 (5.26)	2 (5.26)	36 (94.74)	0 (0.00)	0 (0.00)	0 (0.00)
Average	75	56 (74.76)	15 (18.81)	2 (3.22)	2 (3.22)	13 (17.14)	59 (79.24)	2 (2.67)	0.43 (0.57)	0.43 (0.57)

Note: The numbers in parentheses are the percentage of each region or SSR types.

Table 4. Shared SSRs among the seven species in caesalpinioid legumes.

Species	*C. chuniana*	*C. canadensis*	*T. indica*	*Cera. siliqua*	*L. coriaria*	*M. cucullatum*	*H. brasiletto*
C. chuniana	-						
C. canadensis	19	-					
T. indica	1	0	-				
Cera. siliqua	6	4	1	-			
L. coriaria	4	6	3	7	-		
M. cucullatum	6	5	1	1	8	-	
H. brasiletto	4	3	2	6	6	4	-

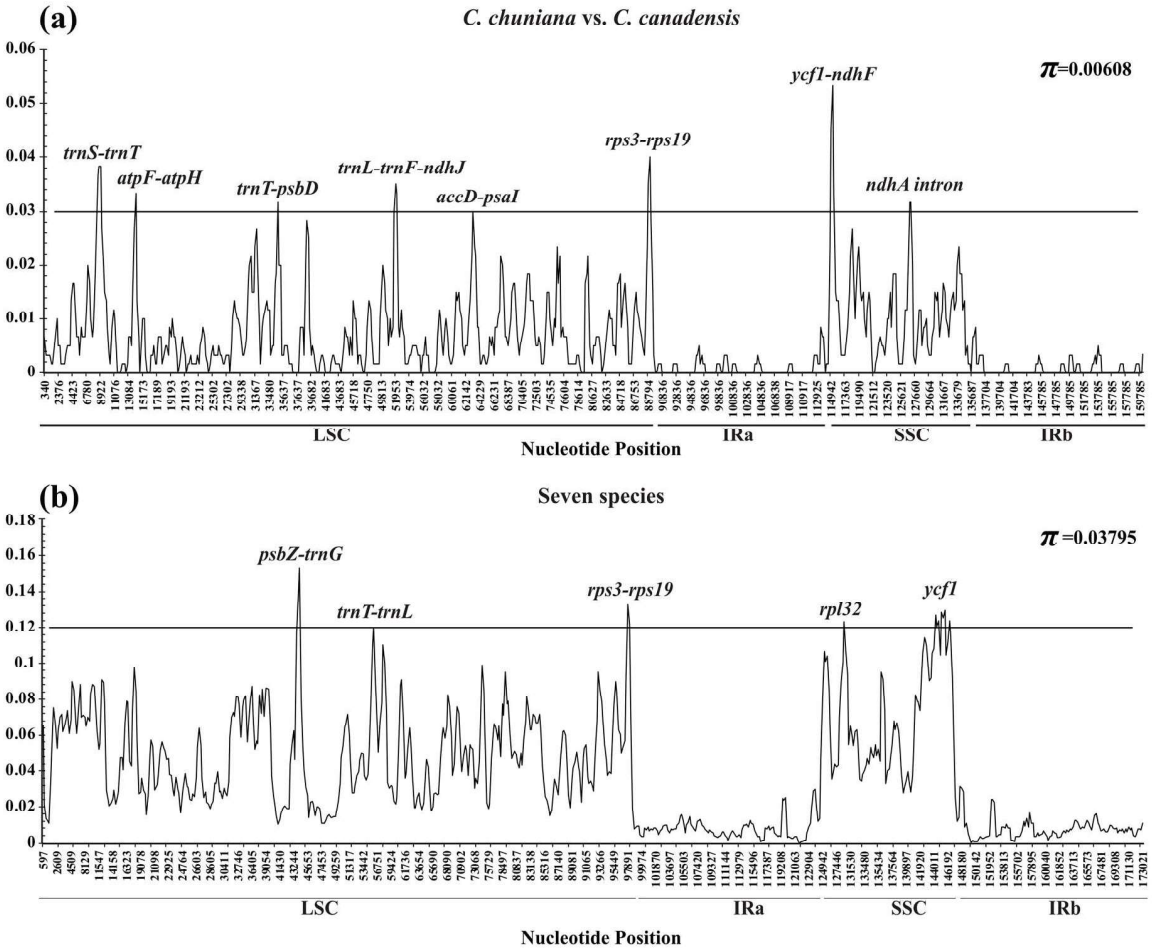

Figure 4. Sliding window analysis of the whole cp genome. (**a**) *C. chuniana* and *C. canadensis*; (**b**) All seven species. *X*-axis: position of the midpoint of a window; *Y*-axis: nucleotide diversity (π) of each window.

2.5. dn/ds Ratio and Kimura 2-Parameter (K2P) Genetic Distance

A total of 76 PCGs in all seven species was used to estimate dn/ds ratios. The dn and ds values range from 0 to 0.1713 and 0.0046 to 0.5330, respectively. If dn or ds is 0, the dn/ds ratio cannot be calculated. Among all genes, 67 proteins possess dn/ds ratios <0.5, indicating purifying selection (Figure 5a). In *ndhD*, Ψycf1, ΨinfA and *rpl23* the dn/ds ratios were >1, indicating positive selection (Figure 5a). Among the different regions, the dn/ds ratio was the highest in the IR regions (0.9022) and the lowest in the LSC region (0.2205). Based on the K2P model, we calculated the interspecific genetic distance among the seven species using 80 PCGs. The average K2P interspecific genetic distance was found to be 0.0373 (Figure 5b). The minimum K2P values were identified in *ndhB* and *rps7* (0.0030) and the maximum in *psaB* (0.2020).

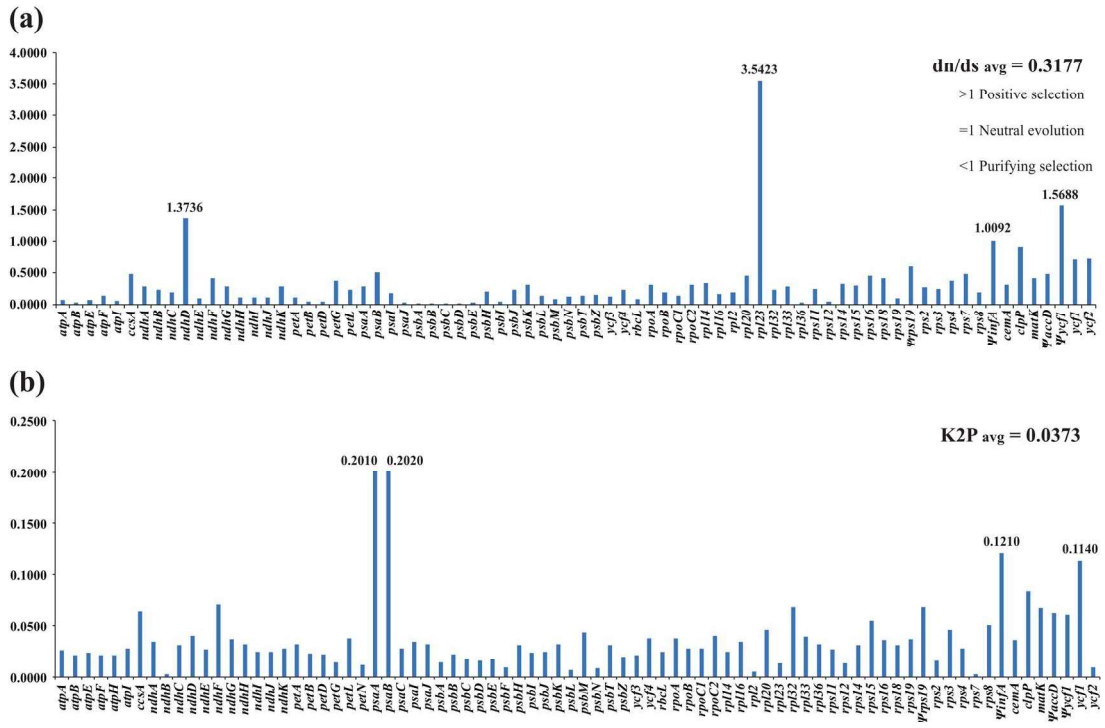

Figure 5. Evolutionary dynamics of genes in the cp genomes. (**a**) The dn/ds ratios for individual genes; (**b**) The K2P values for individual genes.

2.6. Phylogenetic Analyses

A total of 97 representative species from the old Caesalpinioideae and Mimosoideae were selected to reconstruct phylogenetic relationships (Table S4). *Cucumis sativus* (DQ119058) was used as the outgroup. Two phylogenetic methods of Bayesian inference (BI) and maximum likelihood (ML) resulted in highly similar phylogenetic trees based on the complete cp genome sequences and 61 protein-coding genes (PCGs) (Figure 6). The total aligned length was 302,882 bp for the complete cp genome sequences and 69,253 bp for the PCGs, and the number of parsimony-informative sites was 163,470 bp and 25,698 bp, respectively. The trees based on ML exhibit completely congruent topologies with higher bootstrap support values in the tree based on complete cp genome sequences than those based on the PCGs (Figure 6a). The relationship between subfamilies Cercidoideae and Detarioideae was not stable in the BI analysis, but otherwise high posterior probability values were detected in both the ML and BI analyses based on the two data sets (Figure 6b). All analyses recover the monophyly of both the Cercidoideae and Detarioideae with strong support. Our results are consistent with [50] and strongly support the new classification system of the Fabaceae [21].

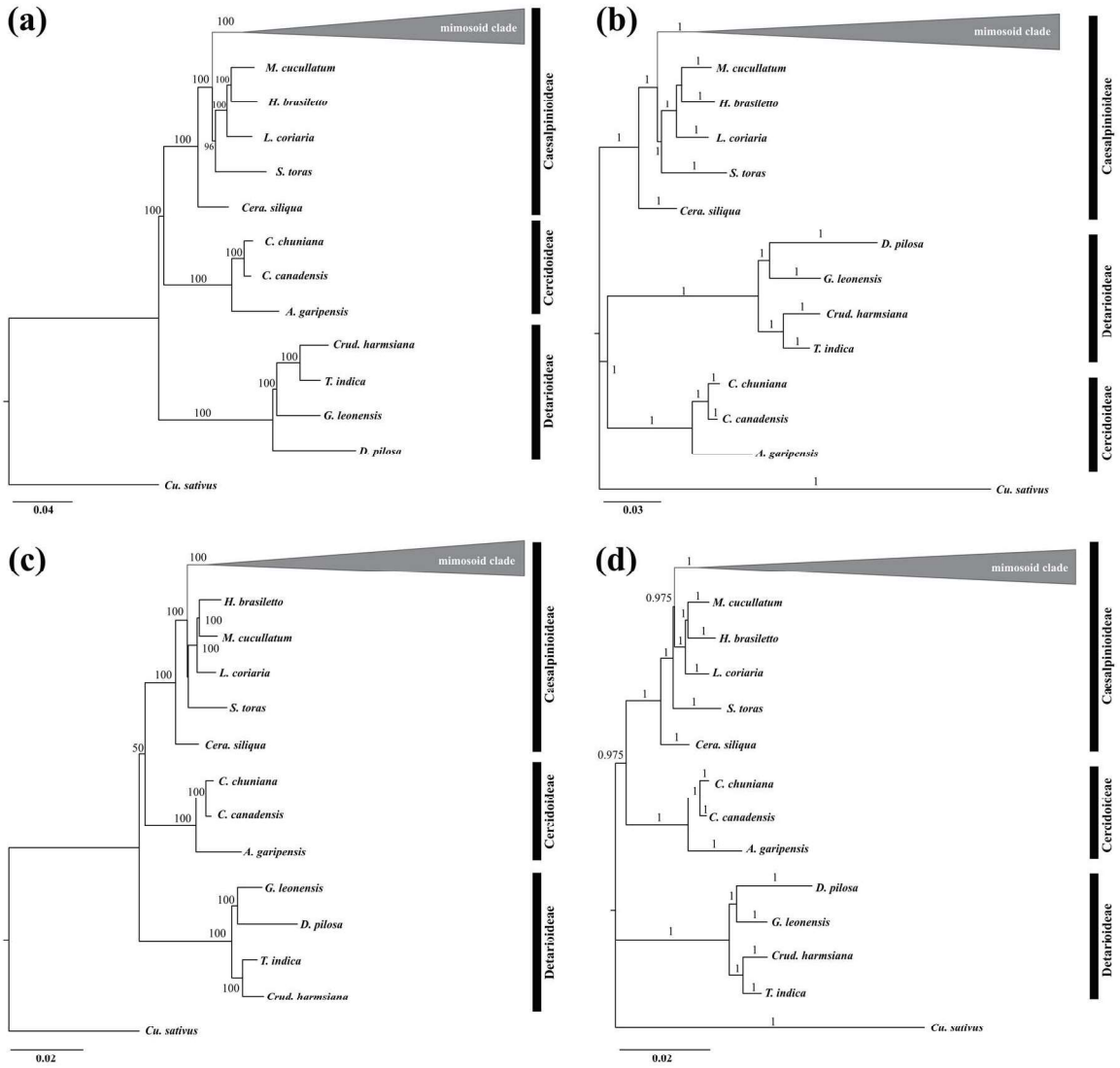

Figure 6. Phylogenetic trees of sampled species inferred from the concatenated whole cp genome sequences and 61 protein-coding genes (PCGs) in the cp genome based on maximum likelihood (ML) and Bayesian inference (BI). (**a**) ML analysis based on whole cp genome sequences; (**b**) BI analysis based on whole cp genome sequences; (**c**) ML analysis based on PCGs; (**d**) BI analysis based on PCGs. Numbers in bold above branches are bootstrap values ≥50% and Bayesian posterior probability values ≥90%.

3. Materials and Methods

3.1. Ethics Statement

Sample collection and transplanting were carried out for scientific purposes. *Cercis chuniana* was collected from the field in Dadongshan Natural Reserve in Guangdong Province, China. One individual seedling was permitted by the management of the reserve to be transplanted and grown in the greenhouse at the College of Life Sciences, South China Agricultural University (SCAU, Guangzhou, China).

3.2. Plant Samples

Fresh leaves were collected from *C. chuniana* growing at SCAU. The voucher (LWZ109) is deposited in the herbarium of SCAU (CANT). The cp genome of *C. canadensis* (KF856619) was downloaded from NCBI and used as the reference sequence in the assembly of *C. chuniana*. Five additional species from the old

Caesalpinioideae were used for comparison, i.e., *Tamarindus indica* (KJ468103), *Ceratonia siliqua* (KJ468096), *Libidibia coriaria* (KJ468095), *Mezoneuron cucullatum* (KU569489) and *Haematoxylum brasiletto* (KJ468097).

3.3. DNA Extraction and PCR Amplification

Total genomic DNA was extracted with the modified Cetyl Trimethyl Ammonium Bromide (CTAB) method [51]. The DNA concentration was quantified with a Nanodrop spectrophotometer (Thermo Scientific, Carlsbad, CA, USA), and a final DNA concentration of >30 ng/μL was used. Sequences of complete cp genome of *C. chuniana* were amplified with fifteen universal primer pairs developed by Zhang et al. [52]. The PCR amplification was performed in a total volume of 25 μL, containing 1 ng of template DNA, 0.12 U of Primerstar GXL DNA Polymerase, 0.2 μM of each primer, 200 μM of each dNTP, 5 μL of 5× PCR Buffer and 13.5 μL of sterilized double-distilled water. Thermocycling conditions were 95 °C (1 min), followed by 32 cycles of denaturation at 94 °C (15 s), annealing at 58 °C (30 s), and extension at 68 °C (10 min), and a final extension of 68 °C (10 min).

3.4. Chloroplast Genome Sequencing, Assembly and Annotation

A paired-end library was constructed with the Nextera XT DNA Library Prep Kit (Illumina Inc., San Diego, CA, USA). The genomic DNA mixture was fragmented into ~300 bp size by the Nextera XT transposome. Library Sequencing acquired 2 × 250 bp paired reads with Illumina MiSeq Desktop Sequencer at South China Botanical Garden, Chinese Academy of Sciences. Reads of the *C. chuniana* cp genome were initially filtered for quality, and then adapters were removed, errors were checked, and contigs and scaffolds generated, all with the A5-miseq pipeline [53]. Scaffolds from the assembly with *k*-mer values of 35 to 145 were matched to reference cp genome sequences, and were used to determine the relative position and direction respectively. We assembled the cp genome using Geneious 9.1.4 (Biomatters Ltd., Auckland, New Zealand) [54] with BLAST 2.0.3+ (National Institutes of Health, Bethesda, MD, USA) [55] and map reference tools. DOGMA (available online: http://dogma.ccbb.utexas.edu/) [56] and Geneious (Biomatters Ltd., Auckland, New Zealand) were used for annotating the cp genome in comparison with that of *C. canadensis* (KF856619) [57]. The annotation of tRNA genes were confirmed with the ARAGORN program (Lund University, Lund, Sweden) [58] and then manually adjusted with Geneious. Contigs with BLAST hits to the consensus sequence from the "map to reference function" were assembled manually to construct the complete cp genome. Finally, the circular genome map of *C. chuniana* was illustrated with the Organellar Genome DRAW tool (OGDRAW, available online: http://ogdraw.mpimp-golm.mpg.de/) [59]. To further refine the draft genome, the quality and coverage of was confirmed by remapping reads. The Sequence Read Archive (SRA) can be found in GenBank under an accession number of SRP118607. The annotated cp genomic sequence of *C. chuniana* was deposited in GenBank (Accession Number: MF741770).

3.5. Genome Comparison

The cp genome sequences from the finalized data set were aligned with MAFFT v7.0.0 (Osaka University, Suita, Japan) [60] and adjusted manually when necessary. The expansion/contraction of the IR regions can lead to changes in the structure of the cp genome, resulting in the length variation of angiosperm cp genomes and contributing to the formation of pseudogenes [9,61,62]. Therefore, we conducted a comparative analysis to detect the variation in the LSC/IR/SSC boundaries among the seven species included in comparisons. Gene synteny analysis was performed with MAUVE (University of Wisconsin, Madison, WI, USA) [63] as implemented in Geneious with default settings. To elucidate the level of sequence divergence, the complete cp genomes were compared and plotted with the mVISTA program in Shuffle-LAGAN mode [64–66].

3.6. Simple Sequence Repeats Analysis

MISA (available online: http://pgrc.ipk-gatersleben.de/misa/misa.html) [67] is a tool for the identification and location of perfect simple sequence repeat loci (SSRs) and compound SSRs (the latter being two individual SSRs that are disrupted by a certain number of bases). We used MISA to search for potential SSRs in the cp genomes of the seven species. The minimum number (thresholds) of SSRs was set as 10, 6, 5, 5, and 5 for mono-, di-, tri-, tetra-, and pentanucleotide SSRs, respectively. All SSRs, motif types and length variants were manually verified and the redundant ones removed. We investigated the shared repeats among the cp genomes of the seven species, based on the criterion that identical lengths located in homologous regions are considered to be shared repeats. Using the program Primer 3-1.1.1 (Premier Biosoft International, Palo Alto, CA, USA) [68], we developed SSR primers specific for *C. chuniana* for potential application in further analysis.

3.7. Sequence Divergence, dn/ds Ratio and K2P Genetic Distance

Comparative analyses of the nucleotide diversity (*Pi*) among the complete cp genomes of the seven species were performed with DnaSP 6 (Universitat de Barcelona, Barcelona, Spain) [69,70], as based on a sliding window analysis. The window length was 600 bp and step size was 200 bp. The 80 PCGs were extracted and aligned with MAFFT. We estimated the dn/ds ratio for each PCG as well as the interspecific genetic distance with DnaSP 6 and MEGA 6.0 (Tokyo Metropolitan University, Hachioji, Tokyo, Japan) [71], as based on the Kimura 2-parameter (K2P) model.

3.8. Phylogenetic Analysis

Altogether 97 representative species from the old Caesalpinioideae and Mimosoideae were selected for phylogenetic analyses (Table S4). *Cucumis sativus* (DQ119058) was used as the outgroup. Two data sets of the complete cp genome sequences and PCGs were used for phylogenetic reconstruction based on two methods of Bayesian inference (BI) and maximum likelihood (ML), respectively. All analyses were performed on the high-performance computer cluster available in the CIPRES Science Gateway 3.3 (available online: www.phylo.org) [72]. Gaps were treated as missing data. BI was performed by using MrBayes v. 3.2.6 (Swedish Museum of Natural History, Stockholm, Sweden) [73] with base frequencies estimated from the data. We ran four Markov Chains Monte Carlo (MCMC) for 50 million generations using default settings for priors and saved one tree every 1000 generations. The first 10% of the trees were discarded, as determined with the aid of the program Tracer version 1.6 (University of Auckland, Auckland, New Zealand) [74]. The posterior probability (PP) of each clade (i.e., the "clade credibility value") was estimated with 50% majority-rule consensus trees. We conducted ML using RAxML 8.2.10 (Heidelberg Institute for Theoretical Studies, Heidelberg, Germany) [75] and the RAxML graphical interface (rxmlGUI v. 1.3) (Research Institute Senckenberg, Frankfurt, Germany) [76]. RaxML was conducted by using Python v.2.7.6 (available online: http://www.python.org/ftp/python/2.7.6/python-2.7.6.msi) with 1000 rapid bootstrap replicates. The general time-reversible (GTR) model was chosen with a gamma model for the rate of heterogeneity.

4. Conclusions

We report the complete cp genome of *C. chuniana* endemic to China, which belongs to *Cercis* L., an intercontinentally disjunct genus. Using a high-throughput sequencing method, we sequenced and annotated the whole genome, detected the arrangement of the genes, and identified SSRs in *C. chuniana*. We compared the cp genomic characteristics of *C. chuniana* to its congener *C. canadensis* and five other species from the old Caesalpinioideae. The current study is the first structural and gene comparison among the cp genomes of seven species from three subfamilies of legumes, including Cercidoideae, Detarioideae and Caesalpinioideae at the genomic level. Nearly 100 representative species from the old Caesalpinioideae and Mimosoideae were used for phylogenetic reconstruction, strongly corroborating

the monophyly of Cercidoideae and Detarioideae in the sense of the new classification of Fabaceae. Our study contributes to the taxonomy, phylogenetic reconstruction and biogeographical research of *Cercis* and other legume species.

Supplementary Materials: Supplementary materials can be found at http://www.mdpi.com/1422-0067/19/5/1286/s1.

Author Contributions: Wanzhen Liu performed most of the experiments and data analyses; Hanghui Kong participated in data analyses and writing the manuscript; Juan Zhou participated in sample collection; Peter W. Fritsch participated in writing the manuscript; Gang Hao supervised the project and provided suggestions for the manuscript; Wei Gong conceived and designed the experiment and research, supervised the project and contributed to the writing of the manuscript.

Acknowledgments: The authors thank Tongjian Liu and Gang Yao lab assistance and data analyses; El Mahdi Bendif for linguistic assistance; and the National Natural Science Foundation of China (31470312; 31470319) and Science and Technology Planning Project of Guangdong Province, China (2016A030303048) for financial support.

Conflicts of Interest: The authors declare no conflict of interest.

Abbreviations

LSC	Large single copy
SSC	Small single copy
IR	Inverted repeat
Cp	Chloroplast
ML	Maximum likelihood
BI	Bayesian inference
A	Adenine
T	Thymine
G	Guanine
C	Cytosine

References

1. Neuhaus, H.E.; Emes, M.J. Nonphotosynthetic metabolism in plastids. *Annu. Rev. Plant Biol.* **2000**, *51*, 111–140. [CrossRef] [PubMed]
2. Inoue, K. Emerging roles of the chloroplast outer envelope membrane. *Trends Plant Sci.* **2011**, *16*, 550–557. [CrossRef] [PubMed]
3. Raubeson, L.A.; Jansen, R.K. Chloroplast genomes of plants. In *Plant Diversity and Evolution: Genotypic and Phenotypic Variation in Higher Plants*; Henry, R.J., Ed.; CABI Publishing: Cambridge, MA, USA, 2005; pp. 45–68.
4. Yang, M.; Zhang, X.; Liu, G.; Yin, Y.; Chen, K.; Yun, Q.; Zhao, D.; Al-Mssallem, I.S.; Yu, J. The complete chloroplast genome sequence of date palm (*Phoenix dactylifera* L.). *PLoS ONE* **2010**, *5*, e12762. [CrossRef] [PubMed]
5. Green, B.R. Chloroplast genomes of photosynthetic eukaryotes. *Plant J.* **2011**, *66*, 34–44. [CrossRef] [PubMed]
6. Wicke, S.; Schneeweiss, G.M.; Müller, K.F.; Quandt, D. The evolution of the plastid chromosome in land plants: Gene content, gene order, gene function. *Plant Mol. Biol.* **2011**, *76*, 273–297. [CrossRef] [PubMed]
7. Roy, S.; Ueda, M.; Kadowaki, K.; Tsutsumi, N. Different status of the gene for ribosomal protein S16 in the chloroplast genome during evolution of the genus *Arabidopsis* and closely related species. *Genes Genet. Syst.* **2010**, *85*, 319–326. [CrossRef] [PubMed]
8. Lei, W.; Ni, D.; Wang, Y.; Shao, J.; Wang, X.; Yang, D.; Wang, J.; Chen, H.; Liu, C. Intraspecific and heteroplasmic variations, gene losses and inversions in the chloroplast genome of *Astragalus membranaceus*. *Sci. Rep.* **2016**, *6*, 21669. [CrossRef] [PubMed]
9. Ivanova, Z.; Sablok, G.; Daskalova, E.; Zahmanova, G.; Apostolova, E.; Yahubyan, G.; Baev, V. Chloroplast genome analysis of resurrection Tertiary relict *Haberlea rhodopensis* highlights genes important for desiccation stress response. *Front. Plant Sci.* **2017**, *8*, 204. [CrossRef] [PubMed]
10. Gaut, B.; Yang, L.; Takuno, S.; Eguiarte, L.E. The patterns and causes of variation in plant nucleotide substitution rates. *Annu. Rev. Ecol. Evol. Syst.* **2011**, *42*, 245–266. [CrossRef]

11. Dong, W.; Xu, C.; Cheng, T.; Zhou, S. Complete chloroplast genome of *Sedum sarmentosum* and chloroplast genome evolution in Saxifragales. *PLoS ONE* **2013**, *8*, e77965. [CrossRef] [PubMed]
12. Duan, Y.; Shen, Y.; Kang, F.; Wang, J. Characterization of the complete chloroplast genomes of the endangered shrub species *Prunus mongolica* and *Prunus pedunculata* (Rosales: Rosaceae). *Conserv. Genet. Resour.* **2018**, 1–4. [CrossRef]
13. Wang, H.; Park, S.; Lee, A.; Jang, S.; Im, D.; Jun, T.; Lee, J.; Chung, J.; Ham, T.; Kwon, S. Next-generation sequencing yields the complete chloroplast genome of *C. goeringii* acc. smg222 and phylogenetic analysis. *Mitochondrial DNA Part B* **2018**, *3*, 215–216. [CrossRef]
14. Lewis, G.P.; Schrire, B.D.; Mackinder, B.A.; Lock, J.M. (Eds.) *Legumes of the World*; Royal Botanic Gardens, Kew: Richmond, UK, 2005.
15. Käss, E.; Wink, M. Molecular evolution of the Leguminosae: Phylogeny of the three subfamilies based on *rbcL*-sequences. *Biochem. Syst. Ecol.* **1996**, *24*, 365–378. [CrossRef]
16. Doyle, J.; Ballenger, J.; Dickson, E.; Kajita, T.; Ohashi, H. A phylogeny of the chloroplast gene *rbcL* in the Leguminosae: Taxonomic correlations and insights into the evolution of nodulation. *Am. J. Bot.* **1997**, *84*, 541–554. [CrossRef] [PubMed]
17. Doyle, J.J.; Chappill, J.A.; Bailey, C.D.; Kajita, T. Towards a comprehensive phylogeny of legumes: Evidence from *rbcL* sequences and non-molecular data. In *Advances in Legume Systematics*; Herendeen, P.S., Bruneau, A., Eds.; Royal Botanic Gardens, Kew: Richmond, UK, 2000; pp. 1–20.
18. Wojciechowski, M.F.; Lavin, M.; Sanderson, M.J. A phylogeny of legumes (Leguminosae) based on analysis of the plastid *matK* gene resolves many well-supported subclades within the family. *Am. J. Bot.* **2004**, *91*, 1846–1862. [CrossRef] [PubMed]
19. Lavin, M.; Herendeen, P.S.; Wojciechowski, M.F. Evolutionary rates analysis of Leguminosae implicates a rapid diversification of lineages during the Tertiary. *Syst. Biol.* **2005**, *54*, 575–594. [CrossRef] [PubMed]
20. The Legume phylogeny Working Group. Legume phylogeny and classification in the 21st century: Progress, prospects and lessons for other species-rich clades. *Taxon* **2013**, *62*, 217–248.
21. The Legume Phylogeny Working Group. A new subfamily classification of the Leguminosae based on a taxonomically comprehensive phylogeny. *Taxon* **2017**, *66*, 44–77.
22. Li, H. Taxonomy and distribution of the genus *Cercis* in China. *Bull. Torrey Bot. Club* **1944**, *71*, 419–425. [CrossRef]
23. Robertson, K.R. *Cercis*: The redbuds. *Arnoldia* **1976**, *36*, 37–49.
24. Hao, G.; Zhang, D.; Guo, L.; Zhang, M.; Deng, Y.; Wen, X. A phylogenetic and biogeographic study of *Cercis* (Leguminosae). *Acta Bot. Sin.* **2001**, *43*, 1275–1278.
25. Davis, C.C.; Fritsch, P.W.; Li, J.; Donoghue, M.J. Phylogeny and biogeography of *Cercis* (Fabaceae): Evidence from nuclear ribosomal ITS and chloroplast *ndhF* sequence data. *Syst. Bot.* **2002**, *27*, 289–302.
26. Fritsch, P.W.; Cruz, B.C. Phylogeny of *Cercis* based on DNA sequences of nuclear ITS and four plastid regions: Implications for transatlantic historical biogeography. *Mol. Phylogenet. Evol.* **2012**, *62*, 816–825. [CrossRef] [PubMed]
27. Dezhao, C.; Dianxiang, Z.; Larsen, S.S.; Vincent, M.A. *Cercis*. In *Flora of China*; Wu, Z.Y., Raven, P.H., Eds.; Science Press: Beijing, China; Missouri Botanical Garden: St. Louis, MO, USA, 2010; Volume 10, pp. 5–6.
28. Metcalf, F.P. Eight new species of Leguminosae from Southeastern China. *Lingnan Sci. J.* **1940**, *19*, 549–563.
29. Coşkun, F.; Parks, C.R. A molecular phylogenetic study of red buds (*Cercis* L., Fabaceae) based on ITS nrDNA sequences. *Pak. J. Bot.* **2009**, *41*, 1577–1586.
30. Coşkun, F.; Parks, C.R. A molecular phylogeny of *Cercis* L. (Fabaceae) using the chloroplast *trnL-F* DNA sequences. *Pak. J. Bot.* **2009**, *41*, 1587–1592.
31. Kong, W.Q.; Yang, J.H. The complete chloroplast genome sequence of *Morus cathayana* and *Morus multicaulis*, and comparative analysis within genus *Morus* L. *PeerJ* **2017**, *5*, e3037. [CrossRef] [PubMed]
32. Guo, X.; Castillo-Ramírez, S.; González, V.; Bustos, P.; Fernández-Vázquez, J.L.; Santamaría, R.I.; Arellano, J.; Cevallos, M.A.; Dávila, G. Rapid evolutionary change of common bean (*Phaseolus vulgaris* L.) plastome, and the genomic diversification of legume chloroplasts. *BMC Genom.* **2007**, *8*, 228. [CrossRef] [PubMed]
33. Williams, A.V.; Boykin, L.M.; Howell, K.A.; Nevill, P.G.; Small, I. Correction: The complete sequence of the *Acacia ligulata* chloroplast genome reveals a highly divergent *clpP1* gene. *PLoS ONE* **2015**, *10*, e138367. [CrossRef] [PubMed]

34. Kaila, T.; Chaduvla, P.K.; Saxena, S.; Bahadur, K.; Gahukar, S.J.; Chaudhury, A.; Sharma, T.R.; Singh, N.K.; Gaikwad, K. Chloroplast genome sequence of Pigeonpea (*Cajanus cajan* (L.) Millspaugh) and *Cajanus scarabaeoides* (L.) Thouars: Genome organization and comparison with other legumes. *Front. Plant Sci.* **2016**, *7*, 1847. [CrossRef] [PubMed]
35. Wang, Y.; Qu, X.; Chen, S.; Li, D.; Yi, T. Plastomes of Mimosoideae: Structural and size variation, sequence divergence, and phylogenetic implication. *Tree Genet. Genomes* **2017**, *13*, 41. [CrossRef]
36. Wang, Y.; Wang, H.; Yi, T.; Wang, Y. The complete chloroplast genomes of *Adenolobus garipensis* and *Cercis glabra* (Cercidoideae, Fabaceae). *Conserv. Genet. Resour.* **2017**, *9*, 635–638. [CrossRef]
37. Choi, I.; Choi, B. The distinct plastid genome structure of *Maackia fauriei* (Fabaceae: Papilionoideae) and its systematic implications for genistoids and tribe Sophoreae. *PLoS ONE* **2017**, *12*, e173766. [CrossRef] [PubMed]
38. Xiang, B.; Li, X.; Qian, J.; Wang, L.; Ma, L.; Tian, X.; Wang, Y. The complete chloroplast genome sequence of the medicinal plant *Swertia mussotii* using the PacBio RS II platform. *Molecules* **2016**, *21*, 1029. [CrossRef] [PubMed]
39. Raman, G.; Park, V.; Kwak, M.; Lee, B.; Park, S. Characterization of the complete chloroplast genome of *Arabis stellari* and comparisons with related species. *PLoS ONE* **2017**, *12*, e183197. [CrossRef] [PubMed]
40. Park, S.; Jansen, R.K.; Park, S.J. Complete plastome sequence of *Thalictrum coreanum* (Ranunculaceae) and transfer of the *rpl32* gene to the nucleus in the ancestor of the subfamily Thalictroideae. *BMC Plant Biol.* **2015**, *15*, 40. [CrossRef] [PubMed]
41. Lu, R.; Li, P.; Qiu, Y. The complete chloroplast genomes of three *Cardiocrinum* (Liliaceae) species: Comparative genomic and phylogenetic analyses. *Front. Plant Sci.* **2017**, *7*, 2054. [CrossRef] [PubMed]
42. Kong, H.; Liu, W.; Yao, G.; Gong, W. A comparison of chloroplast genome sequences in *Aconitum* (Ranunculaceae): A traditional herbal medicinal genus. *PeerJ* **2017**, *5*, e4018. [CrossRef] [PubMed]
43. Piovani, P.; Leonardi, S.; Piotti, A.; Menozzi, P. Conservation genetics of small relic populations of silver fir (*Abies alba* Mill.) in the northern Apennines. *Plant Biosyst.* **2010**, *144*, 683–691. [CrossRef]
44. Wang, T.; Wang, Z.; Chen, G.; Wang, C.; Su, Y. Invasive chloroplast population genetics of *Mikania micrantha* in China: No local adaptation and negative correlation between diversity and geographic distance. *Front. Plant Sci.* **2016**, *7*, 1426. [CrossRef] [PubMed]
45. Der, J.P.; Thomson, J.A.; Stratford, J.K.; Wolf, P.G. Global chloroplast phylogeny and biogeography of bracken (*Pteridium*; Dennstaedtiaceae). *Am. J. Bot.* **2009**, *96*, 1041–1049. [CrossRef] [PubMed]
46. Greiner, S.; Rauwolf, U.; Meurer, J.; Herrmann, R.G. The role of plastids in plant speciation. *Mol. Ecol.* **2011**, *20*, 671–691. [CrossRef] [PubMed]
47. Zhang, Y.J.; Ma, P.F.; Li, D.Z. High-throughput sequencing of six bamboo chloroplast genomes: Phylogenetic implications for temperate woody bamboos (*Poaceae*: Bambusoideae). *PLoS ONE* **2011**, *6*, e20596. [CrossRef] [PubMed]
48. Zhang, Y.; Du, L.; Liu, A.; Chen, J.; Wu, L.; Hu, W.; Zhang, W.; Kim, K.; Lee, S.; Yang, T. The complete chloroplast genome sequences of five *Epimedium* species: Lights into phylogenetic and taxonomic analyses. *Front. Plant Sci.* **2016**, *7*, 306. [CrossRef] [PubMed]
49. Myszczyński, K.; Bączkiewicz, A.; Buczkowska, K.; Ślipiko, M.; Szczecińska, M.; Sawicki, J. The extraordinary variation of the organellar genomes of the *Aneura pinguis* revealed advanced cryptic speciation of the early land plants. *Sci. Rep.* **2017**, *7*, 9804. [CrossRef] [PubMed]
50. Wang, Y.; Wicke, S.; Wang, H.; Jin, J.; Chen, S.; Zhang, S.; Li, D.; Yi, T. Plastid genome evolution in the early-diverging legume subfamily Cercidoideae (Fabaceae). *Front. Plant Sci.* **2018**, *9*, 138. [CrossRef] [PubMed]
51. Doyle, J.J. A rapid DNA isolation procedure for small quantities of fresh leaf tissue. *Phytochem. Bull.* **1987**, *19*, 11–15.
52. Zhang, T.; Zeng, C.X.; Yang, J.B.; Li, H.T.; Li, D.Z. Fifteen novel universal primer pairs for sequencing whole chloroplast genomes and a primer pair for nuclear ribosomal DNAs. *J. Syst. Evol.* **2016**, *54*, 219–227. [CrossRef]
53. Coil, D.; Jospin, G.; Darling, A.E. A5-miseq: An updated pipeline to assemble microbial genomes from Illumina MiSeq data. *Bioinformatics* **2014**, *31*, 587–589. [CrossRef] [PubMed]

54. Kearse, M.; Moir, R.; Wilson, A.; Stones-Havas, S.; Cheung, M.; Sturrock, S.; Buxton, S.; Cooper, A.; Markowitz, S.; Duran, C. Geneious Basic: An integrated and extendable desktop software platform for the organization and analysis of sequence data. *Bioinformatics* **2012**, *28*, 1647–1649. [CrossRef] [PubMed]
55. Altschul, S.F.; Gish, W.; Miller, W.; Myers, E.W.; Lipman, D.J. Basic local alignment search tool. *J. Mol. Biol.* **1990**, *215*, 403–410. [CrossRef]
56. Wyman, S.K.; Jansen, R.K.; Boore, J.L. Automatic annotation of organellar genomes with DOGMA. *Bioinformatics* **2004**, *20*, 3252–3255. [CrossRef] [PubMed]
57. Schwarz, E.N.; Ruhlman, T.A.; Sabir, J.S.M.; Hajrah, N.H.; Alharbi, N.S.; Al Malki, A.L.; Bailey, C.D.; Jansen, R.K. Plastid genome sequences of legumes reveal parallel inversions and multiple losses of *rps16* in papilionoids. *J. Syst. Evol.* **2015**, *53*, 458–468. [CrossRef]
58. Laslett, D.; Canback, B. ARAGORN, a program to detect tRNA genes and tmRNA genes in nucleotide sequences. *Nucleic Acids Res.* **2004**, *32*, 11–16. [CrossRef] [PubMed]
59. Lohse, M.; Drechsel, O.; Kahlau, S.; Bock, R. OrganellarGenomeDRAW—A suite of tools for generating physical maps of plastid and mitochondrial genomes and visualizing expression data sets. *Nucleic Acids Res.* **2013**, *41*, W575–W581. [CrossRef] [PubMed]
60. Katoh, K.; Standley, D.M. MAFFT multiple sequence alignment software version 7: Improvements in performance and usability. *Mol. Biol. Evol.* **2013**, *30*, 772–780. [CrossRef] [PubMed]
61. Kim, K.; Lee, H. Complete chloroplast genome sequences from Korean ginseng (*Panax schinseng* Nees) and comparative analysis of sequence evolution among 17 vascular plants. *DNA Res.* **2004**, *11*, 247–261. [CrossRef] [PubMed]
62. Nazareno, A.G.; Carlsen, M.; Lohmann, L.G. Complete chloroplast genome of *Tanaecium tetragonolobum*: The first Bignoniaceae plastome. *PLoS ONE* **2015**, *10*, e129930. [CrossRef] [PubMed]
63. Darling, A.E.; Mau, B.; Perna, N.T. progressiveMauve: Multiple genome alignment with gene gain, loss and rearrangement. *PLoS ONE* **2010**, *5*, e11147. [CrossRef] [PubMed]
64. Mayor, C.; Brudno, M.; Schwartz, J.R.; Poliakov, A.; Rubin, E.M.; Frazer, K.A.; Pachter, L.S.; Dubchak, I. VISTA: Visualizing global DNA sequence alignments of arbitrary length. *Bioinformatics* **2000**, *16*, 1046–1047. [CrossRef] [PubMed]
65. Brudno, M.; Malde, S.; Poliakov, A.; Do, C.B.; Couronne, O.; Dubchak, I.; Batzoglou, S. Glocal alignment: Finding rearrangements during alignment. *Bioinformatics* **2003**, *19*, i54–i62. [CrossRef] [PubMed]
66. Frazer, K.A.; Pachter, L.; Poliakov, A.; Rubin, E.M.; Dubchak, I. VISTA: Computational tools for comparative genomics. *Nucleic Acids Res.* **2004**, *32*, W273–W279. [CrossRef] [PubMed]
67. Thiel, T.; Michalek, W.; Varshney, R.; Graner, A. Exploiting EST databases for the development and characterization of gene-derived SSR-markers in barley (*Hordeum vulgare* L.). *Theor. Appl. Genet.* **2003**, *106*, 411–422. [CrossRef] [PubMed]
68. Rozen, S.; Skaletsky, H. *Primer3 on the WWW for General Users and for Biologist Programmers; Bioinformatics Methods and Protocols*; Humana Press: Totowa, NJ, USA, 2000; pp. 365–386.
69. Librado, P.; Rozas, J. DnaSP v5: A software for comprehensive analysis of DNA polymorphism data. *Bioinformatics* **2009**, *25*, 1451–1452. [CrossRef] [PubMed]
70. Rozas, J.; Ferrer-Mata, A.; Sánchez-DelBarrio, J.C.; Guirao-Rico, S.; Librado, P.; Ramos-Onsins, S.E.; Sánchez-Gracia, A. DnaSP 6: DNA sequence polymorphism analysis of large data sets. *Mol. Biol. Evol.* **2017**, *34*, 3299–3302. [CrossRef] [PubMed]
71. Tamura, K.; Stecher, G.; Peterson, D.; Filipski, A.; Kumar, S. MEGA6: Molecular evolutionary genetics analysis version 6.0. *Mol. Biol. Evol.* **2013**, *30*, 2725–2729. [CrossRef] [PubMed]
72. Miller, M.A.; Schwartz, T.; Pickett, B.E.; He, S.; Klem, E.B.; Scheuermann, R.H.; Passarotti, M.; Kaufman, S.; O'Leary, M.A. A RESTful API for access to phylogenetic tools via the CIPRES science gateway. *Evol. Bioinform.* **2015**, *11*, S21501. [CrossRef] [PubMed]
73. Ronquist, F.; Teslenko, M.; Van Der Mark, P.; Ayres, D.L.; Darling, A.; Höhna, S.; Larget, B.; Liu, L.; Suchard, M.A.; Huelsenbeck, J.P. MrBayes 3.2: Efficient Bayesian phylogenetic inference and model choice across a large model space. *Syst. Biol.* **2012**, *61*, 539–542. [CrossRef] [PubMed]
74. Drummond, A.J.; Suchard, M.A.; Xie, D.; Rambaut, A. Bayesian phylogenetics with BEAUti and the BEAST 1.7. *Mol. Biol. Evol.* **2012**, *29*, 1969–1973. [CrossRef] [PubMed]

75. Stamatakis, A. RAxML version 8: A tool for phylogenetic analysis and post-analysis of large phylogenies. *Bioinformatics* **2014**, *30*, 1312–1313. [CrossRef] [PubMed]
76. Silvestro, D.; Michalak, I. raxmlGUI: A graphical front-end for RAxML. *Org. Divers. Evol.* **2012**, *12*, 335–337. [CrossRef]

© 2018 by the authors. Licensee MDPI, Basel, Switzerland. This article is an open access article distributed under the terms and conditions of the Creative Commons Attribution (CC BY) license (http://creativecommons.org/licenses/by/4.0/).

Applications in Plant Sciences

PRIMER NOTE

Identification and characterization of microsatellites in *Aconitum reclinatum* (Ranunculaceae), a rare species endemic to North America

Juan Zhou[1], Wanzhen Liu[1], Hanghui Kong[2,3,4], and Wei Gong[1,4]

Manuscript received 18 January 2018; revision accepted 6 March 2018.

[1] College of Life Sciences, South China Agricultural University, Guangzhou 510614, People's Republic of China

[2] Key Laboratory of Plant Resources Conservation and Sustainable Utilization, South China Botanical Garden, Chinese Academy of Sciences, Guangzhou 510650, People's Republic of China

[3] Guangdong Provincial Key Laboratory of Applied Botany, South China Botanical Garden, Chinese Academy of Sciences, Guangzhou 510650, People's Republic of China

[4] Authors for correspondence: wgong@scau.edu.cn, konghh@scbg.ac.cn

Citation: Zhou, J., W. Liu, H. Kong, and W. Gong. 2018. Identification and characterization of microsatellites in *Aconitum reclinatum* (Ranunculaceae), a rare species endemic to North America. *Applications in Plant Sciences* 6(6): e1161.

doi:10.1002/aps3.1161

PREMISE OF THE STUDY: *Aconitum reclinatum* is the only representative species of *Aconitum* subg. *Lycoctonum* in North America, with restricted ranges and endangered populations. Polymorphic microsatellite markers were developed for *A. reclinatum* for further investigation of genetic diversity and population structure.

METHODS AND RESULTS: Using Illumina HiSeq technology, we sequenced a genomic library for identification of simple sequence repeat markers. A total of 12 polymorphic primer pairs were developed and tested on 66 individuals from four populations in North America. The number of alleles ranged from one to seven per locus with an average of 3.48. Levels of observed and expected heterozygosity varied from 0 to 1.000 and 0 to 0.736, respectively, at population level. Three primer pairs were successfully amplified in three of four closely related species.

CONCLUSIONS: The microsatellites isolated in this study will be useful in further research on the genetic diversity and conservation genetics of *A. reclinatum* populations in North America.

KEY WORDS *Aconitum reclinatum*; endangered species; herbal medicine; microsatellites; next-generation sequencing; Ranunculaceae.

Aconitum reclinatum A. Gray, also known as white monkshood, is a perennial herb belonging to *Aconitum* L. subg. *Lycoctonum* (DC.) Peterm. in Ranunculaceae. *Aconitum* subg. *Lycoctonum* is composed of species distributed throughout Eurasia and North America (Jabbour and Renner, 2012). *Aconitum reclinatum* is the only representative species of this subgenus in North America, where it has a restricted geographic range. The largest existing populations of *A. reclinatum* are known to be located in North Carolina in the eastern United States (Hardin, 1964; Brink, 1982). This species is reportedly disturbed and threatened by logging activities and drainage of its habitat (NatureServe, 2007). To date, the genetic diversity and population genetic structure are still unclear for *A. reclinatum* populations.

Although some species in the genus *Aconitum* are highly toxic because of aconite alkaloids, it is popularly used as a traditional herbal medicine in Asia (Liang et al., 2017). Previous research has been conducted to reveal the genetic variation among some populations in *Aconitum*, using traditional molecular markers including amplified fragment length polymorphism (AFLP), inter-simple sequence repeat (ISSR), and random-amplified polymorphic DNA (RAPD) markers (Cole and Kuchenreuther, 2001; Meng et al., 2014; Zhao et al., 2015). Most recently, microsatellites have been developed and characterized for some *Aconitum* species based on next-generation sequencing (He et al., 2015; Ge et al., 2016). However, those microsatellite markers cannot be amplified in *A. reclinatum* successfully due to low interspecific transferability. Therefore, we developed microsatellite markers specific for *A. reclinatum* for further application in the investigation of genetic diversity and population structure. A total of 12 polymorphic microsatellites were isolated and characterized, which will provide information to interpret the fine population structure of this rare and threatened species.

METHODS AND RESULTS

Tender leaves were collected from *A. reclinatum* and dried instantly in silica gel. A total of 66 individuals and four populations were sampled. Total genomic DNA was extracted from the dried leaves of *A. reclinatum* using a modified cetyltrimethylammonium bromide (CTAB) method (Doyle and Doyle, 1987). The DNA concentration was quantified using a NanoDrop spectrophotometer (Thermo Fisher Scientific, Carlsbad, California, USA), and a final DNA concentration of >30 ng/μL was used subsequently.

We used one individual of *A. reclinatum* collected in Three Top Mountain, North Carolina, USA, to construct a genomic DNA

 © 2018 Zhou et al. *Applications in Plant Sciences* is published by Wiley Periodicals, Inc. on behalf of the Botanical Society of America. This is an open access article under the terms of the Creative Commons Attribution License, which permits use, distribution and reproduction in any medium, provided the original work is properly cited.

library with 360-bp inserts. The genomic DNA library was sequenced using an Illumina HiSeq platform at Majorbio (Shanghai, China). Because the original sequencing data have some low-quality reads, we filtered the original data in order to make the subsequent assembly more accurate. After removing the adapter sequences, we excluded those reads that showed no AGCT sequence at the 5′ end, contained high N content (≥10%), or presented short length (<25 bp) after quality trimming. Finally, we only retained reads with high quality scores; 93.4% of the reads were called accurately when using a threshold of Q20. Using SOAPdenovo version 2.04 splicing software (Luo et al., 2012), the assembly of multiple *k*-mer parameters was performed on the optimized sequencer, and gaps in the assembly were then locally closed and bases were corrected using GapCloser within SOAPdenovo. A total of 2,464,714 scaffolds were generated. Using MISA (Thiel et al., 2003), a total of 197,407 simple sequence repeat (SSR) loci were detected from the 2,464,714 scaffolds. Primer pairs for the 105 SSR loci with the longest dinucleotide repeats were designed with Primer3 (Rozen and Skaletsky, 1999).

To screen the SSR primers, we conducted PCR amplification using one individual from each of the four populations. PCR amplification was performed in a total volume of 25 μL, containing 12 ng of template DNA, 1.25 units of *Taq* DNA polymerase, 0.8 μM of forward and reverse primer, 0.2 μM of dNTP, 2 mM of $MgCl_2$, 2.5 μL of 10× PCR buffer, and 14.25 μL of sterilized double-distilled water. Thermocycling conditions were 94°C (5 min); followed by 35 cycles of denaturation at 94°C (40 s), annealing at 58°C (45 s), and extension at 72°C (50 s); and a final extension of 72°C (10 min). A total of 105 primers were designed for *A. reclinatum*. The PCR products of 17 primer pairs produced the expected size (Table 1). The remaining 88 primer pairs presented poor amplification. To test the polymorphism level of the 17 primer pairs, the forward primers were labeled using the fluorescent dye FAM. The amplification products were sent to Invitrogen (Shanghai, China) for genotyping. Sequencing Analysis 5.2 (Applied Biosystems, Carlsbad, California, USA) was used to measure the size of the PCR products in the ABI 3730 DNA sequencer (Applied Biosystems). Among a total of 17 primer pairs, five were monomorphic and 12 produced polymorphic sites.

Genotypes appeared diploid, displaying at most two alleles per locus per individual. For each locus, the number of alleles per locus (A), observed and expected heterozygosity (H_o and H_e), polymorphism information content (PIC), coefficient of inbreeding (F_{IS}), null allele frequency (r), and Hardy–Weinberg equilibrium

TABLE 1. Characteristics of 12 polymorphic and five monomorphic microsatellite loci developed for *Aconitum reclinatum*.

Locus	Primer sequences (5′–3′)	Repeat motif	Allele size range (bp)	T_a (°C)	GenBank accession no.
AR01[a]	F: TTAGACTTACACGGCCCAGG R: GTTCCGGGCTTCTCATAACA	$(TG)_{10}$	416–424	60.1	SRR6476459
AR02[a]	F: GCTGAACTTGCCATTGTTGA R: TTCAGCCCTCAGGTCAGTCT	$(CA)_{13}$	364–374	59.8	SRR6476460
AR03[a]	F: ATGAATGCAAAGTCCCTTGG R: GAAGGAGTGCGGTTGATGAT	$(AG)_{10}$	397–411	59.9	SRR6476457
AR04[a]	F: TGCTGCTTTCAGGAACAATG R: AGGAGGACATTGGTGAATCG	$(TC)_{10}$	288–292	60.0	SRR6476458
AR05[a]	F: GCTGACAGAGCCATGCTGTA R: ATGGTATTCCCATGCTCAGG	$(GT)_{11}$	428–438	60.2	SRR6476455
AR06[a]	F: CGATCTGACTAGGCCCACAT R: GGAGAGGGTGGGAATTAGGA	$(AG)_{14}$	398–428	60.1	SRR6476456
AR07[a]	F: AACACCCTAGAATCCCCCAC R: CGACACACACCGAGTGACAT	$(TG)_{11}$	351–367	60.1	SRR6476453
AR08[a]	F: ACCCATCATACCAATTCCGA R: TCACATTGGGAATCAAAGCA	$(AC)_{10}$	319–325	60.0	SRR6476454
AR09[a]	F: CGAGCCATTTCACTTGTGTG R: AGGAGCGAATGTGAGTTGCT	$(CA)_{13}$	285–317	60.3	SRR6476451
AR10[a]	F: GAAGGGTATTTTCTCCCCCA R: ATCCACAGGGACAAACTTGC	$(CA)_{11}$	292–298	60.1	SRR6476452
AR11[a]	F: ACCAACTCAGGCATTTGGTC R: CTCCTCCAATCCCATCAGAA	$(GA)_{10}$	268–282	60.0	SRR6476466
AR12[a]	F: ACCGTTTGATCTTGGCAATC R: TCCTACCCTTGCATCTTTGG	$(GA)_{13}$	258–276	60.0	SRR6476467
AR13[b]	F: ACCTAACCGAATTGGCTCCT R: GATGTGCATCCCACAATCAA	$(TC)_9$	287	60.3	SRR6476464
AR14[b]	F: TGTTTATACAAGCACCGCGA R: AGTACGGACCCTTGATCGTG	$(GA)_9$	247	60.0	SRR6476465
AR15[b]	F: GGAAAGGGATGAGTCGATGA R: ACACACACGATTCGGGTACA	$(GT)_{10}$	286	59.9	SRR6476462
AR16[b]	F: CATCCCACAGACATGAATGC R: TGCAAATCACTAGTGCCGAG	$(CT)_9$	360	60.0	SRR6476463
AR17[b]	F: GCTGCATTTGGAAATAGGGA R: CCTTCAAACCCAACTCAACC	$(TC)_{12}$	342	59.4	SRR6476461

Note: T_a = annealing temperature.
[a]Tested for polymorphism.
[b]Monomorphic markers.

© 2018 Zhou et al.

TABLE 2. Genetic characteristics of the 12 polymorphic microsatellites developed in *Aconitum reclinatum*.[a]

	US15 (N = 11)						US17 (N = 20)						US22 (N = 16)						US27 (N = 19)					
Locus	A	H_o	H_e^b	PIC	r	F_{IS}	A	H_o	H_e^b	PIC	r	F_{IS}	A	H_o	H_e^b	PIC	r	F_{IS}	A	H_o	H_e^b	PIC	r	F_{IS}
AR01	4	0.909	0.616**	0.539	−0.235	−0.439	5	1.000	0.721***	0.674	−0.175	−0.365	6	1.000	0.613***	0.537	−0.260	−0.611	5	0.895	0.694***	0.645	−0.180	−0.265
AR02	2	0.364	0.397^{ns}	0.318	0.044	0.130	4	1.000	0.548***	0.445	−0.304	−0.818	3	0.750	0.656***	0.375	−0.333	−0.111	4	0.895	0.630***	0.558	−0.219	−0.397
AR03	3	0.818	0.533^{ns}	0.432	−0.213	−0.500	3	0.750	0.611***	0.531	−0.129	−0.203	3	0.938	0.529**	0.421	−0.315	−0.758	3	1.000	0.547***	0.445	−0.307	−0.819
AR04	3	0.364	0.512*	0.444	0.146	0.333	2	0.350	0.289^{ns}	0.247	−0.094	−0.188	2	0.063	0.061^{ns}	0.375	—	—	2	0.526	0.488^{ns}	0.369	−0.038	−0.053
AR05	2	1.000	0.500***	0.375	−0.333	−1.000	3	1.000	0.524***	0.410	−0.320	−0.905	3	0.938	0.525**	0.421	−0.315	−0.772	6	1.000	0.658***	0.597	−0.228	−0.500
AR06	6	0.909	0.711***	0.665	−0.161	−0.235	3	0.250	0.466*	0.395	0.301	0.484	6	0.688	0.736**	0.586	−0.239	0.098	6	0.474	0.683***	0.647	0.170	0.331
AR07	2	0.000	0.165***	0.152	0.888	1.000	3	0.250	0.501***	0.395	0.290	0.520	2	0.000	0.117***	0.000	—	1.000	2	0.000	0.100***	0.095	0.749	1.000
AR08	2	1.000	0.500***	0.375	−0.333	−1.000	2	1.000	0.500***	0.375	−0.333	−1.000	2	1.000	0.500***	0.375	−0.333	−1.000	4	1.000	0.550***	0.448	−0.302	−0.810
AR09	7	0.545	0.661**	0.635	0.106	0.221	3	0.700	0.516^{ns}	0.463	−0.186	−0.333	2	0.063	0.061^{ns}	0.375	—	—	5	0.474	0.591***	0.559	0.113	0.225
AR10	3	0.091	0.169***	0.163	0.451	0.500	1	0.000	0.000	0.000	—	—	3	0.063	0.174**	0.375	—	0.659	2	0.000	0.266***	0.231	0.971	1.000
AR11	3	1.000	0.541*	0.436	−0.310	−0.833	6	1.000	0.613***	0.536	−0.261	−0.617	3	1.000	0.529**	0.419	−0.316	−0.882	7	1.000	0.695***	0.645	−0.201	−0.416
AR12	1	0.000	0.000	0.000	—	—	3	0.500	0.551*	0.461	0.030	0.118	5	0.563	0.531^{ns}	0.640	—	−0.027	5	0.579	0.457^{ns}	0.418	−0.152	−0.241

Note: A = number of alleles; F_{IS} = coefficient of inbreeding; H_e = expected heterozygosity; H_o = observed heterozygosity; HWE = Hardy–Weinberg equilibrium; N = number of individuals sampled; PIC = polymorphism information content; r = null allele frequency.
[a]Locality and voucher information are provided in Appendix 1.
[b]Deviations from HWE using χ^2 tests: *$P \leq 0.05$, **$P \leq 0.01$, ***$P \leq 0.001$, ns = not significant.

TABLE 3. Results of cross-amplification testing showing allele size ranges of microsatellite loci isolated from *Aconitum reclinatum* and tested in four related taxa.[a]

Locus	*A. angustius* (N = 6)	*A. finetianum* (N = 7)	*A. sinomontanum* (N = 6)	*A. barbatum* (N = 7)
AR01	418–424	418–424	—	—
AR02	364–374	364–374	—	364–374
AR03	—	—	—	397–411
AR04	—	—	—	—
AR05	—	—	—	—
AR06	—	—	—	—
AR07	—	351–367	—	—
AR08	319–325	319–325	—	319–325
AR09	—	—	—	285–325
AR10	—	—	—	—
AR11	274–282	274–282	—	—
AR12	258–276	258–276	—	—

Note: — = unsuccessful amplification; N = number of individuals sampled.
[a]Locality and voucher information are provided in Appendix 1.

were analyzed for the four populations. A, H_o, H_e, and Hardy–Weinberg equilibrium were estimated using GenAlEx 6.5 (Peakall and Smouse, 2012). The presence of null alleles was checked using MICRO-CHECKER 2.2.3 (van Oosterhout et al., 2004). Linkage disequilibrium and F_{IS} were estimated using GENEPOP software (Rousset, 2008). CERVUS 3.0.7 was used to calculate PIC and r (Kalinowski et al., 2007).

A varied from one to seven with an average of 3.48. Levels of H_o and H_e ranged from 0 to 1.000 and from 0 to 0.736, respectively, with averages of 0.619 and 0.470. PIC values ranged from 0 to 0.674 with an average of 0.417, and F_{IS} values ranged from −1.000 to 1.000 with an average of −0.177. Null allele frequency values ranged from −0.3330 to 0.971 (Table 2).

We also tested interspecific transferability of these loci in four additional *Aconitum* taxa (*A. angustius* W. T. Wang, *A. barbatum* Pers., *A. finetianum* Hand.-Mazz., and *A. sinomontanum* Nakai). Six or seven individuals were selected from each species and used for amplification (Table 3, Appendix 1). A total of six loci (AR01, AR02, AR07, AR08, AR11, AR12) exhibited successful amplifications in *A. finetianum*, five loci (AR01, AR02, AR08, AR11, AR12) in *A. angustius*, and four loci (AR02, AR03, AR08, AR09) in *A. barbatum*. No microsatellite loci were successfully amplified in *A. sinomontanum*.

CONCLUSIONS

A total of 69 alleles were identified for 12 polymorphic loci in the four populations of *A. reclinatum*. These microsatellite loci will be valuable for further interpretation of the fine population structure and conservation strategies of this rare, threatened species.

ACKNOWLEDGMENTS

The authors thank Dr. Andrew Jenkins and Susan Lutz for their assistance in fieldwork. This research was supported by the National Natural Science Foundation of China (31470312, 31470319) and the Science and Technology Planning Project of Guangdong Province, China (2016A030303048, 2017A030303067).

© 2018 Zhou et al.

DATA ACCESSIBILITY

The raw data has been deposited to the National Center for Biotechnology Information Sequence Read Archive (https://www.ncbi.nlm.nih.gov/sra/SRP129852); the GenBank accession numbers are provided in Table 1. The BioProject ID number is PRJNA427053, and the BioSample accession number is SAMN08218777.

LITERATURE CITED

Brink, D. 1982. Tuberous *Aconitum* (Ranunculaceae) of the continental United States: Morphological variation, taxonomy and disjunction. *Bulletin of the Torrey Botanical Club* 109: 13–23.

Cole, C. T., and M. A. Kuchenreuther. 2001. Molecular markers reveal little genetic differentiation among *Aconitum noveboracense* and *A. columbianum* (Ranunculaceae) populations. *American Journal of Botany* 88: 337–347.

Doyle, J. J., and J. L. Doyle. 1987. A rapid DNA isolation procedure for small quantities of fresh leaf tissue. *Phytochemical Bulletin* 19: 11–15.

Ge, X., H. Tian, and W. Liao. 2016. Characterization of 19 microsatellite loci in the clonal monkshood *Aconitum kusnezoffii* (Ranunculaceae). *Applications in Plant Sciences* 4: 1500141.

Hardin, J. W. 1964. Variation in *Aconitum* of eastern United States. *Brittonia* 16: 80–94.

He, J., Z. Zhang, J. Yang, H. Wang, and J. Meng. 2015. Isolation and characterization of 18 microsatellites for *Aconitum vilmorinianum* Kom. (Ranunculaceae) using next-generation sequencing technology. *Conservation Genetics Resources* 7: 579–581.

Jabbour, F., and S. S. Renner. 2012. A phylogeny of Delphinieae (Ranunculaceae) shows that *Aconitum* is nested within *Delphinium* and that Late Miocene transitions to long life cycles in the Himalayas and Southwest China coincide with bursts in diversification. *Molecular Phylogenetics and Evolution* 62: 928–942.

Kalinowski, S. T., M. L. Taper, and T. C. Marshall. 2007. Revising how the computer program CERVUS accommodates genotyping error increases success in paternity assignment. *Molecular Ecology* 16: 1099–1106.

Liang, X., C. Lan, S. Lei, W. Fei, H. Min, C. He, and Z. Yin. 2017. Diterpenoid alkaloids from the root of *Aconitum sinchiangense* W. T. Wang with their antitumor and antibacterial activities. *Natural Product Research* 31: 2016–2023.

Luo, R., B. Liu, Y. Xie, Z. Li, W. Huang, J. Yuan, G. He, et al. 2012. SOAPdenovo2: An empirically improved memory-efficient short-read de novo assembler. *GigaScience* 1: 18.

Meng, F., M. Peng, R. Wang, C. Wang, and F. C. Guan. 2014. Analysis of genetic diversity in *Aconitum kongboense* L. revealed by AFLP markers. *Biochemical Systematics and Ecology* 57: 388–394.

NatureServe. 2007. NatureServe Explorer: An online encyclopedia of life, Version 6.2. Website http://www.natureserve.org/explorer [accessed 18 August 2017].

Peakall, R., and P. E. Smouse. 2012. GenAlEx 6.5: Genetic analysis in Excel. Population genetic software for teaching and research–an update. *Bioinformatics* 28: 2537–2539.

Rousset, F. 2008. GENEPOP'007: A complete re-implementation of the GENEPOP software for Windows and Linux. *Molecular Ecology Resources* 8: 103–106.

Rozen, S., and H. Skaletsky. 1999. Primer3 on the WWW for general users and for biologist programmers. *In* S. Misener and S. A. Krawetz [eds.], Methods in molecular biology, vol. 132: Bioinformatics: Methods and protocols, 365–386. Humana Press, Totowa, New Jersey, USA.

Thiel, T., W. Michalek, R. K. Varshney, and A. Graner. 2003. Exploiting EST databases for the development and characterization of gene-derived SSR-markers in barley (*Hordeum vulgare* L.). *Theoretical and Applied Genetics* 106: 411–422.

van Oosterhout, C., W. F. Hutchinson, D. P. M. Willis, and P. F. Shipley. 2004. MICRO-CHECKER: Software for identifying and correcting genotyping errors in microsatellite data. *Molecular Ecology Notes* 4: 535–538.

Zhao, F., J. Nie, M. Chen, and G. Wu. 2015. Assessment of genetic characteristics of *Aconitum germplasms* in Xinjiang Province (China) by RAPD and ISSR markers. *Biotechnology and Biotechnological Equipment* 29: 309–314.

APPENDIX 1. Voucher and locality information for *Aconitum* species used in this study.

Species	Voucher specimen accession no.[a]	Population location	*N*	Geographical coordinates
Aconitum reclinatum A. Gray	US15	Mt. Jefferson, North Carolina, USA	11	36°24′N, 81°27′W
	US17	Mt. Three Top, North Carolina, USA	20	36°25′N, 81°35′W
	US22	Hightown, Virginia, USA	16	38°27′N, 79°42′W
	US27	Mitchell County, North Carolina, USA	19	36°05′N, 82°09′W
A. angustius W. T. Wang	LJP195	Shangcheng County, Henan, China	6	31°42′N, 115°31′E
A. barbatum Pers.	ZY57	Huairou District, Beijing, China	7	40°57′N, 116°27′E
A. finetianum Hand.-Mazz.	ZY25	Mt. Junfu, Jiangxi, China	7	26°37′N, 115°19′E
A. sinomontanum Nakai	ZY46	Kai County, Chongqing, China	6	31°39′N, 108°46′E

Note: N = number of individuals sampled.
[a]One voucher was collected for each sampled population. Herbarium vouchers are deposited in the Herbarium of South China Botanical Garden (IBSC).

© 2018 Zhou et al.

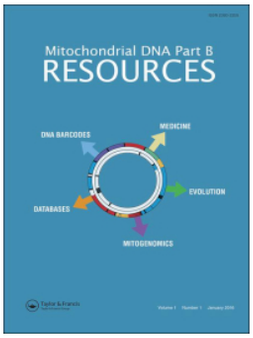

Taylor & Francis
Taylor & Francis Group

Mitochondrial DNA Part B
Resources

ISSN: (Print) (Online) Journal homepage: https://www.tandfonline.com/loi/tmdn20

The complete chloroplast genome of *Aristolochia hainanensis* Merr. (Aristolochiaceae)

Meixiu Lin, Mengxue Feng, Hui Zhou, Wei Gong & Rongjing Zhang

To cite this article: Meixiu Lin, Mengxue Feng, Hui Zhou, Wei Gong & Rongjing Zhang (2022) The complete chloroplast genome of *Aristolochia hainanensis* Merr. (Aristolochiaceae), Mitochondrial DNA Part B, 7:9, 1650-1652, DOI: 10.1080/23802359.2022.2119816

To link to this article: https://doi.org/10.1080/23802359.2022.2119816

© 2022 The Author(s). Published by Informa UK Limited, trading as Taylor & Francis Group.

Published online: 15 Sep 2022.

Submit your article to this journal

Article views: 186

View related articles

View Crossmark data

Full Terms & Conditions of access and use can be found at
https://www.tandfonline.com/action/journalInformation?journalCode=tmdn20

MITOCHONDRIAL DNA PART B
2022, VOL. 7, NO. 9, 1650–1652
https://doi.org/10.1080/23802359.2022.2119816

Taylor & Francis
Taylor & Francis Group

MITOGENOME ANNOUNCEMENT

OPEN ACCESS Check for updates

The complete chloroplast genome of *Aristolochia hainanensis* Merr. (Aristolochiaceae)

Meixiu Lin, Mengxue Feng, Hui Zhou, Wei Gong and Rongjing Zhang

College of Life Sciences, South China Agricultural University, Guangzhou, China

ABSTRACT

Aristolochia hainanensis Merr. 1922, a well-known Chinese medicinal plant, is distributed in Hainan Province and Guangxi Province, China. In the current study, we sequenced the complete chloroplast genome of *A. hainanensis*. The complete plastome genome was 159,764 bp in length, with a GC content of 38.8%, showing a typical quadripartite organization. The genome contained a large single-copy (LSC) of 89,134 bp, a small single-copy (SSC) of 19,306 bp, and a pair of inverted repeats (IRs) of 25,662 bp. A total of 113 genes were annotated, including 79 protein-coding genes, 30 tRNAs, and four rRNAs. The *trnK*-UUU gene contained the longest intron (2644 bp). The topology of the maximum-likelihood tree supported a close relationship between *A. hainanensis* and *A. kwangsiensis*.

ARTICLE HISTORY
Received 7 February 2022
Accepted 27 August 2022

KEYWORDS
Aristolochia hainanensis; chloroplast genome sequencing; phylogenetic analysis

The Aristolochiaceae are composed of approximately 550 species, most of which belong to a large group in the genus *Aristolochia*, which includes 450 species (Bliss et al. 2013; Chase et al. 2016; Qin et al. 2021). In the current study, we focused on the species *Aristolochia hainanensis* Merr. 1922, which is a traditional Chinese medicinal plant mainly distributed in the Wuzhishan Mountain region of Hainan Island. In recent years, with the degradation and loss of their natural growth environment and human harvesting and cutting, *A. hainanensis* has been listed as a Threatened Species with vulnerable (VU) status on the IUCN Red List (https://www.iucnredlist.org/).

Chloroplasts are important organelles of green plants with roles in photosynthesis and nitrogen fixation (Moore et al. 2007). The chloroplast genome is crucial for the taxonomic classification and phylogenetic analysis of land plants (Moore et al. 2007; Yang et al. 2013; Huang et al. 2014). In recent years, many chloroplast genomes of other species in the genus *Aristolochia* have been reported, including *A. kaempferi*, *A. kunmingensis*, *A. macrophylla*, *A. mollissima*, *A. moupinensis*, *A. tagala*, and *A. tubiflora* (Zhou et al. 2017; Li et al. 2019). In the current study, we revealed the chloroplast genome of *A. hainanensis* for the first time, and aimed to provide basic genetic information harbored in the chloroplast and unveil the phylogenetic position of *A. hainanensis*.

We collected several individuals from Mt. Wuzhishan, Hainan, China (E109°42′33.5″, N18°50′03.2″). A specimen was deposited at SCAUB (https://www.cvh.ac.cn/, Rongjing Zhang, zhangrongj@scau.edu.cn) under the voucher number Rong-Jing Zhang 32021. Fresh leaves were sampled for total genomic DNA extraction using a modified CTAB method (Doyle et al. 1987). The DNA library was sequenced using an Illumina NovaSeq 6000 platform with 150 bp pair-end read lengths at Novogene Co. Ltd. (Beijing, China). After filtering low quality reads, a total of 2.38 Gb of clean data with Q30 (92.02%) were obtained and assembled with GetOrganelle (Jin et al. 2020). Annotation was conducted using PGA (Qu et al. 2019) followed by a manual check with Geneious Prime v.2021.2.2 (Biomatters, Auckland, New Zealand, https://www.geneious.com/) to obtain the final annotated data. The complete plastome genome was submitted to GenBank under the accession No. OL943803.

The complete plastome genome was found to be 159,764 bp in length with a GC content of 38.8%, including a large single-copy (LSC) of 89,134 bp and a small single-copy (SSC) of 19,306 bp separated by a pair of inverted repeats (IRs) of 25,662 bp. In total, 113 genes were annotated, including 79 protein-coding genes, four rRNAs, and 30 tRNAs. Among these genes, 15 contained one intron and three contained two introns. The *trnK*-UUU gene included the longest intron at 2644 bp.

To explore the phylogenetic relationship, a phylogenetic tree was generated using five species of the subgenus *Aristolochia* and six species of the subgenus *Siphisia*. Three species of the genus *Piper* were used as outgroups. The sequences used for alignment are available in the GenBank database, including *A. hainanensis* (OL943803.1), *A. kwangsiensis* (MN965793.1), *A. moupinensis* (NC_041454.1), *A. mollissima* (NC_041457.1), *A. kaempferi* (NC_041452.1), *A. manshuriensis* (MN132862.1), *A. delavayi* (MW413320.1), *A. tubiflora* (NC_041456.1), *A. contorta* (NC_036152.1), *A. debilis* (NC_036153.1), *A. tagala* (NC_041455.1), as well as *Piper*

CONTACT Rongjing Zhang zhangrongj@scau.edu.cn; Wei Gong wgong@scau.edu.cn College of Life Sciences, South China Agricultural University, Guangzhou, China

© 2022 The Author(s). Published by Informa UK Limited, trading as Taylor & Francis Group.
This is an Open Access article distributed under the terms of the Creative Commons Attribution License (http://creativecommons.org/licenses/by/4.0/), which permits unrestricted use, distribution, and reproduction in any medium, provided the original work is properly cited.

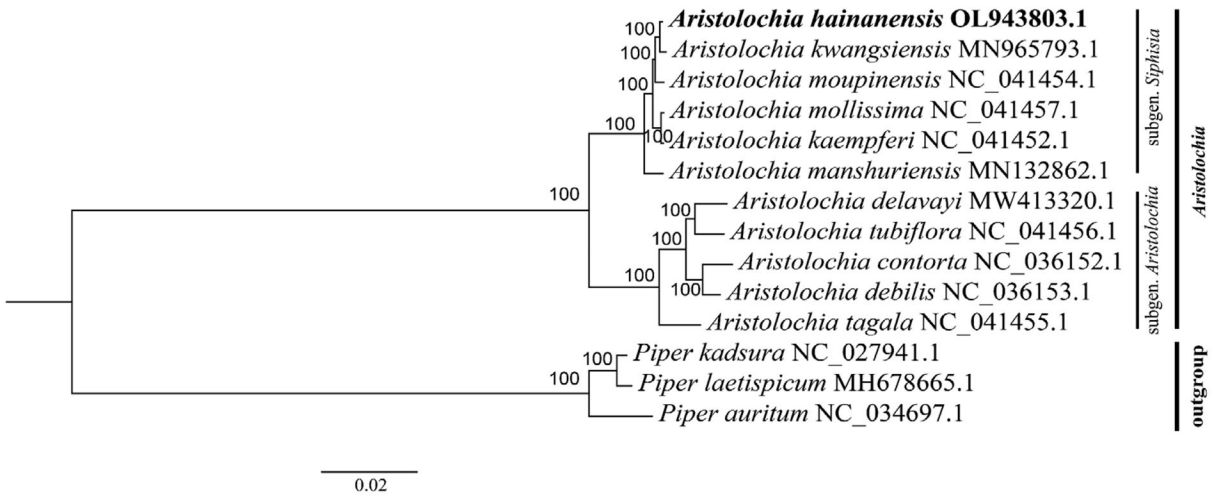

Figure 1. Maximum-likelihood tree based on 11 complete chloroplast genomes of *Aristolochia* and three outgroup species. Numbers in the nodes are bootstrap support values based on 1,000 replications. *A. hainanensis* is highlighted in bold.

kadsura (NC_027941.1), *P. laetispicum* (MH678665.1), and *P. auritum* (NC_034697.1). Sequences were aligned using the MAFFT alignment tool on Geneious Prime v.2021.2.2 (Biomatters, Auckland, New Zealand, https://www.geneious.com/). The best model was generated using jModelTest2 on XSEDE (https://www.phylo.org/, Miller et al. 2010; Darriba et al. 2012). Based on the substitution GTR + I + G model, the maximum-likelihood (ML) phylogenetic tree was produced using RAxML-HPC2 on XSEDE (https://www.phylo.org/) with 1,000 bootstrap replicates (Stamatakis et al. 2008). The topology showed that 11 species of the genus *Aristolochia* occur in the same clade. *A. hainanensis* displayed as a sister to *A. kwangsiensis* based on the ML tree (Figure 1). This study provides a basis for further research and will aid the conservation of this species.

Ethics statement

The authors have complied with the International Union for Conservation of Nature (IUCN) policies research involving species at risk of extinction, the Convention on Biological Diversity and the Convention on the Trade in Endangered Species of Wild Fauna and Flora. Our study has been approved by local authorities (Hainan Administration of Wuzhishan National Nature Reserve). Lei Liu is the Deputy Director (e-mail: 57019386@qq.com).

Author contributions

Conceived and designed the experiments: RJZ, WG, and MXL. Performed the experiments: MXL, MXF, and HZ. Analyzed the data: MXL. Wrote the paper: MXL. Revised the paper: RJZ, WG, MXL, and MXF. Supervised the project and approved the final version to be published: RJZ and WG. All authors agree to be accountable for all aspects of the work.

Disclosure statement

No potential conflicts of interest are reported by the author(s).

Funding

This work was supported by the National Natural Science Foundation of China under Grant Numbers [41001028] and [41471046] and Kadoorie Farm and Botanic Garden of HoogKoon under Grant Number [4600H19501].

ORCID

Meixiu Lin http://orcid.org/0000-0002-6602-553X
Wei Gong http://orcid.org/0000-0002-0881-6130
Rongjing Zhang http://orcid.org/0000-0003-3306-3633

Data availability statement

The genome sequence data that support the findings of this study are openly available in GenBank of NCBI at https://www.ncbi.nlm.nih.gov under the accession no. OL943803. The associated BioProject, SRA, and Bio-Sample numbers are PRJNA795315, SRR17478235, and SAMN24706807, respectively.

References

Bliss BJ, Wanke S, Barakat A, Ayyampalayam S, Wickett N, Wall PK, Jiao Y, Landherr L, Ralph PE, Hu Y, et al. 2013. Characterization of the basal angiosperm *Aristolochia fimbriata*: a potential experimental system for genetic studies. BMC Plant Biol. 13(1):13–26.

Byng JW, Chase MW, Christenhusz MJM, Fay MF, Judd WS, Mabberley D, Sennikov A, Soltis DE, Soltis PS, Stevens P. 2016. An update of the Angiosperm Phylogeny Group classification for the orders and families of flowering plants: APG IV. Bot J Linn Soc. 181(1):1–20.

Darriba D, Taboada GL, Doallo R, Posada D. 2012. JModelTest 2: more models, new heuristics and parallel computing. Nat Methods. 9(8):772.

Doyle JJ, Doyle JL. 1987. A rapid DNA isolation procedure for small quantities of fresh leaf tissue. Phytochem Bull. 19(1):11–15.

Huang H, Shi C, Liu Y, Mao S-Y, Gao L-Z. 2014. Thirteen Camelliachloroplast genome sequences determined by high-throughput sequencing: genome structure and phylogenetic relationships. BMC Evol Biol. 14(1):151.

Jin J-J, Yu W-B, Yang J-B, Song Y, dePamphilis CW, Yi T-S, Li D-Z. 2020. GetOrganelle: a fast and versatile toolkit for accurate de novo assembly of organelle genomes. Genome Biol. 21(1):1–31.

Li X, Zuo Y, Zhu X, Liao S, Ma J. 2019. Complete chloroplast genomes and comparative analysis of sequences evolution among seven Aristolochia (Aristolochiaceae) medicinal species. Int J Mol Sci. 20(5):1045.

Miller MA, Pfeiffer W, Schwartz T. 2010. Creating the CIPRES Science Gateway for inference of large phylogenetic trees. 2010 Gateway Computing Environments Workshop (GCE); Nov 14; New Orleans, LA. p. 1–8.

Moore MJ, Bell CD, Soltis PS, Soltis DE. 2007. Using plastid genome-scale data to resolve enigmatic relationships among basal angiosperms. Proc Natl Acad Sci USA. 104(49):19363–19368.

Qin L, Hu Y, Wang J, Wang X, Zhao R, Shan H, Li K, Xu P, Wu H, Yan X, et al. 2021. Insights into angiosperm evolution, floral development and chemical biosynthesis from the *Aristolochia fimbriata* genome. Nat Plants. 7(9):1239–1253.

Qu XJ, Moore MJ, Li DZ, Yi TS. 2019. PGA: a software package for rapid, accurate, and flexible batch annotation of plastomes. Plant Methods. 15(1):1–12.

Stamatakis A, Hoover P, Rougemont J. 2008. A rapid bootstrap algorithm for the RAxML web servers. Syst Biol. 57(5):758–771.

Yang JB, Yang SX, Li HT, Yang J, Li DZ. 2013. Comparative chloroplast genomes of *Camellia* species. PLOS One. 8(8):e73053.

Zhou J, Chen X, Cui Y, Sun W, Li Y, Wang Y, Song J, Yao H. 2017. Molecular structure and phylogenetic analyses of complete chloroplast genomes of two *Aristolochia* medicinal species. Int J Mol Sci. 18(9):1839.

Conservation Genet Resour
DOI 10.1007/s12686-017-0789-y

TECHNICAL NOTE

Characterization of the whole chloroplast genome of a rare and endangered species *Aconitum reclinatum* (Ranunculaceae) in the United States

Hanghui Kong[1,4] · Wanzhen Liu[2] · Gang Yao[3] · Wei Gong[2]

Received: 27 May 2017 / Accepted: 10 June 2017
© Springer Science+Business Media B.V. 2017

Abstract The complete chloroplast genome (cp genome) of *Aconitum reclinatum* (Ranunculaceae) was characterized through Illumina paired-end sequencing. The cp genome is circle and 157,354 bp in length, consisting of a pair of 26,061 bp inverted repeat regions (IRs) which are separated by a large single copy region (LSC) of 88,269 bp and a small single copy region (SSC) of 16,963 bp. The cp genome contains 135 genes, including 87 protein-coding genes (PCGs), 40 tRNA genes (tRNA) and eight ribosomal RNA genes (rRNA). Among these, seven PCGs, eight tRNA and four rRNA are duplicated. The overall GC content of the *A. reclinatum* cp genome is 38.00%, while the corresponding values of the LSC, SSC and IRs regions are 36.00, 32.80 and 43.00%, respectively. The phylogenetic analysis suggested that *A. reclinatum* is closely related to *A. barbatum* var. *hispidum and A. barbatum* var. *puberulum* with high bootstrap support of 100%.

Keywords *Aconitum reclinatum* · Chloroplast genome · Endangered species · Illumina sequencing · Phylogenetic analysis

✉ Wei Gong
wgong@scau.edu.cn

[1] Key Laboratory of Plant Resources Conservation and Sustainable Utilization, South China Botanical Garden, Chinese Academy of Sciences, Guangzhou 510650, China

[2] College of Life Sciences, South China Agricultural University, Guangzhou 510614, China

[3] College of Forestry and Landscape Architecture, South China Agricultural University, Guangzhou 510614, China

[4] Guangdong Provincial Key Laboratory of Applied Botany, South China Botanical Garden, Chinese Academy of Sciences, Guangzhou 510650, China

Aconitum reclinatum A. Gray, known as trailing white monkshood, belongs to the genus of *Aconitum* in the family of Ranunculaceae. It is an herbaceous perennial plant with greenish white flowers. This species is listed as a national wetland plant, which is rare, threatened and endemic to the states of North Carolina, Tennessee, Virginia, West Virginia and Pennsylvania in the United States (Kintsch and Urban 2002; Lichvar 2013). Aconite produced from the roots of *Aconitum* is widely used for different diseases (Xiao et al. 2005). Many species in the genus *Aconitum* are proved to be essential components in the formulations of traditional herbal medicine in Asia. Even though some species are highly toxic because of aconite alkaloid, they possess a variety of medicinal importance (Semenov et al. 2016; Liang et al. 2016). *Aconitum reclinatum* is the only species of *Aconitum* subg. *Lycoctonum* in the New World (Tamura and Lauener 1979). An improved understanding of *A. reclinatum* genomic information would contribute to formulate the comprehensive conservation strategy to protect and restore this species. However, genomic level of diversity is still unclear for this species. In the current study, we presented the complete chloroplast genome of *A. reclinatum* (GenBank Accession Number: MF155665) based on the Illumina sequencing platform.

Total genomic DNA was extracted from the fresh leaves of a single individual of *A. reclinatum* with the modified CTAB method (Doyle and Doyle 1987). The DNA concentration was quantified using a Nanodrop spectrophotometer (Thermo Scientific, Carlsbad, CA, USA). The final DNA concentration >30 ng/μL were chosen for further Illumina sequencing. The sequences of the cp genome of *A. reclinatum* were amplified using fifteen universal primer pairs developed by Zhang et al. (2016). A paired-end library was constructed by Nextera XT DNA Library Prep Kit (Illumina Inc., San Diego, CA, USA), and then 250 bp paired

Published online: 16 June 2017

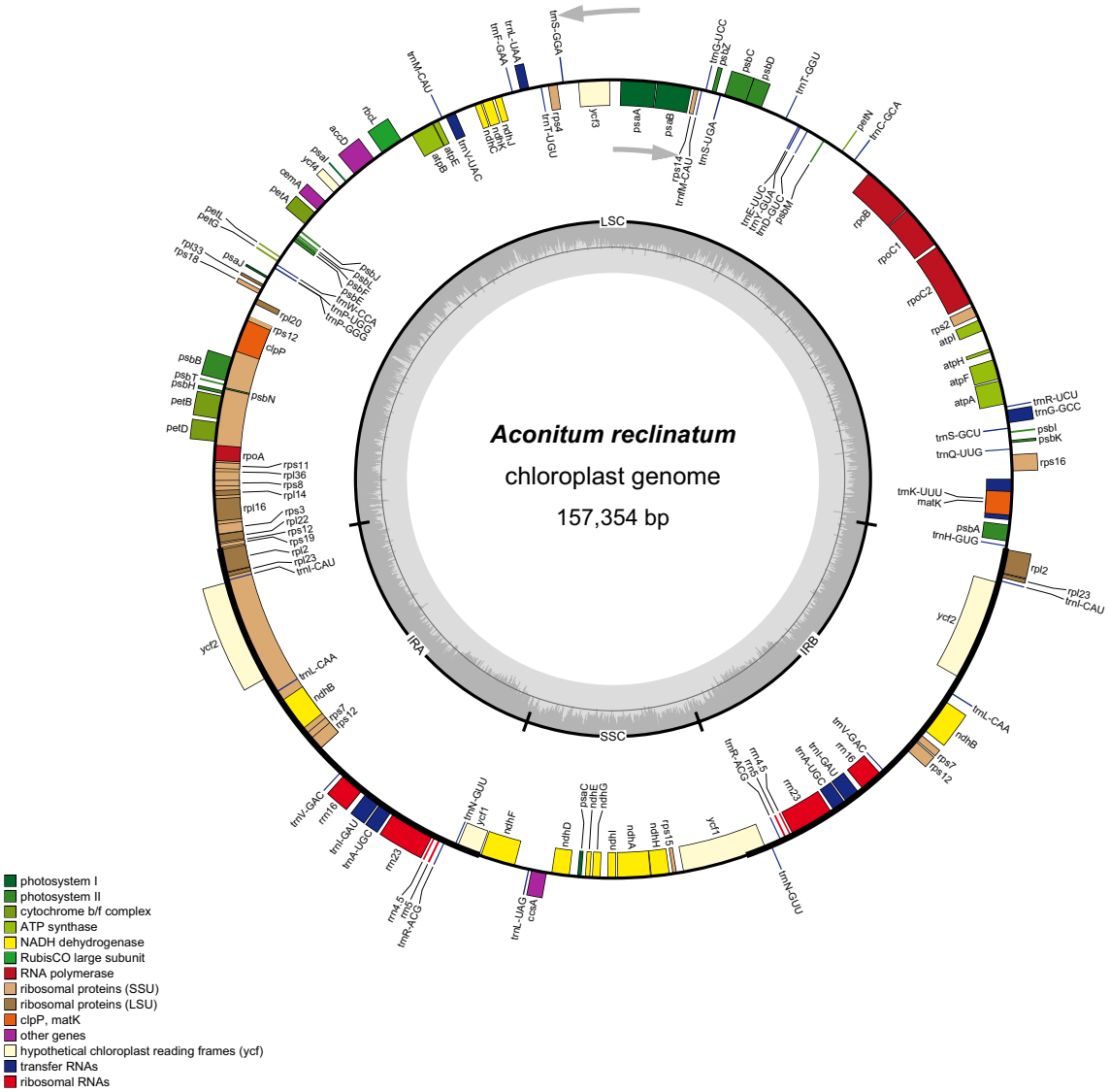

Fig. 1 Gene map of the *Aconitum reclinatum* chloroplast genome

reads were sequenced using the Illumina Miseq Desktop Sequencer. Reads of the *A. reclinatum* cp genome were initially assembled using CLC Genomics Workbench v7.5.1 (CLC Bio., Aarhus, Denmark) with 60 and 64 k-mer respectively. The contigs were checked against the reference cp genome of *A. barbatum* var. *hispidum* (KT820664) and *A. barbatum* var. *puberulum* (KC844054) (Chen et al. 2015). A complete *A. reclinatum* cp genome sequence was subsequently constructed by manual assembling of the hitting contigs. The resulting cp genome sequence was used as a reference, which was subsequently verified by remapping initial reads using GENEIOUS R9.1.4 (Biomatters Ltd., Auckland, New Zealand). The annotation of the *A. reclinatum* cp genome sequence was performed using DOGMA (http://dogma.ccbb.utexas.edu/) (Wyman et al. 2004) and also conducted on the program GENEIOUS R9.1.4 (Biomatters Ltd., Auckland, New Zealand) by comparing with the cp genome of *A. barbatum* var. *hispidum* and *A. barbatum* var. *puberulum*. The annotations of tRNA genes were further confirmed using ARAGORN (Laslett and Canback 2004) followed by manual adjustment. The annotated cp genome sequence of *A. reclinatum* has been submitted to GenBank. Finally, the circular genome map was generated with OGDRAW (http://ogdraw.mpimp-golm.mpg.de/) (Lohse et al. 2013).

The cp genome of *A. reclinatum* (Ranunculaceae) is circle with 157,354 bp in length, displaying a typical quadripartite structure and consisting of a pair of inverted repeat regions (IRs) of 26,061 bp, a large single-copy region (LSC) of 88,269 bp and a small single-copy

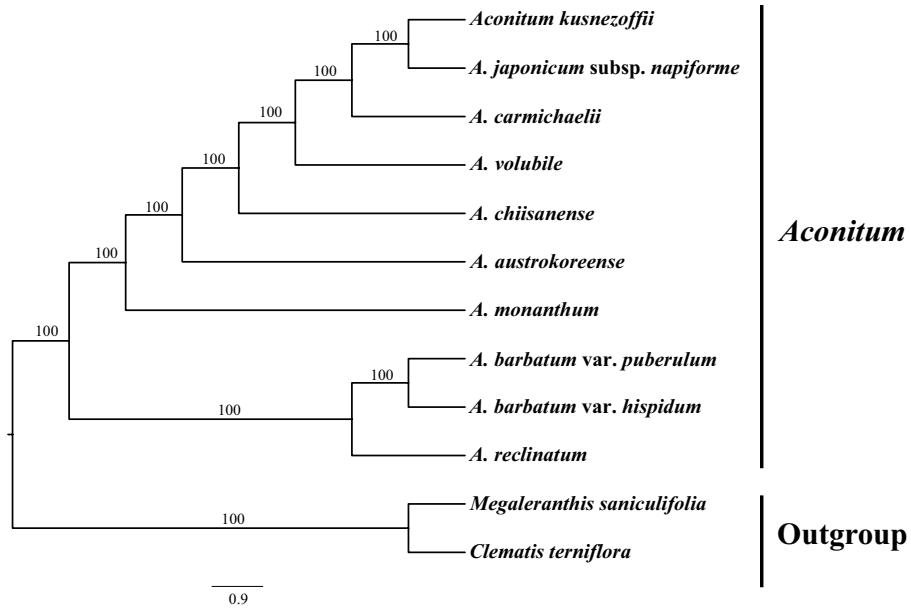

Fig. 2 Phylogenetic reconstruction of eight species and two varieties within *Aconitum* based on the concatenated sequences of 84 to 87 chloroplast PCGs using Maximum Likelihood (ML) analysis. Bootstraps with 1000 replicates were assessed and displayed on the *above of the branches*

region (SSC) of 16,963 bp (Fig. 1). It contains 135 genes, including 87 protein-coding genes (PCGs), 40 transfer RNA genes (tRNA) and eight ribosomal RNA genes (rRNA). Among these, seven PCGs (*ndhB, rpl2, rpl23, rps7, rps12, ycf2* and *ycf15*), eight tRNA (*trnA-UGC, trnI-CAU, trnI-GAU, trnL-CAA, trnN-GUU, trnR-ACG* and *trnV-GAC*) and four rRNA (*rrn4.5, rrn5, rrn16, rrn23*) were revealed to occur in double copies. The overall GC content of *A. reclinatum* cp genome is 38.00%, while the corresponding GC content of the LSC, SSC and IRs regions are 36.00, 32.80 and 43.00%, respectively.

Phylogenetic analysis was conducted based on eight species and two varieties in the genus of *Aconitum*, with *Megaleranthis saniculifolia* and *Clematis terniflora* as outgroup. The cp genome sequences from the finalized data set were aligned with MAFFT v7.0.0 (Katoh and Standley 2013). Altogether 84–87 chloroplast PCGs were used for the phylogenetic reconstruction. Maximum Likelihood (ML) analyses used the identical partition scheme and were conducted using RAxML (Stamatakis 2006) and the RAxML graphical interface [raxmlGUI v.1.3 (Silvestro and Michalak 2012)]. Phylogenetic analysis indicated that all the representative ten species from the genus *Aconitum* formed monophyly, among which *A. reclinatum* clustered with *A. barbatum* var. *hispidum* and *A. barbatum* var. *puberulum* with 100% bootstrap support value (Fig. 2).

Acknowledgements This work was financially supported by the National Natural Science Foundation of China (31470319; 31470312) and Science and Technology Planning Project of Guangdong Province, China (2016A030303048).

Compliance with ethical standards

Conflict of interest The authors report no conflicts of interest.

References

Chen XC, Li QS, Li Y, Qian J, Han JP (2015) Chloroplast genome of *Aconitum barbatum* var. *puberulum* (Ranunculaceae) derived from CCS reads using the PacBio RS platform. Front Plant Sci 6(42):1–9

Doyle JJ, Doyle JL (1987) A rapid DNA isolation procedure for small quantities of fresh leaf tissue. Phytochem Bull 19:11–15

Katoh K, Standley DM (2013) MAFFT multiple sequence alignment software version 7: improvements in performance and usability. Mol Biol Evol 30(4):772–780. doi:10.1007/s12686-017-0789-y

Kintsch JA, Urban DI (2002) Focal species, community representation, and physical proxies as conservation strategies: a case study in the Amphibolite Mountains, North Carolina, USA. Conserv Biol 16(4):936–947

Laslett D, Canback B (2004) ARAGORN, a program to detect tRNA genes and tmRNA genes in nucleotide sequences. Nucleic Acids Res 32:11–16

Liang WJ, Zhang TJ, Li ZJ, Chen ZX, Yan XL, Meng FH (2016) Predicting potential antitumor targets of Aconitum alkaloids by molecular docking and protein-ligand interaction fingerprint. Med Chem Res 25:1115–1124

Lichvar RW (2013) The National Wetland Plant List: 2013 wetland ratings. Phytoneuron 49:1–241

Lohse M, Drechsel O, Kahlau S, Bock R (2013) Organellar Genome DRAW—a suite of tools for generating physical maps of plastid and mitochondrial genomes and visualizing expression data sets. Nucleic Acids Res 41(W1):W575–W581

Semenov AA, Enikeev AG, Snetkova LV, Permyakov AV, Sokolova NA, Dudareva LV (2016) Ortho-phthalic acid esters in lipophilic extract from the cell culture of *Aconitum baicalense* Turcz ex Rapaics 1907. Dokl Biochem Biophys 471:421–422

Silvestro D, Michalak I (2012) raxmlGUI: a graphical front-end for RAxML. Org Divers Evol 12:335–337

Stamatakis A (2006) RAxML-VI-HPC: maximum likelihood-based phylogenetic analyses with thousands of taxa and mixed models. Bioinformatics 22:2688–2690

Tamura M, Lauener LA (1979) A synopsis of *Aconitum* subgenus *Lycoctonum*: II. Notes R Bot Gard Edinb 37:431–466

Wyman SK, Jansen RK, Boore JL (2004) Automatic annotation of organellar genomes with DOGMA. Bioinformatics 20(17):3252–3255

Xiao PG, Wang FP, Gao F, Yan LP, Chen DL, Liu Y (2005) A pharmacophylogenetic study of *Aconitum* L. (Ranunculaceae) from China. Acta Phytotaxon Sin 44:1–46

Zhang T, Zeng CX, Yang JB, Li HT, Li DZ (2016) Fifteen novel universal primer pairs for sequencing whole chloroplast genomes and a primer pair for nuclear ribosomal DNAs. J Syst Evol 54(3):219–227

A comparison of chloroplast genome sequences in *Aconitum* (Ranunculaceae): a traditional herbal medicinal genus

Hanghui Kong[1,4,*], Wanzhen Liu[2,*], Gang Yao[3] and Wei Gong[2]

[1] Key Laboratory of Plant Resources Conservation and Sustainable Utilization, South China Botanical Garden, Chinese Academy of Sciences, Guangzhou, China
[2] College of Life Sciences, South China Agricultural University, Guangzhou, China
[3] College of Forestry and Landscape Architecture, South China Agricultural University, Guangzhou, China
[4] Guangdong Provincial Key Laboratory of Applied Botany, South China Botanical Garden, Chinese Academy of Sciences, Guangzhou, China
[*] These authors contributed equally to this work.

ABSTRACT

The herbal medicinal genus *Aconitum* L., belonging to the Ranunculaceae family, represents the earliest diverging lineage within the eudicots. It currently comprises of two subgenera, *A.* subgenus *Lycoctonum* and *A.* subg. *Aconitum*. The complete chloroplast (cp) genome sequences were characterized in three species: *A. angustius*, *A. finetianum*, and *A. sinomontanum* in subg. *Lycoctonum* and compared to other *Aconitum* species to clarify their phylogenetic relationship and provide molecular information for utilization of *Aconitum* species particularly in Eastern Asia. The length of the chloroplast genome sequences were 156,109 bp in *A. angustius*, 155,625 bp in *A. finetianum* and 157,215 bp in *A. sinomontanum*, with each species possessing 126 genes with 84 protein coding genes (PCGs). While genomic rearrangements were absent, structural variation was detected in the LSC/IR/SSC boundaries. Five pseudogenes were identified, among which Ψ*rps*19 and Ψ*ycf* 1 were in the LSC/IR/SSC boundaries, Ψ*rps*16 and Ψ*inf* A in the LSC region, and Ψ*ycf* 15 in the IRb region. The nucleotide variability (*Pi*) of *Aconitum* was estimated to be 0.00549, with comparably higher variations in the LSC and SSC than the IR regions. Eight intergenic regions were revealed to be highly variable and a total of 58–62 simple sequence repeats (SSRs) were detected in all three species. More than 80% of SSRs were present in the LSC region. Altogether, 64.41% and 46.81% of SSRs are mononucleotides in subg. *Lycoctonum* and subg. *Aconitum*, respectively, while a higher percentage of di-, tri-, tetra-, and penta-SSRs were present in subg. *Aconitum*. Most species of subg. *Aconitum* in Eastern Asia were first used for phylogenetic analyses. The availability of the complete cp genome sequences of these species in subg. *Lycoctonum* will benefit future phylogenetic analyses and aid in germplasm utilization in *Aconitum* species.

Subjects Biodiversity, Evolutionary Studies, Genomics, Plant Science

Keywords *Aconitum*, Chloroplast genome, Herbal medicine, Next generation sequencing, Phylogenetic reconstruction, Ranunculaceae

Submitted 15 June 2017
Accepted 20 October 2017
Published 7 November 2017

Corresponding author
Wei Gong, wgong@scau.edu.cn

Academic editor
Michael Wink

Additional Information and Declarations can be found on page 14

DOI 10.7717/peerj.4018

Copyright
2017 Kong et al.

Distributed under
Creative Commons CC-BY 4.0

OPEN ACCESS

How to cite this article Kong et al. (2017), A comparison of chloroplast genome sequences in *Aconitum* (Ranunculaceae): a traditional herbal medicinal genus. **PeerJ 5:e4018; DOI 10.7717/peerj.4018**

INTRODUCTION

The chloroplast (cp) is an intracellular organelle that plays an important role in the process of photosynthesis and it is widely present in algae and plants (*Neuhaus & Emes, 2000*; *Inoue, 2011*). The cp genome in angiosperms is a circular DNA molecule with a typically quadripartite structure, consisting of two copies of a large inverted repeat (IR) region that separates a large-single-copy (LSC) region from a small-single-copy (SSC) region (*Raubeson & Jansen, 2005*; *Yang et al., 2010*; *Green, 2011*; *Wicke et al., 2011*). Although highly conserved among plants, some differences in gene synteny, copy number and pseudogenes have been observed in cp genome structures (*Roy et al., 2010*; *Lei et al., 2016*; *Ivanova et al., 2017*). A complete cp genome is valuable for plant taxonomical analyses, phylogenetic reconstructions, speciation processes, and biogeographical inferences at different taxonomic levels. The cp genome is useful in investigating the maternal origin in plants, especially those with polyploid species, due to their haploid maternal inheritance and high conservation in gene content and genome structure (*Birky, 1995*; *Soltis & Soltis, 2000*; *Song et al., 2002*). High-throughput sequencing technologies have enabled a rapid increase in the completion of cp genomes and have shifted the study of phylogenetics to phylogenomics. Highly informative universal markers based on indels, substitutions, and inversions of the cp genome have been further developed for various molecular studies in plants.

The genus *Aconitum* L. belongs to the tribe Delphinieae in the Ranunculaceae family and represents one of the earliest diverging lineages within the eudicots APG IV (*Wang et al., 2009*; *Sun et al., 2011*; *The Angiosperm Phylogeny Group et al., 2016*). It is currently divided into two subgenera, *A*. subgenus *Lycoctonum* and *A*. subgenus *Aconitum*, comprising about more than 400 species throughout Eurasia and North America with its diversification center in Eastern Asia (*Utelli, Roy & Baltisberger, 2000*; *Jabbour & Renner, 2012*; *Wang et al., 2013*). Polyploid species were identified in both subgenera, particularly in subg. *Lycoctonum*. One of the tetraploid species in subg. *Lycoctonum* is *A. angustius* ($2n = 4x = 32$), which possesses heterologous chromosomes and is hypothesized to be a hybrid of *A. finetianum* ($2n = 2x = 16$) and *A. sinomontanum* ($2n = 2x = 16$) (*Gao, 2009*; *Kong et al., 2017b*). The three species display intermediate morphological characteristics and overlapping geographical distributions (*Shang & Lee, 1984*; *Yuan & Yang, 2006*; *Gao, 2009*; *Gao, Ren & Yang, 2012*). Based on previous morphological analysis and phylogenetic inference, *A. finetianum* was inferred to be the putative maternal progenitor of *A. angustius* (*Gao, 2009*; *Kong et al., 2017b*).

The genus *Aconitum* is known as a taxonomically and phylogenetically challenging taxon. Early divergence between subg. *Lycoctonum* and subg. *Aconitum* in Europe was suggested based on *trn*H-*psb*A and ITS (*Utelli, Roy & Baltisberger, 2000*). Although high morphological variability within and among populations was detected due to recent speciation, the morphological characteristics are poor indicators of relatedness. *Jabbour & Renner (2012)* conducted a phylogenetic reconstruction focusing on Delphineae based on *trn*L-F and ITS that suggested *Aconitum* was monophyletic clade and a sister group of *Delphinium*. However, few species from Eastern Asia were used, which may have affected

the previous phylogenetic analysis. Most recently, phylogenetic inferences of polyploid species relationships in subg. *Lycoctonum* were made using four cpDNA intergenic regions (*ndh*F-*trn*L, *psb*A-*trn*H, *psb*D-*trn*T, and *trn*T-L) and two nrDNA regions (ITS and ETS) (*Kong et al., 2017b*), *Aconitum finetianum* was inferred as the maternal progenitor of *A. angustius*. With the same cpDNA intergenic regions, taxonomical revision has been conducted based on phylogenetic analyses of subg. *Lycoctonum* by *Hong et al. (2017)*, yet phylogenetic information at the genomics level has been absent.

Although some *Aconitum* species are highly toxic because of aconite alkaloid, many species are essential in the formulation of traditional herbal medicine in Asia (*Zhao et al., 2010*; *Semenov et al., 2016*; *Wada et al., 2016*; *Liang et al., 2017*). The current state of *Aconitum* phylogenetics lacks molecular information of some species in Eastern Asia, and thus inhibits identification and germplasm utilization of this genus. In this study, we report the complete cp genome sequences of three species in subg. *Lycoctonum*; we established and characterized the organization of the cp genome sequences of tetraploid *A. angustius* as well as diploid *A. finetianum* and *A. sinomontanum*. We further compared the structure, gene arrangement and microsatellite repeats (SSRs) with the related species in both subgenera of *Aconitum*. Altogether, 14 species and two varieties from *Aconitum* were used for phylogenetic reconstruction at the genomic level. Seven previously unanalyzed species from the subg. *Aconitum* in Eastern Asia were investigated for phylogenetic relationships, and the maternal origin of *A. finetianum* was explored in the tetraploid, *A. angustius*. Our results provide cp genomic information for taxonomical identification, phylogenetic inference, or the population history of *Aconitum* or Ranunculaceae, which can also aid in the utilization of the genetic resources of *Aconitum* as a traditional herbal medicine.

MATERIALS AND METHODS

Plant samples and DNA extraction

Fresh leaves were collected from *A. angustius*, *A. finetianum* and *A. sinomontanum* growing in the greenhouse of South China Botanical Garden, Chinese Academy of Sciences. Total genomic DNA was extracted from the fresh leaves of *A. angustius*, *A. finetianum* and *A. sinomontanum* using the modified CTAB method (*Doyle & Doyle, 1987*). The DNA concentration was quantified using a Nanodrop spectrophotometer (Thermo Scientific, Carlsbad, CA, USA), and a final DNA concentration of >30 ng/μL was used for Illumina sequencing.

Chloroplast genome sequencing, assembly and annotation

We sequenced the complete cp genome of *A. angustius*, *A. finetianum* and *A. sinomontanum* with an Illumina HiSeq 2000 at Beijing Genomics Institute (BGI) in Wuhan, China. Genomic DNA was fragmented randomly and then the required length of DNA fragments was obtained by electrophoresis. Adapters were ligated to DNA fragments followed by cluster preparation and sequencing. A paired-end library was constructed with 270 bp insert size, and then 150 bp paired reads were sequenced using an Illumina HiSeq 2000.

We assembled the cp genomes using Geneious 9.1.4 (Biomatters Ltd., Auckland, New Zealand) with BLAST and map reference tools, respectively. Using the program

DOGMA (http://dogma.ccbb.utexas.edu/) (*Wyman, Jansen & Boore, 2004*) and Geneious, annotation was performed in comparison with the cp genomes of *A. reclinatum* (MF186593) (*Kong et al., 2017a*), *A. barbatum* var. *puberulum* (KC844054) (*Chen et al., 2015*), and *A. barbatum* var. *hispidum* (KT820664) in subg. *Lycoctonum* as well as 10 species from the subg. *Aconitum* (*Choi et al., 2016*; GB Kim, CE Lim & JH Mun, 2016, unpublished data; *Lim et al., 2017*; D Yang, 2016, unpublished data; SG Yang et al., 2017, unpublished data) (Table 1). Altogether, 14 species and two varieties in both subgenera of *Aconitum* were used for annotation (Table 1). Among those species, *A. angustius*, *A. finetianum*, *A. sinomontanum*, *A. barbatum* var. *hispidum*, and *A. barbatum* var. *puberulum* were collected from China (*Chen et al., 2015*), *A. reclinatum* came from the United States (*Kong et al., 2017a*), while the remaining species were all sampled from Korea (*Choi et al., 2016*; GB Kim, CE Lim & JH Mun, 2016, unpublished data; *Lim et al., 2017*; D Yang, 2016, unpublished data; SG Yang et al., 2017, unpublished data). Chloroplast genome sequences of *Aconitum* species from Europe were not available in GenBank.

The annotation of tRNA genes were confirmed using the ARAGORN program (*Laslett & Canback, 2004*), and then manually adjusted using the program Geneious. Contigs with BLAST hits to consensus sequence from the "map to reference function" were assembled manually to construct complete chloroplast genomes. Finally, the circular genome maps of the three species were illustrated using the Organellar Genome DRAW tool (OGDRAW, http://ogdraw.mpimp-golm.mpg.de/) (*Lohse et al., 2013*). The annotated chloroplast genomic sequences of *A. angustius*, *A. finetianum* and *A. sinomontanum* have been submitted to GenBank (Accession Number: MF155664, MF155665 and MF155666).

Genome comparison and divergence hotspot

The cp genome sequences from the finalized data set were aligned with MAFFT v7.0.0 (*Katoh & Frith, 2012*) and adjusted manually when necessary. Based on many other cp genome studies, the IRs expansion/contraction could lead to changes in the structure of the cp genome, leading to the length variation of angiosperm cp genomes and contributing to the formation of pseudogenes (*Kim & Lee, 2004*; *Nazareno, Carlsen & Lohmann, 2015*; *Ivanova et al., 2017*). Therefore, we conducted comparative analysis to detect the variation in the LSC/IR/SSC boundaries among the species/varieties. Comparative analysis of the nucleotide diversity (*Pi*) among the complete cp genomes of *Aconitum* was performed based on a sliding window analysis using DnaSP 5.10 (*Librado & Rozas, 2009*). The window length was 600 bp and step size was 200 bp. To test and visualize the presence of genome rearrangement and inversions, gene synteny was performed using MAUVE as implemented in Geneious with default settings based on 14 species and two varieties in both subgenera.

Simple sequence repeats analysis

MISA (http://pgrc.ipk-gatersleben.de/misa/misa.html) (*Thiel et al., 2003*) is a tool for the identification and location of perfect microsatellites and compound microsatellites (two individual microsatellites, disrupted by a certain number of bases). We used MISA to search for potential simple sequence repeats (SSRs) loci in the cp genomes of the three species. The minimum number (thresholds) of SSRs was set as 10, 5, 4, 3, and 3 for

Table 1 Summary of characteristics in chloroplast genome sequences of thirteen species and two varieties in *Aconitum*.

	GenBank no.	Voucher number/herbarium	Total genome size (bp)	LSC (bp)	SSC (bp)	IR (bp)	Total number of genes	Protein-coding genes	tRNA genes	rRNA genes	GC content
subg. *Lycoctonum*											
A. angustius	MF155664	ZY37/IBSC	156,109	86,719	16,914	26,225	126	84	38	4	38%
A. finetianum	MF155665	ZY25/IBSC	155,625	86,664	17,107	25,927	126	84	38	4	38%
A. sinomontanum	MF155666	ZY46/IBSC	157,215	88,074	16,926	26,090	126	84	38	4	38%
A. reclinatum	MF186593	US17/IBSC	157,354	88,269	16,963	26,061	127	86	37	4	38%
A.barbatum var. *puberulum*	KC844054	Not provided/-	156,749	87,630	16,941	26,089	127	85	38	4	38%
A.barbatum var. *hispidum*	KT820664	VP0000486327/NIBR	156,782	87,661	16,987	26,067	127	85	38	4	38%
subg. *Aconitum*											
A. austrokoreense	KT820663	VP0000494173/NIBR	155,682	86,388	17,054	26,120	126	83	39	4	38.1%
A.carmichaelii	KX347251	ACAR20151205/-	155,737	86,330	17,021	26,193	124	83	37	4	38.1%
A. chiisanense	KT820665	VP0000494177/NIBR	155,934	86,559	17,085	26,145	125	82	39	4	38.1%
A. ciliare	KT820666	VP0000486323/NIBR	155,832	86,452	17,084	26,148	126	83	39	4	38.1%
A. coreanum	KT820667	VP0000486326/NIBR	157,029	87,622	17,035	26,186	128	86	38	4	38.0%
A. jaluense	KT820669	VP0000494219/NIBR	155,926	86,406	17,090	26,215	126	83	39	4	38.1%
A. japonicum	KT820670	VP0000494223/NIBR	155,878	86,480	17,104	26,147	127	84	39	4	38.1%
A. kusnezoffii	KT820671	VP0000529885/NIBR	155,862	86,335	17,103	26,212	126	84	39	4	38.1%
A. monanthum	KT820672	VP0000529886/NIBR	155,688	86,292	16,996	26,200	125	82	39	4	38.1%
A. volubile	KU556690	MBC_KIOM-2015-73/KIOM	155,872	86,348	16,944	26,290	126	83	38	4	38.1%

mono-, di-, tri-, tetra-, and penta-nucleotides SSRs, respectively. All of the repeats found were manually verified and the redundant ones were removed.

Phylogenetic analysis

Four species and two varieties in subg. *Lycoctonum* and 10 species in subg. *Aconitum* were used for phylogenetic reconstruction, with *Megaleranthis saniculifolia and Clematis terniflorav* as the outgroup. Except for *A. kusnezoffii*, *A. volubile*, and *A. ciliare*, the remaining seven species in subg. *Aconitum* from Korea were first used for phylogenetic analysis. The complete cp genome sequences and PCGs were used for the phylogenetic reconstruction of *Aconitum* species in Eastern Asia. Three different methods including Bayesian Inference (BI), Maximum Parsimony (MP), and Maximum Likelihood (ML) were employed. In all analyses, gaps were treated as missing.

Bayesian Inference (BI) of the phylogenies was performed using MrBayes v.3.2 (*Huelsenbeck & Ronquist, 2001*; *Ronquist & Huelsenbeck, 2003*). The best model was determined for each sequence partition, after comparisons among 24 models of nucleotide substitution using Modeltest v.3.7 (*Posada & Crandall, 1998*). We performed MP using PAUP* v.4.0b10 (*Swofford, 2002*). We calculated the bootstrap values with 1,000 bootstrap replicates, each with 10 random sequence addition replicates holding a single tree for each run. We conducted ML using RAxML (*Stamatakis, 2006*) and the RAxML graphical interface (raxmlGUI v.1.3 (*Silvestro & Michalak, 2012*)) with 1,000 rapid bootstrap replicates. The general time-reversible (GTR) model was chosen with a gamma model for the rate of heterogeneity.

RESULTS AND DISCUSSION

Genome organization and features

Using the Illumina HiSeq 2000 sequencing platform, a total number of 2 × 150 bp pair-end reads ranging from 9,879,068 to 27,530,148 bp were produced for the three species in subg. *Lycoctonum*. Altogether, 1,270 Mb of clean data were produced for *A. angustius*, 3,586 Mb for *A. finetianum,* and 3,590 Mb for *A. sinomontanum*. The assembly generated an average of 6,713 contigs with a N50 length of 732 bp for *A. angustius*, an average of 6,201 contigs with a N50 length of 801 bp bp for *A. finetianum*, and an average of 6,999 contigs with a N50 length of 769 bp for *A. sinomontanum*. Scaffolds from the assembly with k-mer values of 35 to 149 were matched to reference cp genome sequences, which were used to determine the relative position and direction respectively. We generated a new draft chloroplast genome by manually identifying the overlapping regions. To further refine the draft genome, the quality and coverage of each was double-checked by remapping reads. The complete cp genome sequences of the three species with full annotations were deposited into GenBank.

The size of the cp genomes was 156,109 bp for *A. angustius*, 155,625 bp for *A. finetianum* and 157,215 bp for *A. sinomontanum* (Table 1). The chloroplast genomes displayed a typical quadripartite structure, including a pair of IRs (25,927–26,225 bp) separated by LSC (86,664–88,074 bp) and SSC (16,914–17,107 bp) regions (Fig. 1 and Table 1). The GC content of the three cp genomes was 38.00%, demonstrating congruence with other *Aconitum* species (38.00% or 38.10%) (Table 1).

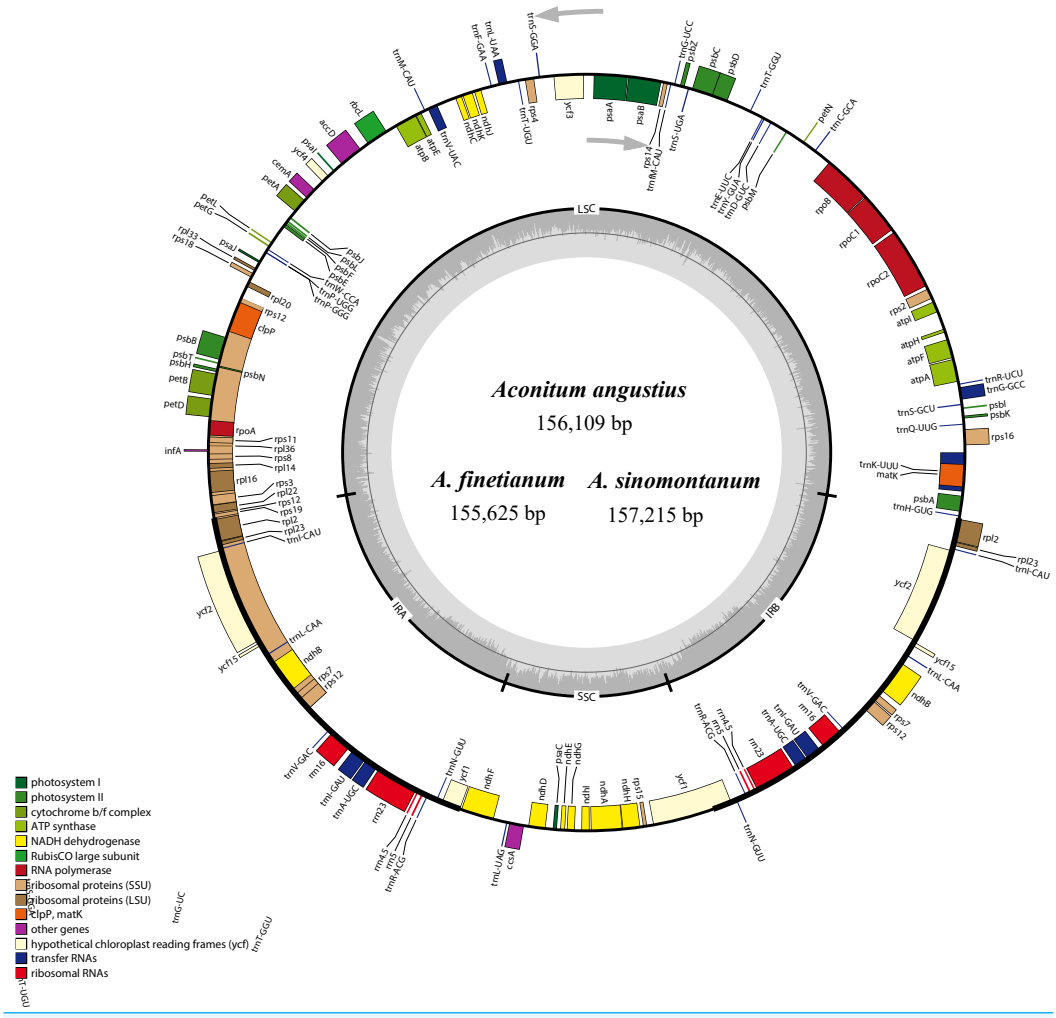

Figure 1 The gene maps of *Aconitum angustius*, *A. finetianum*, and *A. sinomontanum*. The genes lying inside and outside the circles are transcribed in the clockwise and counterclockwise directions, respectively. Different colors denote the genes belonging to different functional groups. The thicknesses indicate the extent of the inverted repeats (IRa and IRb) that separate the small single-copy (SSC) region from the large single-copy (LSC) region. The dark gray in the inner circle corresponds to GC content, and the light gray to AT content.

Full-size DOI: 10.7717/peerj.4018/fig-1

When duplicated genes in the IR regions were counted only once, each of the three cp genomes of *A. sinomontanum* 126 predicted functional genes, including 84 PCGs, 38 tRNA genes, and four rRNA genes. The remaining non-coding regions include introns, intergenic spacers, and pseudogenes. Altogether 18 genes were duplicated in the IR regions, including seven PCGs, seven tRNA genes, and four rRNA genes (Fig. 1; Table S1). Each of the thirteen genes (eight PCGs and five tRNA genes) contained one interval, and three PCGs (*clp*P, *ycf* 3 and *rps*12) had two intervals each (Table S1). The maturase K (*mat* K) gene in the cp genomes of the three species is located within *trn*K intron, which is similar in most of the other plants species (*Kong & Yang, 2017*). In the IR regions, the four rRNA genes and two tRNA genes (*trn*I and *trn*A) are clustered as 16S-*trn*I-*trn*A-23S-4.5S-5S. This has also been

reported in the cp genomes of *A. barbatum* var. *hispidum*, *A. barbatum* var. *puberulum*, and many other plant species (*Mardanov et al., 2008*; *Wu et al., 2014*; *Chen et al., 2015*).

Comparative analysis of genomic structure

Synteny analysis identified a lack of genome rearrangement and inversions in the cp genome sequences of the *Aconitum* species. No gene rearrangement and inversion events were detected (Fig. S1). Genomic structure, including gene number and gene order, is highly conserved among the *Aconitum* species; however, structural variation was still present in the LSC/IR/SSC boundaries (Fig. 2). The genes *rps*19-*rp*12-*trn*H and *ycf* 1-*ndh*F were located between the junction of the LSC/IR and SSC/IR regions. The *rps*19 gene crosses the LSC/IRa junction region in *A. sinomontanum*, *A. barbatum* var. *puberulum* and *A. barbatum* var. *hispidum* of subg. *Lycoctonum*, as well as in *A. jaluense*, *A. volubile*, *A. carmichaelii*, *A. kusnezoffii* and *A. monanthum* of subg. *Aconitum*. As a result, the *rps*19 gene has apparently lost its protein-coding ability due to being partially duplicated in the IRb region, thus a producing pseudogenized Ψ*rps*19 gene. The same was found with the *ycf* 1 gene, as the IRb/SSC junction region is located within the *ycf* 1 CDS region and only a partial gene is duplicated in the IRa region, resulting in a pseudogene. This is a general structure among the dicots. The Ψ*ycf* 1 pseudogene in the IR region was 1,279 bp for two varieties in subg. *Lycoctonum* and seven species in subg. *Aconitum*. However, length variation was present in the IR of the remaining six species: 1,292 bp in *A. angustius*, *A sinomontanum*, and *A. reclinatum*; 1,165 bp in *A. finetianum*; 1,274 bp in *A. chiisanense*; 1,356 bp in *A. volubile*; and 1,263 bp in *A. carmichaelii* (Fig. 2; Table 2).

Three pseudogenes, Ψ*ycf* 15, Ψ*rps*16, and Ψ*inf* A, were identified in the gene annotations (Table 2). The Ψ*ycf* 15 gene is pseudolized in *A. austrokoreense* and *A. chiisanense* with four base insertions and pseudolized in *A. monanthum* with a one base insertion, contributing to several internal stop codons. The Ψ*inf* A region is pseudogenized with two nonsynonymous substitutions producing internal stop codons in all of the members of subg. *Lycoctonum*. This pseudogenized Ψ*inf* A gene has also been found in other angiosperm chloroplast genomes (*Roman & Park, 2015*; *Lu, Li & Qiu, 2017*). The gene *rps*16 encodes the ribosomal protein S16 and is present in the cp genome of most if the higher plants. However, *rps*16 has been functionally lost in various plant species (*Roy et al., 2010*). A pseudogene Ψ*rps*16 was also present in the cp genomes of *A. angustius*, *A. finetianum* and *A. reclinatum* in subg. *Lycoctonum* as well as in the nine species in subg. *Aconitum* due to the loss of one CDS region (Table 2). As has been revealed in other studies, the functional loss of the *rps*16 gene might be compensated by the dual targeting of the nuclear *rps*16 gene product (*Keller et al., 2017*).

Sequence divergence among the species in *Aconitum*

The average nucleotide variability (*Pi*) values were estimated to be 0.00549, ranging from 0 to 0.03856, based on the comparative analysis of cp genome sequences in *Aconitum* species. The highest variation was found in the LSC and SSC regions, with an average $Pi = 0.007140$ and 0.008368, respectively. The IR regions had a much lower nucleotide diversity with

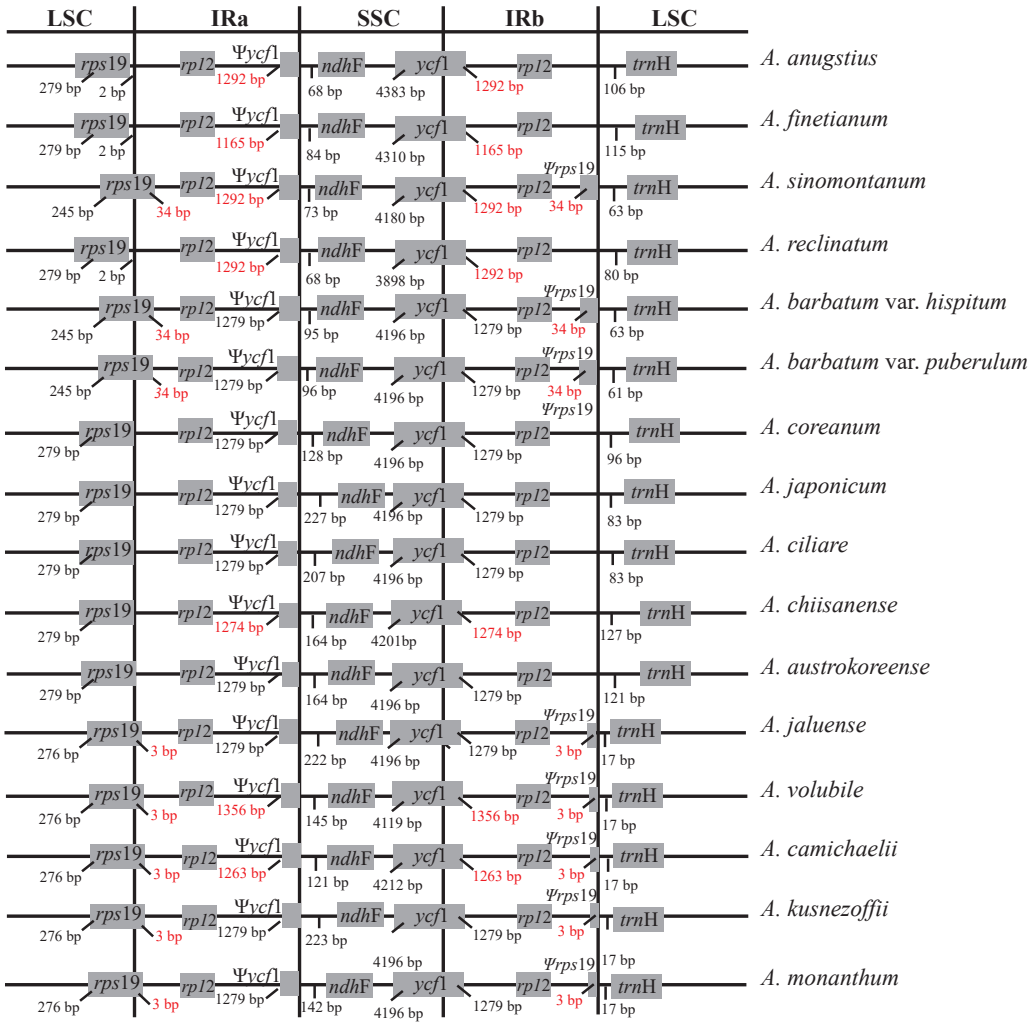

Figure 2 Comparison of the border positions of LSC, SSC and IR repeat regions among fourteen species and two varieties in *Aconitum*. Genes are denoted by grey boxes and the gaps between the genes and the boundaries are indicated by the base lengths (bp). Extensions of the genes are also indicated above the boxes.

Full-size DOI: 10.7717/peerj.4018/fig-2

Pi = 0.001079 and 0.001459. Eight intergenic regions (*trn*H-*psb*A, *trn*K-*rps*16, *trn*D-*trn*Y, *trn*Y-*trn*E, *trn*E-*trn*T, *trn*T-*trn*L, *rpl*12-*clp*P and *trn*H-*trn*R) were highly variable, with *Pi* value ~0.023 (Fig. 3). The former eight loci are present in the LSC, while the pseudogene Ψ*ycf* 1 is in the SSC region. The single-copy regions have been demonstrated to be highly variable with loci clustered in 'hot spots' (*Kong & Yang, 2017*). Among the eight intergenic regions, *trn*H-*psb*A and *trn*T-*trn*L are variable and useful for phylogenetic reconstruction in the subg. *Lycoctonum* (*Utelli, Roy & Baltisberger, 2000*; *Kong et al., 2017b*). However, the other intergenic regions, even with higher nucleotide variability, have never been involved in the phylogenetic analysis for the genus *Aconitum*. The highly variable loci detected in the current study may provide a basis for further phylogenetic characterization of this

Table 2 The distribution of the five pseudogenes in *Aconitum*.

Locations	LSC		LSC/IRa	IRa	IRa/SSC
Genes	Ψ*rps*16	Ψ*inf* A	Ψ*rps*19	Ψ*ycf* 15	Ψ*ycf* 1
Aconitum* subg. *Lycoctonum					
A. angustius	+				+/1,292 bp
A. finetianum	+				+/1,165 bp
A. sinomontanum		+	+/34 bp		+/1,292 bp
A. reclinatum	+	+			+/1,292 bp
A. barbatum var. *puberulum*		+	+/34 bp		+/1,279 bp
A. barbatum var. *hispidum*		+	+/34 bp		+/1,279 bp
Aconitum* subg. *Aconitum					
A. austrokoreense	+			+/4 bp indel	+/1,279 bp
A. carmichaelii	+		+/3 bp		+/1,263 bp
A. chiisanense	+			+/4 bp indel	+/1,274 bp
A. ciliare	+				+/1,279 bp
A. coreanum	+				+/1,279 bp
A. jaluense	+		+/3 bp		+/1,279 bp
textitA. japonicum	+				+/1,279 bp
A. kusnezoffii	+		+/3 bp		+/1,279 bp
A. monanthum	+		+/3 bp	+/1 bp indel	+/1,279 bp
A. volubile	+		+/3 bp		+/1,356 bp

Notes.
+, indicating the presence of pseudogenes.

genus. The observed divergence hotspot regions provide abundant information for marker development in phylogenetic analysis or conservation genetics of *Aconitum*.

Characterization of simple sequence repeats

MISA was used to identify SSRs with minimum a of 10 bp repeats among the three species. In *A. angustius*, 60 SSRs were found, while 62 SSRs were found in *A. finetianum*, and 58 in *A. sinomontanum*. This result is comparable with *A. reclinatum* (61 SSRs), *A. barbatum* var. *hispidum* (53 SSRs), and *A. barbatum* var. *puberulum* (57 SSRs). An average of 59 SSRs were identified in subg. *Lycoctonum*, which is relatively higher than that of subg. *Aconitum* (47). In both subgenera, most SSRs are in the LSC regions, accounting for an average of 85.31% and 80.85% in subg. *Lycoctonum* and subg. *Aconitum*, respectively. Among all of the SSRs, the mononucleotide A/T repeat units occupied the highest proportion, with 64.41% and 46.82% of the total SSRs in subg. *Lycoctonum* and subg. *Aconitum*, respectively. Although few SSRs were detected in subg. *Aconitum*, a higher proportion of di-, tri-, tetra- and penta-nucleotide repeats were detected (Table 3). The SSRs have a remarkably high A/T content with only seven SSRs, namely $(ATCT)_3$, $(TTCT)_3$, $(CTTT)_3$, $(TAAAG)_3$, $(TTTC)_3$, $(ATAC)_3$ and $(CATT)_3$, that contain one C or G nucleotide.

A total of 11 cp SSR loci were shared among the cp genomes of tetraploid *A. angustius* and diploid *A. finetianum*. No common cp SSRs were specifically found between *A. angustius* and *A. sinomontanum*. This result provides evidence of the maternal origin of the tetraploid *A. angustius* from diploid *A. finetianum*, which is consistent with previous research

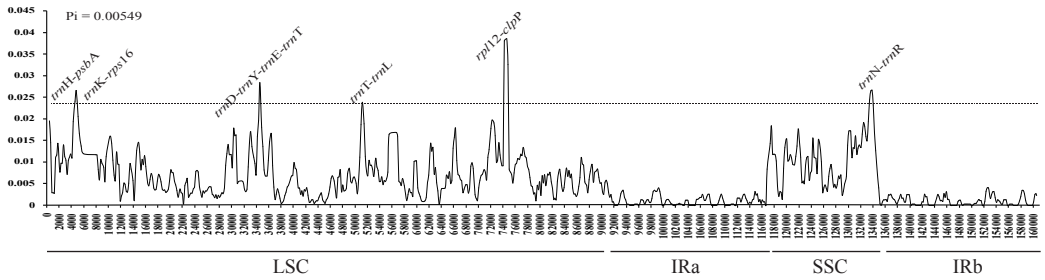

Figure 3 Sliding window analysis of the whole cp genome for fourteen species and two varieties in *Aconitum*. *X*-axis, position of the midpoint of a window; *Y*-axis, nucleotide diversity (*Pi*) of each window.

Full-size DOI: 10.7717/peerj.4018/fig-3

(*Gao, 2009*; *Kong et al., 2017b*). Among the three species, the highest number of unique SSRs loci were present in *A. sinomontanum* (11) followed by *A. angustius* (7), *A. finetianum* (6), and *A. reclinatum* (5).

Phylogenetic analyses

In the present study, three phylogenetic methods (BI, MP and ML) resulted in identical phylogenetic trees within each data set. Different analyses based on the two datasets generated largely congruent topologies (Fig. 4). The total aligned length with parsimony informative loci was 178,392 bp with 4,342 for the complete cp genome sequences, and 106,535 bp with 3,164 for PCGs, respectively. All of the phylogenetic trees support that *Aconitum* comprises two monophyletic subgenera. High Bayesian posterior probabilities and bootstrap values were detected at most nodes, particularly based on the complete cp genomes (Fig. 4A).

The phylogenetic relationship of Korean species in subg. *Aconitum* was investigated for the first time. The monophyletic clade was formed by *A. ciliare*, *A. carmichaelii*, *A. japonicum* subsp. *napiforme* and *A. kusnezoffii*, with strong support values (Fig. 4). The clade comprised of *A. jaluense* subsp. *jaluense* and *A. volubile* exhibited moderate-to-high support, forming a monophyletic sister group. The positions of the four species *A. ciliare*, *A. carmichaelii*, *A. austrokoreense*, and *A. chiisanense*, demonstrated inconsistencies based on the two data sets. Obviously, these species received stronger support based on the sequences of the complete cp genome rather than PCGs, indicating that whole genomes are more efficient in determining phylogenetic relatedness in *Aconitum* than PCGs alone.

Based on the phylogenetic tree, the tetraploid *A. angustius* was always closely related with diploid *A. finetianum*, which further supports previous research (*Kong et al., 2017b*). The two species co-occur on several mountains in southeast China and even grow very closely within a community (*Yuan & Yang, 2006*). They show similar morphological characteristics in having three-part leaves, the cylindric upper sepals and retrosely pubescent pedicels, resulting in common misidentification (*Gao, Ren & Yang, 2012*). *Aconitum finetianum* is the most likely maternal progenitor of *A. angustius* based on both molecular phylogenetic and morphological evidence (*Kong et al., 2017b*); therefore, it is reasonable to see that the two species have a close phylogenetic relationship.

Table 3 Number of chloroplast SSRs in different regions or different types present in *Aconitum* species.

Species						Number of SSRs in different regions			
	Homo (>10)	Di (>5)	Tri (>5)	Te(>3)	Pen (>3)	LSC	SSC	IR	Total
subg. *Lycoctonum*	38 (64.41%)	10 (16.95%)	3 (4.80%)	8 (12.99%)	0 (0.00%)	50 (85.31%)	7 (11.02%)	2 (3.39%)	59
A. angustius	40	9	2	8	1	50	8	2	60
A. finetianum	42	9	2	8	1	51	9	2	62
A. sinomontanum	36	12	2	8	0	50	6	2	58
A. reclinatum	42	10	2	7	0	53	6	2	61
A. barbatum var. *puberulum*	36	10	2	8	0	49	5	2	56
A. barbatum var. *hispidum*	32	10	7	7	0	49	5	2	56
subg. *Aconitum*	22 (46.81%)	15 (31.91%)	1 (21.28%)	7 (14.89%)	1 (21.28%)	38 (80.85%)	7 (14.89%)	2 (4.36%)	47
A. austrokoreense	22	15	0	7	0	32	10	2	44
A. carmichaelii	21	16	1	7	0	37	6	2	45
A. chiisanense	21	16	1	7	2	39	6	2	47
A. ciliare	23	16	1	7	1	41	5	2	48
A. coreanum	39	14	1	7	1	50	10	2	62
A. jaluense	17	14	1	6	2	33	6	2	41
A. japonicum	20	16	1	7	1	37	6	2	46
A. volubile	17	15	1	6	1	35	3	2	40
A. kusnezoffii	19	16	1	7	1	37	5	2	44
A. monanthum	18	13	0	7	2	36	9	2	47

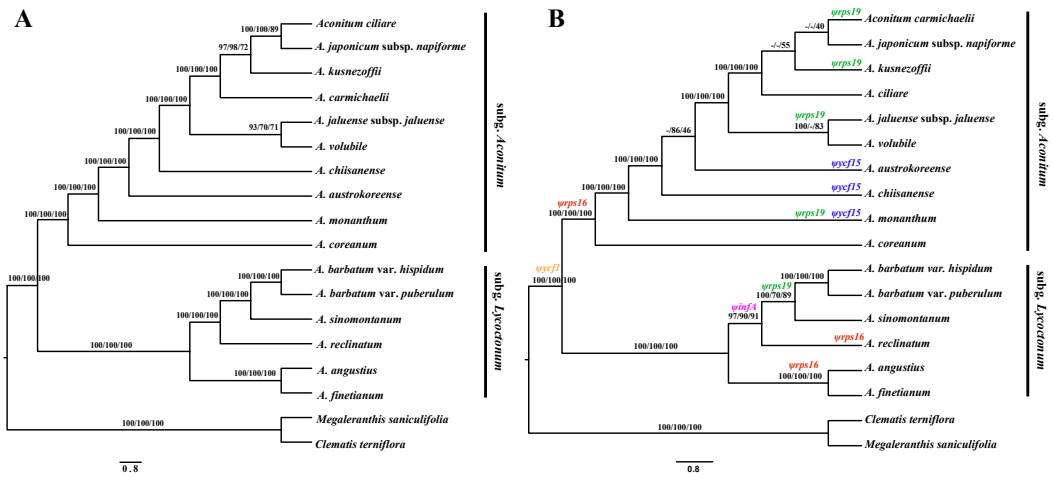

Figure 4 Phylogenomic relationship among *Aconitum* species. Based on the two data sets of complete cp genome sequences (A) and PCGs (B), respectively, phylogenetic reconstruction was conducted using three methods: Bayesian Inference (BI), Maximum Parsimony (MP) and Maximum Likelihood (ML). Numbers above the branches represent BI posterior probabilities, MP and ML bootstrap values. The pseudogenes are indicated above the branches in different colors on the phylogenetic tree based on PCGs (B).
Full-size DOI: 10.7717/peerj.4018/fig-4

The five pseudogenes exhibit different evolutionary histories from each other. Concerning the evolution of Ψ*ycf15*, it occurs in only three species *A. monanthum*, *A. austrokoreense*, and *A. chiisanense* of subgen. *Aconitum*, which was probably pseudogenized once in each species independently and subsequently restored to a functional copy. We propose that Ψ*rps16* was pseudogenized during the divergence between the two subgenera and restored to a functional copy within the *A. sinomontanum*-*A. barbatum* clade of subgen. *Lycoctonum*. With respect to Ψ*rps19*, it appears to have been pseudogenized multiple times independently in phylogenetically distant species of the two subgenera. Ψ*ycf1* is commonly found among cp genomes of plant species. Within *Aconitum*, Ψ*ycf1* exhibits length variation and multiple convergent mutation events, which are not consistent with the phylogenetic relationships of the genus. Only Ψ*infA* shows an evolutionary history congruent with the phylogeny of *Aconitum* (Fig. 4B; Table 2). Overall, our results show that similarities among pseudo-gene sequences do not necessarily predict phylogenetic relationships among species.

ACKNOWLEDGEMENTS

We would like to provide a special thank to Dr. Tongjian Liu for his assistance in lab work and data analyses. We thank Dr. AJ Harris and LetPub (http://www.letpub.com) for their linguistic assistance during the preparation of this manuscript.

A. austrokoreense
A. coreanum
A. sinomontanum
A. austrokoreense
A. chiisanense
A. coreanum
A. sinomontanum

ADDITIONAL INFORMATION AND DECLARATIONS

Funding

This work was supported by the National Natural Science Foundation of China (31470319; 31470312) and Science and Technology Planning Project of Guangdong Province, China (2016A030303048; 2017A030303067). The funders had no role in study design, data collection and analysis, decision to publish, or preparation of the manuscript.

Grant Disclosures

The following grant information was disclosed by the authors:
National Natural Science Foundation of China: 31470319, 31470312.
Science and Technology Planning Project: 2016A030303048, 2017A030303067.

Competing Interests

The authors declare there are no competing interests.

Author Contributions

- Hanghui Kong and Wei Gong conceived and designed the experiments, analyzed the data, wrote the paper, prepared figures and/or tables, reviewed drafts of the paper.
- Wanzhen Liu performed the experiments, analyzed the data, contributed reagents/materials/analysis tools.
- Gang Yao wrote the paper, prepared figures and/or tables, reviewed drafts of the paper.

DNA Deposition

The following information was supplied regarding the deposition of DNA sequences:

Accession data available from GenBank (MF155664, MF155665 and MF155666) and from figshare (https://dx.doi.org/10.6084/m9.figshare.5092414.v1).

Data Availability

The following information was supplied regarding data availability:

Raw data for whole cp genome matrix: Kong, Hanghui (2017): cp_whole.nex. figshare. https://dx.doi.org/10.6084/m9.figshare.5092414.v1.

Raw data for CDs matrix: Kong, Hanghui (2017): CDS.fas.nex. figshare. https://dx.doi.org/10.6084/m9.figshare.5092420.v1.

The of cp genome sequences are contained at the GenBank accession numbers in Table 1.

Supplemental Information

Supplemental information for this article can be found online at http://dx.doi.org/10.7717/peerj.4018#supplemental-information.

REFERENCES

Birky CW. 1995. Uniparental inheritance of mitochondrial and chloroplast genes: mechanisms and evolution. *Proceedings of the National Academy of Sciences of the United States of America* **92(25)**:11331–11338 DOI 10.1073/pnas.92.25.11331.

Chen XC, Li QS, Li Y, Qian J, Han JP. 2015. Chloroplast genome of *Aconitum barbatum* var. *puberulum* (Ranunculaceae) derived from CCS reads using the PacBio *RS* platform. *Frontiers in Plant Science* **6(42)**:1–9 DOI 10.3389/fpls.2015.00042.

Choi JE, Kim GB, Lim CE, Yu HJ, Mun JH. 2016. The complete chloroplast genome of *Aconitum austrokoreense* Koidz (Ranunculaceae), an endangered endemic species in Korea. *Mitochondrial DNA Part B. Resources* **1(1)**:688–689 DOI 10.1080/23802359.2016.1219644.

Doyle JJ, Doyle JL. 1987. A rapid DNA isolation procedure for small quantities of fresh leaf tissue. *Phytochemical Bulletin* **19**:11–15.

Gao Q. 2009. Taxonomic revision of *Aconitum* L. subgenus *Lycoctonum* (DC.) *Peterm. (Ranunculaceae)* from China. D. Phil. Thesis, Institute of Botany, the Chinese Academy of Sciences, Beijing, China.

Gao Q, Ren C, Yang QE. 2012. Taxonomic status and distributional range of *Aconitum angustius* (Ranunculaceae) based on cytological evidence. *Nordic Journal of Botany* **30**:1–13 DOI 10.1111/j.1756-1051.2012.01506.x.

Green BR. 2011. Chloroplast genomes of photosynthetic eukaryotes. *The Plant Journal* **66**:34–44 DOI 10.1111/j.1365-313X.2011.04541.x.

Hong Y, Luo Y, Gao Q, Ren C, Yuan Q, Yang QE. 2017. Phylogeny and reclassification of *Aconitum* subgenus *Lycoctonum* (Ranunculaceae). *PLOS ONE* **12(1)**:e0171038 DOI 10.1371/journal.pone.0171038.

Huelsenbeck JP, Ronquist F. 2001. MRBAYES: Bayesian inference of phylogenetic trees. *Bioinformatics* **17**:754–755 DOI 10.1093/bioinformatics/17.8.754.

Inoue K. 2011. Emerging roles of the chloroplast outer envelope membrane. *Trends in Plant Science* **16(10)**:550–557 DOI 10.1016/j.tplants.2011.06.005.

Ivanova Z, Sablok G, Daskalova E, Zahmanova G, Apostolova E, Yahubyan G, Baev V. 2017. Chloroplast genome analysis of resurrection Tertiary relic *Haberlea rhodopensis* highlights genes important for desiccation stress response. *Frontiers of Plant Sciences* **8**:Article 204 DOI 10.3389/fpls.2017.00204.

Jabbour F, Renner SS. 2012. A phylogeny of *Delphinieae* (Ranunculaceae) shows that *Aconitum* is nested within *Delphinium* and that Late Miocene transitions to long life cycles in the Himalayas and Southwest China coincide with bursts in diversification. *Molecular Phylogenetics and Evolution* **62**:928–942 DOI 10.1016/j.ympev.2011.12.005.

Katoh K, Frith MC. 2012. Adding unaligned sequences into an existing alignment using MAFFT and LAST. *Bioinformatics* **28(23)**:3144–3146 DOI 10.1093/bioinformatics/bts578.

Keller J, Rousseau-Gueutin M, Martin GE, Morice J, Boutte J, Coissac E, Ourari M, Aïnouche M, Salmon A, Cabello-Hurtado F, Aïnouche A. 2017. The evolutionary fate of the chloroplast and nuclear *rps16* genes as revealed through the sequencing and comparative analyses of four novel legume chloroplast genomes from *Lupinus*. *DNA Research* **24(1)**:343–358 DOI 10.1093/dnares/dsx006.

Kim KJ, Lee HL. 2004. Complete chloroplast genome sequences from Korean ginseng (Panax *schinseng* Nees) and comparative analysis of sequence evolution among 17 vascular plants. *DNA Research* **11**:247–261 DOI 10.1093/dnares/11.4.247.

Kong HH, Liu WZ, Yao G, Gong W. 2017a. Characterization of the whole chloroplast genome of a rare and endangered species *Aconitum reclinatum* (Ranunculaceae) in the United States. *Conservation Genetics Resources* Epub ahead of print June 16 2017 DOI 10.1007/s12686-017-0789-y.

Kong WQ, Yang JH. 2017. The complete chloroplast genome sequence of *Morus cathayana* and *Morus multicaulis*, and comparative analysis within genus *Morus* L. *PeerJ* **5**:e3037 DOI 10.7717/peerj.3037.

Kong HH, Zhang Y, Hong Y, Barker MS. 2017b. Multilocus phylogenetic reconstruction informing polyploid relationships of *Aconitum* subgenus *Lycoctonum* (Ranunculaceae) in China. *Plant Systematics and Evolution* **303**:727–744 DOI 10.1007/s00606-017-1406-y.

Laslett D, Canback B. 2004. ARAGORN, a program to detect tRNA genes and tmRNA genes in nucleotide sequences. *Nucleic Acids Research* **32**:11–16 DOI 10.1093/nar/gkh152.

Lei WJ, Ni DP, Wang YJ, Shao JJ, Wang XC, Yang D, Wang JS, Chen HM, Liu C. 2016. Intraspecific and heteroplasmic variations, gene losses and inversions in the chloroplast genome of *Astragalus membranaceus*. *Scientific Reports* **6**:21669 DOI 10.1038/srep21669.

Liang X, Chen L, Song L, Fei W, He M, He C, Yin Z. 2017. Diterpenoid alkaloids from the root of *Aconitum sinchiangense* W.T. Wang with their antitumor and antibacterial activities. *Natural Product Research* **11**:1–8 DOI 10.1080/14786419.2016.1272113.

Librado P, Rozas J. 2009. DnaSP v5: a software for comprehensive analysis of DNA polymorphism data. *Bioinformatics* **25**:1451–1452 DOI 10.1093/bioinformatics/btp187.

Lim CE, Kim GB, Baek S, Han SM, Yu HJ, Mun JH. 2017. The complete chloroplast genome of *Aconitum chiisanense* Nakai (Ranunculaceae). *Mitochondrial DNA A* **28(1)**:75–76 DOI 10.3109/19401736.2015.1110805.

Lohse M, Drechsel O, Kahlau S, Bock R. 2013. OrganellarGenomeDRAW—a suite of tools for generating physical maps of plastid and mitochondrial genomes and visualizing expression data sets. *Nucleic Acids Research* **41(W1)**:W575–W581 DOI 10.1093/nar/gkt289.

Lu RS, Li P, Qiu YX. 2017. The complete chloroplast genomes of three *Cardiocrinum* (Liliaceae) species: comparative genomic and phylogenetic analyses. *Frontiers of Plant Sciences* **7**:Article 2054 DOI 10.3389/fpls.2016.02054.

Mardanov AV, Ravin NV, Kuznetsov BB, Samigullin TH, Antonov AS, Kolganova TV, Skyabin KG. 2008. Complete sequence of the duckweed (*Lemna minor*) chloroplast genome: structural organization and phylogenetic relationships to other angiosperms. *Journal of Molecular Evolution* **66**:555–564 DOI 10.1007/s00239-008-9091-7.

Nazareno AG, Carlsen M, Lohmann LG. 2015. Complete chloroplast genome of *Tanaecium tetragonolobum*: the first Bignoniaceae plastome. *PLOS ONE* **10**:e129930 DOI 10.1371/journal.pone.0129930.

Neuhaus HE, Emes MJ. 2000. Nonphotosynthetic metabolism in plastids. *Annual Review of Plant Biology* **51**:111–140 DOI 10.1146/annurev.arplant.51.1.111.

Posada D, Crandall KA. 1998. Modeltest: testing the model of DNA substitution. *Bioinformatics* **14**:817–818 DOI 10.1093/bioinformatics/14.9.817.

Raubeson LA, Jansen RK. 2005. Chloroplast genomes of plants. In: Henry RJ, ed. *Plant diversity and evolution: genotypic and phenotypic variation in higher plants*. Cambridge: CABI Press, 45–68.

Roman G, Park S. 2015. Analysis of the complete chloroplast genome of a medicinal plant, *Dianthus superbus* var. *longicalyncinus*, from a comparative genomics perspective. *PLOS ONE* **10(10)**:e0141329 DOI 10.1371/journal.pone.0141329.

Ronquist F, Huelsenbeck JP. 2003. MrBayes 3: Bayesian phylogenetic inference under mixed models. *Bioinformatics* **19**:1572–1574 DOI 10.1093/bioinformatics/btg180.

Roy S, Ueda M, Kadowaki K, Tsutsumi N. 2010. Different status of the gene for ribosomal protein S16 in the chloroplast genome during evolution of the genus *Arabidopsis* and closely related species. *Genes and Genetic Systems* **85**:319–326 DOI 10.1266/ggs.85.319.

Semenov AA, Enikeev AG, Snetkova LV, Permyakov AV, Sokolova NA, Dudareva LV. 2016. Ortho-phthalic acid esters in lipophilic extract from the cell culture of *Aconitum baicalense* Turcz ex Rapaics 1907. *Doklady Biochemistry and Biophysics* **471**:421–422 DOI 10.1134/S1607672916060120.

Shang XM, Lee CL. 1984. Chromosome studies of ten species of *Aconitum* in China. *Acta Phytotaxonomica Sinica* **22**:378–385.

Silvestro D, Michalak I. 2012. raxmlGUI: a graphical front-end for RAxML. *Organisms Diversity & Evolution* **12**:335–337 DOI 10.1007/s13127-011-0056-0.

Soltis PS, Soltis DE. 2000. The role of genetic and genomic attributes in the success of polyploids. *Proceedings of the National Academy of Sciences of the United States of America* **97(13)**:7051–7057 DOI 10.1073/pnas.97.13.7051.

Song BH, Wang XQ, Wang XR, Sun LJ, Hong DY, Peng PH. 2002. Maternal lineages of *Pinus densata*, a diploid hybrid. *Molecular Ecology* **11**:1057–1063 DOI 10.1046/j.1365-294X.2002.01502.x.

Stamatakis A. 2006. RAxML-VI-HPC: maximum likelihood-based phylogenetic analyses with thousands of taxa and mixed models. *Bioinformatics* **22**:2688–2690 DOI 10.1093/bioinformatics/btl446.

Sun G, Dilcher DL, Wang HS, Chen ZD. 2011. A eudicot from the Early Cretaceous of China. *Nature* **471**:625–628 DOI 10.1038/nature09811.

Swofford DL. 2002. PAUP*: phylogenetic analysis using parsimony (* and other methods). Version 4.0b10. Sunderland: Sinauer Associates. *Available at http://paup.scs.fsu.edu/*.

The Angiosperm Phylogeny Group, Chase MW, Christenhusz MJM, Fay MF, Byng JW, Judd WS, Soltis DE, Mabberley DJ, Sennikov AN, Soltis PS, Stevens PF. 2016. An update of the Angiosperm Phylogeny Group classification for the orders and families of flowering plants: APG IV. *Botanical Journal of the Linnean Society* **181**:1–20 DOI 10.1111/boj.12385.

Thiel T, Michalek W, Varshney R, Graner A. 2003. Exploiting EST databases for the development and characterization of gene-derived SSR-markers in barley

(*Hordeumvulgare* L.). *Theoretical Application of Genetics* **106**:411–422 DOI 10.1007/s00122-002-1031-0.

Utelli AB, Roy BA, Baltisberger M. 2000. Molecular and morphological analyses of European *Aconitum* species (Ranunculaceae). *Plant Systematics and Evolution* **224**:195–212 DOI 10.1007/BF00986343.

Wada K, Takeda K, Haraguchi M, Abe Y, Kuwahara N, Suzuki S, Terui A, Masaka T, Munakata N, Uchida M, Nunokawa M, Yamashita H, Goto M, Lee KH. 2016. Four new diterpenoid alkaloids from *Aconitum japonicum*. *Planta Medica* **81(S01)**:S1–S381 DOI 10.1055/s-0036-1596757.

Wang W, Liu Y, Yu SX, Gao TG, Chen ZD. 2013. *Gymnaconitum*, a new genus of Ranunculaceae endemic to the Qinghai-Tibetan Plateau. *Taxon* **62**:713–722 DOI 10.12705/624.10.

Wang W, Lu AM, Ren Y, Endress ME, Chen ZD. 2009. Phylogeny and classification of Ranunculales: evidence from four molecular loci and morphological data. *Perspectives in Plant Ecology Evolution and Systematics* **11**:81–110 DOI 10.1016/j.ppees.2009.01.001.

Wicke S, Schneeweiss GM, DePamphilis CW, Müller KF, Quandt D. 2011. The evolution of the plastid chromosome in land plants: gene content, gene order, gene function. *Plant Molecular Biology* **76**:273–297 DOI 10.1007/s11103-011-9762-4.

Wu Z, Gui S, Quan Z, Pan L, Wang S, Ke W, Liang D, Ding Y. 2014. A precise chloroplast genome of *Nelumbo nucifera* (Nelumbonaceae) evaluated with Sanger, Illumina MipSeq, and PacBio RS II sequencing platforms: insight into the plastid evolution of basal eudicots. *BMC Plant Biology* **14**:289 DOI 10.1186/s12870-014-0289-0.

Wyman SK, Jansen RK, Boore JL. 2004. Automatic annotation of organellar genomes with DOGMA. *Bioinformatics* **20(17)**:3252–3255 DOI 10.1093/bioinformatics/bth352.

Yang M, Zhang XW, Liu GM, Yin YX, Chen KF, Yun QZ, Zhao DJ, Al-Mssallem IS, Yu J. 2010. The complete chloroplast genome sequence of date palm (*Phoenix dactylifera* L.). *PLOS ONE* **5(9)**:e12762 DOI 10.1371/journal.pone.0012762.

Yuan Q, Yang QE. 2006. Polyploidy in *Aconitum* subgenus *Lycoctonum* (Ranunculaceae). *Botanical Journal of the Linnean Society* **150**:343–353 DOI 10.1111/j.1095-8339.2006.00468.x.

Zhao Y, Bu G, Zhou Y, Lv L, Yan G, Chen B, Wang L, Cen X. 2010. Mechanism study of *Aconitum*-induced neurotoxicity in PC12 cells: involvement of dopamine release and oxidative damage. *Neurotoxicology* **31**:752–757 DOI 10.1016/j.neuro.2010.06.005.

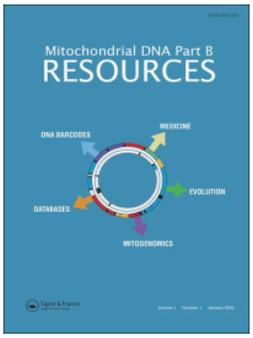

Taylor & Francis
Taylor & Francis Group

Mitochondrial DNA Part B

Resources

ISSN: (Print) (Online) Journal homepage: https://www.tandfonline.com/loi/tmdn20

The complete chloroplast genome of *Sedum tricarpum* Makino. (Crassulaceae)

Jing Chen, Hui Zhou & Wei Gong

To cite this article: Jing Chen, Hui Zhou & Wei Gong (2022) The complete chloroplast genome of *Sedum tricarpum* Makino. (Crassulaceae), Mitochondrial DNA Part B, 7:1, 15-16, DOI: 10.1080/23802359.2021.2005489

To link to this article: https://doi.org/10.1080/23802359.2021.2005489

© 2021 The Author(s). Published by Informa UK Limited, trading as Taylor & Francis Group.

Published online: 10 Dec 2021.

Submit your article to this journal

View related articles

View Crossmark data

Full Terms & Conditions of access and use can be found at
https://www.tandfonline.com/action/journalInformation?journalCode=tmdn20

MITOCHONDRIAL DNA PART B
2022, VOL. 7, NO. 1, 15–16
https://doi.org/10.1080/23802359.2021.2005489

Taylor & Francis
Taylor & Francis Group

MITOGENOME ANNOUNCEMENT

OPEN ACCESS Check for updates

The complete chloroplast genome of *Sedum tricarpum* Makino. (Crassulaceae)

Jing Chen[a], Hui Zhou[b] and Wei Gong[b]

[a]College of Life Science, Zhejiang Chinese Medical University, Hangzhou, China; [b]College of Life Sciences, South China Agricultural University, Guangzhou, China

ABSTRACT

Sedum tricarpum Makino., is a perennial succulent herb, which was first discovered and established as a new species ten years ago. Here, we report the complete chloroplast genome of *S. tricarpum*. It shows a typical quadripartite structure with a total length of 149,349 bp, including the large single-copy region (LSC) of 81,644 bp, the small single-copy region (SSC) of 16,643 bp, and two separated inverted regions (IRs) of 25,531 bp, respectively. For the whole genome, there are a total of 131 genes, including 85 protein-coding genes (PCGs), 8 rRNA genes, and 37 tRNA genes. The overall GC content of the cp genome is 37.8%. A well-supported phylogenetic tree revealed monophyly formed by *S. tricarpum* and *S. sarmentosum*, suggesting a relatively closer phylogenetic relationship with the clade consisting of *S. lineare* and *Graptopetalum amethystinum.* The complete chloroplast genome of *S. tricarpum* provides valuable information for further phylogenetic reconstruction of the Crassulaceae family.

ARTICLE HISTORY
Received 2 September 2021
Accepted 6 November 2021

KEYWORDS
Sedum tricarpum; chloroplast genome; succulent herb; illumina sequencing

Sedum tricarpum Makino., a perennial succulent herb, belongs to the family of Crassulaceae. It was first found to occur in Anhui Province, China and established as a new species (Hong et al. 2013). It normally grows on rocks along small streams at an altitude of about 200–400 m. In the current study, we report the first complete chloroplast (cp) genome of *S. tricarpum* in order to provide valuable information for further phylogenetic reconstruction of the Crassulaceae family.

One individual was collected in Shunxin, Lin'an, Zhejiang Province (23.08°, 113.22°). A specimen was deposited at the herbarium of College of Life Sciences, Zhejiang Chinese Medical University (Jing Chen; cj00123@zcmu.edu.cn) under the voucher number 20150614-050-031). Tender leaves were collected and instantly put into the silica gel for drying and preservation. Total genomic DNA was extracted using a modified CTAB method (Doyle and Doyle 1987). The paired-end (2 × 150 bp) library was sequenced by Illumina PE150 at Novogene Co. Ltd (Beijing, China). A total of 2.34 Gb clean reads were obtained after removing low-quality reads and adaptor sequences., We assembled the complete cp genome of *S. tricarpum* using GetOrganelle (Jin et al. 2020) and SPAdes (Bankevich et al. 2012). Manual adjustment and annotation were conducted with the aid of Geneious prime 2019.2.1 (Kearse et al. 2012). The tRNA genes were annotated with ARAGORN (Laslett and Canback 2004). The cp genomes of 13 species of Crassulaceae were downloaded from the GenBank database, including *Aeonium arboreum* (MW206792), *Crassula perforata* (MW206794), *Graptopetalum amethystinum* (MW206795), *Hylotelephium ewersii* (MN794014), *Kalanchoe daigremontiana* (MT954417), *Phedimus aizoon* (MN794321), *Phedimus takesimensis* (KF954541), *Rhodiola sacra* (MN109978), *Sedum lineare* (MT755626), *Sedum sarmentosum* (JX427551), *Sinocrassula densirosulata* (MW206800), *Sinocrassula indica* (MN794334), and *Umbilicus rupestris* (MN794335). *Hamamelis mollis* (MH191387) of Hamamelidaceae was used as an outgroup. A total of 14 cp genomes were aligned with online software MAFFT on CIPRES (https://www.phylo.org, Miller et al. 2015). Maximum likelihood (ML) analyses were performed using RAxML-HPC v.8.2.10 on XSEDE (https://www.phylo.org) with 1,000 bootstrap replicates. Substitution model of GTR + I + G (Stamatakis 2014) was applied which was determined by the Bayesian information criterion (BIC) in jModeltest v2.1.10 (Darriba et al. 2012).

The *S. tricarpum* cp genome has been deposited in GenBank (Accession No.: MZ519883). The total length is 149,349 bp with the typical quadripartite structure. It consists of a pair of inverted regions (IRs) of 25,531 bp separated by a large single-copy region (LSC) of 81,644 bp and a small single-copy region (SSC) of 16,643 bp, respectively. The overall GC content of the cp genome is 37.8%. The whole cp genome of *S. tricarpum* contains 131 genes with 85 protein-coding genes (PCGs), 37 tRNA genes, and eight rRNA genes. Among these genes, 63 PCGs and 22 tRNA genes are located in the LSC region, while 12 PCGs and one tRNA gene occur in the SSC region. All of the eight rRNA genes are duplicated in the IR regions. Additionally, IR regions contain five PCGs and seven tRNA genes, if counting only once. Among the annotated genes, 15 genes (*trnK-UUU, trnL-UAA, rps16, trnV-*

CONTACT Wei Gong wgong@scau.edu.cn College of Life Sciences, South China Agricultural University, Guangzhou, China

© 2021 The Author(s). Published by Informa UK Limited, trading as Taylor & Francis Group.
This is an Open Access article distributed under the terms of the Creative Commons Attribution License (http://creativecommons.org/licenses/by/4.0/), which permits unrestricted use, distribution, and reproduction in any medium, provided the original work is properly cited.

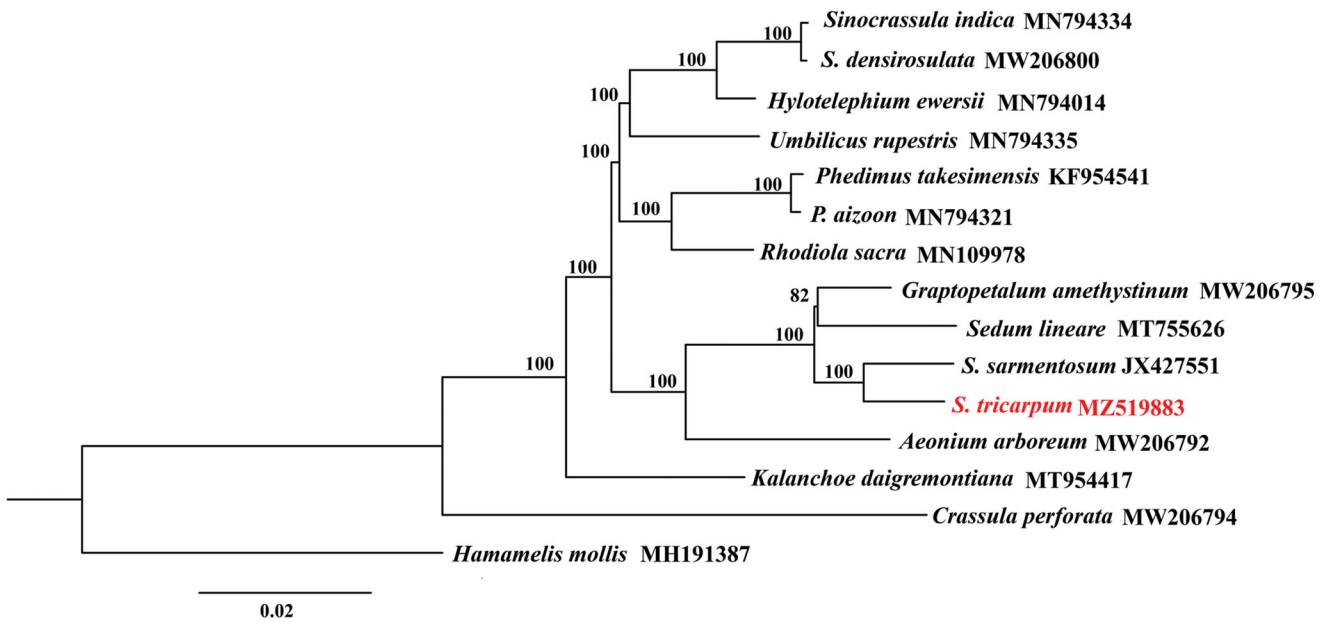

Figure 1. ML tree based on 15 complete chloroplast genomes of Crassulaceae and one outgroup species. Numbers at the nodes are bootstrap support values based on 1000 replicates. GenBank accession numbers are listed beside the species. The species *S. tricarpum* is highlighted in red.

UAC, rpl2, ndhB, trnG-UCC, trnI-GAU, trnA-UGC, atpF, ndhA, rpoC1, petD, petB, and rpl16) contain one intron, while three genes (*clpP, ycf3,* and *rps12*) possess two introns. A well-supported phylogenetic tree based on ML analysis was reconstructed, suggesting monophyly formed by *S. tricarpum* and *S. sarmentosum* (Figure 1). The two species demonstrate a comparably closer phylogenetic relationship with the clade that consists of *S. lineare* and *Graptopetalum amethystinum*.

Disclosure statement

No potential conflict of interest was reported by the authors.

Funding

This research was supported by the Key Research and Development Program in Zhejiang Province [2020C03052] and the National Natural Science Foundation of China [31470312].

Data availability statement

The complete chloroplast genome sequence data that support the findings of this study are openly available in GenBank of NCBI at (https://www.ncbi.nlm.nih.gov/) under the accession no. MZ519883. The associated BioProject, SRA, and Bio-Sample numbers are PRJNA749476, SRR15239711, and SAMN20371514 respectively.

References

Bankevich A, Nurk S, Antipov D, Gurevich AA, Dvorkin M, Kulikov AS, Lesin VM, Nikolenko SI, Pham S, Prjibelski AD, Pyshkin AV, et al. 2012. SPAdes: a new genome assembly algorithm and its applications to single-cell sequencing. J Comput Biol. 19(5):455–477.

Darriba D, Taboada GL, Doallo R, Posada D. 2012. jModelTest 2: more models, new heuristics and parallel computing. Nat Methods. 9(8):772.

Doyle JJ, Doyle JL. 1987. A rapid DNA isolation procedure for small quantities of fresh leaf tissue. Phytochem Bull. 19:11–15.

Hong X, Li ZL, Zhou SB. 2013. A new record of Sedum L. From East China. J Zhejiang University. 30:797–798.

Jin JJ, Yu WB, Yang JB, Song Y, dePamphilis CW, Yi TS, Li DZ. 2020. GetOrganelle: a fast and versatile toolkit for accurate de novo assembly of organelle genomes. Genome Biol. 21(1):241.

Kearse M, Moir R, Wilson A, Stones-Havas S, Cheung M, Sturrock S, Buxton S, Cooper A, Markowitz S, Duran C, et al. 2012. Geneious basic: an integrated and extendable desktop software platform for the organization and analysis of sequence data. Bioinformatics. 28(12): 1647–1649.

Laslett D, Canback B. 2004. ARAGORN, a program to detect tRNA genes and tmRNA genes in nucleotide sequences. Nucleic Acids Res. 32(1): 11–16.

Miller MA, Schwartz T, Pickett BE, He S, Klem EB, Scheuermann RH, Passarotti M, Kaufman S, O'Leary MA. 2015. A RESTful API for access to phylogenetic tools via the CIPRES science gateway. Evol Bioinform Online. 11:43–48.

Stamatakis A. 2014. RAxML version 8: a tool for phylogenetic analysis and post-analysis of large phylogenies. Bioinformatics. 30(9): 1312–1313.

Taylor & Francis
Taylor & Francis Group

Mitochondrial DNA Part B
Resources

ISSN: (Print) (Online) Journal homepage: https://www.tandfonline.com/loi/tmdn20

The complete chloroplast genome of *Hylotelephium erythrostictum* (Miq.) H. Ohba (Crassulaceae)

Jing Chen, Hui Zhou & Wei Gong

To cite this article: Jing Chen, Hui Zhou & Wei Gong (2022) The complete chloroplast genome of *Hylotelephium erythrostictum* (Miq.) H. Ohba (Crassulaceae), Mitochondrial DNA Part B, 7:2, 365-366, DOI: 10.1080/23802359.2022.2036648

To link to this article: https://doi.org/10.1080/23802359.2022.2036648

© 2022 The Author(s). Published by Informa UK Limited, trading as Taylor & Francis Group.

Published online: 09 Feb 2022.

Submit your article to this journal

Article views: 502

View related articles

View Crossmark data

Citing articles: 1 View citing articles

Full Terms & Conditions of access and use can be found at
https://www.tandfonline.com/action/journalInformation?journalCode=tmdn20

MITOCHONDRIAL DNA PART B
2022, VOL. 7, NO. 2, 365–366
https://doi.org/10.1080/23802359.2022.2036648

Taylor & Francis
Taylor & Francis Group

MITOGENOME ANNOUNCEMENT

OPEN ACCESS Check for updates

The complete chloroplast genome of *Hylotelephium erythrostictum* (Miq.) H. Ohba (Crassulaceae)

Jing Chen[a], Hui Zhou[b] and Wei Gong[b]

[a]College of Life Science, Zhejiang Chinese Medical University, Hangzhou, PR China; [b]College of Life Sciences, South China Agricultural University, Guangzhou, PR China

ABSTRACT

The species *Hylotelephium erythrostictum* is well known as an ornamental plant in China. Here, we report the complete chloroplast genome (cp) of *H. erythrostictum* using the next-generation sequencing. It shows a total length of 151,707 bp with typical quadripartite structure. The genome is composed of the large single copy region (LSC) of 83,070 bp, the small single copy region (SSC) of 17,018 bp, and two separated inverted regions (IRs) of 25,793 bp, respectively. It contains 134 genes, including 80 protein-coding genes (PCGs), 8 rRNA genes, and 37 tRNA genes. The overall GC content of the cp genome is 37.7%. Maximum likelihood (ML) tree based on ten complete chloroplast genomes of Crassulaceae and one outgroup species suggested a monophyly formed by *H. erythrostictum* together with *Hylotelephium ewersii*, which demonstrate a comparably closer phylogenetic relationship. The complete chloroplast genome of this *H. erythrostictum* provides valuable information and further phylogenetic reconstruction of the Crassulaceae family.

ARTICLE HISTORY
Received 27 July 2021
Accepted 27 January 2022

KEYWORDS
Hylotelephium erythrostictum; chloroplast genome; ornamental plant; Crassulaceae

The genus *Hylotelephium,* belonging to the family of Crassulaceae, shows a wide geographical distribution range in Euro-Asia and North America. *Hylotelephium erythrostictum* (Miq.) H. Ohba 1977 is a perennial succulent herb in this genus. This species has been widely used in urban greening and ecological landscaping in China due to its strong stress-resistance and highly ornamental value. In this study, we report the first complete chloroplast (cp) genome of *H. erythrostictum*, on the purpose of further phylogenetic reconstruction of the Crassulaceae family.

Before we carried out the project, we got ethical approval and permission from the Natural Reserve of Tianmu Mountain. Field studies have been carried out in accordance with guidelines and comply with local legislation. One individual was collected from Tianmu Mountain, Zhejiang Province (N23.08°, E113.22°). A specimen was deposited at the herbarium of College of Life Science, Zhejiang Chinese Medical University (Jing Chen; cj00123@zcmu.edu.cn) under the voucher number 20150720-051-021. Tender leaves were sampled and instantly put into the silica gel for drying and preservation (Jing Chen; cj00123@zcmu.edu.cn). Total genomic DNA was extracted by using a modified CTAB method (Doyle and Doyle 1987). The paired-end (2×150 bp) library was sequenced by Illumina PE150 at Novogene Co. Ltd (Beijing, China). A total of 2.19 Gb clean reads were obtained after removing low quality reads and adaptor sequences. Using GetOrganelle (Jin et al. 2020) and SPAdes (Bankevich et al. 2012), we assembled the complete cp genome of *H. erythrostictum* followed by manual adjustment and annotated it by the aid of Geneious prime 2019.2.1 (Kearse et al. 2012), using default parameters to predict protein-coding genes (PCGs) and rRNA genes. The tRNA genes were annotated on ARAGORN (Laslett and Canback 2004). The cp genomes of nine species of Crassulaceae were downloaded from GenBank database, including *Aeonium arboreum* (MW206792), *Cotyledon tomentosa* (MW206793), *Crassula perforata* (MW206794), *Graptopetalum amethystinum* (MW206795), *Hylotelephium ewersii* (MN794014), *Kalanchoe fedtschenkoi* (MW206796), *Kalanchoe tomentosa* (MN794319), *Rosularia alpestris* (MN794333), and *Sedum lineare* (MT755626). *Eucommia ulmoides* (KU204775) of Eucommiaceae was used as an outgroup. Totally, 11 cp genomes were aligned with online software MAFFT on CIPRES (https://www.phylo.org, Miller et al. 2015). Maximum likelihood (ML) analyses were performed by using RAxML-HPC version 8.2.10 on XSEDE (https://www.phylo.org) with 1000 bootstrap replicates and the substitution GTR + I + G model (Stamatakis 2014), the latter of which was determined by the Bayesian information criterion (BIC) in jModeltest version 2.1.10 (Darriba et al. 2012).

The *H. erythrostictum* cp genome has been deposited in GenBank (Accession No.: MZ519882). The total length is 151,707 bp with the typical quadripartite structure. It consists of a pair of inverted regions (IRs) of 25,793 bp separated by large single copy region (LSC) of 83,070 bp and small single copy region (SSC) of 17,018 bp, respectively. The overall GC

CONTACT Wei Gong wgong@scau.edu.cn College of Life Sciences, South China Agricultural University, Guangzhou, PR China

© 2022 The Author(s). Published by Informa UK Limited, trading as Taylor & Francis Group.
This is an Open Access article distributed under the terms of the Creative Commons Attribution License (http://creativecommons.org/licenses/by/4.0/), which permits unrestricted use, distribution, and reproduction in any medium, provided the original work is properly cited.

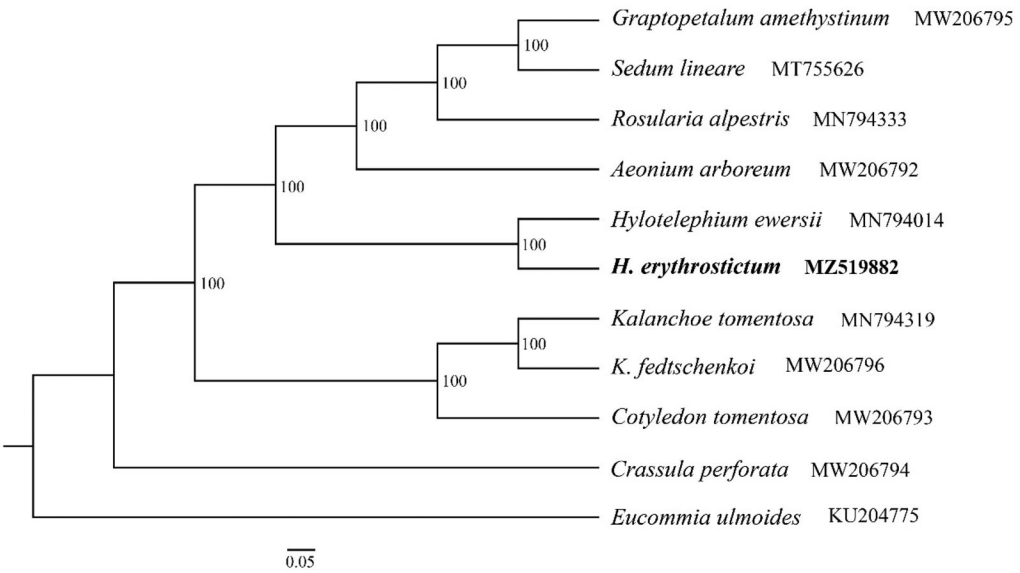

Figure 1. ML tree based on 10 complete chloroplast genomes of Crassulaceae and one outgroup species. Numbers at the nodes are bootstrap support values based on 1000 replicates. GenBank accession Numbers are listed beside the species. The species *H. erythrostictum* is highlighted in bold.

content of the cp genome is 37.7%. The whole cp genome of *H. erythrostictum* contains 134 genes with 80 PCGs, 37 tRNA genes, and 8 rRNA genes. Among these genes, 60 PCGs and 22 tRNA genes are located in the LSC region, while 12 PCGs and one tRNA gene occur in the SSC region. All these eight rRNA genes are duplicated in the IR regions. IR regions contain six PCGs and seven tRNA genes, if counting only once. Among the annotated genes, a total of 15 genes contain one intron, which are *trn*K-UUU, *trn*L-UAA, *rps*16, *trn*V-UAC, *rpl*2, *ndh*B, *trn*G-GCC, *trn*I-GAU, *trn*A-UGC, *atp*F, *ndh*A, *rpo*C1, *pet*D, *pet*B, and *rpl*16, while three genes including *clp*P, *ycf*3, and *rps*12 possess two introns. The numbers and genes that contain one or two introns are exactly the same as *Sedum tricarpum*, which is largely due to the low variation based on cpDNA genome and the relatively close phylogenetic relationship between *H. erythrostictum* and *Sedum tricarpum* in the Crassulaceae family. A well supported phylogenetic tree is reconstructed, suggesting a monophyly formed by *H. erythrostictum* together with *H. ewersii* (Figure 1). The two species demonstrate a comparably closer phylogenetic relationship with the clade consisting of *Graptopetalum amethystinum, Sedum lineare, Rosularia alpestris,* and *Aeonium arboreum.*

Author contributions

Wei Gong and Jing Chen conceived and designed the project. Wei Gong and Hui Zhou analyzed and interpreted the data. Wei Gong and Jing Chen wrote the paper and revised it for intellectual content. All authors agree to be accountable for all aspects of the work.

Disclosure statement

No potential conflict of interest was reported by the authors.

Funding

This research was supported by the National Natural Science Foundation of China [82174272, 31470312], the Research Project of Zhejiang Chinese Medical University [2020ZG33].

Data availability statement

The complete chloroplast genome sequence data that support the findings of this study are openly available in GenBank of NCBI at [https://www.ncbi.nlm.nih.gov] (https://www.ncbi.nlm.nih.gov/) under the accession no. MZ519882. The associated BioProject, SRA, and Bio-Sample numbers are PRJNA749471, SRR15239599, and SAMN20371389, respectively.

References

Bankevich A, Nurk S, Antipov D, Gurevich AA, Dvorkin M, Kulikov AS, Lesin VM, Nikolenko SI, Pham S, Prjibelski AD, Pyshkin AV, et al. 2012. SPAdes: a new genome assembly algorithm and its applications to single-cell sequencing. J Comput Biol. 19(5):455–477.

Darriba D, Taboada GL, Doallo R, Posada D. 2012. jModelTest 2: more models, new heuristics and parallel computing. Nat Methods. 9(8):772.

Doyle JJ, Doyle JL. 1987. A rapid DNA isolation procedure for small quantities of fresh leaf tissue. Phytochem Bull. 19:11–15.

Jin JJ, Yu WB, Yang JB, Song Y, dePamphilis CW, Yi TS, Li DZ. 2020. GetOrganelle: a fast and versatile toolkit for accurate de novo assembly of organelle genomes. Genome Biol. 21(1):241.

Kearse M, Moir R, Wilson A, Stones-Havas S, Cheung M, Sturrock S, Buxton S, Cooper A, Markowitz S, Duran C, et al. 2012. Geneious basic: an integrated and extendable desktop software platform for the organization and analysis of sequence data. Bioinformatics. 28(12):1647–1649.

Laslett D, Canback B. 2004. ARAGORN, a program to detect tRNA genes and tmRNA genes in nucleotide sequences. Nucleic Acids Res. 32(1):11–16.

Miller MA, Schwartz T, Pickett BE, He S, Klem EB, Scheuermann RH, Passarotti M, Kaufman S, O'Leary MA. 2015. A RESTful API for access to phylogenetic tools via the CIPRES science gateway. Evol Bioinform Online. 11:43–48.

Stamatakis A. 2014. RAxML version 8: a tool for phylogenetic analysis and post-analysis of large phylogenies. Bioinformatics. 30(9):1312–1313.